aval Research Laboratory
shington, DC 20375-5000 NRL Publication 158-4831 June 1990

NRL REVIEW

Original contains color plates: All DTIC reproductions will be in black and white

DISCLAIMER NOTICE

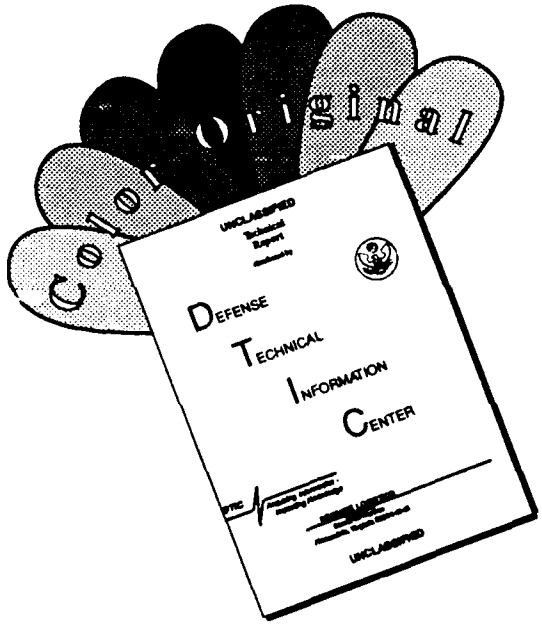

THIS DOCUMENT IS BEST QUALITY AVAILABLE. THE COPY FURNISHED TO DTIC CONTAINED A SIGNIFICANT NUMBER OF COLOR PAGES WHICH DO NOT REPRODUCE LEGIBLY ON BLACK AND WHITE MICROFICHE.

Naval Research Laboratory

NRL REVIEW

In this Review, NRL presents highlights of the unclassified research and development programs for fiscal year 1989. The 1990 date on the spine reflects the printing year. This book fulfills a dual purpose: it provides an exchange of information among scientists, engineers, scholars, and managers; and it is used in recruiting science and engineering professionals. As you read this Review, *you will become even more aware that the Laboratory is a dynamic team working together to promote the programs, progress, and innovations that will continue to foster discoveries, inventiveness, and scientific advances for the Navy of the future.*

REFLECTIONS FROM TOP MANAGEMENT ...

Thirty years ago at the Naval Academy, when we were doing war games about how to operate carriers in the Tonkin Gulf, I occasionally thought about what a military career might be like in a time of peace, a time of smaller, not larger, military forces. Now, given recent world events and my promotion, some of that might not only come true, but come true during my watch.

How then to face the prospect of a decreasing Navy, reduced force structures, and constant competition for budget resources as the old begrudgingly gives way to the new? One way is to concentrate on quality and on the end result. In ten years, we will have a smaller Navy, but we will still have a Navy, because we remain an island nation that depends on world commerce. We also remain an active member of the world community that wants peace among our peers. That Navy will be a better, higher quality, productive, and protective national asset if we concentrate on the end result.

So, too, for NRL, the strength of which has always been its people, and that will not change. In the years since World War II, NRL has grown and prospered, and it has developed a very successful method of dealing with the shore establishment and the operating forces through a complex but effective network of relationships at the branch level. I believe that when you are successful, you shouldn't change, but at the same time, NRL must concentrate on the result it wants to attain. A good example is the prospect that both NRL and the Navy as a whole will have to seek out a prudent level for activity in space. The next ten years could well be the decade that determines whether or not NRL continues as a major national trust.

I believe that the Lab will grow in quality along with the rest of the Navy. As Dr. Coffey points out in his companion piece, most of NRL's leadership will change in the next decade. If that leadership maintains a vision of the end result—of quality and of professional dedication to science and country—then NRL will surely prosper. As our Nobel Laureate, Dr. Jerry Karle, recently told us, he believes that we will need all levels of management to become more proactive in showing the Navy, Congress, and the American people what NRL is and what we as a laboratory can contribute.

The opportunities are there if we take them. We should seek increased technology transfer through cooperative agreements with industry and increased awareness and participation at all levels in the Navy decision process. Add to that an increased sense of community with schools, local government, and people from all walks of life. The opportunities are there, and I am very grateful that I have had the good fortune to be part of the NRL family at this particular time and to help envision such an end result.

RADM (Sel) John J. Donegan, Jr., USN
Commanding Officer

... AS WE MOVE TOWARD THE YEAR 2000

As we enter the 1990s, there is much speculation in the media regarding the state of the world as it will be in the year 2000. It is of course not possible to predict with any certainty what the world situation will be by the year 2000—in science and technology or politics or economics. There are, however, a number of trends to which we will respond over the next decade. Our collective response to these trends will determine the situation that actually exists by the turn of the century. We can expect that economic competition among the world's nations will increase. This increased competition will exacerbate the problem of vanishing global raw material sources. The increased competition will be in conflict with a growing awareness of the environmental consequences of the competition. All of these pressures will filter down to NRL in the form of national policy regarding military, social, and commercial affairs. NRL will be expected to be a major player in reconciling what will become increasingly conflicting requirements. Namely, how does one simultaneously maintain an adequate national defense, respond to an accelerating high technology competition, and protect the environment? These conflicting requirements will present some marvelous opportunities for NRL to create advances in science and technology. I expect that NRL will maintain its historic involvement with the development of sensors of all kinds. I expect, however, that we will move from the development of basic sensors to the development of increasingly sophisticated and intelligent sensors. This movement is being driven by advances in computer technology and by an ever increasing ability to develop materials with specifically designed properties. NRL will become increasingly involved with the use of computer simulation in almost all the areas it pursues, from the design of molecules and materials to the behavior of complex systems to the actual engineering design of military equipment and systems.

As we respond to the opportunities and requirements that will confront us, we will be faced with a large number of complex problems. The most important and perhaps the most complex problem will be that of maintaining a scientific and technical staff that is able to respond to the challenges. Current NRL demographics indicate that there will be a very significant turnover in personnel between now and the year 2000. This turnover will present a great opportunity to renew NRL's workforce. NRL must, however, be provided the tools to accomplish this renewal. The second great challenge will be to provide the facilities required to conduct the research and technology developments of the 21st century. NRL will need all of its persuasive powers to obtain the computer resources, the clean rooms, the material fabrication facilities, the analytical instrumentation, and the other equipment and facilities needed to fulfill its function as the Navy's Corporate Research Laboratory.

Clearly, the research, technology, and management challenges that will confront us in this decade are quite profound. Some would say they are worrisome. We could, of course, worry about them. I would rather get on with meeting them. We are entering what will be one of the most exciting decades in the history of the Laboratory. Although I cannot predict the state of the world in the year 2000, I will predict that NRL in the year 2000 will look back with pride upon its accomplishments in the decade of the 1990s.

Dr. Timothy Coffey
Director of Research

MISSION

To conduct a broadly based multidisciplinary program of scientific research and advanced technological development directed toward new and improved materials, equipment, techniques, systems, and related operational procedures for the Navy.

RESPONSIBLE FOR NAVY-WIDE LEADERSHIP IN:

- The performance of primary in-house research for the physical and engineering sciences;
- The conduct of a broadly based exploratory and advanced development program in response to identified and anticipated Navy needs;
- The development of space systems for the Navy.

CONTENTS

The Naval Research Laboratory

THE NAVAL RESEARCH LABORATORY

"I believe [that] the Government should maintain a great research laboratory, jointly under military and naval and civilian control. In this could be developed the continually increasing possibilities of . . . all the technique of naval progression ....

"When the time came, if it ever did, we could take advantage of the knowledge gained through this research work and quickly produce the very latest and most efficient instruments ... "

Thomas A. Edison
The New York Times Magazine
May 30, 1915

THE NAVAL RESEARCH LABORATORY

Our Heritage

Today, when government and science seem inextricably linked, when virtually no one questions the dependence of national defense on the excellence of national technical capabilities, it is noteworthy that in-house defense research is relatively new in our Nation's history. The Naval Research Laboratory (NRL), the first modern research institution created within the United States Navy, began operations in 1923.

Thomas Edison's Vision—The first step came in May 1915, a time when Americans were deeply worried about the great European war. Thomas Edison, asked by a *New York Times* correspondent to comment on the conflict, argued that the Nation should look to science. "The Government," he proposed in a published interview, "should maintain a great research laboratory.... In this could be developed...all the technique of military and naval progression without any vast expense." Secretary of the Navy Josephus Daniels seized the opportunity created by Edison's public comments to enlist Edison's support. He agreed to serve as the head of a new body of civilian experts—the Naval Consulting Board—to advise the Navy on science and technology. The Board's most ambitious plan was the creation of a modern research facility for the Navy. Congress allocated $1.5 million for the institution in 1916, but wartime delays and disagreements within the Naval Consulting Board postponed construction until 1920.

The Laboratory's two original divisions, Radio and Sound, pioneered in the fields of high-frequency radio and underwater sound propagation. They produced communications equipment, direction-finding devices, sonar sets, and, perhaps most significant of all, the first practical radar equipment built in this country. They also performed basic research, participating, for example, in the discovery and early exploration of the ionosphere. Moreover, the Laboratory was able to work gradually toward its goal of becoming a broadly based research facility. By the beginning of World War II, five new divisions had been added: Physical Optics, Chemistry, Metallurgy, Mechanics and Electricity, and Internal Communications.

The War Years and Growth—Total employment at the Laboratory jumped from 396 in 1941 to 4400 in 1946, expenditures from $1.7 million to $13.7 million, the number of buildings from 23 to 67, and the number of projects from 200 to about 900. During the war, scientific activities necessarily were concentrated almost entirely on applied research. New electronics equipment—radio, radar, sonar—was developed. Countermeasures were devised. New lubricants were produced, as were antifouling paints, luminous identification tapes, and a sea marker to help save survivors of disasters at sea. A thermal diffusion process was conceived and used to supply some of the ^{235}U isotope needed for one of the first atomic bombs. Also, many new devices that developed

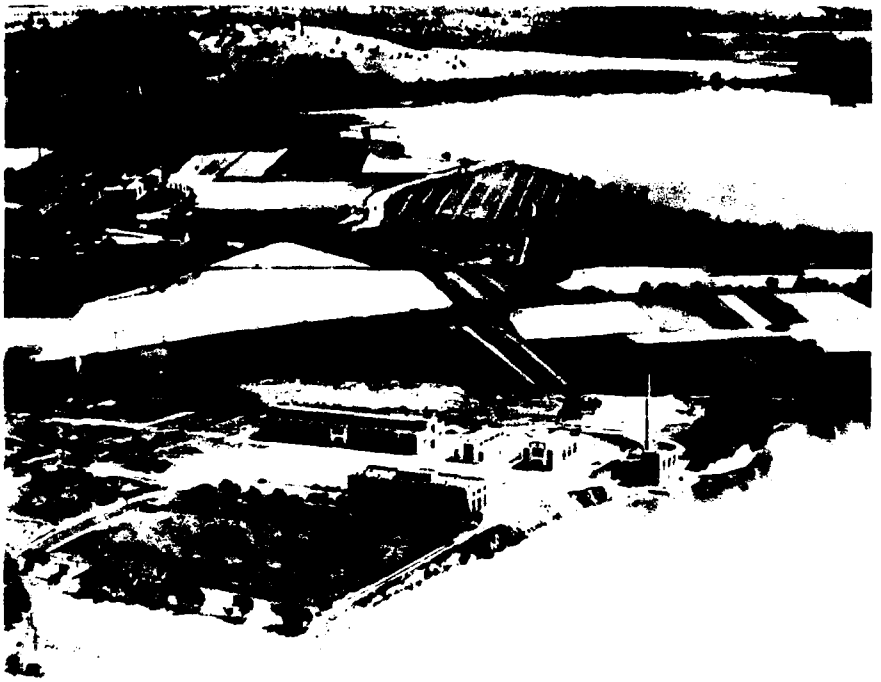

The original Naval Research Laboratory in 1923 among the farmlands of Blue Plains as viewed from the Potomac River

from booming wartime industry were type tested and then certified as reliable for the Fleet.

NRL Reorganizes for Peace—Because of the major scientific accomplishments of the war years, the United States emerged into the postwar era determined to consolidate its wartime gains in science and technology and to preserve the working relationship between its armed forces and the scientific community. While the Navy was establishing its Office of Naval Research (ONR) as a liaison with and supporter of basic and applied scientific research, it was also encouraging NRL to broaden its scope and become, in effect, its corporate research laboratory. There was a transfer of NRL to the administrative oversight of ONR and a parallel shift of the Laboratory's research emphasis to one of long-range basic and applied investigation in a broad range of the physical sciences.

However, rapid expansion during the war had left NRL improperly structured to address long-term Navy requirements. One major task—neither easily nor rapidly accomplished—was that of reshaping and coordinating research. This was achieved by transforming a group of largely autonomous scientific divisions into a unified institution with a clear mission and a fully coordinated research program. The first attempt at reorganization vested power in an executive committee composed of all the division superintendents. This committee was impracticably large, so in 1949 a civilian director of research was named and given full authority over the program. Positions for associate directors were added in 1954.

The Breadth of NRL—During the years since the war, the areas of study at the Laboratory have included basic research concerning the Navy's environments of Earth, sea, sky, and space. Investigations have ranged widely from monitoring the sun's behavior, to analyzing marine atmospheric conditions, to measuring parameters of the deep oceans. Detection and communication capabilities have benefited by research that has exploited new portions of the electromagnetic spectrum, extended ranges to outer space, and

The staff of NRL, circa 1935

provided means of transferring information reliably and securely, even through massive jamming. Submarine habitability, lubricants, shipbuilding materials, fire fighting, along with the study of sound in the sea, have also been steadfast concerns.

The Laboratory has pioneered naval research into space, from atmospheric probes with captured V-2 rockets, through direction of the Vanguard project—America's first satellite program—to involvement in such projects as the Navy's Global Positioning System. Today, NRL is the Navy's lead laboratory in space systems research, fire research, tactical electronic warfare, microelectronic devices, and artificial intelligence. NRL has also evaluated new issues, such as the effects of intense radiation and various forms of shock and vibration on aircraft, ships, and satellites.

Many significant accomplishments occurred in 1989, and a few are recorded here. Two new research centers were established—the Center for Bio/Molecular Science and Engineering and the Center for Advanced Space Sensing. Researchers at NRL developed an automated crystal growth system to produce large single protein crystals for use in X-ray diffraction studies. An instrument that measures mechanical properties and surface forces of thin films was also developed at the Laboratory. Scientists here were successful in creating magnetic superlattices for use in nonvolatile, radiation-hardened memory devices for information storage and digital computer systems. Scandia was identified as a corrosion-resistant stabilizer for zirconia. Zirconia is used as a thermal coating to help increase the efficiency of gas turbines and other engines. NRL researchers were successful in the creation of a chemically resistant epoxy lining for use in aircraft carrier collection-holding-transfer discharge piping systems. Laboratory researchers and engineers also participated in several satellite-based experimental studies during 1989. NRL efforts in this regard included the contribution of instruments for the Nickel Carbonyl Release Experiment (NICARE) and the Beam Experiment Aboard Rocket (BEAR) program. As part of the SDI Program, the Low-Power Atmospheric Compensation Experiment (LACE) satellite, designed and built by NRL, was readied for launch in early 1990.

Two Navy Cooperative Research and Development Agreements were signed. These agreements are authorized under the Federal Technology Transfer Act of 1986. One agreement, with the Electric Power Research Institute (EPRI) and the Lectromechanical Design

Company (Letromec), makes possible the study of multifactor stress effects on the deterioration of electrical insulation materials. The other, with the Shipley Company, provides for further development of a new lithographic technique for fabricating ultrahigh-resolution patterns on a variety of solid substrates.

One goal, however, has guided NRL's diverse activities through the years—to conduct pioneering scientific research and development that will provide improved materials, equipment, techniques, systems, and operations for the Navy, for the Department of Defense (DoD), and for the U.S. Government.

NRL Today

ORGANIZATION AND ADMINISTRATION

The position of NRL within the Navy is that of a field command under the Chief of Naval Research.

Heading the Laboratory with joint responsibilities are the naval commanding officer, Capt. John J. Donegan, Jr., USN, and the civilian director of research, Dr. Timothy Coffey. Line authority passes from the commanding officer and the director of research to six associate directors of research and the director of one technology center. Research is performed in the following areas:

- General Science and Technology
- Warfare Systems and Sensors Research
- Materials Science and Component Technology
- Naval Center for Space Technology.

Further details of the Laboratory's organization are given on the organizational chart appearing in the "General Information" section.

NRL operates as a Navy Industrial Fund (NIF) activity. As a NIF activity, all costs, including overhead, must be charged to various research projects. Funding in 1989 came from the Chief of Naval Research, the Naval Systems Commands, and other government agencies, such as the Defense Advanced Research Projects Agency, the Department of Energy, and the National Aeronautics and Space Administration as well as several nongovernment activities. NRL's relationship with its sponsoring agencies, both inside and outside DoD, is defined by a comprehensive policy on interagency support agreements.

Besides funding for scientific work, NRL receives Navy monies for general construction, maintenance, and operations.

PERSONNEL DEVELOPMENT

At the end of 1989, NRL employed 3860 personnel—52 military officers, 108 enlisted men and women, and 3700 civilians. In the research staff, there are 767 employees with doctorate degrees, 390 with masters degrees, and 667 with bachelors degrees. The support staff assists the research staff by providing administrative, computer-aided designing, machining, fabrication, electronic construction, publication, personnel development, information retrieval, large mainframe computer services, and contracting and supply management services.

Opportunities for higher education and other professional training for NRL employees are available through several programs offered by the Employee Development Branch. These programs provide for graduate work leading to advanced degrees, advanced training, college course work, short courses, continuing education, and career counseling. Graduate students, in certain cases, may use their NRL research for thesis material.

NRL today as viewed from the east

For non-NRL employees, several post-doctoral research programs exist. There are also cooperative education agreements with several universities, summer and part-time employment programs, and various summer and interchange programs for college faculty members, professional consultants, and employees of other government agencies.

NRL has active chapters of Women In Science and Engineering, Sigma Xi, Toastmaster's International, and the Federal Executive and Professional Association. Three personal computer clubs meet regularly—Edison Atari, NRL IBM-PC, and Edison Commodore. An amateur radio club, a wives' club, a drama group—the Showboaters, and several sports clubs are also active. NRL has a recreation club that provides swimming, sauna, whirlpool bath, gymnasium, and weight-room facilities. The recreation club also offers classes in karate, aerobics, swimming, and cardiopulmonary resuscitation.

A community outreach program at NRL provides tutoring for local students, science fair judging, participation in high school and college career day programs, an art and essay contest during Black History Month, and a Christmas party with gifts donated by Laboratory employees for disadvantaged children.

NRL has an active, growing Credit Union with assets of $113 million and a membership numbering 15,000. Public transportation to NRL is provided by Metrobus.

For more information on these programs, see the *Review* chapter entitled "Programs for Professional Development."

SCIENTIFIC FACILITIES

In addition to its main campus of about 130 acres and 152 buildings, NRL maintains 12 other research sites including a vessel for fire research and a Flight Support Detachment. The many diverse scientific and technological research and support facilities are described in the following paragraphs.

Research Facilities

• Space Science

NRL is the Navy's main laboratory for conducting basic research and development in the space sciences. The Space Science Division has a number of commitments for space experiments in the areas of upper atmospheric, solar, and astronomical research aboard NASA, DoD, and other space projects. Division scientists are involved in major research thrusts that include remote sensing of the upper atmosphere by using ultraviolet sensing, studies of the solar atmosphere by using spectrographic techniques, and studies of astronomical radiation ranging from the ultraviolet through the cosmic rays. The division maintains facilities to design, construct, assemble, and calibrate space experiments. A network of VAX computers, an array processor, image processing hardware, a PDS microdensitometer, and CRAY and Connection Machine access are used to analyze and interpret space data.

• Computational Physics and Fluid Dynamics

The Laboratory for Computational Physics and Fluid Dynamics (LCP&FD) has developed a Graphical and Array Processing System (GAPS). The system provides communications and common memory for large simulations on parallel array processors and immediate displays of results from other sources on high-resolution, high-speed graphics monitors. The system is front ended by two VAX 11/780s that provide control and communication to other sites at NRL and outside laboratories. A 1.4-gigabyte high-speed disk is incorporated for simulations storage and replay. The computational engines are six 30-megaflop array processors supported by a vectorizing Fortran compiler. The current graphics devices are a Tektronix and a Metheus with 1024 × 1280 color raster resolution and high-speed block data transfer capability, and an IRIS 4D vector display. A 64-million word Convex C210 has recently been installed and incorporated into the NRL network.

The LCP&FD also maintains fluid dynamic laboratory facilities that include a 30-m wind/wave tank to study nonlinear ocean wave processes and fluid/structure interactions; a 20-m stratified tow channel to study geophysical flows, jets, and wakes; and blow-down water tunnels to study hydroacoustics, turbulent boundary layers, and non-Newtonion flows. Experimental efforts using these facilities are supported by flow measurement systems including multicomponent laser velocimeters and anemometers; digital image processing of flow visualization; hydrophones; imaging infrared radiometers; and a variety of microwave radar measurement systems for remote sensing studies of hydrodynamic processes. On-line experiment control, data acquisition, and processing are achieved with a central HP1000 system or one of a number of smaller, portable units.

• Condensed Matter and Radiation Sciences

Ion Implantation Facility—The facility consists of a 200-keV ion implanter with specialized ultrahigh vacuum chambers and associated *in situ* specimen analysis instrumentation. The facility is used to develop advanced surface treatments of materials to modify their properties and improve corrosion and wear resistance.

3-MeV Tandem Van de Graaff—This facility is used to study charged particle radiation damage effects such as occur in space, to perform Rutherford backscattering spectroscopy and nuclear reaction analysis to provide high-sensitivity composition depth profiles, and to perform MeV energy implants in materials.

60-MeV Electron Linear Accelerator (LINAC)—The LINAC produces intense electron beams with 10 to 65 MeV energies. Pulse rates from 1 to 360 s and widths from 50 ns to 1.4 ms are selectable. This facility is widely used to study radiation effects on microelectronics and materials

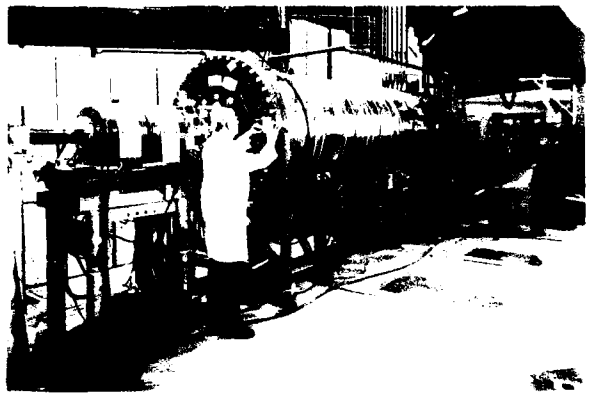

Bob Gossett working near the 3 MeV Tandem Van de Graaff accelerator

for both NRL and other important DoD satellite and missile programs. It is also used to study radiation effects on the new, high-critical-temperature superconductors. Single beam pulses can be analyzed and stored in a fast multichannel digitizer system.

Hypervelocity Impact Facilities—Three facilities are used for ballistics research at speeds exceeding 6 km/s with toxic or explosive targets. The projectile velocity, orientation, and dynamic projectile-target interaction can be measured.

Synchrotron Radiation Facility—An intense monochromatic X-ray photon source, tunable from 10 eV to 12 keV, is available on the NRL-developed beam lines at the National Synchrotron Light Source at Brookhaven National Laboratory. Environmental target chambers can span a pressure range from ambient to several hundred kbar and temperatures from 10 to 1500 K. A six-circle computer controlled goniometer is used to control and position targets.

• Plasma Physics

The Plasma Physics Division is the major center for in-house Navy and DoD plasma physics research. The division conducts a broad experimental and theoretical program in basic and applied research in plasma physics, which includes laboratory and space plasmas, pulsed-power sources, intense electron and ion beams, atomic physics, laser physics, and numerical simulations. The facilities include an extremely high-power laser, PHAROS III, for the laboratory simulation of space plasmas and high-latitude nuclear explosion effects studies. The division has developed a variety of pulsed power sources to

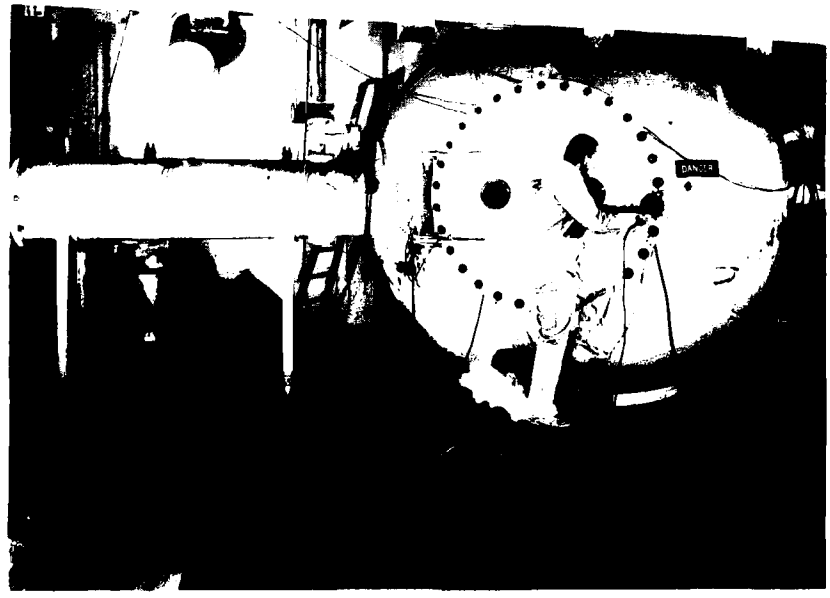

The 12-foot diameter hypervelocity impact chamber can withstand a blast from 20 lbs of TNT

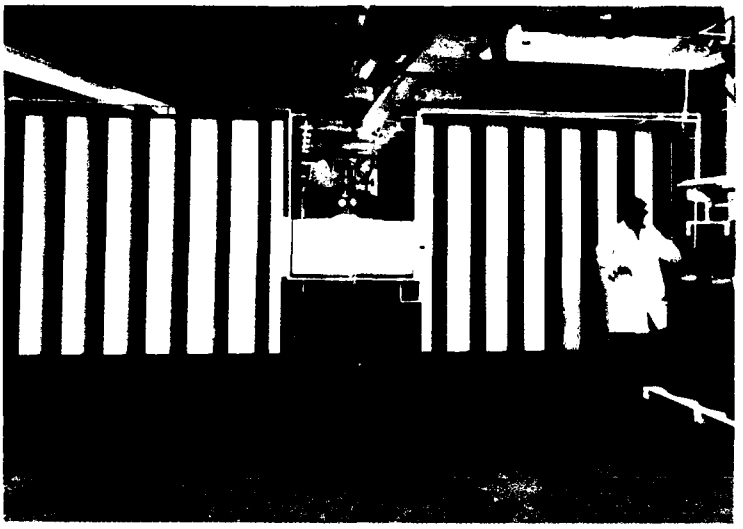

The ZFX Power Generator is a 350-kJ pulsed-power generator capable of driving up to 2 MA in 630 ns into a 100-nH load

generate electron and ion beams, powerful discharges, and various types of radiation. The largest of these pulsers, GAMBLE II, is used to study the production of megampere electron beams and for producing very hot, high-density plasmas. Other generators are used to produce particle beams that are injected into magnetic fields and/or cavities to generate intense microwave pulses. A charged-particle-beam (CPB) propagation facility exists for testing advanced CPB propagation (both endo- and exoatmospheric) concepts. A 5-MW generator injects pulses of electron current into preheated ionization channels to study the effectiveness of propagation under various conditions. This division also operates a modified betatron facility for studying methods to accelerate high-current electron beams to energies in the 25- to 50-MeV range.

- Acoustics

NRL's facilities in support of acoustical investigations are located at the main Laboratory site and in Orlando, Florida, at the Underwater Sound Reference Detachment (USRD). At the main Laboratory site, there are two research tanks instrumented to study echo characteristics of targets and to develop devices. There is also an underwater acoustic holography facility for

NRL's P-3 aircraft configured for Global Positioning System (GPS) interferometric navigation airborne gravity measurements

research in acoustic fields and a water tunnel having a large blow-down channel with a 15-m test section used for acoustic and flow-induced vibration studies of towed line arrays and flexible cables. NRL is investigating dynamic GPS interferometric navigation to extend the capabilities of their fixed-wing airborne gravity measurement system, which is accurate to better than 3 mGal (3×10^{-5} m/s^2), to operation over land. In addition to providing the accurate positioning necessary for airborne gravimetry, GPS interferometric altimetry, in conjunction with radar altimeters, may be used in the future to study oceanographic phenomena and to obtain accurate ice profiles in glaciated parts of the world. The

Connection Machine, an experimental facility that exploits the natural computational parallelism inherent in data-intensive research problems, has been established for use by researchers both within and outside the Laboratory. The USRD facilities are described with NRL's field stations.

• Radar

NRL has gained worldwide renown as the "Birthplace of Radar" and has maintained its reputation as a leading center for radar-related research and development for a half century. An impressive array of facilities managed by NRL's Radar Division continues to contribute to this reputation. These include land-based, airborne, and laboratory radar cross section measurement systems; an airborne APS-116 radar with ISAR image processing; and an airborne adaptive array laboratory. Also, the division manages and maintains a radar display test bed, an IFF ground station, a digital signal processing facility, a digital image processing laboratory, and a radar cross section prediction facility. A radar research and development activity is located at the Chesapeake Bay Detachment (CBD), Randle Cliff, Maryland. It has separate facilities for specific types of systems that range from high-frequency, over-the-horizon systems to millimeter wave radars. The SENRAD radar test bed, a flexible and versatile system for demonstrating new developments in radar, is also located at CBD.

• Information Technology

The Information Technology Division, which includes the Navy Center for Applied Research in Artificial Intelligence, is at the forefront of DoD research and development in telecommunication, computer science, and artificial intelligence. The division maintains a local area computer network to support its research.

The network comprises a Gould 9005 UNIX machine, Symbolics, LISP machines, SUN and Apollo workstations, laser printers, network gateways, and terminal servers. A Butterfly 128-node parallel processor is also part of the division's computer resources. The network is connected to NRL's Central Computing Facility and to the MILNET, ARPANET, and other university networks. The network will become part of the Strategic Defense Initiative (SDI) Battle Management Technology validation facility.

• Electronic Warfare

The scope of research and development at NRL in the field of electronic warfare covers the entire electromagnetic spectrum, from basic technology research, component and subsystem development, to system design and effectiveness evaluation. Major emphasis is placed on providing the methods and means to counter enemy hostile actions in all battle phases, from the beginning—when enemy forces are mobilized for an attack—through the final engagement stages. For this purpose, NRL has constructed special research and development laboratories, anechoic chambers, and facilities for modeling and simulating. NRL is also in the process of adding extensive new facilities where scientists can focus on the coordinated use of all organic defensive and offensive resources now present in the Fleet.

Building 210 houses the Tactical Electronic Warfare Division. Here an antenna range is shown on the roof, and a wind tunnel and simulated ship mast are shown on the left-hand side of the building.

• Laboratory for Structure of Matter

The Laboratory investigates the atomic arrangement of matter to improve old materials or to invent new materials. Various diffraction methodologies are used to make these investigations. Subjects of interest include the structural and functional aspects of energy conversion, ion transport, device materials, and physiologically active substances such as drugs, antibiotics, and antiviral agents. Theoretical chemistry calculations are used to complement the structural research. A real-time graphics system aids in modeling and molecular dynamics studies.

• Center for Bio/Molecular Science and Engineering

The Center for Bio/Molecular Science and Engineering conducts research in biotechnology aimed at solutions of Navy and Department of Defense problems. Long-term research directions focus on complex biomolecular systems and are aimed at gaining a fundamental understanding of the structures and functions of biologically derived systems. The staff of the Center is an interdisciplinary team performing basic and applied research in a number of diverse areas including biochemistry, biophysics, synthesis, and thin-film fabrication. Because of the interdisciplinary nature of this work, most of the research being performed in the Center is of a collaborative nature. The Center Associate concept is a key way of establishing this collaboration. Center Associates come from other research areas within NRL as well as universities, industry, and other Government laboratories.

• Chemistry

NRL has been a major center for chemical research in support of Navy operational requirements since the late 1920s. The Chemistry Division continues its tradition with a broad spectrum of basic and applied research programs concerned with fuels and combustion, corrosion, advanced polymeric materials, ultrasensitive detection methods for chemical agents, and special materials for electronic warfare applications. Modern facilities for research include a wide range of the most modern optical, magnetic, and ion-based spectroscopic devices, a 325-m^3 (11,400 ft^3) fire research chamber (Fire I), multiple facilities for materials synthesis and physical/chemical characterization, high- and low-temperature equipment, and extensive surface-analytical instrumentation. The division has recently developed the 475-ft ex-*Shadwell* (LSD-15) into an advanced fire research ship.

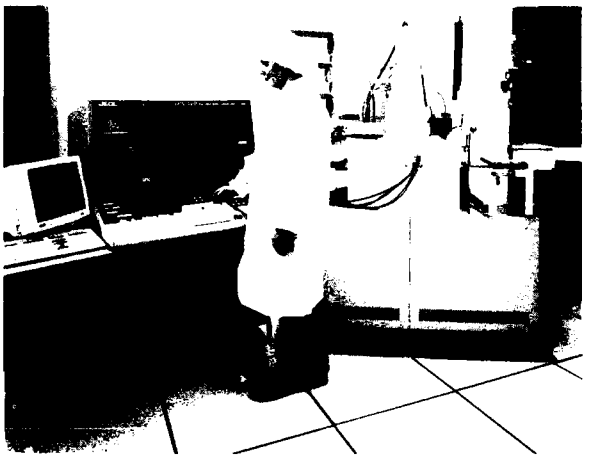

The JEOL-5D II electron beam lithography system is capable of writing patterns with linewidths smaller than 50 nm

• Materials

NRL has capabilities for X-ray and electron diffraction analysis and for electron and Auger spectroscopy. It has a secondary ion mass spectrometer for surface analysis that significantly extends the diagnostic capability of the technique. A high-resolution, reverse-geometry mass spectrometer is used to probe reactions between ions and molecules. The Laboratory has a fully equipped fatigue and fracture laboratory, a modern vacuum arc melting furnace for reactive metals, an ultrasonic gas atomization system for making metal powders, and hot isostatic press facilities. The Laboratory's cryogenic facilities include dilution refrigerators and superconducting magnetic sensors for measuring ultrasmall

magnetic fields. Also available are two molecular beam epitaxy devices for growing thin films.

• Optics

Ultralow-Loss, Fiber-Optic Waveguides—NRL has developed record-setting ultrahigh transparency infrared waveguides. These fluoride glass materials offer the promise of long-distance communications without the need of signal amplification or repeaters.

Focal Plane Evaluation Facility—This facility has extensive capabilities to measure the optical and electrical characteristics of infrared focal plane arrays being developed for advanced Navy sensors.

IR Missile-Seeker Evaluation Facility—This facility performs open-loop measurements of the susceptibilities of infrared tracking sensors to optical countermeasures.

Large Optic, High-Precision Tracker—NRL has developed a tracker system with an 80-cm primary mirror for atmospheric transmission and target signature measurements. By using a quadrant detector, the servo system has demonstrated a 12-mrad tracking accuracy. An optical correlation tracker system tracks objects without a beacon.

High-Energy Pulsed Hydrogen Fluoride, Deuterium Fluoride Laser—NRL has constructed a pair of pulsed chemical lasers each capable of producing up to 30 J of laser energy at 2.7 to 3.2 mm and 3.8 to 4.5 mm in a 2-ms pulse. This facility is used to investigate a variety of research areas including stimulated Brillouin scattering, optical phase conjugation, pulsed laser amplification, propagation, and beam combining.

Fiber-Optics Sensors—The development and fabrication of fiber-optic sensor concepts, including acoustic, magnetic, and rate-of-rotation sensors, are conducted in several facilities within the Laboratory's Optical Sciences and Acoustics Divisions. Equipment includes facilities for evaluating optical fiber coatings, fiber splicers, an acoustic test cell, a three-axis magnetic sensor test cell, a rate table, and various computers for concept analysis.

Digital Processing Facility—This facility is used to collect, process, analyze, and manipulate infrared data and imagery from several sources.

Emittance Measurements Facility—NRL routinely performs measurements of directional hemispherical reflectance from 2 to 16 mm in the infrared by using a diffuse gold integrating sphere and a Fourier Transform Spectrophotometer (FTS). Sample temperatures can be varied from room temperature to 250°C and incidence angles from 0° to 60°.

• Electronics Science

In addition to specific equipment and facilities to support individual scientific and technology programs in electronics and electronic-materials growth and analysis, NRL operates two major central facilities that provide services to electronics programs throughout the Laboratory and to external organizations. The latter two facilities are the nanoelectronics processing facility and the high magnetic field facility.

Nanoelectronics Processing Facility—This facility provides support for NRL programs that require microelectronics processing skills and equipment. The facility recently acquired a nanowriter that fabricates nanoscale (80 Å) structures and, in general, supplies NRL programs with a range of items from discrete structures and devices to complete integrated circuits with very large scale integration (VLSI) complexity based on silicon metal oxide semiconductors (MOS) submicrometer technology.

High Magnetic Field Facility—This facility is used to support research projects throughout NRL, DoD, and, to a limited extent, the local scientific community. The facility provides the capability to determine the response of materials and devices to high magnetic fields up to 17 T with a variety of electrical, optical, and magnetic probes.

Dr. Randall P. Shumaker is the acting Superintendent of the Information Technology Division at NRL. Prior to this assignment, he was director of NRL's Navy Center for Applied Research in Artificial Intelligence. Dr. Shumaker has wide experience in computer science and digital electronics, with particular interests in computer languages, digital control, and artificial intelligence.

Dr. Homer W. Carhart, Director of the Navy Technology Center for Safety and Survivability, spearheads highly active Navy R&D programs particularly in the areas of damage control, fire and chemical warfare protection, and fuels and enclosed atmospheres. He and his group introduced into the Fleet items such as firefighting foams, dry chemicals, improved and safer fuels, the Naval Firefighters Thermal Imager (NFTI), submarine atmosphere control, insulations, and HALON simulants. They have also developed nitrogen pressurization for extinguishing fires in enclosed spaces.

Mr. Robert E. Eisenhauer, Superintendent of the Space Systems Development Department, leads the Naval Center for Space Technology's research and development team in the development of advanced spacecraft data collection, data management systems, onboard data processing, and communication systems. He also heads the development of C^3 systems in support of the Navy's space program.

Dr. Warren E. Pickett, head of the Electronic Structure Section of the Complex Systems Theory Branch, is involved in research on the copper-oxide high-temperature superconductors and on diamond films. A Fellow of the American Physical Society, he has been a pioneer in the application of supercomputers to theoretical studies of superconductivity, magnetism, and bandgaps in crystalline solids.

• Naval Center for Space Technology

In its role as a center of excellence for space systems research, NRL establishes and supports the development of spacecraft, systems that use these spacecraft, and their ground command and control stations. The Naval Center for Space Technology (NCST) designs, builds, analyzes, tests, and operates spacecraft, as well as identifies and conducts promising research to improve spacecraft and their support systems. NCST facilities that support this work include large and small anechoic radio frequency chambers, clean rooms, shock and vibration facilities, an acoustic reverberation chamber, large and small thermal/vacuum test chambers, and modal analysis test facilities. NCST has a 31-m, computer-controlled wind and wave tank and special airborne instrumentation for developing electromagnetic remote sensing systems; a facility for long-term testing of satellite clock time/frequency standards under thermal/vacuum conditions linked to the Naval Observatory; a 5-m optical bench laser laboratory; and a hologram research laboratory to conduct research in support of the development of space systems.

• Center for Advanced Space Sensing

The Center for Advanced Space Sensing conducts a broad program in sensing applications at wavelengths from radio to optical. This program includes space experiments, radio, IR, and optical astronomy using ground based facilities operated by the Center of national facilities (such as the Very Large Array of the National Radio Astronomy Observatory) and relevant technology applications to remote sensing, precise tracking, navigation, and imaging. To accomplish these programs, the Center operates Maryland Point Observatory, which consists of 84- and 85-ft radio antennas, which are used primarily for Very Long Baseline Interferometry (VLBI) and background environmental emissions at radio wavelengths. For the processing of VLBI data, the Center is a partner in the Washington, DC, Correlator Facility. For actively illuminated objects at radio wavelengths, the Center has a SAR image processing facility consisting of high-density digital recorders, super minicomputers, and software to process images. The Center is also developing space based sensor technology. The Middle Atmosphere Sounder is a limb-scanning microwave spectrometer designed to fly on the space shuttle. At optical wavelengths, an interferometer capable of precision measurements of the size and positions of celestial objects is operated on Mount Wilson, California. To satisfy the computing needs generated for image processing and other data processing needs, the Center has an Alliant VFX-40 visualization graphics supercomputer.

Research Support Facilities

• Technical Information Services

The Ruth H. Hooker Technical Library contains more than one million items including 1700 current journals. Its collections can be searched by computer-based catalogs. The Library also provides interlibrary loans, on-line literature searches, access to CD ROM databases, loans of microcomputer software, and a full range of reference services, including assistance in selecting and using microcomputer software.

Publication services include writing, editing, composition, phototypesetting, and publications consultation. The primary focus is on using computer-assisted publication techniques to produce scientific and technical information containing complex artwork and equations.

The diversity of the research conducted at NRL requires a corresponding diversity of graphic support, such as technical and scientific illustrations, computer graphics, design services, photographic montages/composites, airbrushing/photographic retouching, calligraphy, display panels, and framing.

Photography services include motion picture, video, and still-camera coverage for data documentation both at NRL and in the field.

The ribbon-cutting ceremony officially opening the Microcomputer Software Support Center located in the Technical Information Division's Library. Shown are Mr. Dennis Blakey, center manager, Ms. Laurie Stackpole, NRL's head librarian, and CAPT John Donegan, Commanding Officer.

Information specialists prepare written and visual materials for dissemination to the public, for use at exhibitions, professional meetings and seminars, and for internal information.

The DICOMED computer graphics system produces high-resolution, high-quality color images on 35-mm slides, 8 × 10 in. viewgraphs, 16-mm movies, or microfiche. It is driven by tapes generated on many different computer systems.

• Central Computing Facility

The Central Computing Facility (CCF) consists of a Cray X-MP/24 Class 6.5 supercomputer supported by five DEC/VAX 700/8000 front-end processors. The Class 6.5 supercomputer is a balanced vector and a very high-speed scalar processor. The peak processing speed of the two processor Class 6.5 supercomputers is 488 million floating point operations per second (MFLOPS) with a sustainable speed of 105 MFLOPS per processor. It has four million (64-bit) words of static MOS memory in sixteen interleaved banks, and three interconnected I/O processors with four million words of shared buffer memory.

The Class 6.5 system is accessed by VAX minicomputers at the central computing site, by local area networks, by the Defense Data Network (MILNET/ARPANET), and by SURANET/NSFNET at remote sites. The front-end systems recognize and exploit the features of typical modern terminals whether they are connected by dial-up, direct line, local area networks, or DDN/MILNET. It also provides database management, document processing, and graphics support. FORTRAN, PASCAL, C, and ADA are the primary programming languages for the Class 6.5 system. A wide range of scientific, statistical, and mathematical software is also available. MAC NASTRAN and ABAQUS are available on the Cray. PATRAN and ABAQUS are available on the front ends.

A high-quality, high-performance pen plotter and a high-speed electrostatic plotter/printer are available. Plots can also be previewed on graphics terminals. Plotting software can generate tapes for the DICOMED system, located in the Technical Information Division.

FIELD STATIONS

NRL has acquired or made arrangements over the years to use a number of field sites or auxiliary facilities for research that cannot be conducted in Washington, DC. They are located in Maryland, Virginia, California, Colorado, Alabama, and Florida. The two largest facilities are the Chesapeake Bay Detachment (CBD) and the Underwater Sound Reference Detachment (USRD).

• Chesapeake Bay Detachment (CBD)

CBD occupies a 168-acre site near Chesapeake Beach, Maryland, and provides facilities and services for research in radar, electronic warfare, fire research, optical devices, materials, communications, and other subjects. Because of its location on the west shore of the Chesapeake Bay, unique experiments can be performed. Radar antennas 50 to 60 m above the water overlook the bay. Another site, Tilghman Island, is 16 km across the bay from CBD and in a direct line of sight from CBD. This creates a unique environment for low clutter and generally

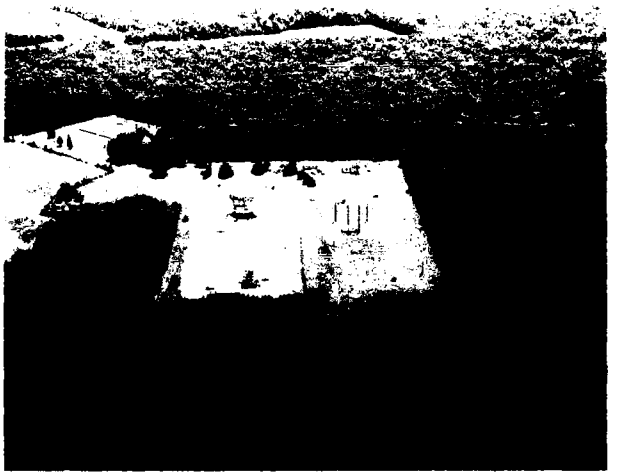

Satellite Tracking and Calibration Facility located in Pomonkey, Maryland

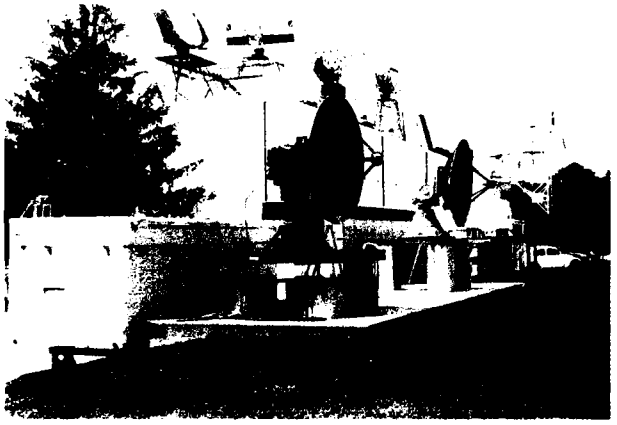

The Radar Division's test site, Building 75, at the Chesapeake Bay Detachment, Chesapeake Beach, Maryland, showing antennas used in experimental radar development

The Midway Research Center (MRC) Space Tracking Facility, Stafford, Virginia

low background radar measurements. Experiments involving dispensing chaff over water and radar target characterizations of aircraft and ships are examples of military-oriented research. Basic research is also conducted in radar antenna properties, testing of radar remote sensing concepts, use of radar to sense ocean waves, and laser propagation.

- Underwater Sound Reference Detachment (USRD)

Located at Orlando, Florida, USRD functions as a link in the traceability of underwater sound measurements to the National Institute of Standards and Technology and also performs R&D for sonar transducers and related acoustic materials. Its semitropical climate and two clear, quiet lakes (the larger 11-m deep and nearly circular) are distinct assets to its research and development on sonar transducers and underwater reference standards and to its improvement of techniques to calibrate, test, and evaluate underwater acoustic devices. USRD has an anechoic tank for simulating ocean depths to approximately 700 m and smaller pressure tanks for simulating depths to approximately 7000 m. A spring-fed lake, located in a remote area about 40 miles north of USRD (the Leesburg Facility), provides a natural tank for water depths to 52 m with an ambient noise level 10 dB below that for sea state zero; larger objects can be calibrated here. The detachment has provided acoustic equipment and calibration services not only to hundreds of Navy activities and their contractors but also to private firms and universities not engaged in DoD contracts.

- Marine Corrosion Test Facility

Located on Fleming Key at Key West, Florida, this facility offers an ocean air environment and clear, unpolluted, flowing seawater for studies of environmental effects on materials. Equipment is available for experiments involving weathering, general corrosion, fouling, and electrochemical phenomena, as well as coatings, cathodic protection devices, and other means to combat environmental degradation.

- Flight Support Detachment (NRL FSD)

Located on the Naval Air Station Patuxent River at Lexington Park, Maryland, NRL FSD provides facilities and service for airborne research. Four P-3 variant aircraft are maintained and operated by NRL and Detachment personnel.

- Other Sites

Some field sites have been chosen primarily because they provide favorable conditions to operate specific antennas and electronic subsystems and are close to NRL's main site. Maryland Point, south of NRL, operates two radio telescopes (25.6 and 26 m in diameter) for radio astronomy research. NRL's Waldorf Facility, south of NRL, operates 18.3-m, X-band and S-band antennas for space and communications research. Pomonkey, a field site south of NRL, has a free-space antenna range to develop and test a variety of antennas. The antenna model measurement range in Brandywine, Maryland, has a 4.6-m diameter turntable in the center of a 305-m diameter ground plane for conducting measurements on scale-model shipboard and other antenna designs.

- Research Platforms

NRL uses ships and aircraft to conduct some of its research. For airborne research, NRL uses four four-engine turboprop P-3 Orion aircraft, which are maintained by the Flight Support Detachment at the Patuxent River Naval Air Station, Maryland. These airplanes annually log over 2000 hours of flying time on a wide variety of projects ranging from bathymetry and electronic countermeasure research to studies of radar signal reflections. Oceangoing research ships are obtained from a pool of vessels maintained by the Naval Oceanographic Office, Bay St. Louis, Mississippi.

NRL in the Future

To continue its growth and provide preeminent research for tomorrow's Navy, NRL must maintain and upgrade its scientific and technological facilities at the forefront. Its physical plant to house these facilities must also be adequate. NRL recently embarked on a Corporate Facilities Investment Plan (CFIP) to renew its physical plant. This plan and future facility plans are described below.

THE CORPORATE FACILITIES INVESTMENT PLAN (CFIP)

The CFIP is a financial spending plan to provide modern research facilities at NRL by the year 2000. The plan calls for both Congressional and Laboratory investment and is updated and altered as changes occur in scientific emphasis and congressional attitude. Over the past several years, congressionally approved military construction (MILCON) funds were used to construct the new Electro-Optics laboratory and to complete the final phase of the Tactical Electronic Warfare facility. At this time, funds are being requested to build a second wing to the Electro-Optics building and a facility to house the Naval Center for Space Technology.

In the past years, NRL general and administrative (G&A) funds were used to renovate Buildings 16, 32, 34, 35, 46, 47, 56, 58, and major portions of several other buildings. Approximately $4 million of Laboratory funding is budgeted for modernization each year.

- Vacuum Ultraviolet Space Instrument Test Facility

The Space Science Division will soon install a new vacuum ultraviolet space instrument test facility. This facility will be capable of housing space instrumentation up to 2 m in diameter and 5 m in length. While exposed to high vacuum (10^{-7} torr), instruments can be illuminated by a simulated solar spectrum for alignment and verification tests. The facility will also include a 13-m evacuated extension containing sources to simulate the solar corona. An externally mounted 1-m diameter heliostat will be employed to project a beam from the sun directly into the vacuum chamber. In the near future, the facility will be used to test space instruments that are presently under development for flight on NASA's Orbiting Solar Laboratory spacecraft and European Space Agency's Solar and Heliospheric Observatory spacecraft. The facility will be fully operational in 1991.

- Plasma Physics Facilities

A major, 2-kJ krF-laser facility will be established in the Plasma Physics Division by the end of FY 93. This facility is being initiated to provide intense radiation for studying inertial confinement fusion target heating at short wavelengths. A new 3-MJ, 10-MA pulsed-power facility, Rook, is being constructed for inductive energy storage research and should be ready in the FY 90-91 time frame.

- Center for Materials Research

The Department of the Navy is in the process of programming construction of a special-purpose laboratory. This special facility will provide stringently clean laboratories with carefully controllable temperature, humidity, vibration isolation, ambient dust, and power for investigations in the rapidly evolving fields of electronic technology and nanometrics.

- Offboard Countermeasures Wind Tunnel

A wind tunnel facility has been developed to permit the study of the flowfield around various bodies of interest and the resulting force and moment data on the body. The facility provides a test environment for dynamic testing of deployment systems and propulsion devices. It is specially suited to the study of subsonic low Reynolds number aerodynamics because of its low

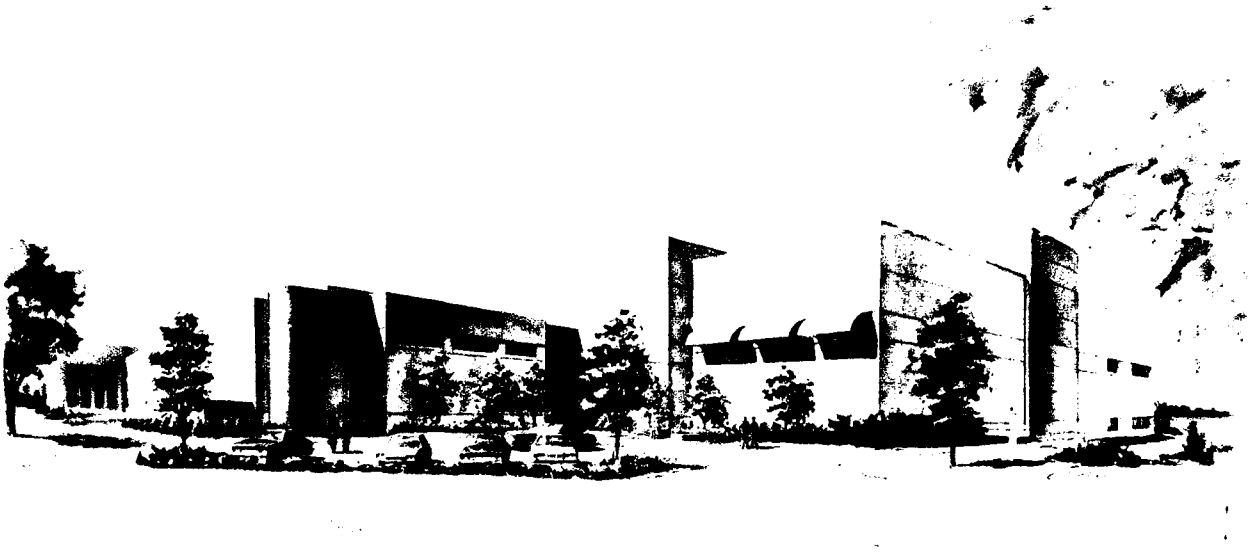

Artist's concept of the Optical Sciences Division's Electro-optic Laboratory. Phase II construction is planned for fiscal year 1991.

turbulence intensity. The tunnel speed range is 50 to 200 knots for aerodynamic testing and 50 to 160 knots for propulsion testing.

- EW Scale Model Analysis Facility (SMAF)

The newly completed addition to NRL's TEWD Building 210 includes an anechoic chamber with radar-source analogs operating in the submillimeter range. The radar cross sections (RCS) of objects can be studied here by means of physical scale models in which the target and environment are reduced in size by some convenient scaling factor. For a mid-X-band base frequency, scaling ratios of from 70:1 to 200:1 can be produced. Ratios in this range are well suited to the study of ship and ship-system RCS. Both phase and amplitude of scatterers can be determined as a function of polarization. The facility will provide analysis capabilities ranging from the identification and characterization of individual scatterers to the measurement of full target illumination with multipath.

The SMAF chamber is a class 10,000 clean room with a high degree of vibration isolation and environmental control.

This special facility is expected to become operational during the first half of FY 90.

- Midway Research Center

NRL's newest field site, the Midway Research Center (MRC), is located on a 158-acre site in Stafford County, Virginia. Located adjacent to the Quantico Marine Corps Base, the MRC consists of a 5000 ft^2 operations/administration building and two of three programmed 60-ft diameter parabolic antennas housed in 100-ft radomes. The third MRC antenna is scheduled for construction in the 1990-91 time frame. When completed, the MRC, under NRL Code 8000, will provide NRL with a state-of-the-art facility dedicated solely to space communications and research.

- Electronics Science and Technology

An enhanced effort in narrow energy gap semiconductors has been initiated, and a new molecular beam epitaxy (MBE) machine has been received for this program. In collaboration with the Materials Science and Technology Division, this program will be broadened to include other electronic materials by acquisition of a second

MBE, which will be linked to the first. Continued improvement of the Nanoelectronics Processing Facility will include greater capability in the processing of GaAs and fabrication of nanoscale (80 Å) structures with the Division's acquired nanowriter. A recently acquired scanning tunneling microscope (STM) is being used to characterize nanostructures.

• Fire Research Facility

Construction is under way at the Fire Research Facility at CBD to expand the current facilities. Once completed the facility will have a 50 × 50 × 50-ft burn building with an attached control center, three lab/office complexes of about 2500 ft^2 each, and a new, large, concrete minideck (to simulate air-capable ship decks) for expanded large-scale fire-fighting studies. FIRE-I, NRL's 325-m^3 (11,400-ft^3) pressurizable fire research chamber, is being relocated to this site.

• Radar Mode Test System

The Radar Division has acquired the Radar Mode Test System to evaluate the performance of NATO compliant Mark XI IFF radar mode (RM) equipment. It has been used to test equipment from the United Kingdom and will have application to the evaluation of NRL- and contractor-developed RM equipment

REHABILITATION OF SCIENTIFIC FACILITIES

Specialized facilities are being installed or upgraded in several of the research and support divisions.

• Information Technology

An expanded computer/communication network is being implemented that will provide each researcher in the division with an office workstation (SUN, Apollo, or equivalent) connected to all the major scientific networks. Special test facilities are also being planned in support of specific R&D tasks. Facilities to support human-computer interaction research include an eye-monitoring system, touch screens and tablets, speech I/O hardware, high-resolution graphic displays, a 6-D tracker, a wall-sized display, and time-stamped video and audio recording equipment for monitoring experiments. An information security testbed is being planned to enable the interconnection of communication security and computer security devices to address network and system security problems.

• Plasma Physics

An inductive energy storage facility, PAWN, is being upgraded to increase the output power from 0.1 up to as much as 1.0 terawatt. This facility will be more than an order of magnitude more compact than similar generators when final development stages are completed. PAWN will be used for intense electron and ion beam generation research and in X-ray laser development. A low-frequency (300 MHz to 10 GHz), high-power microwave facility, which uses a relativistic klystron concept, is being upgraded to produce multigigawatt coherent radiation pulses. A new laser facility is also planned. It will use a powerful KrF laser and a target chamber to conduct inertial confinement fusion research.

• Engineering Services

An advanced technology and fabrication facility is being planned. It will be used to study fabrication methods by using new and/or unusual materials, processes, and techniques (such as powdered-metal mixtures, ion implantations, various composites, and laser machining of composites) developed by NRL research divisions or other Navy laboratories. Longer range plans call for new machines—both computer-controlled drives by our new computer-aided device/computer-aided manufacture (CAD/CAM) system, and human-controlled drives with enhanced precision capability using new and unusual material fabrication.

• Radar

The Radar Division has installed a computer-aided engineering (CAE) facility to aid in digital system design. The system has seven full-color graphics workstations to provide capabilities for circuit design and simulation and printed circuit board layout. The facility has been used to design systems based on commercially available components as well as advanced systems incorporating VHSIC and gate array technologies. It has proven to be a valuable tool in evaluating new technologies for radar signal-processing requirements. The facility is currently being expanded to include three SUN workstations and ADAS software, which will allow designs to be modeled and simulated at the system level. Future plans call for acquiring VHDL (VHSIC Hardware Description Language) software for the workstations, which is supported by ADAS. This would provide designers with an integrated toolset to model and simulate their designs from the system level down to the device level.

• Acoustics-Target Research Tank

Tank facilities for acoustic target research in the Acoustics Division will be significantly expanded to extend the range of target sizes. The expanded model tank is planned to contain a water volume of approximately 30,000 m^3.

• High-Pressure Acoustic Test Facility

A new tank facility at NRL's Underwater Sound Reference Detachment (USRD) in Orlando, Florida, will be used for underwater acoustic-materials research, development, test, and evaluation of much larger objects at significantly increased pressures and lower frequencies. This new tank is patterned after the smaller, lower pressure anechoic tank that has been used to develop virtually every submarine and torpedo transducer in the Fleet today. It will be operational in 1991 and will simulate ocean depths to 2100 m.

• Materials Science and Technology

Renovation is proposed for Building 3, which is now made up of two of the original five buildings at NRL, to contain modern laboratories for studies of thin film deposition and characterization, superconducting materials, magnetic materials, and other materials science projects. The new space will feature the most modern molecular beam epitaxy and other materials synthesis and processing equipment, an up-to-date fatigue and fracture laboratory and state-of-the-art diagnostic equipment, including electron microscopes, spectrometers, and electron and X-ray diffraction equipment. The renovated building will also contain a modern conference and meeting room facility, as well as offices for the MS & T Division's administrative staff and office and laboratory space for approximately 70 technical personnel.

Further Information: The NRL *Fact Book* gives more details about the Laboratory and its operations. It lists major equipment, current fields of research, field sites, and outlying facilities. It also presents information about the responsibilities, organization, key personnel, and funding of the divisions, detachments, and other major organizational units.

Information on the research described in this *Review* may be obtained by contacting Dr. George Abraham, Head, Technology Transfer and Special Programs, Code 1003.2, (202) 767-3744. General information about NRL may be obtained from Information Services, Code 4810, (202) 767-2541. The sources of information on the various nonresearch programs at NRL are listed in the *Review* chapter entitled "Programs for Professional Development."

HIGHLIGHTS OF NRL RESEARCH IN 1989

Mount Wilson Optical Interferometer

The imaging capabilities of interferometry at optical wavelengths have been demonstrated by successfully fabricating a variable 4- to 34-m baseline addition to the Mount Wilson Optical Interferometer. This provides knowledge of the diameters of many giant and supergiant stars and the precise orbits of close binary stars. The result of long baseline optical interferometer technology is the development of an instrument to image stars with an angular resolution four orders greater than is now accomplished with ground-based observations.

***

Progress in the Development of the Modified Betatron Accelerator at NRL

The lifetime of the circulating electron beam in the NRL modified betatron has substantially increased from a few microseconds to ≥ 700 μs by adding strong focusing windings to the device. The beam acceleration has been confirmed not only by the X-ray attenuation technique but also with the detection of photoneutrons from the reaction $D(y,n)H$. Experiments are in progress to locate and eliminate the field error(s) that excite the resonances and thus to accelerate the electron ring to even higher energy.

***

Wide-Area Rapid Acoustic Predictions (WRAP) Research Program

The unified wave field theory research program has developed new algorithms incorporating eigenvalue and nonlinear signal processing methods into their previously developed wave acoustics techniques. With its new range-dependent, surface-noise model, the present capability is evolving into a full-scale numerical laboratory for studying the complete problem of extracting signals masked in partially coherent noise in a complex ocean. An important recent outgrowth of this research is the new concept of environmental symmetry breaking, i.e., the ocean itself can be used as an integral part of a signal processing aperture by taking advantage of known anisotropies of the environment.

***

VHSIC Technology Digital Sidelobe Canceler Development

Radar in a wartime scenario must contend with enemy jamming interference that is intentionally directed at the receiving antenna and that enters the antenna sidelobes. Adaptive cancellation techniques have long offered the potential for greatly reducing the adverse effects of sidelobe jamming on radar performance. The Radar Division is significantly advancing the state-of-the-art in jammer suppression with sidelobe cancellers technology.

***

Microlithography

Naval Research Laboratory/Office of Naval Research 6.1 research funds, aided by Office of Naval Technology, Defense Advanced Research Projects Agency, and, most recently, MANTECH support, enabled NRL to develop a technique for lithography capable of 0 25-μm resolution. The work has been licensed by the Shipley Company with sizable royalty payments to NRL and the inventors. NRL and the Shipley Company signed a Cooperative Research and Development Agreement to further develop the lithographic technique. The expertise of the Microelectronic Fabrication Facility and the Bio/Molecular Science and Engineering Center, combined with Shipley's expertise in photoresist fabrication and metallization, provide the necessary resources to bring the technology from the laboratory to the manufacturing environment.

***

Chaos in Solid State Systems

The quantification of spin-wave chaotic trajectories in yttrium iron garnet (YIG) spheres took a major step forward with the calculation of the Lyapunov exponents of both the transient chaos and the permanent chaos as a function of the driving radio frequency (RF) field. The functional dependence of the exponents on the RF field resembled the simple case of period-halving cascades in simple maps above the threshold for chaos, suggesting that such a phenomenon is occurring in bulk YIG. These calculations also show, for the first time, that it is possible to extract meaningful Lyapunov exponents from experimental data on chaotic transients.

***

Fly's Eye Program

The Fly's Eye program has, for the first time, verified an IR threat warning system. The Naval Research Laboratory has developed a data measurements sensor that has been used to obtain a unique set of ground-based and airborne data to test an NRL- developed algorithm. The results of the data analysis show that the staring IR threat warning system has a high probability of detection and a low false alarm rate. The staring IR array approach can be implemented in a small sensor with minimal impact on the aircraft and can provide full-aspect, long-range warning of threats to U.S. aircraft.

***

All-Optical Towed Array

A highly successful sea test of the all-optical towed array was completed. This test included new high-scale factor fiber-optic hydrophones and fiber-optic heading, temperature, and depth sensors. The self-noise performance of the new hydrophones surpassed all expectations. Various state-of-the-art fiber-optic sensor multiplexing techniques were demonstrated in the laboratory, including a 10-sensor multiplexed array. This is the largest number of fiber-optic sensors multiplexed to date.

***

Observation of Nuclear Radiation from Soviet Space Reactors

In February 1987, the Soviet Union launched COSMOS 1818. Within a day of its launch, radiation monitors on board NASA's Solar Maximum Mission Satellite (SMM) began detecting clouds of positrons

and electrons. Detection of these particles enabled the power source on COSMOS to be unambiguously identified as a nuclear reactor. This Soviet satellite was one of 18 containing nuclear reactors that were detected by the SMM spectrometer from 1980 to 1988.

***

Numerical Simulation of Three-Dimensional Bluff-Body Near-Wake Instabilities

A finite-difference numerical model has been developed for the three-dimensional simulation of bluff-body near-wake turbulent flows. The model allows the study of the large-scale features of spatially evolving plane wakes. Understanding the evolution and structure of these shear flows has important applications for external flows over bodies such as ships, submarines, torpedoes, and planes.

***

Direct Simulation of Turbulence Near a Free Surface

The incompressible three-dimensional Navier-Stokes equations are solved by psuedospectral methods for a turbulent flow in the vicinity of a free surface. The computational grid is sufficient to allow the resolution of all essential turbulent scales without resort to subgrid models. A large number of turbulence statistics are computed in the vicinity of the free surface, and complete determinations of the balances of the exact Reynolds stress, turbulence kinetic energy, and isotropic dissipation rate equations are reported for the first time. The results show near-surface anisotropic behavior leading to preferential redistribution of the turbulence kinetic energy into the spanwise component of kinetic energy.

***

Development of a New Structural Probe of Thin Films to Determine the Body-Centered Cubic Phase of Epitaxially Grown Cobalt on GaAs

The first extended absorption fine structure study on a thin epitaxial film was carried out by using a new conversion electron technique. Epitaxial cobalt grown on GaAs was shown by this technique to be definitely body-centered cubic, confirming NRL's claim to have grown the first true metastable phase of a magnetic element that is not naturally occurring.

***

Quasi-Optical Gyrotron Research

The quasi-optical gyrotron (QOG) is under development as an efficient, high average power millimeter-wave source for fusion plasma heating and DoD applications. Recent experiments demonstrated tunable operation from 95 to 130 GHz at powers up to 148 kW and efficiencies up to 12% for 20- to 28-cm mirror separation. To demonstrate scaling to higher power, a new experiment with a more powerful (95 kV, 50 A) electron gun and smaller resonator mirrors for increased output coupling (~ 5% at 120 GHz) was set up and tested in FY 89. During initial operation, this device achieved an output power of 320 kW at a frequency of 125 GHz and an efficiency of 10%. A maximum efficiency of 15% was achieved at 160 kW output power.

***

AXSAR, A Target Strength Prediction with Increased Frequency Range

A prediction for acoustic scattering from submerged elastic structures has been developed that is valid for higher frequency than previous models. This model is also valid for axisymmetric structures of otherwise arbitrary geometry, and it includes both the effects of fluid loading and of elastic waves propagating in the structure. The improvements in this model approximately double the low frequency range over which predictions can be made.

***

Radar Display and Distribution System and Ships Sensor Integrated Display and Distribution System (RADDS/SSIDDS)

Conducting certain operations in combat information centers on U.S. Navy ships, other than those using NTDS, are difficult because they are carried out in a noisy, error-prone environment. RADDS and its expanded version SSIDDS have been developed to facilitate handling and to display sensor information—primarily radar—in such a manner as to make such information more usefully available for ship operation and to eliminate many error sources.

***

A Tri-Service Data Item Description (DID) for IEEE/ANSI 1076 Hardware Description Language (VHDL) Documentation

The Naval Research Laboratory provided the leadership and technical expertise to establish a DoD-level DID for the delivery of digital hardware documentation in a manageable, reusable, and understandable format. This effort resulted in the creation of a working document that now has the official designation of DI-EGDS-80811. The DID, which did not exist 2 years ago, is already in place on several important systems contracts generating VHDL deliverables, including the AN/UYS-2 Matrix processor, the Advanced Tactical Fighter, and the Advanced Spaceborne Computer Modules efforts.

***

BaRT—A Bayesian Reasoning Tool

Research has investigated computational schemes for managing uncertainty in target classification problems. This investigation has led to the development of a computer program called BaRT that efficiently and rationally computes the impact of uncertain evidence on target hypotheses. This effort will help reduce the time required to make good judgments and enable decision makers to cope with more complex problems under time constraints.

***

HF Skywave Propagation Through an Artificially Modified Ionosphere

Ionospheric modification by direct chemical injection was used to create a "hole" in the ionosphere. An HF channel probe was used to monitor the effects on HF skywave propagation. Chemicals were transported by a rocket launched from Wallops Island, Virginia, to ionospheric heights, where they were released at an altitude of about 300 km. Results indicate some focusing of the preexisting skywave signal and the sudden appearance of some multipath returns related to the ionospheric disturbance. Changes were subtle and will require further analysis to determine the full extent of the effect.

***

Analysis of a Low-Frequency, High-Powered, Compact Underwater Acoustic Source

The Navy needs a high-power, low-cost, low-frequency expendable acoustic source to be used in an air-deployed, active sonobuoy system. A composite transducer, consisting of a ceramic cylinder encased in a coaxial metal cylinder (both of which have a common axial slot cut through their thickness dimensions), is a possible candidate for this application. A predictive acoustic finite element program was developed as a tool for design optimization, and the results were compared to those obtained experimentally. A predictive model can then be used to examine various materials and geometry configurations to meet design specifications before a prototype is built.

***

Development of an Improved Reliability Submarine Sonar Connector

An improved reliability underwater electrical cable plug, called the Extended Life Portsmouth Connector (EXLPC), has been developed to replace an unreliable underwater cable plug used on sonar systems aboard ballistic missile submarines. This new plug is completely compatible—form, fit, and function—with the plug it replaces; it increases the average service life of the cable plug from 3 years to years.

***

X-ray Characterization of Molecular Structures and Physical Properties of High-Density Explosives and Propellants

The Laboratory for Structure of Matter (LSM) has performed X-ray analyses of 63 new materials synthesized in the ONR-sponsored government, university, and industrial laboratories during FY 89. These analyses provide detailed molecular structures, solid-state properties, and crystal-packing schemes. Among these materials are a number of solid-state complexes of CL-20*, which are expected to have enhanced combustion efficiency compared to CL-20.

***

Explosive-Drive, Water-Filled Conical Shock Tube

Sonar transducers and related components mounted on surface ships and submarines are required to pass an appropriate explosive shock test performed in open water at the West Coast Shock Facility (WCSF). The water-filled conical shock tube that has been developed at the Underwater Sound Reference Detachment of NRL is an inexpensive, rapid-turnaround alternative to the WCSF. It reproduces the WCSF shock test for small devices that can fit into the 15-cm diameter muzzle end of the shock tube. A 50-cm diameter shock tube is being developed for testing larger devices such as submarine spherical array transducers.

***

Atomistic Computational Experiments (ACE)

NRL has developed and validated a large-scale, general code (ACE) for carrying out atomistic simulations of metallurgical systems under conditions corresponding to those of laboratory experiments. NRL has also developed techniques for carrying out constant-pressure molecular-dynamics simulations in

a fashion that can incorporate three-body interactions. These techniques will allow us to perform computational experiments on systems that are not accessible in laboratory experiments and to extract thermodynamic information needed as parameters for large-scale, continuum models. The techniques can further be applied to the study of detailed atomistic mechanisms that are important in interface motion during phase transformations.

***

Infrared Countermeasure Technology Program

An infrared countermeasure technology (IRCM) program was initiated to develop a countermeasure system to defeat advanced missile threats against U.S. tactical aircraft. The program integrates state-of-the-art technologies into a system and demonstrates the capability to defeat a wide class of infrared guided missile threats. The program defines the most effective approach, acquires major subsystems, integrates these subsystems into an aircraft, and defeats a missile in a live-firing demonstration.

***

Diamond and Nondiamond Carbon Growth in Hydrocarbon-Oxygen Flames

The diamond/carbon deposition in an oxygen-acetylene combustion flame has been analyzed over a range of oxygen/acetylene flow ratios R_f and substrate temperatures T_s. Diagrams relating diamond, microcrystalline graphite, and amorphous carbon growth to P_f and T_s have been developed. In addition, the dependences of particle morphology and growth rate on R_f and T_s were examined. Higher quality diamond growth was achieved in an oxygen-acetylene-hydrogen flame. Improvement and control of the diamond nucleation and growth, resulting in single crystal and heteroepitaxial growth, will enable high-temperature and radiation-hardened semiconductor devices to be produced.

***

Efficient Generation of Blue Light by Nonlinear Frequency Conversion of Laser Diode Emission

Blue light was efficiently generated by frequency doubling of AlGaAs laser diode emission at 800 nm and by nonlinear mixing of an Nd:YAG 1064-nm laser emission with the laser diode output. Using a monolithic resonant cavity fabricated in a $KNbO_3$ nonlinear crystal, 65 mW of blue was generated by frequency doubling 240 mW of the infrared fundamental with an optical efficiency of 27%, and 126 mW of blue was generated by sum frequency mixing of 220 mW of laser diode emission with 4.7 W of 1064 nm radiation. Conventional laser sources for generating blue radiation have electrical-to-optical conversion efficiencies of less than 0.1%, which are too low for the application where the power and space available are limited. The blue light developed at NRL has a sufficiently high efficiency and power to make it useful in these applications.

***

Theory of Structural Aging of Compacted Glasses

In many areas of science and technology, glasses are produced in a compacted nonequilibrium state. The structure of the glass subsequently ages and relaxes in time back to its equilibrium state. This influences the properties of the material for processing and applications. The structural aging is a nonlinear process that retains memory of the sample history and processing. For this reason it has been very difficult to

formulate theoretically. Development of an NRL coupling model of relaxation has resulted in quantitive predictions of structural aging of glasses for different sample treatments. Applications have been made to SiO_2 on Si and polymeric glasses.

***

Multimission Advanced Tactical Terminal (MATT) Development

MATT, which is a miniaturized, highly integrated, and modular ultrahigh frequency (UHF) communications terminal, has been developed. MATT incorporates a multichannel and space diversity transceiver, multimode modem, embedded communications security (COMSEC), message processing, and multiple types of user interfaces. The MATT design represents a substantial achievement in miniaturization and packaging. More than four times the capability has been incorporated in approximately one-sixteenth the volume of the existing equipment.

***

Microwave Study of Optical Detection by High-T_c Superconducting Films

A method of investigating light detection by thin films of high-T_c metal oxide superconductors has been developed. This method relies on the change in surface resistance of a sample positioned in a microwave bridge spectrometer when light is absorbed. Since neither contacts nor a complete conductive path are needed, the microwave approach is more flexible and informative than the conventional dc-biased photoconductivity experiments commonly used to study the light detection.

***

Two-Dimensional Modeling of Radar Ocean Surface Signatures Relating to Bottom Topography

The spatially modulated radar cross section for perturbed Bragg resonant waves by M2 tides flowing over a complex bottom topography has been modeled for Phelps Bank, Nantucket Shoals, Massachusetts. The procedure followed is general and applicable to other coastal areas. The numerical computational procedure developed provides a simple and cost-effective means for predicting the two-dimensional ocean surface signatures relating to complex bottom topography near coastal zones. This is the first time the two-dimensional properties of tidal currents have been included in the prediction of radar ocean surface signatures.

***

Theoretical Studies of Solid State Fusion Based on the Bose Bloch Condensate

Using very general quantum mechanical ideas, NRL has identified a natural limit within a solid in which the infusion of deuterium into a metallic host can lead to the possibility of nuclear interactions among nucleons separated by macroscopic distances. This is made possible by the creation of a cooperative state named the Bose Bloch Condensate (BBC). Under suitable conditions, the population of the BBC state leads to an entirely new form of nuclear interaction, solid-state fusion, in which large amounts of heat and nonconventional nuclear fusion products (chiefly helium) are released. This shows the possibility of generating heat without pollutants through the solid-state fusion process.

COLOR PRESENTATION

For visual interest, we present here some of NRL's latest scientific achievements and state-of-the-art equipment.

A colliding pulse modelocked dye laser is being used to study chemical reactions taking place within the timescale of 50 to 100 femtoseconds (a femtosecond is 10^{-15} seconds). (A. Baronavski, Code 6110)

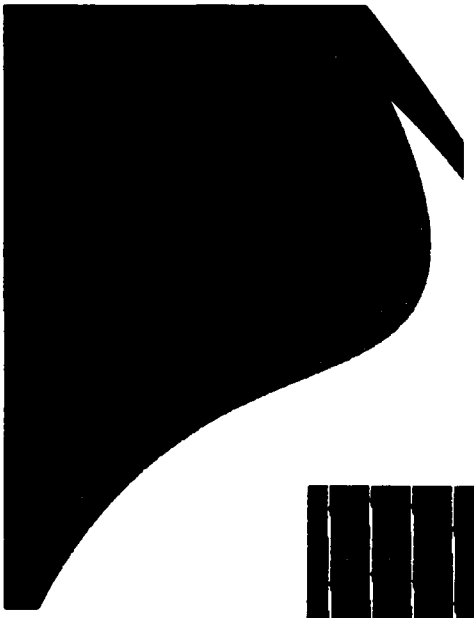

The charged particle dynamics in Earth's magnetotail is chaotic. This system has well-defined entry and exit regions in the phase space. The tear-drop shaped region is an entry region in the phase space for stochastic orbits showing the pre-image of two distinct exit regions. Each pixel corresponds to an orbit and is color coded (red and yellow) according the eventual exit mode. Inset is a small subregion enlarged by a factor of 2×10^5. The generic features are the nonfractal (solid) red and yellow bands. The space between various bands contains similar band structures on finer scales, intertwined *ad infinitum*. (J. Chen, Code 4781)

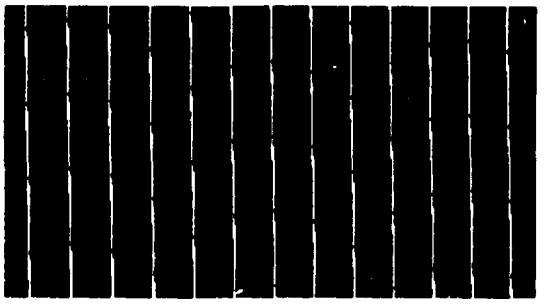

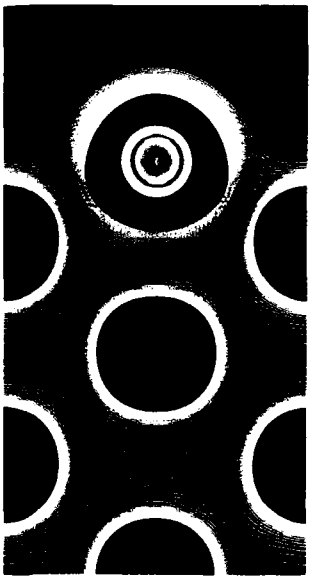

A theoreticians view of corrosion, in this case a monolayer of sulfur on an iron surface. This colored-contour plot of the electron charge density in a (110) plane shows a single sulfur atom (top) bonded chemically to the iron surface atoms. Similar studies of oxygen on iron show that oxygen-iron bond formation weakens the bonding of the surface iron layer to the subsurface iron and alters its magnetic properties. (W. Pickett, Code 4692)

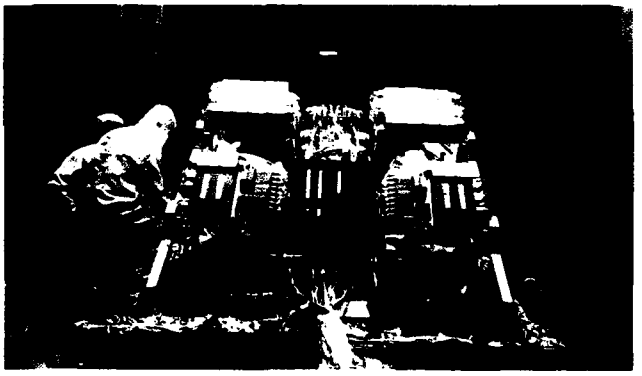

Oriented Scintillation Spectrometer Experiment (OSSE) undergoing preparations for thermal vacuum test at Ball Aerospace Systems Group in Boulder, Colorado. (J. Kurfess, Code 4150)

Visualization: Ship RCS Range Profile vs. Aspect Angle ("Waterfall" Plot)

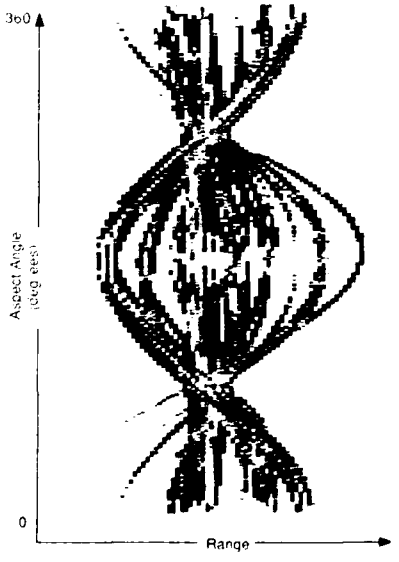

This "waterfall plot" is a visualization depicting simulated high-resolution radar measurements for a ship radar target. The *x* and *y* coordinates of a color picture element (pixel) correspond, respectively, to position in range and to aspect angle of the target as it is rotated 360° relative the measurement radar. The pixel color indicates the magnitude of radar cross section (RCS) at a particular position in range and aspect angle. (A. Goldberg, Code 5753)

Ultrahigh vacuum RF/DC sputtering system used to prepare films of both commercial and oxide superconductors. Inset is a fractal structure synthesized by RF sputtering. (W.T. Elam, Code 4683 and S.A. Wolf, Code 6340)

Isodensity contours of the upper half of an artificial plasma cloud released in Earth's atmosphere. Earth's magnetic field is aligned along the z axis. Shown are contour levels of 1.8×10^6 (red) and 8×10^5 (blue) electrons/cc. The cloud is initially in a stable waterbag configuration, with both contours nearly coincident. However, diffusive processes both along the magnetic field and perpendicular to it quickly evolve the cloud into a nonwaterbag state as seen by the large differences in the isodensity contours as time progresses. In this new configuration the cloud is unstable and subsequently breaks up. (S. Zalesak, Code 4781)

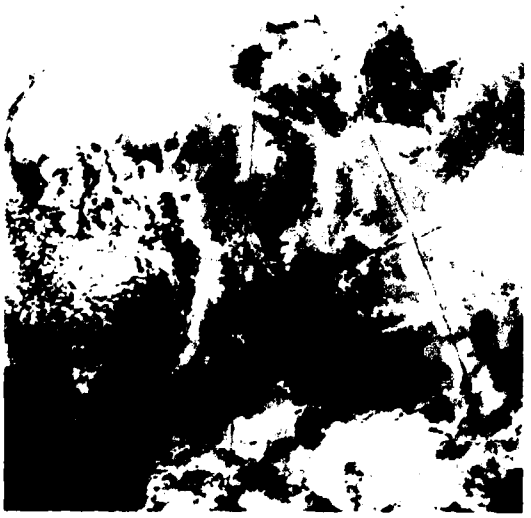

To assess the effectiveness of a satellite-borne infrared sensor to detect aircraft movements, maps of clouds as a function of altitude are constructed from infrared and visible images gathered by the NOAA meteorological satellites. The original infrared image is stretched into an altitude distribution map by compensating for the temperature variation of surface and atmosphere from tropical to arctic. The figure shows a cloud distribution map for Western Europe and the North Atlantic. In this three-color image, the unstretched infrared image is used for the blue component; the stretched infrared image is green; and visible image is displayed in red. Clouds are seen as various shades of gray, varying from white pixels containing high clouds to dark gray pixels containing low clouds. The cloud-free surface appears black in most places. However, where the surface is covered with ice or snow, the strong visible component makes it appear red. (N. Stone, Code 6520)

NASA's Long Duration Exposure Facility as photographed from the space shuttle just after being released on April 7, 1984. NRL's Heavy Ions in Space experiment is located in the two trays circled in white. This experiment collects data on energetic heavy ions that are known to upset the operation of computers in space. These data will be used to influence the design of new space computers so that they will tolerate the error rates resulting from energetic heavy ions. (L. Beahm, Code 4154.3)

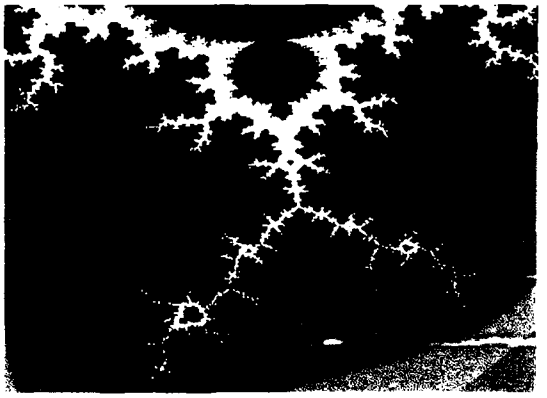

Mandelbot set, a chaotic fractal image. The different colors represent the rate of divergence of the mapping $z_{n+1} = z_n^2 + z_0$ in the complex $z = x + iy$ plane. It is interesting that such a simple mapping can give rise to chaotic behavior. This image was calculated on an HP 9816S computer and displayed on the NRL Dicomed system. (W.H. Carter, Code 8304)

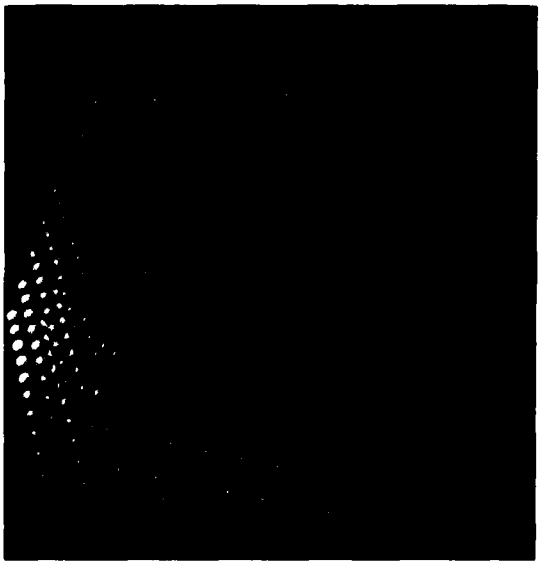

Representative cluster of 1000 atoms used in molecular dynamics simulations for studying cluster stability and melting of solids. The image, produced by a Stellar GS2000 minisupercomputer on an associated graphics terminal, corresponds to illumination by a variety of colored lights placed in various directions. (L. Boyer, Code 4691)

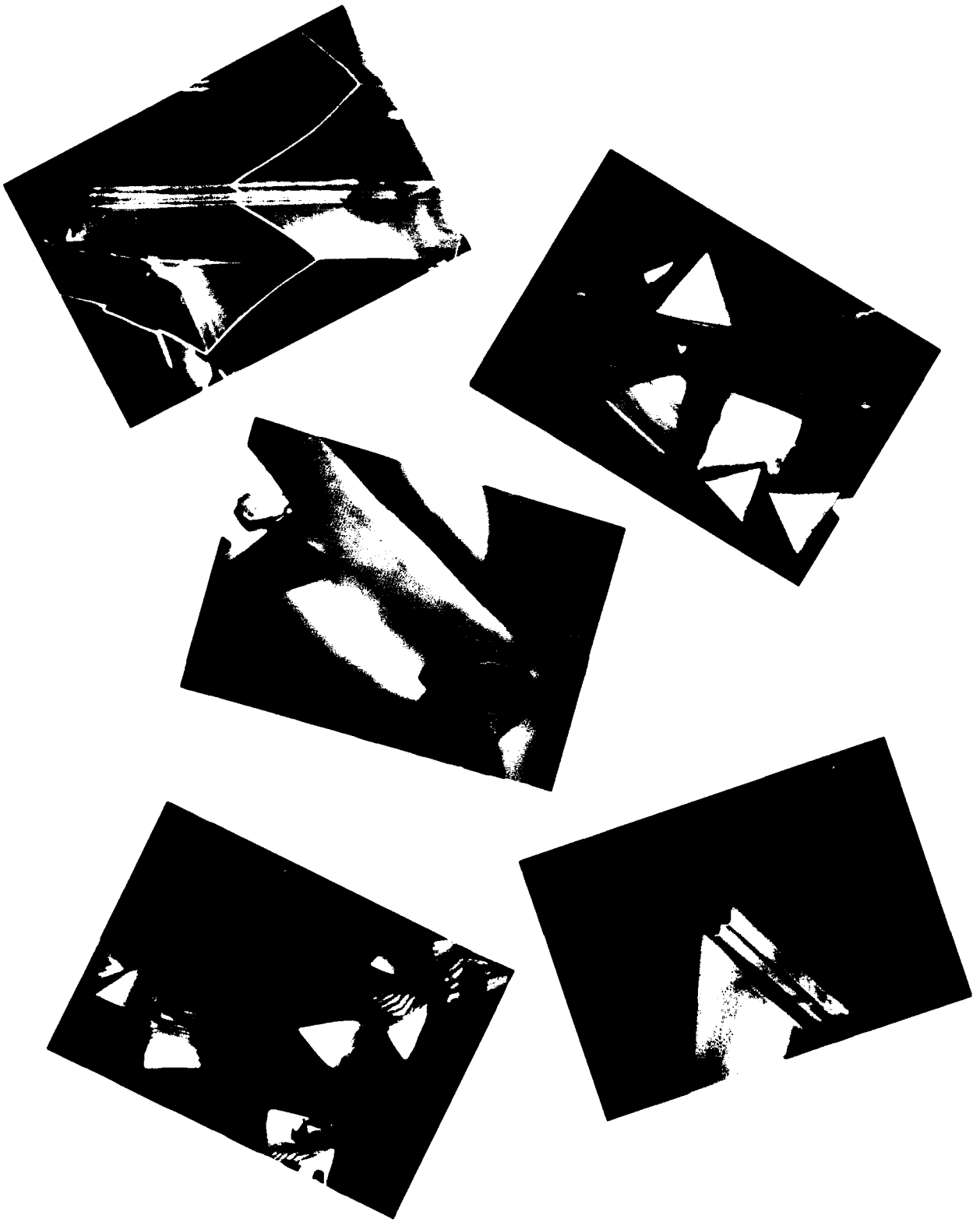

Color-enhanced, laser microscope images of synthetic diamond deposits in the oxygen-acetylene flame. (J. Butler, Code 6174, and T. Saito, Lasertec)

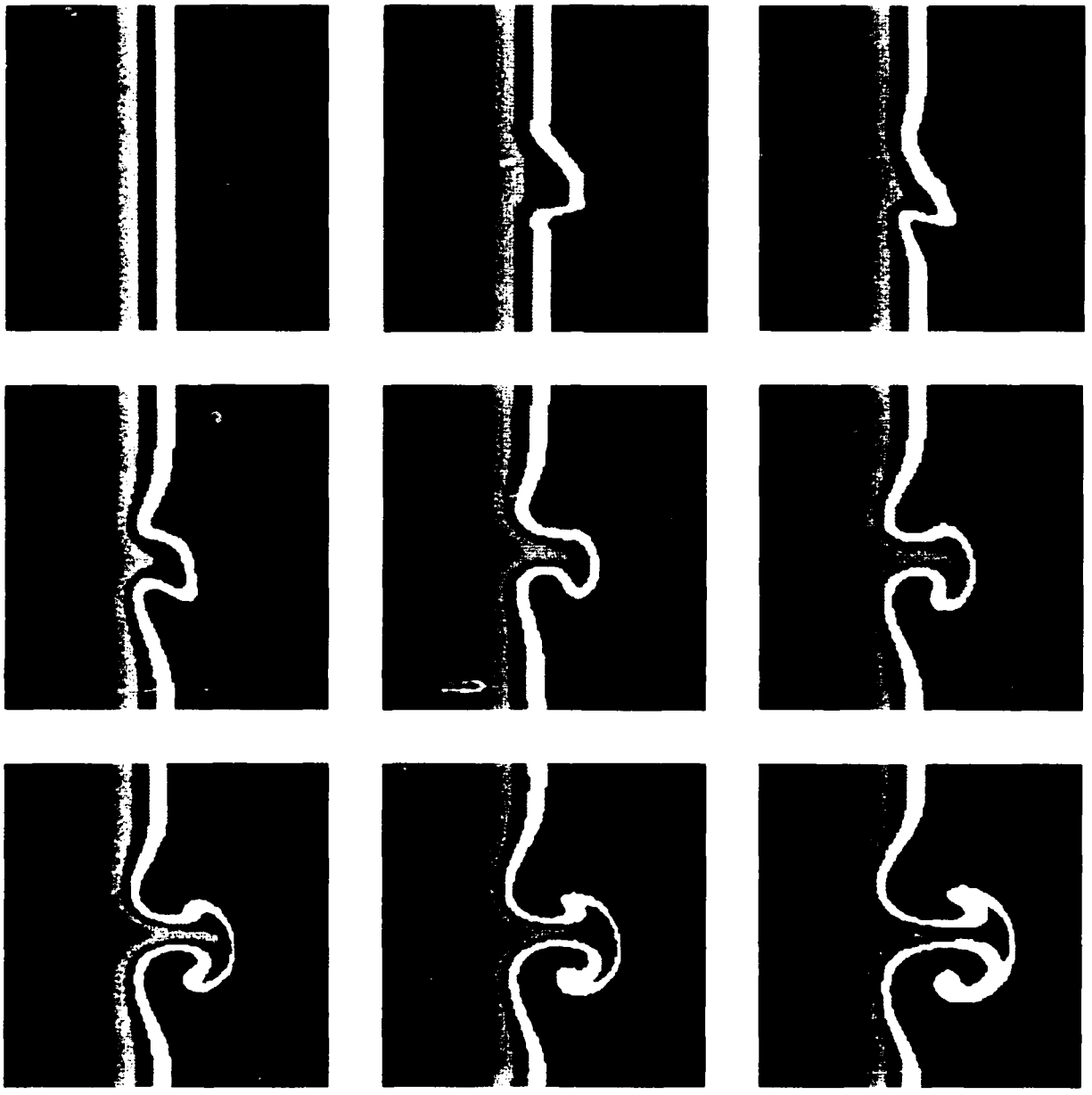

A plan view of the ocean surface in a 140 × 140 km^2 numerical model. Shown is the evolution of a simulated sea surface temperature pattern at times T (in days) resulting from ejection of a mass of fluid from a boundary region. For a fluid pulse in the Northern Hemisphere (here shown directed to the east), the Coriolis force causes deflection to the right ($0.2 \leq T \leq 0.6$) and the asymmetry in the mushroomlike pattern ($T \geq 1.0$) is due to flow nonlinearities. (R. Mied, Code 5142)

Featured Research at NRL

FEATURED RESEARCH AT NRL

Since its inception, NRL has grown in stature, has become the Navy's Corporate Research Laboratory, and has become a national and international leader in research and development in areas of naval interest. Multifaceted research programs embrace acoustics, artificial intelligence, biomolecular engineering, ceramics and composites, chemistry, electronics, ocean technologies, optics, plasmas, materials and their properties, radiation, sonar, space (near and far), and tactical electronic warfare, to name a few. This chapter is devoted to an in-depth look at the latest developments in solid-state supercomputing, electronics research, global weather observation, and parallel and supercomputing technology .

Solid-State Supercomputing

Larry L. Boyer, Barry M. Klein, Dimitrios A. Papaconstantopoulos, and Warren E. Pickett
Condensed Matter and Radiation Sciences Division

Introduction

The scientist, perhaps in a Navy uniform, sits down at a computer terminal and starts to create a data file named "Ball Bearing for Reactor Turbopump for the Trident VIII." Next, the scientist types in quantities such as elastic constants, hardness and melting temperature, and then the command, "GO." In seconds, the laser printer yields a sheet of paper looking similar to a recipe from a cookbook, giving parameters such as metal composition, formation temperature procedures, and ion-beam implantation parameters. The scientist gives the paper to the foundry foreman who completes the ball bearing a day later and hands it off to a systems integrator specialist for final testing. The time is the year 2020. This futuristic tale would have been considered a pure pipe dream just ten years ago, but now the concept of theoretical materials engineering is taken a lot more seriously. Scientists at the Naval Research Laboratory have been leaders in the application of supercomputers to solid-state science, which could make such a fable a reality. Here we convey some of the recent progress leading to the possibility that such scenarios might take place in our lifetime with enormous scientific and technological implications.

NRL has long supported major efforts in the theory of solids, most having applications to experimental programs in the Navy and the Department of Defense (DoD). During this time, in parallel with the growth in computer speed and memory capacities, computational methods and computer algorithms have evolved. These have enabled quantitative theoretical predictions of materials properties to be on the same scale of accuracy as experimental determinations. In the field of solid-state supercomputing, NRL scientists have assumed the lead, pioneering roles in developing, implementing, and applying methodologies on the computer to add understanding to experimental studies and to make explicit predictions of materials properties.

NRL's entry into this field began with major efforts in the 1970s in the areas of first-principles studies of X-ray emission and absorption from solids, magnetism, and especially in the area of transition-metal superconductivity, where the NRL group performed some of the earliest calculations of the fundamental parameters entering into the theory. This expertise positioned NRL to marshal a strong effort in the theory of superconductivity for the recently discovered high-T_c cuprates. As successes have mounted, particularly during the 1980s, the field of computational, solid-state physics has assumed greater credibility and importance in the search for new materials with enhanced desirable properties. In this article, we highlight several of the approaches and applications generated by theoreticians in the field of solid-state supercomputing in the newly formed Complex Systems Theory Branch.

Supercomputers

A supercomputer is, by definition, the best there is. Although increasingly competitive supercomputers are coming from Japan, the name Cray has become the supercomputer equivalent of "frigidaire" or "jello." Since early 1985, NRL has had a Cray XMP-24, with the "24" denoting "2" very high-speed processors (upgraded from NRL's original version) and "4" megawords of

64-bit "core" memory. Other versions of Crays—Cray 2 and the "Y" series—can be several times faster and have a hundred times more memory. The Texas Instruments' ASC supercomputer installed at NRL in the mid-70s was the predecessor to the NRL Cray and allowed NRL scientists to perform some of the earliest large-scale, solid-state calculations. NRL also has two Connection Machines with highly parallel architectures and 8K and 16K processors respectively. These offer great potential for solid-state studies.

Total Energy Methods

On the microscopic level, solids consist of vast numbers (roughly $10^{23}/cm^3$) of electrons and nuclei interacting strongly through their electric charges, making it appear that a first-principles description of their quantum mechanical behavior is beyond the reach of theory and computation. However, the inherent periodicity of solids reduces the semi-infinite problem to one that is tractable. This periodicity causes the discrete atomic energy levels of the constituent atoms to broaden into energy bands, hence the name "band theory."

The foundation of most modern band theory methods rests on the density functional theorems of Hohenberg, Kohn, and Sham (H-K-S) [1] who establish that the ground state total energy of the electrons and nuclei can be determined from the electronic density alone. Besides normal electrostatic energy terms that have classical analogues, there is an exchange-correlation energy E_{xc}, which accounts for the fact that electrons are indistinguishable spin-1/2 particles. E_{xc} is intrinsically many-body in nature, and only approximate forms are known. A fairly simple but highly effective approximate form is the local density approximation (LDA) that uses the value at each point in the solid from a homogeneous electron gas at the same density. Figure 1 illustrates the computational problem that results. The most computer-intensive part of the calculation is solving the Schrödinger equation, which involves setting up and diagonalizing large matrices, sometimes of the order of 1000 × 1000 or larger.

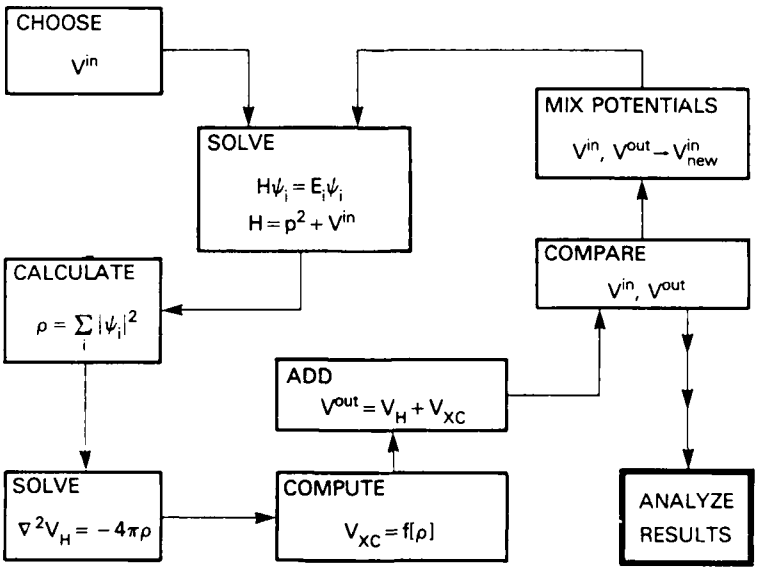

Fig. 1 - Flow chart for a self-consistent band calculation. After a starting potential V^{in} is chosen, the steps are: SOLVE the Schrödinger equations, CALCULATE the density, SOLVE Poisson's equation for the Coulomb potential, COMPUTE the exchange-correlation potential, ADD them together to obtain the output potential V^{out}, and COMPARE it with V^{in}. If they differ, then one must MIX POTENTIALS and repeat the procedure; if they are essentially the same, convergence has been attained and one can ANALYZE RESULTS.

Examples of properties that can be calculated are crystal structures, cohesive energies, lattice vibrations (from the difference in total energies between displaced and undisplaced lattices), elastic behavior, Fermi surfaces, and superconducting properties. Some results obtained from total energy approaches are described in the following sections.

Ordered Alloys

Various technological applications require materials that are strong and ductile at high temperatures but also are light in weight. Over the last few decades, metallurgists have discovered such materials by experimentation, often depending on the Edisonian trial-and-error approach. Recently the local density approximation, aided by the advent of larger and faster computers, has provided the means for reliable theoretical predictions of physical quantities that affect strength and ductility in metals and alloys.

We have applied these methods to determine the equation of state in a variety of ordered intermetallic alloys. The equilibrium properties are found by calculating the total energy as a function of the unit cell volume for cubic systems or as a function of volume and *c/a* ratio for noncubic substances. The total energy E vs volume V results are least-squares fitted to an equation of state. This function then readily provides the equilibrium lattice spacing that corresponds to the minimum total energy. The curvature of the $E(V)$ function gives the bulk modulus, which is a very sensitive test of the accuracy of these calculations. The method is also capable of distinguishing which one of various possibilities is the most stable structure. For example, these calculations bear out the experimental fact that for copper, nature prefers the face-centered cubic structure to the body-centered cubic, and vice versa for vanadium. But the capabilities of this method go even farther; the shear modulus and elastic constants of a crystal can also be computed by straining the crystal and relating the energy change to the elastic moduli. An example is the calculation of the difference $c_{11} - c_{12}$ for CoAl, whose unit cell is shown in Fig. 2. With strain parameters $e_2 - e_1$ and e_3 chosen to conserve the crystal volume, $c_{11} - c_{12}$ is obtained from a polynomial fit to the energy change $\Delta E = 3V(c_{11} - c_{12})e_1$.

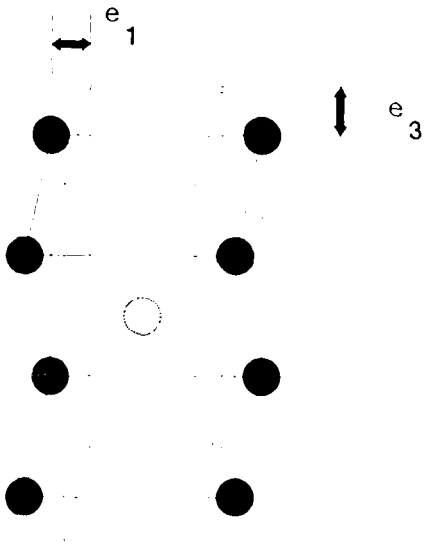

Fig. 2 – Crystal structure of CoAl with the dashed lines denoting the shape of the unit cell when distorted to calculate the shear modulus

In an effort led by Mehl [2], we applied this methodology to the intermetallic alloys SbY (NaCl structure), CoAl and RuZr (CsCl structure), and NbIr (tetragonal $L1_0$ structure). The results are summarized in Table 1. The calculated lattice spacings are within 2% of the experimental values. The bulk modulus for the cubic materials CoAl and SbY are also in excellent agreement with measured values. For the tetragonal material NbIr, the calculated bulk modulus differs by 6% from the experiment. For the shear modulus of the cubic materials, the discrepancy between theory and experiment is approximately 8%. The only serious problem appears in the shear modulus of NbIr, where the discrepancy is at the 30% level. Table 1 also shows the melting temperatures. The calculated values of T_m were found by using an empirical formula that relates the c_{11} elastic constant to T_m. Therefore the values of T_m are not the result of first principles calculations like the

Table 1 — Comparison of Parameter-Free Calculations of Lattice Spacings and Elastic Moduli with Experiment (R. B. Fleischer)

Compound	SbY	CoAl	RuZr	NbIr
Lattice spacings (Å)				
Theory				
a	6.12	2.80	3.22	3.99
c	---	---	---	3.86
Experiment				
a	6.16	2.86	3.25	4.03
c	---	---	---	3.86
Bulk modulus (Mbar)				
Theory	0.67	1.57	2.25	3.20
Experiment	0.66	1.62	---	3.01
Shear modulus (Mbar)				
Theory	0.38	1.05	0.90	1.40
Experiment	0.40	1.14	---	0.99
Melting temperature (K)				
Theory	1590	2070	2700	2800
Experiment	2310	1648	---	2200

other quantities given in Table 1; they simply represent an estimate of T_m that can be very valuable in the exploration of new intermetallic alloys. In that respect, for RuZr, where there are no measurements, our value of $T_m \approx 2700$ K as well as the elastic moduli are predictions worthy of further attention by the experimentalists. We emphasize that our theoretical values for the bulk and shear moduli of CoAl are also predictions of our theory that were subsequently verified experimentally.

Disordered Alloys: These results assume a regular ordered periodic arrangement of the atoms in a solid. However, real solids deviate from periodicity and contain vacancies, impurities, dislocations, or random substitutions by other kinds of atoms. The theories that we have discussed have been extended to cover disorder and randomness of the atomic constituents. This was done by employing the coherent potential approximation (CPA), which is a mean field theory designed to calculate the electronic states of disordered materials. The basic idea of the CPA is that the electrons in a solid can be regarded as moving in an effective medium, the Hamiltonian of which is determined self-consistently by the condition that the average scattering of electrons by the potential of each atom site is zero on the average. The CPA method has been applied by the NRL group to calculate the electronic densities of states for a great variety of systems ranging from metal hydrides and hydrogenated amorphous silicon to the new, high-temperature superconductors. These results often justify expectations derived from calculations for periodic structures, but the results also show their limitations.

Heavy Fermion Compounds

The acquisition of the Cray computer was instrumental in extending NRL's electronic structure studies to more complicated structures than basic metals, semiconductors, and insulators.

In the spring of 1985, as soon as the Cray was operational, a study began on UBe_{13}. This compound is interesting for a number of reasons. First, it is a heavy fermion (HF) metal, whose huge increase in linear specific heat coefficient and magnetic susceptibility at low temperature reflects very heavy electrons. Second, it becomes superconducting just below 1 K, which is surprising because the huge rise in the magnetic susceptibility below 20 K suggests that it is about to become magnetic. Finally, its crystal structure, shown in Fig. 3, is quite unusual and difficult for a band structure study.

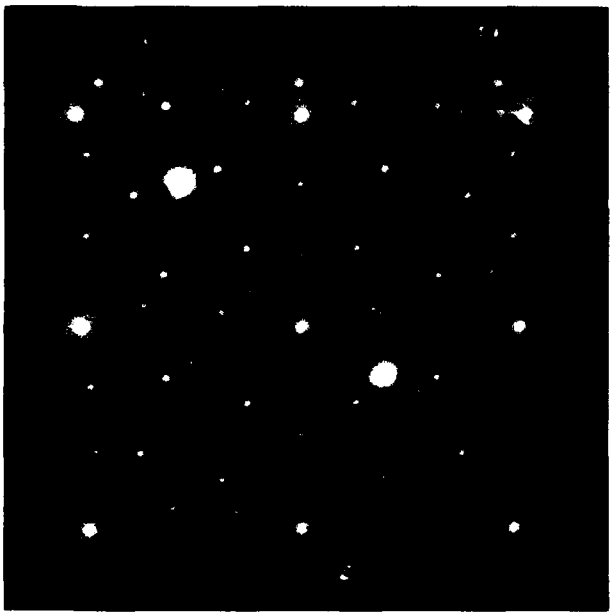

Fig. 3 – Crystal structure of UBe_{13}. The large red spheres are uranium atoms, each of which is surrounded by 24 Be (blue) atoms. The green atoms are Be atoms that are inequivalent to the blue ones and, like the U atoms, lie on a simple cubic lattice.

Because UBe_{13} and other HF compounds are metals in which the electrons are very highly correlated, questions arose as to whether local density methods would have any applicability at all. These questions were only answerable by carrying out the calculations and comparing the results with experimental data. Calculations on UBe_{13} requiring 60 to 70 hours of (CPU) time were carried out immediately when the NRL Cray came on-line. These calculations revealed that the crystal volume was predicted just as well as for normal metals. They also made specific predictions about the energy bands and Fermi surface; however, because of complications related to its heavy fermion nature, it has still not been possible to check these predictions experimentally. Parallel calculations were carried out for UPt_3 with the distinction that for this metal (whose fermions are not quite so heavy), it was possible to measure the Fermi surface with standard, but highly sophisticated, methods. The Fermi surface for this metal was predicted [3] to be extraordinarily complicated, with six separate sheets centered at various positions in momentum space. Experimental data have verified the correctness of these predictions in detail; the intricate topology is correct and the cross-sectional areas are off by only 5 to 20%. Discrepancies such as these are typical in much simpler, normal metals. It is thus established that band theory provides a cornerstone for a quantitative theory of heavy fermion behavior, although some of the most interesting phenomena remain to be explained.

High-Temperature Superconductors

The discovery in 1986 by Bednorz and Müller [4] of high critical temperature (T_c) superconductivity in the layered copper-oxide compounds has had a profound influence on the community of condensed matter scientists. Not only was no significant increase in T_c expected at the time, but the new superconductors proved to be drastically different from the previous best ones. The most notable difference was the large concentration of oxygen in the new compounds (typically 50%). With few exceptions, it had been observed that adding oxygen to superconductors drastically hindered their superconducting properties. Soon it came to light that these copper oxides were unusual in other ways, such as being near (in the phase diagram) to antiferromagnetic insulating compounds and being black, brittle ceramics rather than shiny, ductile metals. In some ways, though, they appeared to resemble other

superconducting materials, such as being associated with soft-mode structural transitions.

Their unusual properties, and most of all their incredible superconductivity, led to widespread speculation that even in their nonsuperconducting ($T > T_c$) metallic state, they were qualitatively distinct from more typical metals—a controversy that is not yet completely resolved. Thus, in this respect, they presented the same questions posed by the HF compounds a few years previously: can local density-band calculations provide any information about their electronic structure and properties? Again, the question could only be answered by long and intricate calculations.

During late December 1986, within three weeks of the announcement of the discovery of high critical temperature superconductivity, we began calculations on the La_2CuO_4 material with $T_c = 35$ K. Together with a few other groups doing similar calculations, we learned that the band calculations predicted that the important states were an antibonding combination of Cu d states and O p states [5]. The distinguishing feature of this copper oxide, compared with other transition metal oxides, is that the Cu d and O p bands are wide (8 to 9 eV) and that they are centered close to the same energy, resulting in strong hybridization. At the same time, it was possible to alloy on the La site with Ba or Sr until the insulator became metallic and superconducting.

During the next three years, a number of various layered cuprate properties (now having confirmed T_c values up to 125 K), have been explained qualitatively and, in some cases, semiquantitatively within the context of band theory. On the negative side, a description of the antiferromagnetic insulating materials, from a band point-of-view, is still lacking. Since the magnetic properties diminish very rapidly as the material is converted from the insulating phase to the metallic superconductor, it seems likely that, interesting as these phases are, the microscopic interactions leading to magnetism are weak in the metallic phase and not essential to an understanding of their superconductivity.

Continuing from this vantage point, we have embarked on an ambitious and highly successful study of the structural (in)stability and lattice dynamics by using the parameter-free, local density, total energy methods. Ronald Cohen (NRL's Complex Systems Theory Branch) performed most of the extensive calculations of a size and complexity that have not been contemplated by any other group. It was first established [6] that the computational methods gave *quantitatively correct results* for La_2CuO_4 for both the unstable tilt mode (thereby accounting for the observed tetragonal-to-orthorhombic structural transition) and for a number of phonon frequencies that have been observed by light (Raman) scattering and neutron scattering experiments.

Although it is generally considered that the same superconducting mechanism must be operating in La_2CuO_4 as in the other cuprates discovered since that have pushed T_c up to 125 K, that conceptual step is by no means certain. Certainly, it is crucial to determine whether comparably accurate results can be obtained for the more exotic compounds. We chose $YBa_2Cu_3O_7$, which has been more widely studied than the others and whose crystal structure is well established and extended the studies of lattice instability and vibrational frequencies to this compound. Figure 4 shows the complicated crystal structure that necessarily leads to complexities in determining normal vibrational modes, since any given mode will involve motions of many, if not all, of the atoms in the cell. For this reason and because the unit cell is twice as large as that of La_2CuO_4, calculations for $YBa_2Cu_3O_7$ were much more demanding than those for La_2CuO_4.

For long wavelength modes, symmetry arguments can be applied to separate the dynamical matrix that describes the forces among all sublattices of atoms into block diagonal form.

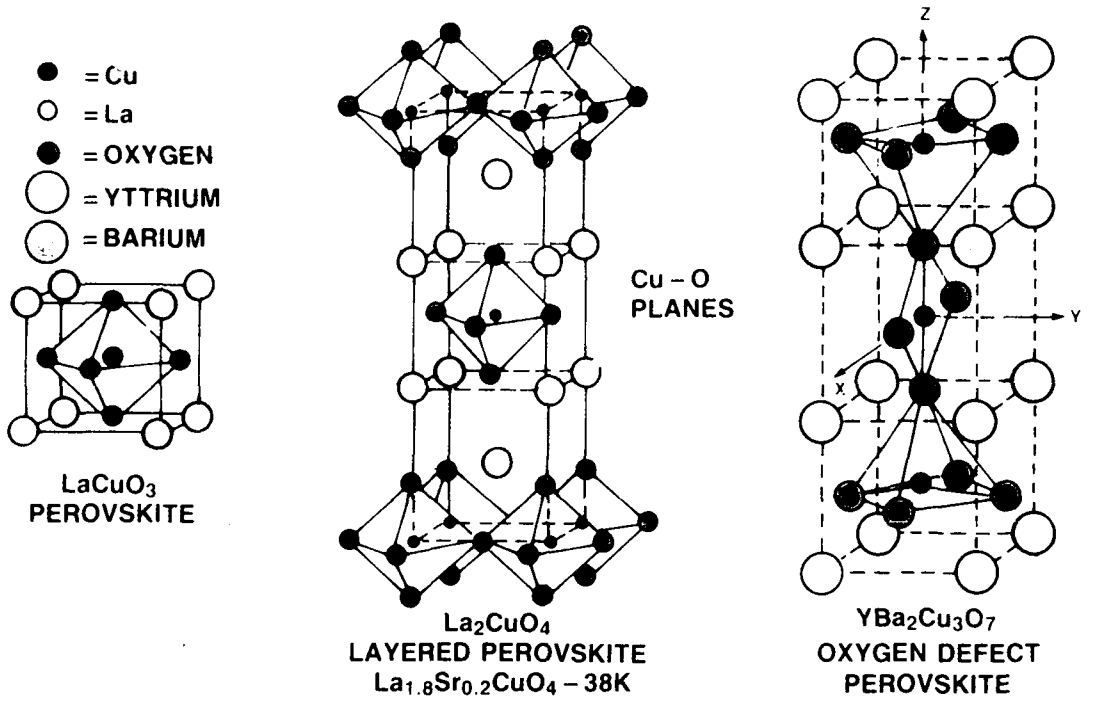

Fig. 4 – Crystal structure of $YBa_2Cu_3O_7$, showing the Cu–O planes and chains separated by Y and Ba ions.

Attention was focussed on the Raman-active modes, five each of symmetry A_{1g}, B_{2g}, and B_{3g}, all of which involved the motion of five atoms. These calculations, which are the most ambitious and demanding of their kind ever undertaken and requiring the equivalent of 2000 Cray XMP hours and were carried out at the National Center for Supercomputing Applications in Illinois, allow a direct comparison with the experiment and, therefore, a stringent test of the theory. The outcome shows that with the exception of one mode that may be 15 to 20% off, all modes are predicted as accurately as would have been expected for a completely normal material of comparable complexity. There was one discrepancy that may be due to nonadiabatic renormalization (which lies beyond current theories) or possibly to unusually low energy electronic excitations of an unknown nature.

We carried out one other calculation in which we determined the change in energy caused by a buckling of the Cu–O chain; this buckling consists of motions of the O ions perpendicular to the chains. In agreement with potential induced breathing (PIB) calculations suggesting that this motion was unstable, a very wide (0.75 Å) and anharmonic double-well potential was found. Experiments involving X-ray studies of detwinned crystals that had been carried out simultaneously with the calculations found this chain-buckling mode to be unstable; the total energy calculations were again proved to be accurate.

These results have far-reaching consequences for any theory of the properties of layered cuprates. One way to summarize these results is to say that local density band theory gives the correct density response of the cuprates. It is still unclear whether dynamical processes exist that renormalize the band eigenstates and must be taken into account in describing superconductivity. However, our results establish that if such processes exist (and are not implicit within band theory), they must provide a negligible effect on

the static density response. This realization implies a limit on the strength of such processes.

The usefulness of these calculations does not end there. As a by-product, a number of detailed quantities are obtained that allow one to compute the electron-phonon coupling strength and evaluate whether this coupling is large enough to account for the very high values of T_c. These calculations are still in progress. However, one novel and undoubtedly important result has emerged. Although these materials are reasonably good metals, they retain a strong ionic character that gives rise to long-range (nonlocal) Madelung potential shifts when atoms vibrate that do not occur in normal metals. An example of these novel nonlocal contributions to electron-phonon coupling are shown in Figure 5—a contour plot of the change in electron charge density when the bridging oxygen atom is displaced perpendicular to the CuO_2 layer. The crucial point to notice is that this displacement leads to a redistribution of charge on the Cu and O atoms in the layer and on the Cu atom in the chain, reflecting the change in the potential. It is the dichotomy between metallic conduction and ionic potential shifts that may distinguish the cuprates from previous superconductors. These characteristics are, in fact, just the properties that spurred Bednorz and Müller to search for superconductivity in these compounds.

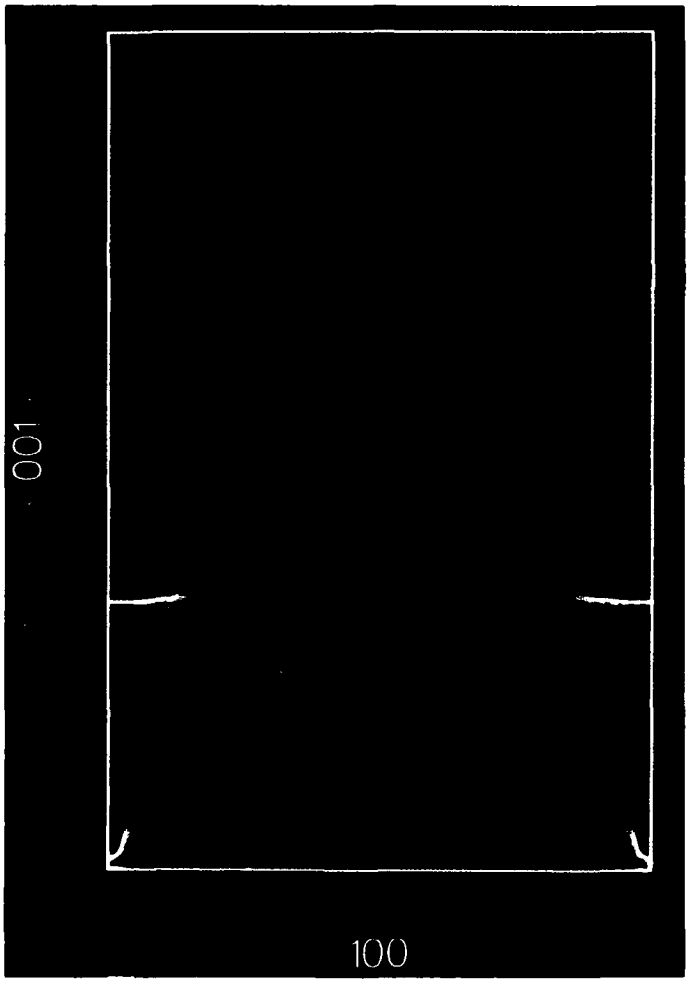

Fig. 5 – Contour plot of the change in charge density in a (010) plane of $YBa_2Cu_3O_7$ when the bridging oxygen atom (where most of the contours lie) is displaced upward. Note particularly the nonlocal changes on the Cu atoms, in the Cu–O plane (above), and in the Cu–O chain (below the displaced atom).

Modeling Phase Transitions

In this section we describe *ab initio* models (AIMs) for applying LDA in total energy calculations and show how this approach has led to a better understanding of the mechanisms for structural transitions in condensed matter. While the governing principle for developing AIMs is general, the simplest candidate materials are systems whose bonding can be described by interactions among closed shell atoms or ions. Fortunately, such systems provide a rich assortment of phase transitions that are described rather well by AIMs.

In a selfconsistent band calculation, the charge density is allowed to relax without constraint from some starting density to that of the ground state. In an AIM, the charge density is deliberately constrained in a way that simplifies the calculation of total energy, and hopefully, captures the essential physics of the problem. Both approaches use a local density ansatz for relating energy to charge density. A band calculation gives the electronic kinetic energy exactly, because the charge density in a band calculation is expressed in terms of single, electron-wave functions with well-defined kinetic energies. AIMs use, in addition, a local density expression for kinetic energy.

Let us examine a very simple AIM, the so-called rigid-ion (RI) model. In the RI model, we assume the total energy is given by a sum over pair-wise interactions. The charge density in each ion pair is assumed to be the sum of individual free ions. In other words, we assume the charge density $n(r)$ of a single ion is undistorted by contact with another; hence the name rigid ion. The repulsive part of the interaction between ions arises from the increase in kinetic energy of the electrons in the overlap region. In a formulation derived over fifty years ago [7], the kinetic-energy density is proportional to $n^{2/3}$ Thus the increase in kinetic energy caused by the overlap of an ion A with another ion B is given by

$$C \int [(n_A + n_B)^{5/3} - n_A^{5/3} - n_B^{5/3}] dv,$$

where C is a known constant and the integration is over all space. Similar expressions give the contribution from electron exchange and correlation. These contributions plus that caused by electrostatic forces combine to give the total pair interaction.

For many years the only use for this formulation was in the qualitative understanding it provided. Rather than attempting to evaluate the pair potentials *ab initio*, workers introduced empirical models with parameters that were determined by fitting to experimental results for the particular solid being studied. Efforts to improve accuracy produced models with more complex interactions, that is, with enough parameters to give the desired accuracy. In 1972, Gordon and Kim [8] evaluated pair potentials for alkali halide and rare gas atom interactions by numerically evaluating the expressions outlined above, assuming n_A and n_B are the densities of free atoms or ions. Application of this RI AIM to halide materials has led to a better understanding of the mechanisms for various types of phase transitions and to the prediction of new materials.

An example of a predicted new material is $NaCaF_3$. Based on molecular dynamics simulations using the RI AIM, it is expected to have a distorted perovskite structure with a large ferroelectric polarization, 21 $\mu C/cm^2$, at room temperature. The prediction should be reliable because the same theory correctly accounts for the structures and phase transitions in the existing isomorphs, $KCaF_3$ and $RbCaF_3$, which have paraelectric ground states. The ferroelectric transition temperature, computed to be ~ 550 K in molecular dynamics simulations, could presumably be tuned by doping with potassium, making it a potentially useful material for applications.

The mechanisms for phase transitions, be they continuous (or nearly so) or largely first order in

character, refer to the pathways in configuration space between energy minima, which allow the transition to occur. The minimum energy pathway defines the so called "order parameter" and the corresponding energy surface defines a "double well." Double wells are associated with various types of transitions between condensed matter phases.

The well known soft-mode theory of displacive transitions originated from work based on empirical models. This theory assumes the existence of a temperature-dependent force constant that causes the frequency of a mode to approach zero, which in turn causes the transition. Further change in the force constant converts the potential well for the soft mode from a single to a double well. Results of AIM calculations suggest a somewhat different interpretation. The soft mode should not be viewed as the cause of the transition, as was originally envisioned, but as a symptom of the presence of a double well. The soft-mode response results from anharmonicity associated with the double well, which itself, is essentially independent of temperature. In $RbCaF_3$, for example, calculations show that the double well is present even at very high temperatures, near melting (~ 1400 K), while the soft-mode transition occurs at ~ 200 K. The order parameter describes a coordinated rotation of corner-shared CaF_6 octahedra. The computed energy barrier gives a good approximation for the transition temperature T_0 by equating energy per atom to $kT_0/2$.

Double wells have been associated with transitions between crystalline and disordered condensed matter phases. For example, the fluorine ions in CaF_2 are dynamically disordered in a temperature range beginning about 200 K below the melting temperature, $T_m = 1630$ K. This superionic transition appears to be related to a highly anharmonic double-well mode with a symmetry that only involves motion of the F^- ions. In this case, the double well forms with increasing volume. At the volume corresponding to the superionic phase, the double-well is shallow, too shallow for the fluorine ions to condense into a lower symmetry lattice; as a result, ions can move approximately one-third the distance to neighboring sites with no substantial change in potential energy. This extreme anharmonicity presumably contributes to and may be the primary cause of the disorder in the superionic state and may contribute to the high ionic conductivity. The similarly wide and shallow double well in $YBa_2Cu_3O_7$ likely contributes to the high conductivity of oxygen ions observed to occur along the chains at high temperatures.

Transitions between solid and liquid phases may be related to double wells where the pathway between energy minima is given by parameters that define dynamically allowed (symmetric) shear-strain tensors. Thus far, calculations have only been carried out for NaF, aluminum, and a model potential suitable for rare gas elements. Figure 6 illustrates the finding with results for the model potential. Two motivations exist for associating such double wells with melting. First the barrier height correlates approximately with T_m and second, the parameters defining the distortion are consistent with the main structural difference between a solid and a liquid—the liquid's lack of resistance to shear stress.

These examples of phase transitions are difficult to treat by standard methods of statistical mechanics because of the highly anharmonic vibrations near the transition. Now we consider an example of a phase transition that is easy to treat with statistical mechanics—the transition between B1 and B2 crystal structures that occurs as a function of pressure P in many alkali halides. In this case, the Gibb's energies of the two phases can be calculated accurately by using a quasiharmonic approximation. For KCl, the RI AIM described gives a thermodynamic transition pressure that is nearly independent of temperature, with a value of ~ 13 kbar (experimental value of 19 kbar). Here the pathway between minima is described by a volume and shear parameter (Fig. 7). The shear

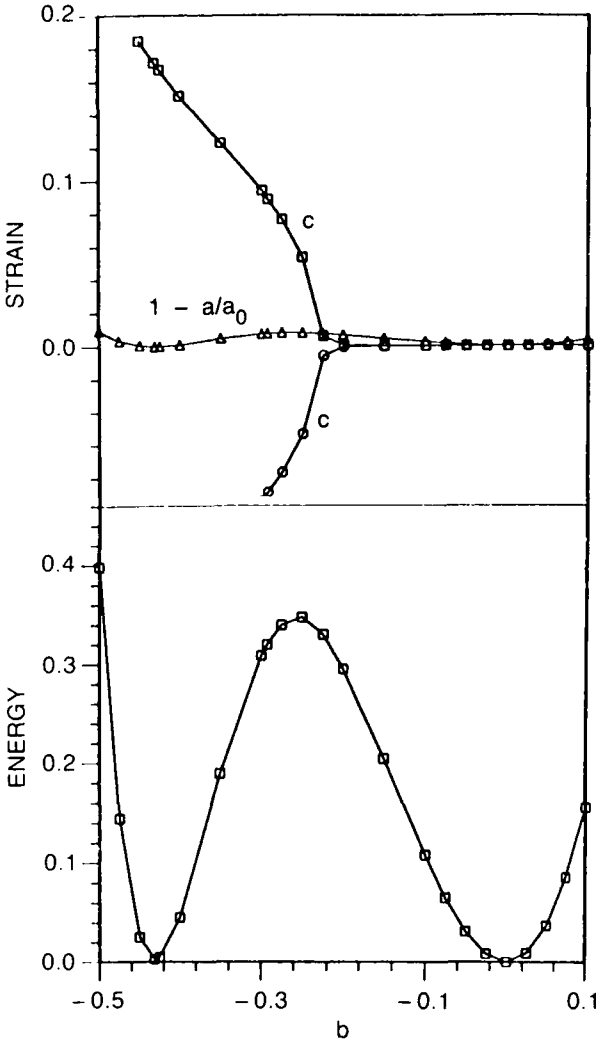

Fig. 6 – Double well and corresponding strain parameters for the minimum energy path between equivalent fcc structures in a model rare-gas crystal; atoms interact by means of the potential $4\epsilon(1/r^{12} - 1/r^{6})$; a/a_0 denotes lattice dilation; b and c denote shear strain corresponding, respectively, to the C_{11}–C_{12} and C_{44} elastic moduli; the melting temperature for this model is $0.67\epsilon/k$

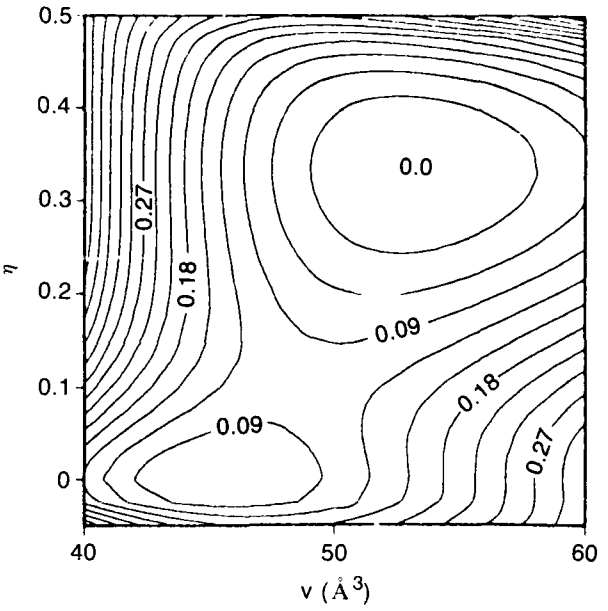

(a)

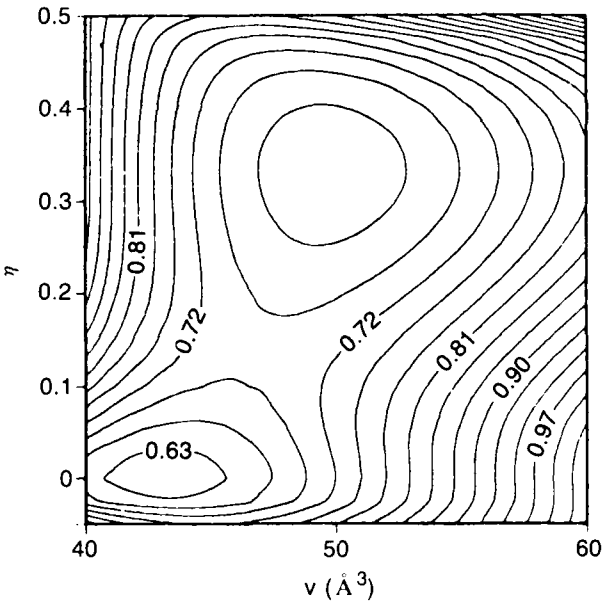

(b)

Fig. 7 – Contour plot of the zero temperature Gibb's energy per molecule of KCl (units of eV) as a function of volume/molecule and shear strain η, corresponding to the C_{44} elastic modulus); (a) for P = 0 and (b) P = 20 kbar

strain η is that corresponding to the C_{44} elastic modulus. The minimum at $\eta = 0$ is the B2 structure, and the minimum at $\eta = 1/3$ is the B1 structure.

The logical next step beyond the RI model is to allow the ions to deform in the simplest manner possible; for instance, one can change its radial charge distribution or "breathe," in response to changes in its environment. This is absolutely necessary for oxides because the O^{--} ion is unstable as a free ion. The PIB model stabilizes the oxygen ion by a charged shell whose potential is equated to the Madelung potential of the solid. Ron Cohen has applied the PIB model to many oxides with great success in predicting equations of state and elastic properties. Its application to La_2CuO_4 and $YBa_2Cu_3O_7$ led to the more accurate self-consistent calculations described here. In keeping with the theme of this section, we note that a major triumph of the La_2CuO_4 study was the association of a calculated double well with an experimentally observed structural transformation.

Perhaps the most important ferroelectric material from a theoretical and technological standpoint is $BaTiO_3$. It has three ferroelectric phases below 400 K and is paraelectric with the cubic perovskite structure above 400 K. The PIB model wrongly predicts a stable cubic structure at zero temperature. This suggests that the type of ferroelectric ground state found in $BaTiO_3$ requires a polarizable oxygen ion. Indeed, a polarizable-ion AIM was developed by Paul Edwardson in our group that correctly predicts the sequence of phase transitions in $KNbO_3$, which are the same as in $BaTiO_3$, but at higher temperature (cubic above 700 K). Once again, the mechanism for this sequence of transitions is described in terms of double wells; the order parameter is given essentially by the coordinated displacement of the Nb ions in their octahedral cages with oxygens at

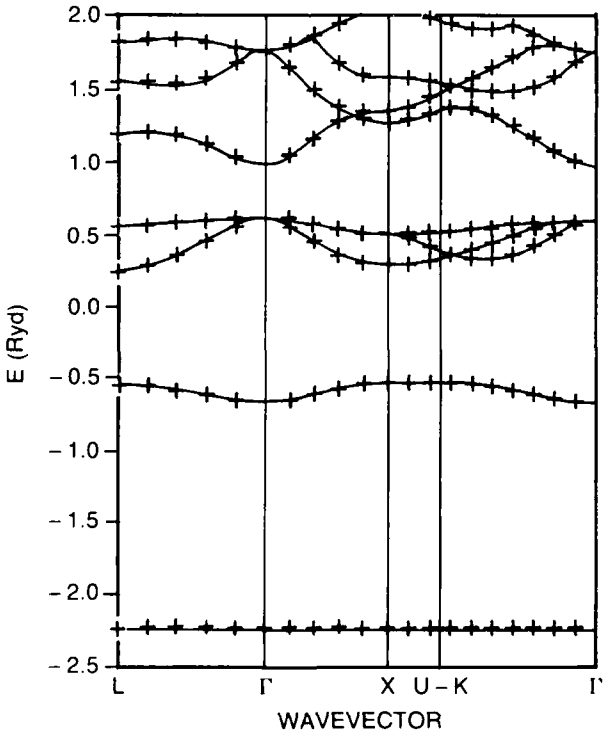

Fig. 8 – Comparison of the PIB model band structure (symbols) for MgO with that derived self-consistently (solid curves); they are nearly identical.

the corners. Displacement in any one of the eight (111) directions gives the deepest minimum and the rhombohedral ground state. With increasing temperature, the Nb ions acquire enough thermal energy to fluctuate from site to site—first, between two adjacent sites, giving the orthorhombic phase; next, among four sites each having a component of displacement along one of the six cubic directions, producing the tetrahedral phase; and finally, over all eight sites, giving the cubic structure.

The success of AIMs in describing displacive-type phase transitions in ionic crystals was completely unanticipated. The prevailing wisdom was that the small displacements associated with such transitions must originate from subtle changes in the forces between ions, changes that presumably had a complicated quantum mechanical origin. Fortunately, this is not the case. Simple AIMs for the charge density, together with LDA for relating charge density to energy, provide sufficient accuracy for most purposes.

The potential accuracy of an AIM can be easily tested by comparing its band structure (from a nonself-consistent potential derived from the model density) with that of a self-consistent calculation. For example, the results in Fig. 8 show that the PIB model band structure for MgO is almost identical to that derived by the self-consistent method. This bodes well for the future of AIMs; it shows that their success is not accidental and points the way for making improved models. AIMs provide a simplified bonding picture and are several orders of magnitude more efficient than self-consistent methods. Their greater efficiency is absolutely necessary, for example, in molecular dynamics simulations of phase transitions.

Acknowledgments: Work in this article was done in collaboration with Henry Krakauer (College of William and Mary), Paul Edwardson (Mission Research Corp. and former NRC-NRL postdoctoral fellow), and John Hardy (University of Nebraska). Robert B. Fleisher (General Electric Company, Schnectady, N.Y.) provided the calculations used in Table 1. Also contributing were Michael J. Mehl and Ronald E. Cohen of NRL's Complex Systems Theory Branch.

References

[1] P. Hohenberg and W. Kohn, "Inhomogeneous Electron Gas," Phys. Rev. **36**, B864–871 (1964); W. Kohn and L.J. Sham, "Self-Consistent Equations Including Exchange and Correlation Effects," *Phys. Rev.* **140**, A1133–1138 (1965).

[2] M.J. Mehl, J.E. Osburn, D.A. Papaconstantopoulos, and B.M. Klein, "Structural Properties of Ordered High-Melting-Temperature Intermetallic Alloys from First Principles Total Energy Calculations," submitted to *Phys. Rev. B.*

[3] C.S. Wang, M.R. Norman, R.C. Albers, A. M. Boring, W. E. Picket, H. Krakauer, and N.E. Christensen, "Fermi Surface of UPt_3 within the Local Density Approximation," *Phys. Rev. B.* **35**, 7260 (1987).

[4] J.G. Bednorz and K.A. Müller, *Z. Physik B* **64**, 189 (1986).

[5] W.E. Pickett, H. Krakauer, D.A. Papaconstantopoulos, and L.L. Boyer, "Evidence of Conventional Superconductivity in La-Ba-Cu-O Compounds," *Phys. Rev. B* **35**, 7252–7255 (1987).

[6] R.E. Cohen, W.E. Pickett, and H. Krakauer, "First Principles Phonon Calculations for La_2CuO_4," *Phys. Rev. Lett.* **62**, 831–834 (1989).

[7] M. Born and K. Huang, *Dynamical Theory of Crystal Lattices*, Section 1 (Oxford Press, London, 1954).

[8] R.G. Gordon and Y.S. Kim, "Theory for the Forces between Closed-Shell Atoms and Molecules," *J. Chem. Phys.* **56**, 3122(1972).

THE AUTHORS

LARRY L. BOYER graduated from Doane College in Crete, Nebraska, in 1965 with a B.A. degree and majors in mathematics and physics. He received an M.S. and a Ph.D. in physics from the University of Nebraska in 1968 and 1970, respectively, where his thesis involved the development of theoretical methods for treating dislocations in metals. His post-doctoral research between 1970 and 1973, at the University of Nebraska and Princeton University, was in deriving simple models for interactions in complex ionic materials—$Gd_2(MoO_4)_3$, a ferroelectric material and apatite, the main constituent mineral of bones and teeth. He joined NRL in September 1973 to do theoretical and experimental work on complex interactions in simple ionic materials and multiphonon infrared absorption in alkali halides. The following year he joined Klein and Papaconstantopoulos in applying and developing self-consistent electronic structure methods. He has made major contributions in developing techniques for band-structure calculations, applying and developing simplified models for the electronic structure and dynamics of ionic materials, and in relating results of lattice dynamics to phase transitions.

BARRY M. KLEIN graduated from the New York University College of Engineering with a B.S. in engineering physics in 1962. He continued his education at N.Y.U., obtaining M.S. and Ph.D. degrees in physics in 1965 and 1969, respectively. From 1969 to 1971, Dr. Klein was a National Research Council Post-Doctoral Associate at NRL. Dr. Klein was a lecturer (part time) at George Mason University from 1972 to 1975; served as a program director for condensed matter theory at the National Science Foundation in 1984 and 1985; and he has remained active on numerous national committees, especially those related to the NSF.

Dr. Klein joined the NRL staff in 1971 as a research scientist in the X-ray Optics Branch, where he did experimental and theoretical work on X-ray fluorescence analysis and X-ray plasma spectroscopy, while developing a research program on solid-state theory. In subsequent years, his research efforts evolved into first-principles electronic structure theory with particular emphasis on superconducting materials and defects in solids. From 1978 to 1985, he headed the Electronic Structure of Solids Section in the X-ray Optics and Condensed Matter Physics Branches, becoming branch head for the latter in 1985. In 1988, he became branch head for the newly formed Complex Systems Theory Branch, which is his current position. Also in 1988, he spent a year as the General Science and Technology Directorate representative on the Office of Strategic Planning Staff. Dr. Klein is the author of over 80 technical publications and has given more than 100 presentations.

DIMITRIOS A. PAPACONSTANTOPOULOS was born in Athens, Greece, and graduated from the University of Athens with a B.S. degree in physics in 1961. He received a Ph.D. in theoretical solid state physics from the University of London, England, in 1966. He was a professor of physics at George Mason University from 1967 to 1977 and chairman of the physics department from 1974 to 1977. He worked at NRL as a consultant from 1970 to 1977 and as a government employee from 1977 until the present. He was acting branch head in 1986 and in 1989. He is currently head of the Alloy Theory Section in the Complex Systems Theory Branch. His areas of expertise include band structure calculations, superconductivity, and theory of alloys. He has authored approximately 120 journal papers, 1 book, and has given over 100 presentations at professional meetings. He has won three NRL best paper awards. He has been a Fellow of the American Physical Society since 1981.

WARREN PICKETT graduated from Wichita State University with a double major (B.S.) in physics and mathematics in 1969 and obtained an M.S. in physics there in 1971. He received his Ph.D. in physics from State University of New York (SUNY) at Stony Brook in 1975, one year of which was spent studying at the Cavendish Laboratory in Cambridge, England. After a series of postdoctoral appointments at the University of Bristol, England, at the University of California, Berkeley, and at Northwestern University, he joined NRL in late 1979. As a participant in the Advanced Graduate Research Program, he spent the academic year 1983-1984 at Daresbury Laboratory, England. Since joining the theory group in the X-ray Optics Branch in 1979 (presently the Complex Systems Theory Branch), Dr. Pickett has worked on a wide range of theoretical topics involving metals, semiconductors, and insulators. Providing a deeper theoretical understanding of the mechanism of superconductivity and suggesting ways of raising the critical temperature has been a favorite topic of research. His work centers on providing accurate numerical tests of theories, which require access to state-of-the-art computational facilities. He has used ten different supercomputers throughout the U.S. and Europe.

New Frontiers in Electronics at NRL

Gerald M. Borsuk
Electronics Science and Technology Division

Introduction

Electronics is a crucial ingredient of our successful Navy. Electronic systems form the backbone of the Navy's command, control, communications, radar, electronic warfare, surveillance, weapons, and data processing capabilities. To maximize the impact of its limited assets, either in diversity or force multiplication, the Navy depends on state-of-the-art electronics. Electronic components must be capable of surviving the harsh environments of radiation, high humidity, temperature extremes, and countermeasures by adversaries. For these reasons, the Navy maintains robust and forward-looking electronics programs. At the Naval Research Laboratory, these programs involve hands-on research across a broad spectrum of scientific and technological disciplines, and this article outlines the NRL effort that focuses on nonsystem electronics research.

New Materials for Electronics

The materials that are important for paving the way for future naval electronics components are semiconductor bulk crystals, epitaxially structured materials, and grown or deposited materials that are an integral part of the fabrication process. We are making progress in the areas of materials science and engineering, chemistry, and most recently, bioengineering.

Semiconductor Materials: Crystalline semiconductors form the common denominator in most solid-state electronics except for those niches applicable to superconductors and amorphous semiconductors. A convenient way to delineate research activities in semiconductors is to group them by bandgap, a key electronic attribute that controls critical electrical properties. Those semiconductors that have midrange bandgaps (1.1 to 1.6 eV) have the widest technological application. However, new growth and characterization tools and methods have increased opportunities for those semiconductors with "narrow" bandgap (<0.5 eV), "wide" bandgap (>2.2 eV), and the so-called "engineered" bandgap, where the bandgap is determined by the scientist. Bulk crystal materials form the host substrate for solid-state devices and circuits. The required physical properties of these materials include low surface dislocation density, lattice parameters that match those of any grown epitaxial layers, and well-characterized and controlled defects. Technological requirements include the ability to produce these materials in large volume, in large diameter wafers with well-controlled surface topographies, and at low cost relative to the total cost of wafer fabrication.

The two most technologically advanced bulk semiconductor materials for electronics are silicon (Si) and the compound semiconductor, gallium arsenide (GaAs). Silicon has been and will be the predominant starting material for digital, ultra-large-scale-circuit monolithic chips. Most silicon starting material is grown by the Czochralski method in which a boule of single crystal silicon is pulled from a silicon melt. The quality and availability (albeit from foreign sources) of this material are adequate for present and near-term extensions of military and commercial silicon-based technologies. GaAs, the starting material of most solid-state

radio-frequency (RF) and electro-optic technologies of importance to the Navy (and possibly future nanoelectronic technologies), is not as advanced as Si. Significant effort is expended by NRL to understand, control, and reduce defects and dislocations in GaAs, and important advances have recently been made to this end by the development of a vertical zone, melt-growth technique. This method of crystal growth serves to improve the purity of the crystalline material over that obtained by present liquid-encapsulated, Czochralski crystal-growth methods. In addition, this new method leads to reductions of dislocations and defects in the material by achieving a more uniform and controlled temperature distribution during solidification. This crystal growth method is being rapidly transitioned to industry under the sponsorship of the Microwave/Millimeter-wave Monolithic Integrated Circuit (MIMIC) Program. Research is under way to apply this crystal growth technique to cadmium telluride (CdTe)—a difficult material to grow in large quantity and high quality. Cadmium telluride is the starting material for a class of infrared focal-plane arrays used by the Navy for a host of imaging applications.

Epitaxial and Multilayered Semiconductor Materials: Nonequilibrium growth and synthesis techniques have produced new, artificially structured, epitaxial materials with unique electrical, optical, and mechanical properties. The ability to deposit multilayers of specific species of atoms or molecules on semiconductor substrates in the thickness of one atomic layer with a given stoichiometry will be the essence of electronic materials of the next century. The methods used to synthesize these multilayers include molecular beam epitaxy (MBE), metal-organic chemical-vapor deposition (MOCVD), liquid- and solid-phase epitaxy, and sputtering- and ion-beam deposition. Of these approaches, MBE is used most frequently in research that requires the greatest control over layer interface abruptness. MBE is a low-temperature, ultrahigh vacuum growth method. The major impediments in using it as a production technique are the slow growth rate of layers and the need for frequent recharging of constituent materials. However, metal-organic MBE techniques may allow the latter limitation to be circumvented by providing a continuous supply of reagents to the system without the need to break the vacuum integrity of the unit. MOCVD is a low (or atmospheric) pressure, low-temperature method for multilayer material deposition. This method holds great promise for economical production of layered materials for future solid-state devices because of its ability to deposit epitaxially controlled thin layers over large areas.

NRL has several major epitaxial growth programs centered around both MBE and MOCVD research systems. These multidisciplinary programs include research into growth science and technology, characterization of the physical and electronic properties of the materials, and growth of materials for device-physics research. One facility, the EPI-CENTER, a cooperative undertaking among personnel specializing in electronics science and others in materials science, is just becoming operational. In this facility, two isolated MBE systems, each growing epitaxial layers in different materials systems (one is solely for the growth of narrow bandgap III-V compound semiconductor materials while the other is solely for the growth of wide bandgap II-VI compound semiconductor materials) are connected by a common sample transport system in an ultrahigh-vacuum-transfer apparatus. Layered materials of a species grown in one MBE can be passed to the other MBE for layered growth of a radically different species, all within the confines of an ultrapure environment. The possible payoff will be new types of electronic devices—some having integrated functional capability and others having a unique functional capability to which there is no present analogue. Other MBE growth programs are centered on Si, GaAs (and its lattice-matched and strained-layered materials derivatives), and indium antimony (InSb). Research programs in MOCVD are under way to address a host of diverse

materials systems. They include major research efforts on GaAs and its derivatives, indium phosphide (InP) and its derivatives, silicon carbide (SiC), diamond, and yttrium barium copper oxide (YbBaCuO), a high-temperature superconductor.

Nanoelectronics

The convergence of interest of diverse scientific disciplines and evolving advanced electronics is nowhere as strong today as the drive to continue the downscaling of electronic solid-state components to ever smaller dimensions. The silicon transistor, and its incorporation into evermore complex, planar-digital integrated circuits, has been the key element driving the rapid advances in information, computer, and electronic technologies. These high technologies have been action multipliers for economic growth, productivity enhancement, and force multiplication for the Navy. However, there are technical signs that the powerful advantages gained in speed, power, and density achieved by the traditional device and circuit scaling of silicon-integrated circuits will be compromised as feature sizes reach the 0.2 μ m regime. The fabrication processes necessary to advance to and go beyond the 0.2 μ m regime are presently being put in place, and the ability to investigate the electronic, chemical, and physical properties of materials on an atomic scale is evolving at an astounding rate. The question becomes which will we have in the 21st century—continued exponential growth in the down scaling of solid-state devices and circuits to the nanoscale or a leveling off of feature-size reductions? In either case, the down scaling will proceed apace. If feature-size reduction does abate, new approaches will evolve for higher levels of integration. Wafer-scale integration and three-dimensional integrated circuits (ICs) are early manifestations of some of these approaches. However, there is much promise for continued feature-size reductions. Rapid scientific advances across a wide spectrum of technical areas are already paving the way for nanoelectronic components in electronic systems of the 21st century. NRL is an active participant and contributor to the scientific and technological aspects of nanoelectronics.

The NRL nanoelectronics program centers on the three cornerstones of the field: engineered semiconductor multilayer, thin-film materials; processing science; and novel device phenomena. Materials growth is centered on III-V materials systems and is an extension of the ongoing MBE research. The effort is being concentrated on "atomic layer" growth. Semiconductor layers are grown one atomic layer at a time to form sharper interfaces and possibly new crystalline stoichiometry, e.g., several atomic layers of Ga sandwiched between GaAs layers. The physical and electronic properties of such engineered layers are influenced strongly on the nanoscale by two-dimensional effects; however, in three dimensions, new phenomena are manifested. The processing science of nanofabrication, another area of intense research, requires maintaining the integrity of selected areas of the grown material while at the same time having the ability to form various sizes and shapes on and within the material. NRL is performing nanofabication research in both problem areas. Lithography on the nanoscale is being accomplished by using electron-beam exposure of resists. Figure 1 shows the principal tool for this work, a JEOL JBX-5DII. This tool, specifically designed for nanolithography, exposes resists using a 50-keV electron beam whose spot diameter can be as small as 80 Å. Figure 2 shows an example of a pattern of a 200-Å grid exposed by the JEOL in polymethyl methacrylate resist. Lithography research is also being conducted by using the low-energy (several eV) electrons from the tip of a scanning tunneling microscope (STM) as the means of exposure. Low-energy electrons do not cause the deleterious degradation of resolution created by the "straggling" that is present in resists exposed by high-energy electrons. But STM lithography is crucially dependent on the exposure sensitivity of

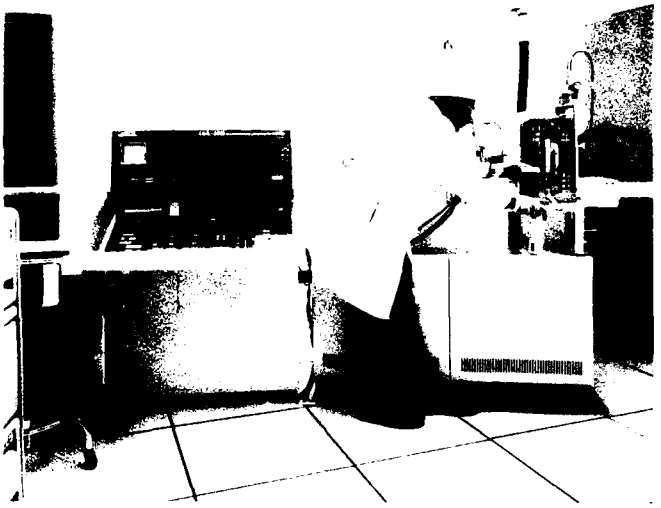

Fig. 1 — NRL's JEOL JBX-5DII electron beam nanofabrication tool

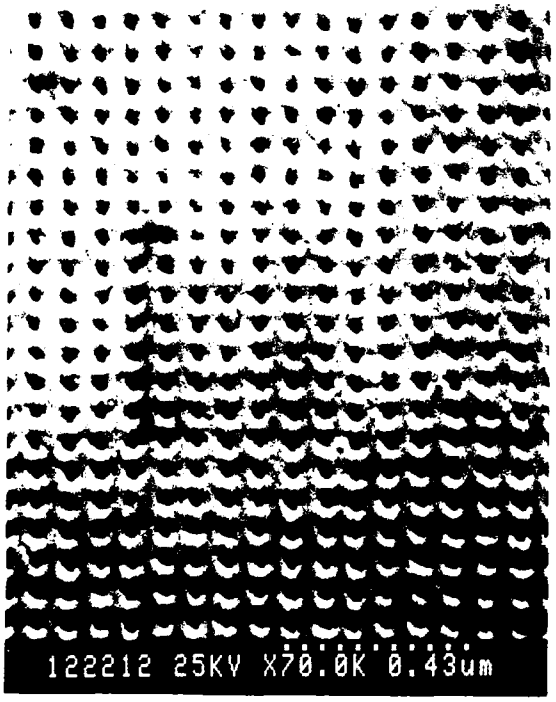

Fig. 2 — Pattern of a grid of 200-Å wires exposed in PMMA resist by the JBX-5DII

the resist because that determines the time it takes the beam to expose the pattern. Research is being conducted to understand exposure mechanisms in a host of novel resist materials, some formed by bioengineering. Figure 3 shows the patterning made by a vacuum STM. The feature size is 200 Å. As the feature size of novel material structures approaches the characteristic de Broglie wavelength of charge carriers in that medium, the wave nature of the charge carriers cannot be ignored. New phenomena, such as quantum-well confinement, resonant tunneling, large linear- and nonlinear-optical processes, and electron-wave function interactions, become apparent. These phenomena and others yet to be discovered will form the basis for nanoelectronic devices.

Microelectronics

The silicon digital integrated circuit is the driving force of the "high tech" revolution occurring in the second half of the 20th century, and in-house Department of Defense (DoD) laboratories are active participants in silicon technology research and development.

The NRL microelectronics research program addresses issues of principal military importance—the radiation effects and hardening of advanced materials and devices, the physics of failure, and the development of microelectronic components for highly efficient analog processing of sensor signals. An investigation into fundamental mechanisms of radiation degradation of silicon-metal-oxide semiconductor devices, a long-time Navy concern, is being persued as is

Fig. 3 — Pattern of 200 Å feature size exposed by a vacuum scanning tunneling microscope (STM)

research into new materials systems, such as silicon on insulator, using silicon MBE. Reliability of novel and emerging microfabricated electronic components is being assessed by investigating their physics of failure. This approach focuses on understanding how the fabrication process affects component reliability and identifies the physical mechanisms of electronic degradation.

A significant advantage in size, weight, and power can be achieved by processing complex sensor signals, e.g., "neural networks." However, well-known limitations to such circuits hinge on the ability to perform an accurate vector-matrix multiplication function. Novel device structures based on capacitive storage for setting the analog weight have been developed at NRL and Fig. 4 is a photomicrograph of an integrated circuit designed and tested here. The chip was fabricated using the MOSIS Si p-well complementary metal oxide semiconductor (CMOS) process.

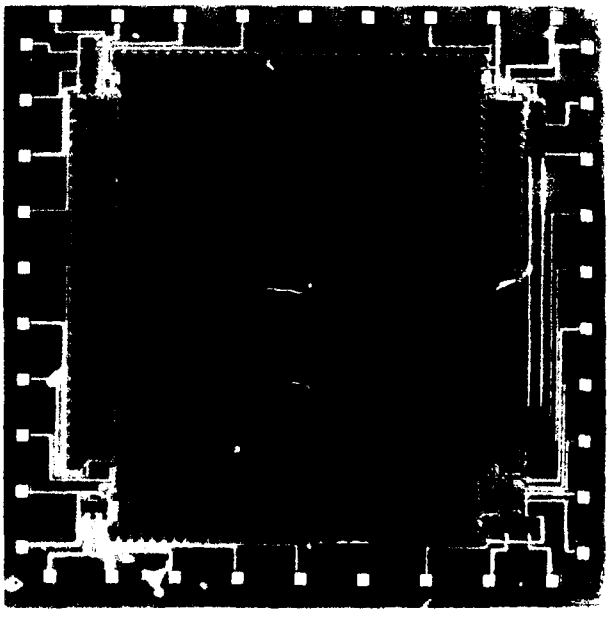

Fig. 4 — Photomicrograph of a neural network IC

RF Solid-State Heterostructure Components

Solid-state RF components have evolved over the last 20 years to fill an important niche in naval military systems. They are highly miniaturized as required in complex systems, use low voltages, and have proven reliability. Their electronic performance characteristics in the power-frequency regime (illustrated parametrically in Fig. 5) have set the standards for the state of the art. In the UHF- to F-band frequency range, silicon device technologies have proven adequate, and in the range of frequencies above 4 GHz, device technologies based on III-V materials have dominated. In particular, GaAs metal semiconductor field-effect transistor (MESFET) technology is predominate in both sensor and low-power RF applications in the microwave regime. In addition, indium phosphide two-terminal devices have dominated the millimeter-wave regime. Material advances, specifically in the area of epitaxial heterostructures formed by MBE, have set the stage for a new generation of devices, which have shown improved performance at both microwave and millimeter-wave frequencies. This family of emerging high-frequency heterostructure devices includes modulation-doped field-effect transistors, resonant tunneling diodes, and heterojunction bipolar transistors.

The research work at NRL in the area of high-frequency, solid-state devices includes the fundamental material growth and characterization efforts described earlier and basic research into novel heterostructures, such as quantum well and superlattice. Applied research devices fabricated and tested at NRL include SiC-junction FETs, GaAs/AlGaAs-modulation-doped FETs and digital IC-test circuits, InGaAs/InP-pseudomorphic-modulation-doped FETs, and GaAs optoelectric detector amplifier arrays.

Vacuum Electronics

Microwave- and millimeter-wave vacuum-power tubes are the basic building blocks in the majority of the Navy's active radiating electronics systems. Figure 5 shows that these devices provide coherent RF source capabilities in a range of frequencies that are not accessible by other technologies.

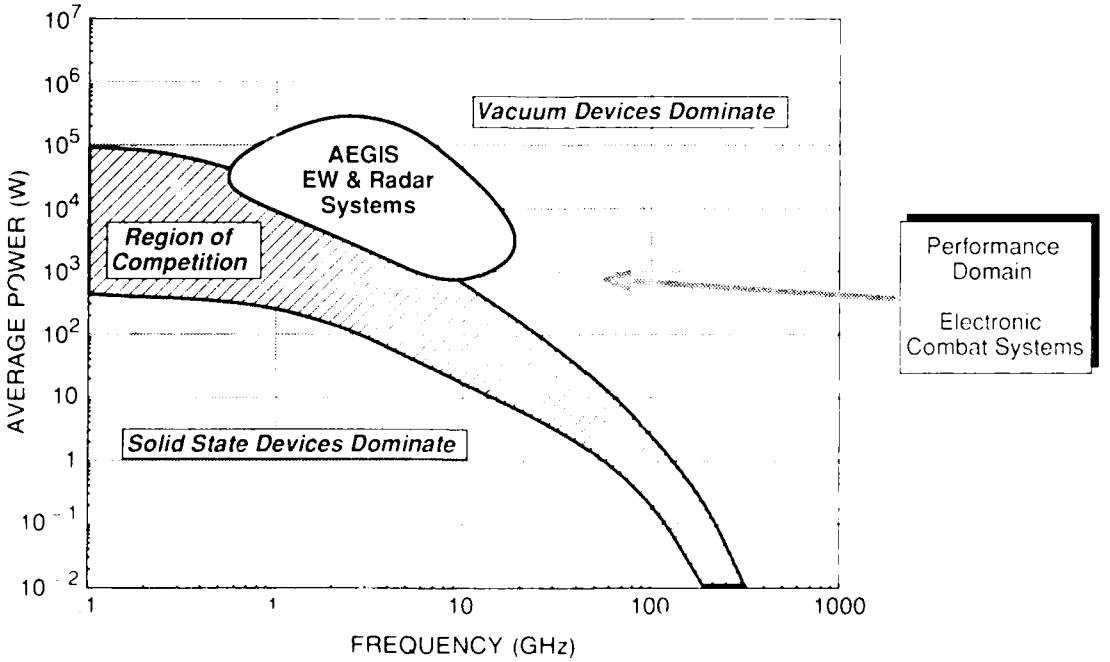

Fig. 5 — A frequency-power parametric plot showing the areas of predominance for vacuum and solid-state electronics

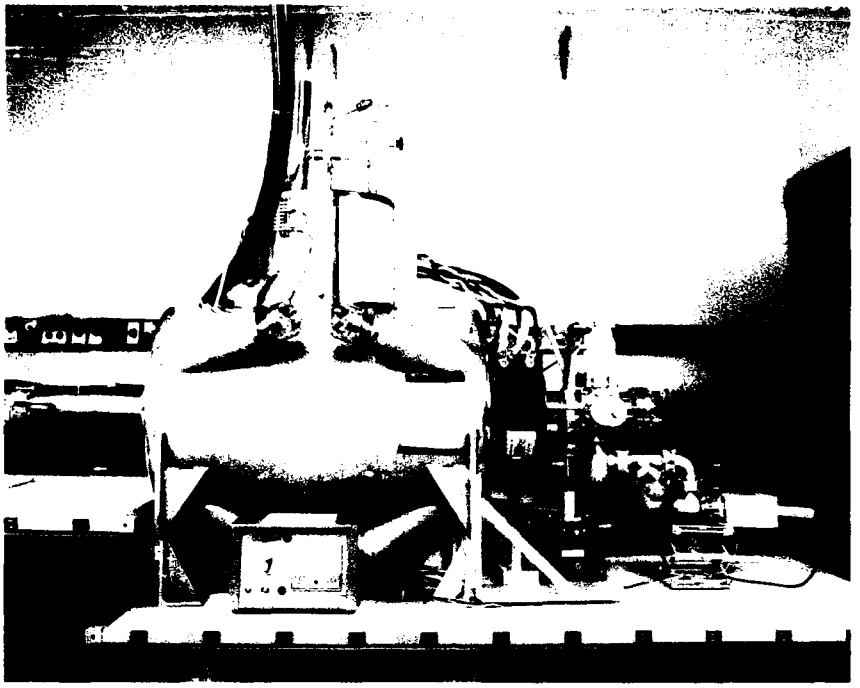

Fig. 6 — A Ka-band gyrotron-TWT fast-wave millimeter amplifier

Besides maintaining the technology-base expertise in vacuum electronics, NRL is actively developing high-power, millimeter-wave, fast-wave amplifiers, integrating advanced scientific electromagnetic computer codes to the design of vacuum electronic devices, and researching the scientific and technological aspects of vacuum microelectronics. An example of a fast-wave amplifier being actively investigated by NRL is the tapered gyrotron traveling wave tube shown in Fig. 6. The device constructed here is a wideband millimeter-wave, high-power amplifier for possible use in Navy electronic warfare and point defense radar applications. It is a cyclotron resonant device that incorporates axial tapering of both the interaction circuit and the magnetic field for broadband, low-voltage operation. Initial experiments explored the basic stability limits of the device in a single-stage, reflection-type configuration. Subsequent tests of a second-generation device have been operated stably at full beam current providing a significant small-signal gain over a wide bandwidth at millimeter-wave frequencies with a peak power output of 1.6 kW.

Optoelectronics

Optoelectronics research is a generic activity pursued in several divisions at NRL; this section addresses only IR-imaging, solid-state sensors because of a large electronics involvement. In the last 25 years, there has been a tremendous increase in the use of the IR region of the electromagnetic spectrum (from 3 to 5 μ m and 8 to 12 μ m in wavelength) to enhance Navy capabilities. Sensors operating in these bands have high payoff for the Navy in missile guidance (for example, the Navy-developed Sidewinder air-to-air missile), search and track, threat warning, and passive surveillance. IR-sensor technology has evolved from single detector elements to the present-day approach of a focal plane array wherein many detector elements are placed together in a two-dimensional planar architecture by using integrated circuit (IC) technology. The two major variants of this focal plane array technology are hybrid arrays and monolithic arrays. Hybrid arrays consist of a two-dimensional array of mercury-cadmium-telluride (HgCdTe)

IR-sensitive photodiodes connected to a two-dimensional Si multiplexer IC by indium bump connectors. The monolithic IR focal plane array technology uses either InSb or HgCdTe materials in an integrated array. These arrays have the unique property that both the sensor and electrical signal output circuits are together on the same chip. Both approaches, however, are limited in array size by the quality and uniformity of the IR-sensitive materials.

The NRL electronics research program has two separate thrusts. One program is devoted to investigating reliability and radiation effects in advanced IR focal-plane arrays fabricated under contract to the Laboratory. This work addresses both fundamental mechanisms of failure in Si ICs at cryogenic temperatures as well as the interfacial properties of HgCdTe sensor materials at these temperatures. The other basic research thrust is centered on the epitaxial growth by MBE and characterization of a host of non-mercury-based compound semiconductors. One of these new materials systems being investigated may allow the fabrication of large, focal-plane arrays with both high sensitivity and uniformity. This development would give the Navy new sensor capability in this important part of the electromagnetic spectrum.

Advanced Development Programs

NRL plays an important DoD role in executing five major advanced-development electronics programs. They are the MIMIC Program, the Infrared Focal Plane Array Producibility Program, the National X-ray Lithography Program, the Navy's AEGIS Cross-Field Amplifier Program, and the NRL High-Temperature Superconductor Space Experiment Program. In these seemingly unrelated programs, the common thread of Laboratory participation is to promote the rapid insertion of diverse advanced electronics technologies into Navy and DoD systems.

The MIMIC Program, a DARPA/Tri-Service effort, was established to develop an affordable microwave and millimeter-wave monolithic IC chip technology. The genesis of this program has deep and diverse roots in the DoD solid-state RF community, including the Navy's exploratory development program. In the mid-1980s, the Navy sponsored an industrial effort to develop "affordable" monolithic microwave integrated circuits (MMICs). It was clear to NRL's scientists and engineers that the fabrication methodology of Si IC mass production needed to be applied to the fledgling microwave GaAs IC technology. This was deemed a prerequisite to achieve components inexpensive enough to be used in the great numbers required for new radar, communications, electronic warfare, and smart weapons being designed by NRL system engineers and others in the U.S. defense community. Figure 7 shows a representative GaAs MIMIC. This chip is one of several being produced by the Navy's MIMIC contractor for use in an electronic-warfare demonstration brassboard.

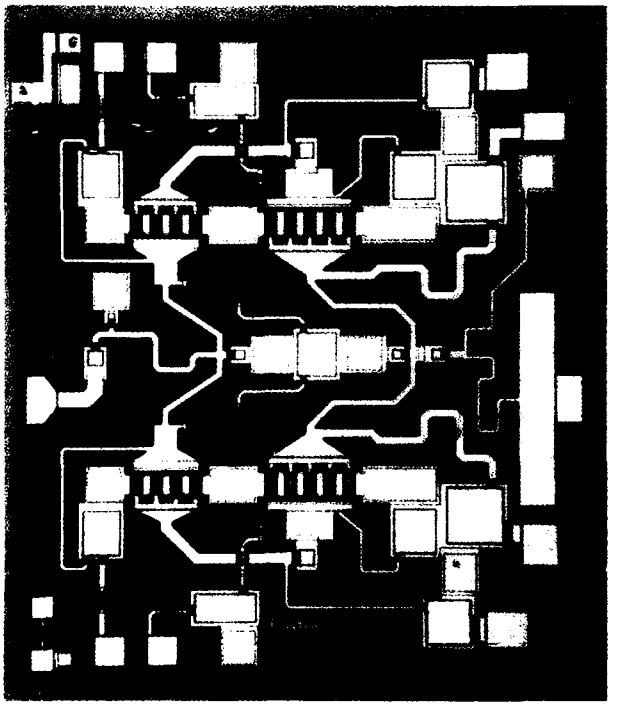

Fig. 7 — A GaAs monolithic microwave-integrated circuit fabricated on the Navy's MIMIC Program by a Raytheon/Texas Instruments joint venture

An important in-house program performed by NRL scientists in support of the MIMIC Program is to test the contractor-produced ICs to ensure that they meet performance specifications and are suitable for use in a military environment. By determining the physics of failure, NRL scientists identify basic failure mechanisms and radiation effects, thus ensuring the development of MIMICs that will meet the harsh temperature, shock, and radiation environments experienced by Navy electronic systems in the field.

The Infrared Focal Plane Producibility Program is also a DARPA Tri-Service effort—to improve the yield of solid-state IR focal-plane arrays used in military systems to make them more available and affordable. Two IR focal-plane array technologies are being pursued. They are the platinum (Pt)-silicide charge-couple device array mid-wavelength technology for very low cost, smart weapons; and the HgCdTe long-wavelength technology for search and track, missile seekers, surveillance, and passive imaging forward-looking infrared. The Navy's program is administered by the Office of Naval Technology. NRL provides technical support and in-house evaluation of contractor-produced components for performance verification and reliability testing.

The National X-ray Lithography Program is a DARPA-sponsored program aimed at establishing an entirely new approach to lithography for the next generation of submicrometer microelectronic ICs. The program originated at NRL, where leading-edge research has been performed in X-ray sources and lithographic materials. A number of government laboratories, universities, and the industrial community are participating in this effort. Major development thrusts are the creation of a viable production-oriented X-ray mask technology, demonstration of these technologies in an IC-manufacturing environment, and the transition of X-ray lithography to the domestic IC manufacturing community. The latter is achieved by establishing resource centers for X-ray mask fabrication and wafer exposure. Besides NRL's technical management of the program, work is also ongoing here to pattern X-ray masks by using the JEOL electron-beam nanolithography tool and to determine the properties of bioengineered monolayer resists. Figure 8 shows a scanning electron microscope of an X-ray mask test structure patterned by the NRL JEOL.

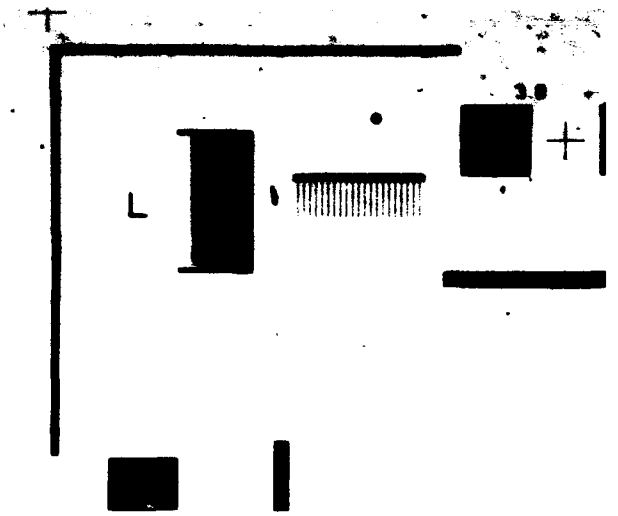

Fig. 8 — A transmission-electron-microscope photomicrograph of an X-ray test-mask structure patterned by the JEOL at NRL

The Navy's *Ticonderoga* class cruiser, expected to serve well into the 21st century, uses the AEGIS SPY-1 radar system as an integral part of its weapons system in defense of the battle group. Recognizing the continual need to improve capability in this sophisticated system, the Navy is planning to insert products of several newly evolving technological advances. One of these concerns vacuum tubes. The SPY-1 radar uses the largest number of RF power tubes of any fielded DoD system. Advanced tubes made by NRL's exploratory development efforts in cathode driven, cross-field amplifier tube technology will be inserted into a production upgrade of the SPY-1 radar. These tubes promise more RF output power and superior noise characteristics than present components. These improvements will give the AEGIS system the new capability to meet air-attack threats of the 21st century.

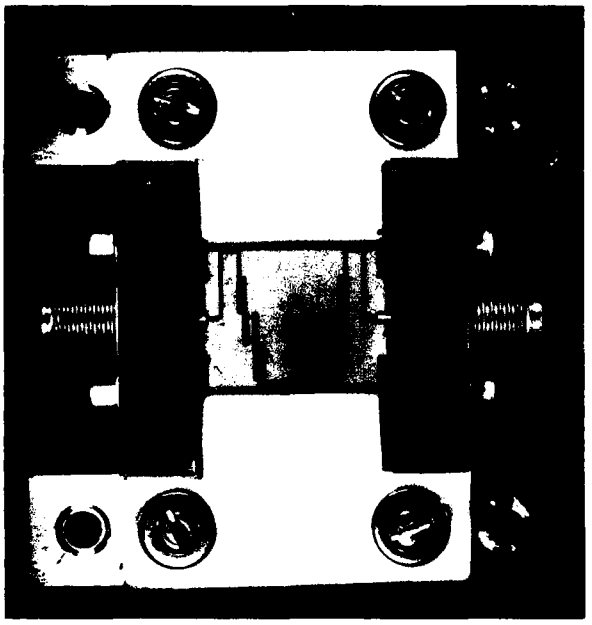

Fig. 9 — A stripline microwave bandpass filter using a high-temperature YBCO thin film conductor element

The discovery in 1986 of a new class of ceramic superconductors with high transition temperatures set off a worldwide scramble in the scientific community to learn more about these materials. To rapidly transition new, high-temperature superconductor technologies into demonstrable applications of devices with military relevance, NRL established the High Temperature Superconductor Space Experiment Program. The space environment is one in which the benefits of low temperature come about naturally, but it is also a hostile environment, promising to offer a significant test of any newly developed devices. An early and promising application for these materials is in thin-film form for passive microwave electronic components. It is possible to achieve superior sensitivity, selectivity, and power management in sensor systems employing these materials. Figure 9 shows an example of the advances made in these areas at NRL. This device is a stripline microwave frequency bandpass filter formed in a laser ablated thin film of yttrium barium copper oxide. Figure 10 shows the performance of this device in the range from 9.5 to 11.5 GHz when cooled to low temperature. These and similar results for other microwave passive components made from high-temperature superconductor materials are very encouraging. These devices and other high - temperature

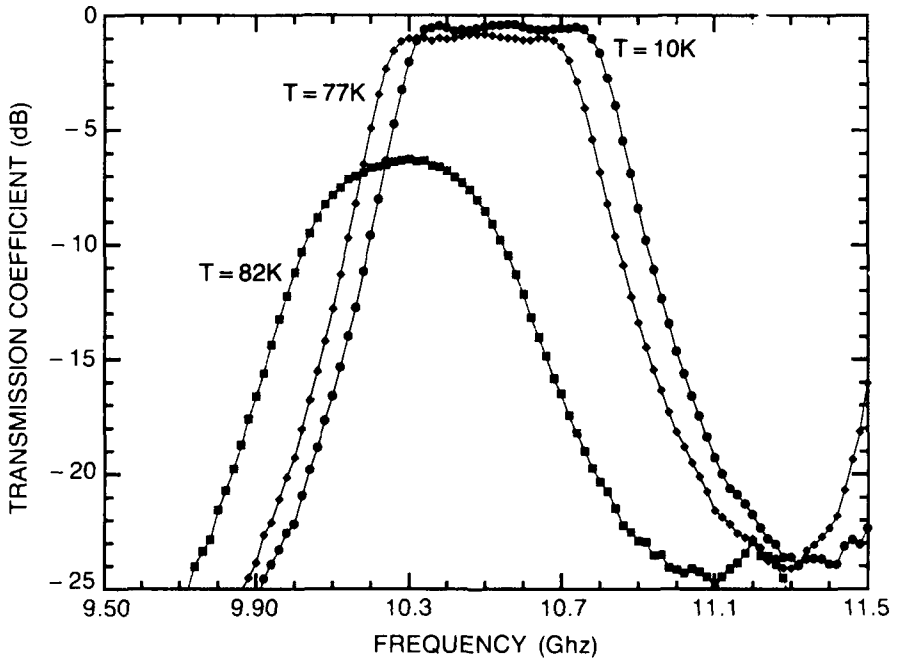

Fig. 10 — The microwave performance of the superconductor microstrip bandpass filter. Notice the sharp filter skirts and low insertion loss when the device is cooled to liquid nitrogen's temperature of 77 K.

superconductor experiments are scheduled for satellite launch into Earth's orbit in 1992.

Conclusions

NRL leads research in many important areas of electronics ranging from basic materials to sophisticated devices and circuits. This knowledge base has found important applications in formulating and executing major Navy and DoD programs. The contribution to scientific knowledge in electronics and the translation of such contributions into military programs are two ways NRL continues to prove its value to the Navy and the Nation.

Acknowledgments

I gratefully acknowledge and thank the contributors from the Electronics Science and Technology Division staff to this article; Fig. 2 by E. Dobisz and M.C. Peckerar; Fig. 3 by C.K. Marrian; Fig. 4 by F. Kub; Fig. 5 by R. Parker; Fig. 6 by C. Armstrong, Fig. 8 by M.C. Peckerar; and Figs. 9 and 10 by J. Pond, H. Newman, L. Allen, and D. Chrisy.

THE AUTHOR

GERALD M. BORSUK is the Superintendent of the Electronics Science and Technology Division. In this position he is responsible for the in-house execution of a multidisciplinary program of basic and applied research into electronic materials and structures, solid-state devices, vacuum electronics, and circuits. He serves as the Office of Naval Research (ONR) Subelement Monitor for Electronics and as the Block Manager for the Navy's principal exploratory development program in electronics. He is the Navy's Deputy Program Manager and Technical Director for the DARPA/Tri-Service MIMIC Program.

Dr. Borsuk received a Ph. D. in Physics from Georgetown University in 1973. He then joined the Electro-Physics Laboratory in Columbia, Maryland, as a staff physicist, where he worked on the use of charge-coupled devices for imaging and signal-processing applications. In 1976, he joined the Westinghouse Advanced Technology Laboratory in Baltimore, Maryland, where he worked on silicon integrated circuits and device physics. He performed original work in photodetectors used with acousto-optic processors, and he headed the Westinghouse VHSIC effort in advanced submicron VLSI device technology. Dr. Borsuk was department manager of solid-state sciences when he left Westinghouse in 1983 to join the Naval Research Laboratory as the Superintendent of the Electronics Science and Technology Division.

Dr. Borsuk has 35 technical publications and seven patents. He is a Senior Member of the IEEE, a member of the American Physical Society, a member of the Sigma Xi, and the Navy's Deputy Member to the Advisory Group on Electron Devices (AGED). Dr. Borsuk also serves on the Editorial Board of the IEEE Proceedings.

Global Weather Observations with the SSM/I

James Hollinger and Glenn Sandlin
Space Systems Technology Department

Introduction

The modern Navy's high-technology systems and global operations have an ever-increasing dependence on detailed knowledge of surface and weather conditions. Remote sensing of environmental parameters from space is the most timely and cost-effective way to obtain this information. The polar-orbiting, Special Sensor Microwave/Imager (SSM/I) is a joint Navy/Air Force operational instrument that measures critical atmospheric, oceanographic, and land parameters both day and night on a global scale. The SSM/I retrieves near real-time synoptic maps over the ocean of cloud concentration and water content, precipitation, humidity, marine windspeed, and sea-ice location, age, and concentration. Further, the SSM/I provides measurements of land-surface temperature, snow-water content, soil moisture, and precipitation over land for military, agricultural, and geological purposes. Table 1 gives a summary of the environmental parameters retrieved by the SSM/I along with the spatial resolution, parameter range, and accuracy information.

Table 1 — Environmental Parameters Retrieved by the SSM/I

Parameter	Geometric Resolution (km)	Range Values	Quantization Levels	Absolute Accuracy
Ocean Surface Wind Speed	25	3 to 25 m/s	1	± 2 m/s
Ice				
° Area Covered	25	0 to 100%	5	± 12%
° Age	50	1st year, multiyear	1 yr, >2 yr	None
° Edge Location	25	N/A	N/A	± 12.5 km
Precipitation Over Land Areas	25	0 to 25 mm/h	0, 5, 10, 15, 20, ≥ 25	± 5 mm/h
Cloud Water	25	0 to 1 kg/m^2	0.05	± 0.1 kg/m^2
Integrated Water Vapor	25	0 to 80 kg/m^2	0.10	± 2.0 kg/m^2
Precipitation Over Water	25	0 to 25 kg/m^2	0, 5, 10, 15, 20, ≥ 25	± 5 mm/h
Soil Moisture	50	0 to 60%	1	None
Land Surface Temperature	25	180 to 340 K	1	None
Snow Water Content	25	0 to 50 cm	1	± 3 cm
Surface Type	25	12 types	N/A	N/A
Cloud Amount	25	0 to 100%	1	± 20%

The first SSM/I was launched in June 1987 aboard the Defense Meteorological Satellite Program Block 5D-2 Spacecraft F8 (Fig. 1). The SSM/I is a seven-channel, four-frequency (19.35, 22.235, 37.0 and 85.5 GHz), linearly polarized, radiometric system. The SSM/I incorporates several innovations that result in improved performance compared to previous satellite based, microwave-radiometric systems. These include (1) the first satellite-based, high-resolution, 85 GHz radiometer; (2) an accurate, end-to-end, absolute calibration scheme including the feedhorn that results in excellent stability and repeatability; and (3) the use of a total power radiometer that provides a factor of 2 improvement in sensitivity over conventional "Dicke" switched radiometers. The sensitivity to brightness temperatures for all operating channels ranges from about 0.4 to 0.8 K, and the long-term (1987 to 1989) repeatability level is better than 1 K. Since the dynamic range of radiometric temperatures within weather systems, particularly storms, can exceed 200 K at 85 GHz, the SSM/I provides excellent dynamic resolution of the internal physical processes in the atmosphere. Because of the high stability of the SSM/I, long term effects of wind, rain, or fire damage to terrain, which may be recorded as temperature differences within a range of about 10 K, also may be observed and analyzed at surface resolutions up to 12.5 km or better. Figure 2 illustrates the concentric scan geometry of the SSM/I. Figure 3 presents a view of the world at 19.35 GHz.

Remote Sensing with Microwaves

Microwave remote sensing originated in the 1960s. It is new compared with aerial visual photography that has been used for over 100 years and aerial optical spectroscopy that has been in use for over 40 years. The successful use of visual and infrared (IR) photography, and more recently of Geostationary Operational Environmental Satellite (GOES), Advanced Very-High Resolution Radiometer (AVHRR), and LANDSAT images from space, is well known. Microwave radiometry has the advantages that microwave radiation penetrates clouds and vegetation, is independent of solar illumination, and provides information complementary to that available in the visible and IR regions.

The radiation emitted by Earth, which has an average surface temperature of 288 K, is predominantly in the IR and microwave portions of the spectrum. The measured intensity (brightness temperature) of the radiation is a function of frequency, polarization, incidence angle, emissivity of the scene, and transmission through and radiation by the atmosphere. Since atmospheric water vapor and clouds are more absorptive at IR than at microwave frequencies, a microwave sensor receives a proportionally greater amount of the radiation from the surface and lower atmosphere. Ice clouds (cirrus) that are dense enough to completely obscure the ground optically and at IR frequencies are almost completely transparent to microwaves. Not only is visual radiation almost completely reflected, scattered, or absorbed by clouds and aerosols, but a large fraction of the total upwelling radiance is from the atmosphere, making visual spectroscopy of the surface difficult. Even in the IR primary atmospheric windows, aerosols, water vapor, and unresolved clouds in apparently cloud-free areas emit, reflect, and scatter radiation that obscures the signal from below. High-contrast microwave maps of areas, such as Greenland and Antarctica, can be produced day or night with almost no cloud effect. The effect of clouds on the transmission of microwaves increases with decreasing wavelength so that microwave radiation measured by the SSM/I in the range of 1.5 to 0.3 cm contains information about cloud water content. Thus the SSM/I can sense the type of land or ice and the sea surface roughness beneath the clouds, as well as the atmospheric water content.

The physical state and amount of water in Earth's atmosphere and on its surface provides

Fig. 1 — DMSP Block 5D-2 satellite

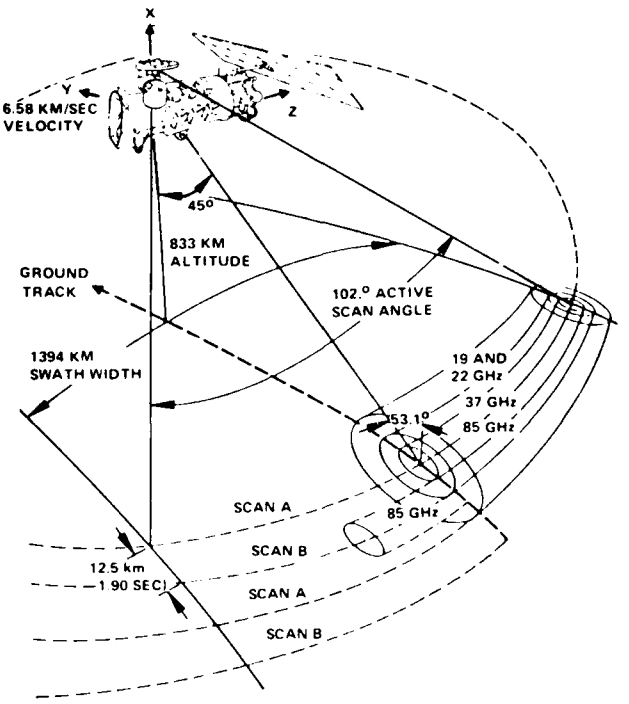

Fig. 2 — SSM/I scan geometry

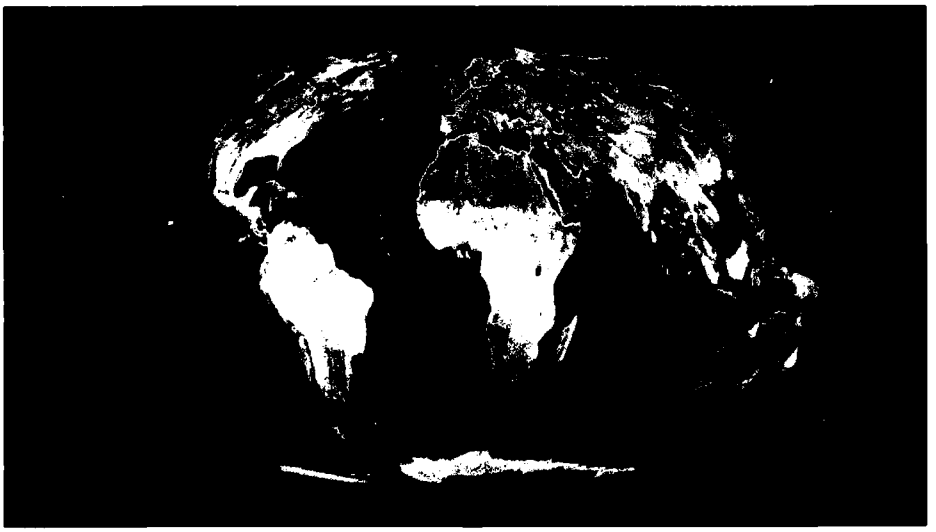

Fig. 3 — World view at 19.3 GHz

valuable information about the energy processes associated with the hydrological cycle—a major determinant of climate. Since microwave transmission is sensitive to the physical state of water in the medium observed, the microwave spectrum is dependent upon humidity, clouds, and rain and is ideal for the remote sensing of Earth's weather. The microwave intensity of a scene also depends upon the properties of the surface. For example, the microwave emissivity of the ocean increases with the surface roughness caused by wind, allowing the remote determination of marine wind speed. Further, the emissivity of sea ice is dramatically higher for first year ice than for multiyear ice, and the microwave radiation from the land depends upon soil moisture, snow water content, vegetation, and surface type. Through proper choice of instrumental parameters (wavelength, polarization, and viewing angle), it is possible to establish useful relations between the brightness temperatures measured by the multifrequency radiometers and specific terrestrial or atmospheric parameters of interest.

Naval Research Laboratory (NRL) Contributions

NRL has made significant contributions to the science of microwave remote sensing (active and passive) since the original development of radar at NRL beginning in 1922. Radiometric techniques have been used in extraterrestrial observations since the 1940s and in terrestrial observations since the late 1960s. In 1968, NRL made the first observations verifying the dependence of microwave radiation on capillary waves (a few centimeters in length and a few millimeters in height) and sea foam, a dependence that allows the remote determination of marine windspeed. During the 1970s and 1980s, numerous original field experiments were conducted to evaluate the use of passive microwave sensors for meteorological, oceanographic, and military applications. For example, in 1973 and 1974, NRL demonstrated that multifrequency passive microwave techniques could be used to determine oil-slick thickness and to direct oil cleanup operations. In the same years, NRL made the first microwave measurements of sea-ice characteristics over a wide frequency range. In the 1980s, NRL's airborne measurements at millimeter wavelengths were formative in defining the SSM/I. NRL led the multidisciplinary team that conducted the DMSP SSM/I calibration/validation effort to ensure that the instrument and the environmental retrieval algorithms performed within specifications.

An important contribution of the SSM/I is that all of its products can be measured quantitatively and consistently on a global scale, including regions where measurements of these products would not exist otherwise. The products of Table 1 are sent routinely to the National Environmental Satellite Data and Information Service for archival purposes and are available to the public. Figure 4 shows examples of the gridded products in the world maps.

SSM/I Observations of Tropical Storms

A major feature of the hydrological cycle is the equatorial trough, or Intertropical Convergence Zone (ITCZ), where the atmospheric energy and water (vapor, cloud, and rain) are greatest (shown in Fig. 4). The ITCZ normally is partitioned into clusters of clouds, each several hundred kilometers across, where the atmospheric energy is the most turbulent. About one in ten of the cloud clusters of the ITCZ may deepen into a tropical cyclone. A tropical cyclone is named as a tropical storm when the maximum sustained windspeed reaches 17.5 m/s (35 knots) and as a full hurricane or typhoon when the windspeed exceeds 33 m/s (66 knots). Approximately 60 typhoons or tropical storms occur in the Pacific each year, and about 10 occur in the Atlantic and Caribbean. Of these, about 20 affect Department of Defense installations and 3 affect the U.S. mainland. Tropical cyclones, on approaching landfall, may inundate the coastal region with oceanic storm surges as high as

4 to 8 m, causing heavy losses of lives and property. Seven storms, each wreaking damage estimated in excess of $1 billion, have struck the United States since 1972.

The SSM/I has monitored the development and course of 75% of the tropical storms that have occurred since the launch of the DMSP. The SSM/I completes 14.1 revolutions per day along a sun-synchronous track above the solar terminator. With an observational swath width of 1400 km, there is an 89% probability of viewing a storm in the tropics at least once a day. A second SSM/I, scheduled for launch in 1990, will increase the probability to 99%. Because the microwave radiation from storms can penetrate the dense overlying cirrus clouds, it reveals physical details not always depicted by visible and IR images, including the eye of the vortex and the structure of deeply convective regions (for example, Fig. 5). The locations of storms at sea can be fixed with greater precision and consistency by the SSM/I than is permitted by conventional imagery. When the windspeeds are contoured, the thirty-knot radii delineating the near-gale warning line for ships at sea can be determined quickly and routinely, day or night (Fig. 5). Wind directions can be computed simply from the SSM/I windspeeds and the pressure gradients read from 1000-mb synoptic sea-surface charts (as seen in Fig. 6). Furthermore, when the SSM/I images are enhanced with the digital color-image processing developed at NRL (Figs. 5, 7, and 8), they greatly augment other techniques for analyzing the physical processes in storms.

The most damaging hurricane ever to strike the U.S. mainland—Hugo (Fig. 7)—was tracked by the SSM/I in near real time. Within 3 hours of the overpass of the SSM/I, windspeed data were relayed to the Naval Eastern Oceanography Center (NEOC) in Norfolk, Virginia, to be included in the marine weather updates until landfall. After landfall, tracking with the SSM/I imagery continued until Hugo ceased to be a tropical storm. The SSM/I products were valuable not only in tracking the storm but in assessing the damage as well. Figures 8 and 9 portray a small part of the Hugo event and its effect on the eastern seaboard.

Tracking the Storm

Forecasters need accurate information on a storm's past and current location and strength to predict the storm track and intensity over 1 to 3-day periods. Historically, a precise fix on the storm's position could be provided by a WC-130 aircraft flying into the eye of the storm to obtain temperature, humidity, and barometric pressure data. In recent years, satellite imagery has been used as an aid in locating the eye and in determining the storm's intensity from cloud patterns (the Dvorak technique). Visual and IR imagery have been provided by civilian satellites, such as GOES. These views, however, tend to be limited to the top and middle levels of a storm. Microwave imagery is three dimensional and more heavily weighted toward the surface. Analyses by NRL and field work by the Joint Typhoon Warning Center (JTWC) indicate that the SSM/I products increase the precision of tracking by satellite to a level approaching that of all previous techniques combined.

The primary determinant of the precision in tracking is the forecaster's ability to locate the center of the eye at the surface—defined as the point of lowest pressure at that level. Since SSM/I imagery is primarily of the low atmosphere, many of the atmospheric products are useful for an interpretation of the storm's structure near the surface. An enhanced image of 85.5 GHz radiation reveals both the eye and the atmospheric windstreaming in the planetary boundary layer with 12-km resolution. Both imagery and wind vectors define the windstreaming. Alternatively, the center can be located in images of SSM/I retrievals of cloud water and water vapor with an uncertainty on the order 12 to 25 km.

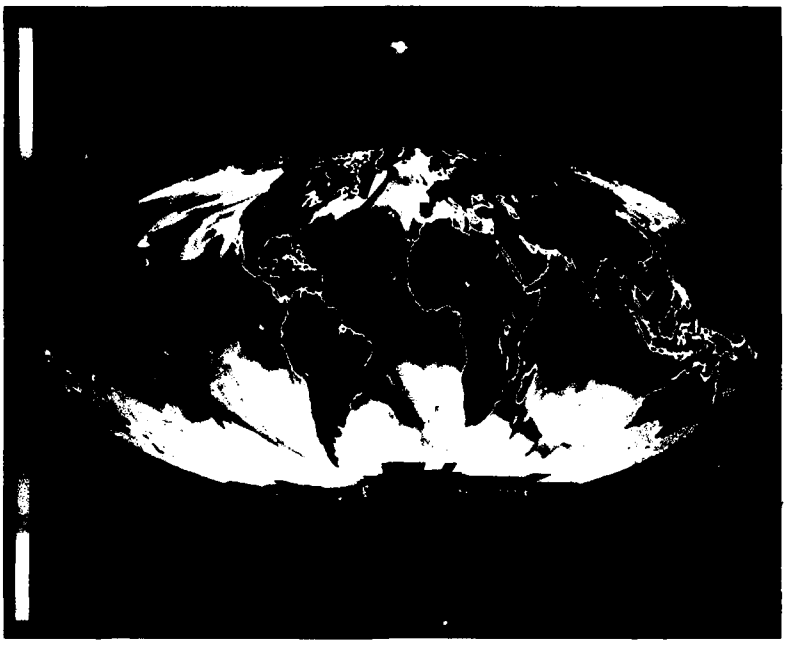

(a)

(b)

Fig. 4 — SSM/I global maps of (a) water vapor, (b) cloud liquid water (CLW), (c) rain rates, and (d) marine windspeed as displayed in the ranges and accuracies of Table 1. (The dark gray areas correspond to locations where the environmental product was not retrieved, except for (b) where rain rate was retrieved over land.) The Mollweide equal-area projection is composed of SSM/I data from 58 consecutive revolutions of the DMSP over the period, 7 to 10 October 1989. They illustrate the overall microwave view of the global circulation system and major features of the hydrological cycle. Water vapor, CLW, and rain typically tend toward maxima in the equatorial regions where solar heating is greatest. For example, two-thirds of global precipitation (annual average 1 m) falls in the tropics and subtropics. The condensation of water vapor to CLW and rain releases heat inside the atmosphere, and this is a principal driver for the global-scale motions in the troposphere, as evident in the wind and water-vapor maps. This process concentrates the tropical rainfall into a latitudinally thin region called the intertropical convergence zone (ITCZ), and also generates the worldwide meridional circulation that restricts the latitudinal temperature gradients (see Fig. 3) and the prevailing wind intensities (average 10 m/s). The ITCZ generally is partitioned into about 30 individual cloud clusters, each several hundred

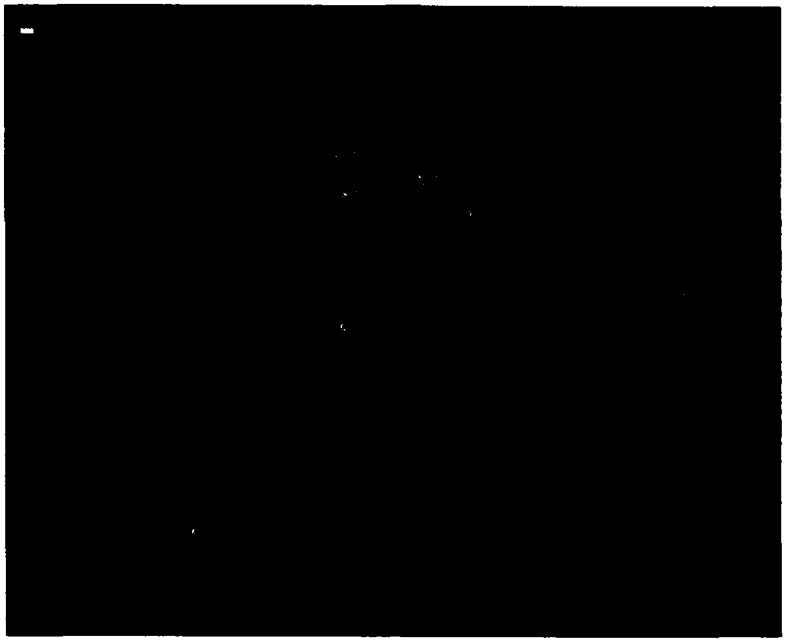

(c)

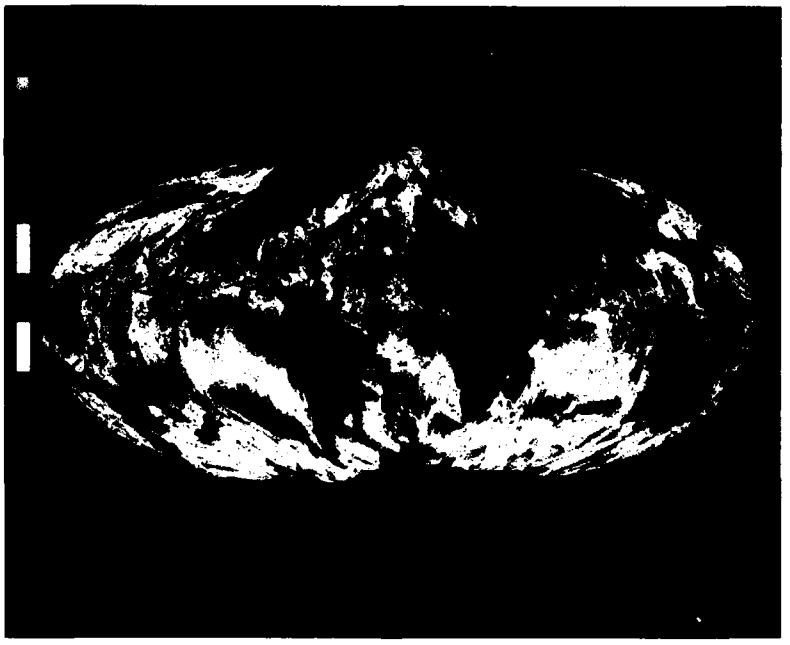

(d)

(Continued)
kilometers across and each triggered or modulated by local inhomogeneities in the winds and lower boundary conditions. Convection within the cloud clusters is enhanced (where CLW is 0.3 to 1.0 kg/m^2) in numerous cumulonimbus "hot towers" that are essential in driving the meridional circulation and in forming tropical cyclones. About one in ten of the cloud clusters deepens into a tropical cyclone in certain favored locations within the ITCZ, where wind, water vapor, CLW, and rain are concentrated into a storm. They are identified by the red regions in (a) where the columnar CLW derivatives are about 1.0 kg/m^2 or greater. For example, the red region off the coast of Florida locates Tropical Storm Jerry, which followed Hurricane Hugo. The Atlantic frontal system receding eastward from Nova Scotia is what remains of the dissipated Hugo, which had followed a track curving northward over land from Charleston, SC, along the Appalachian Mountains to the Great Lakes. The rain from tropical cyclones may be as much as 35% of the annual average rain in many parts of the tropics and subtropics; consequently, they are important to the ecology and well-being of certain tropical countries. Japan considers itself a nation "blessed by typhoons."

(a) — Operational Linescan System (OLS) visual image for Typhoon Sperry, 29 June 1987

(b) — Typhoon Sperry at 85 GHz (horizontal) 29 June 1987

Fig. 5 — Comparison of microwave and visual imagery of Typhoon Sperry. The SSM/I reveals storms hidden by clouds or darkness. Figure 3(a) shows Typhoon Sperry, partially seen in visible light at local sunset time near the Philippines on 29 June 1987. The core of the storm, as well as thunderclouds outside the gale envelope, and the island of Mindanao (lower left) are veiled by the dense overlying cirrus clouds at 50,000 ft. To the east (right), much of the lower atmosphere is hidden in the darkness behind the setting sun. The SSM/I senses the scene below 50,000 ft and produces (b) a detailed microwave (85.5 GHz) image of the eye and eyewall of the Typhoon Mindanao (white) in the southwest, and the band of thunderclouds (numbered 1 to 6) streaming from the direction of Mindanao (under cloud 6) toward the southeastern flank of the typhoon. The brighter colored parts of the thunderclouds are deeply convective regions containing rain and hail, The darker outside regions indicate precipitation that is likely to be mostly rain. The SSM/I also permits a view of the lower level clouds and windstreaming in the darkness to the east. In the upper right and left corners of the image, frontal lines separate the humid cyclonic air from the drier, high-pressure regions through which the typhoon is passing. The orange isopleth is the near-gale warning line; note that it lies outside the rain flagged region identified by the green isopleth.

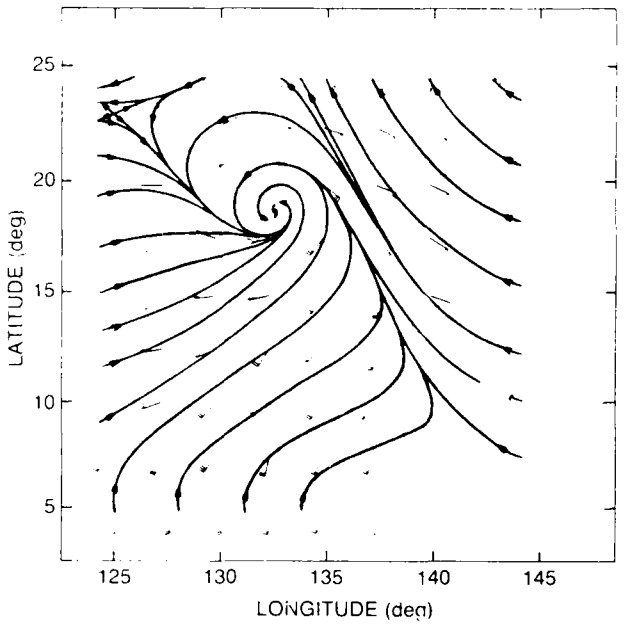

Fig. 6 — SSM/I wind field for Typhoon Sperry. By use of a new technique, wind directions within a typhoon have been determined from space with the use of passive microwave radiometers. The sea surface roughness, sensed through the cirrus clouds, provided information about the frictional force reacting against the wind at the surface of the troposphere. When the frictional force was quantized in terms of the derived windspeeds, the direction of the wind could be computed with the application of Ekman boundary layer dynamics. Wind directions and speeds are presented in standard meteorological notation. Air Force Global Weather Central has independently determined the streamlines of the wind for Sperry based on ship reports and aircraft reconnaissance. The streamlines have been superimposed on the SSM/I wind field for Sperry to show the degree of accuracy of the computed directions. The accuracy was as good as or better than that (20°) generally associated with active (radar) measurements with a device known as a scatterometer. Currently, there is no scatterometer operating in space. Moreover, since the SSM/I wind directions do not have the 90° ambiguity associated with scatterometer measurements, the SSM/I is expected to become an even more important sensor of global winds for meteorologists, oceanographers, and naval operations.

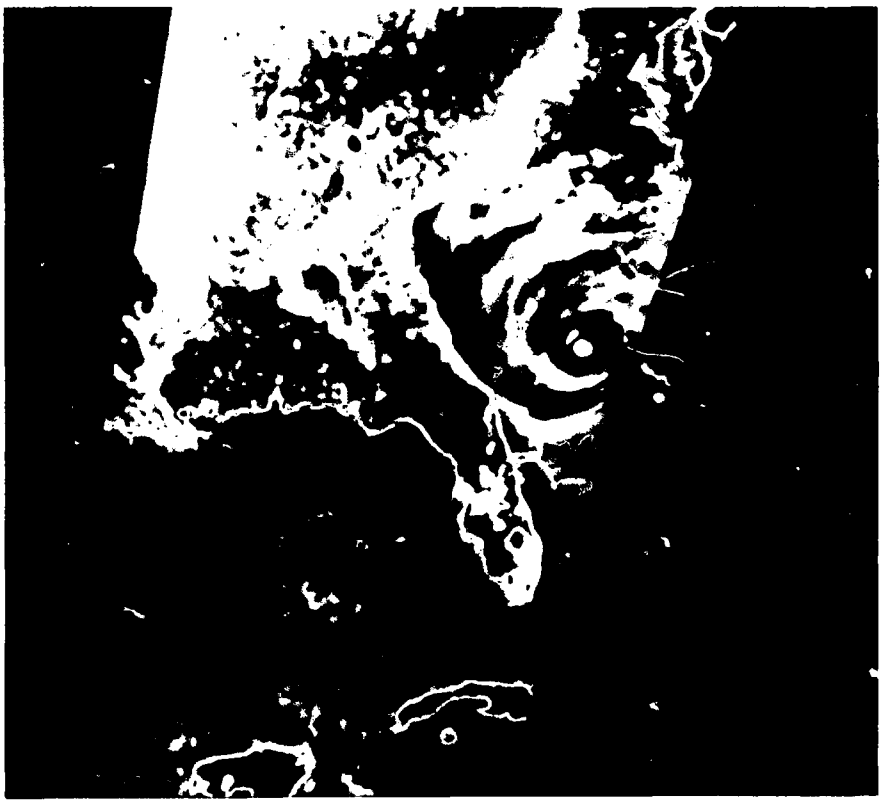

Fig. 7 — Landfall of Hurricane Hugo. Hurricane Hugo moved inland across Charleston, SC, during the evening of 21 September 1989. The maximum reported windspeeds near the eyewall were 135 knots. the SSM/I passed over the storm near 2400Z. The 1400 km swath of 85H brightness temperatures (Tb) ranges from the Yucatan Peninsula to the Delmarva Peninsula. The radius of gale-force oceanic winds determined with the SSM/I was approximately 150 km. Heavy rain bands (19 to 25 mm/h and greater) imaged with the SSM/I extended over 850 km westward from the eye: they were approximately coincident with the deeply convective (turquoise) regions of Hugo. Lighter rain (5 to 18 mm/h) extended into the Midwest. Shown are the blue-identified, normal-oceanic background Tb, Lake Okeechobee, the Mississippi River (resolved beneath the cirrus overcast), and regions over land where hydrometeors (large raindrops, hail, and graupel) scattered and absorbed microwave radiation from below. The degree of microwave backscatter from hydrometeors was sufficient to obscure the coast near Charleston. The coastline and major lakes have been simulated in red by computer. White identified primarily clouds and water vapor with emissivities above ocean background. The band along the Gulf Coast identified the region of dry air immediately south of the Hugo system where the total atmospheric water vapor was below normal background.

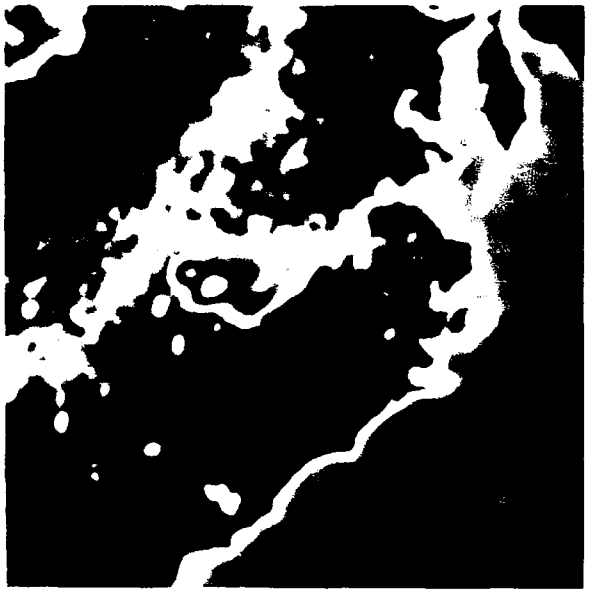

(a) An 85H image of the eastern seaboard on 30 August 1989, 20 days before Hugo arrived. The nominal resolution at the surface is 12.5 km. The swath extends from Florida to the Delmarva Peninsula. The color bar is the same as that for Fig. 5. The greens and browns identify low-altitude terrain, green representing the highest brightness temperature (Tb). White identifies primarily clouds but also high-altitude terrain, such as the tops of the Appalachian mountains. Blue identifies the ocean, Lakes Marion and Moultrie, north of Charleston, SC, and also the deeply convective regions of clouds where precipitation is expected. The remaining colors (turquoise, gray, and yellow) identify the increasingly deeper convective regions within storms where hydrometeors are present. Except for widely scattered thunderstorm activity near the Appalachian regions, the eastern U.S. is clear. The emissivity of the terrain for a given land type is proportional not only to land temperature but also to the density of live vegetation and inversely proportional to the amount of surface ground water. Note the dark green expanse throughout the Carolinas.

(b) The eastern seaboard on 23 September 1989, within two days after landfall. The scene north of Florida and east of the Appalachian Mountains is free of clouds. (The four, thin, black arcs across this region indicate data dropouts.) The average Tb in the vicinity of the Chesapeake Bay is approximately the same as that in Fig. 6(a); in the pathway of Hugo, however, the average Tb has decreased. This can be interpreted partly as an effect of increased ground water. It is possible that part of the decrease in Tb is caused by defoliation. Note also the differences for Lakes Marion and Moultrie; the increase in ground water is evident.

Fig. 8 — The eastern seaboard before and after Hurricane Hugo

Fig. 9 — Water vapor image of Hurricane Hugo. The columnar water vapor measurement for the scene ranges from 14 kg/m^2 south of the weather front (turquoise) to 71 kg/m^2 in the eye of Hugo (white). Water vapor over land is not measured by the SSM/I.

A new SSM/I algorithm for retrieving wind direction in addition to speed can aid in determining the windstreams for tropical cyclones. The algorithm is simple and uses only Ekman boundary layer dynamics and routine surface pressure analyses. The computations for SSM/I scenes have been made by applying first order Ekman equations, which imply a balance among the pressure gradient, the Coriolis, and the frictional forces (defined by the windspeeds) in the planetary boundary layer.

Wind measurements over the global oceans reported by ships of opportunity and buoys constitute approximately 900 to 1000 reports per synoptic hour. The majority of these reports originate in shipping lanes and along coast lines and come from latitudes outside the tropics. This constitutes a very poor spatial sampling even if the measurements were distributed uniformly over the oceans. In one DMSP overpass of the tropical zone requiring only 13 minutes, the SSM/I can sense the marine wind in over 26,000 locations with 50 km resolution. FNOC can provide the data to the U.S. Fleet in near real time.

Ships typically avoid storms and generally report winds much less than 30 knots. Observations of wind from aircraft flights into developed tropical cyclones (winds > 50 knots) usually are concentrated toward the inner vortex within a 225-km radius. Thus wind sampling has been especially limited in the outer-gale to near-gale region (winds 30 to 40 knots), which may exceed 400 km in hurricanes or typhoons. Comprehensive coverage of the oceans by the SSM/I is routinely providing wind fields up to gale force (and occasionally to greater winds inside the gale envelope) that have an accuracy ± 4 knots (2 m/s) 85% of the time. The uncertainties in wind direction outside the gale envelope are on the order of ± 20 degrees 66% of the time (Fig. 6).

Currently there are two basic limitations on windspeed retrievals inside the gale envelope—the exceptionally large quantities of rain and hail and the resolution of the instrument. Microwave

radiation emitted from the wind-roughened ocean surface that contains information about windspeed must pass through the water-laden atmosphere before being measured by the SSM/I. If the windspeed signature is attenuated by scattering from rain and ice to a level below instrumental noise, then meaningful windspeed retrievals are no longer possible. The extent of these areas in and around hurricanes may be as little as 2% or as great as 50% within a 1400-km radius. The uncertain areas, flagged by the retrieval algorithm according to the amount of atmospheric loss present, normally lie inside the 30- or 40-knot radii and have little effect on the SSM/I ability to track the storms. Even in rain-free cases, the SSM/I windspeeds in excess of 40 knots, retrieved from the inner vortex of storms, will have greater uncertainties because the average windspeed gradients inside the gale envelopes are on the order of 0.5 knot/km and approach about 4 knots/km near the eyewall. The effective resolution of the algorithm, 50 km, is limited by the resolving power of the SSM/I antenna at 19, 22, and 37 GHz. The high spatial gradients in windspeed, therefore, are smoothed by the surface resolution. For maritime operations, however, quantitative knowledge of the outer gale regions is the most important for weather avoidance.

The eyes of typhoons are known to be quiescent, rain-free regions. Cloud liquid water (CLW) is expected to have minimum values in the eye, with very steep gradients at the inner edge of the eyewall where convection is deepest. Therefore, the cloud water isopleths can be an aid in fixing the position and size of the eye. However, since the eyewall, defined by cloud water, may not be perfectly vertical, the apparent eye at the top of the clouds may be slightly skewed relative to its position at the sea surface. Therefore, the cloud water isopleths should be used in conjunction with other SSM/I imagery, such as the 85H and the water vapor distributions.

Water vapor is the fuel that maintains the energy of the storm. The vortex of a tropical low accumulates water vapor not only from the surrounding moist air but also from increased evaporation of the sea surface. Convection carries the water vapor to higher levels of the atmosphere where it cools and condenses to cloud water and rain. During the intensification stage of storms, water vapor begins to increase in asymmetric plateaus (such as to the west and southeast of typhoon Sperry) and to attain slightly higher values in the eye. As the storm matures, the vortex fills, the plateau closes around the eye, and water vapor density tends to increase with decreasing radius through the vortex to a maximum in the eye, as in Hurricane Hugo (Fig. 9). This implies that the image of water vapor can be used as an aid in center fixing.

The evidence from all storms analyzed by NRL and other investigators and compared with aircraft reconnaissance data indicates that center fixes can be determined from SSM/I 85H images alone within an uncertainty of ± 25 km. When the wind vectors, CLW, and water vapor products are used to improve the interpretation of the 85H imagery, the positional uncertainty decreases to 12 km.

A further consideration of hurricane tracking is the distance a storm may move between the time of an SSM/I overpass and the dissemination of information to maritime users—currently 1 to 3 hours. A storm center typically moves at a rate of 10 to 40 km/hr along fairly predictable paths. Standard prediction techniques usually are accurate to within the order of a degree (110 km)/day, given accurate center fixes. The added uncertainty for SSM/I tracking is about 4 to 6 km/h. Tracking with low-level aircraft is also not instantaneous. Depending on the structure and location of the storm and the number of flight crossings required to find the center, an aircraft can require 1 to 3 hours to make a center fix after arriving at the storm. The aircraft may make 1 or 2 center fixes per day, which is comparable to the SSM/I frequency of overpass.

The SSM/I spatial, as well as temporal, uncertainties in center fixing are comparable to those for aircraft reconnaissance. The absolute

uncertainty in center fixing from aircraft depends on the inertial navigation system (INS) errors, the particular storm, and the technique for finding the center. The INS errors are a function of flight path and flying time. They typically propagate at the rate of 2 to 4 km/h. For straight-line flight in the same latitudes, the INS error will have minimum values of ±4 km/day. The technique—which may be wind, pressure, or temperature centering—depends on the structure of the storm and the size of the eye; it may add as much as ±16 km to the uncertainty. In a storm with a well-defined and constricted eye, as in Hurricane Gilbert, the center fix was accurate to within ±4 km, according to NOAA; for Hurricane Paine, with a broad eye, the accuracy was ±20 km. Satellite imagery often is used as a guide for the initial bearings of reconnaissance aircraft. The better the initial estimate, the less the final INS uncertainty. The initial estimate can be in error by as much as 8 km when the eye at cirrus level is skewed from the surface position or as much as 170 km when no eye is visible, as in Hurricane Floyd. In this case an aircraft may be required to make multiple crossings of the storm to locate the center, increasing the INS uncertainty. The SSM/I low-level imagery is expected to be an improved aid in center fixing tropical cyclones.

Future Directions

The use of remote sensing with the SSM/I marks the beginning of a new era in meteorology. The SSM/I products provide global, consistent, quantitative information with accuracies at least as good as those of buoys and ships—and they can be obtained day or night, under any kind of cloud cover, in distant strategic areas, or unique regions that are inaccessible by other means.

SSM/I products will continue to be evaluated for new applications, and new products will be developed. For example:

(1) The Naval Environmental Prediction and Research Facility (NEPRF) has concluded that the SSM/I windspeeds can be successfully assimilated into the Navy Operational Global Atmospheric Prediction System (NOGAPS).

(2) The new algorithm for wind direction has been validated and is being tested in NOGAPS and other predictive models.

(3) Following curtailment of aircraft reconnaissance flights in the western Pacific, the JTWC depends exclusively on satellite imagery, and they have found the SSM/I to be a valuable replacement for storm tracking. Their assessment shows that NRL-SSM/I techniques can reduce the conventional center-fix uncertainty by at least a factor of 3 and that the uncertainty in tracking will decrease with the use of SSM/I water-vapor structure.

(4) A new SSM/I algorithm for determining wind stress is being developed and validated by NRL experiments. Wind stress affects the concentration and distribution of surfactants, oceanic clutter, acoustical degradation lengths, and the depths of atmospheric evaporation ducts (for long-range communications). Wind stress (a more basic quantity than windspeed) is an essential input to all atmospheric and oceanic circulation models.

(5) Products not discussed above but presently derived from the SSM/I include sea-ice concentration, ice-edge location, soil moisture, land-surface type, land-surface temperature, and snow burden. Ice concentration is particularly important to the Navy because it is associated with acoustic noise generation. A new algorithm to determine ice age and amount is being developed along with algorithms for numerous other land products.

Six more SSM/I imagers will be launched in this decade. Five additional instruments, called SSM/IS, that incorporate the SSM/I along with the atmospheric temperature and water-vapor sounders, are currently being developed and will provide environmental products well into the next century. Sounders retrieve air-temperature profiles by means of pressure-broadening in the 50 Ghz region of the oxygen spectrum and also water vapor profiles by pressure broadening of water

molecules at resonances 22 and 183 GHz. With sounder air temperatures, it may be feasible to use known techniques to deduce surface winds inside the 30-knot radii of tropical cyclones (at least, to 50 knots) more accurately than with the current SSM/I.

Finally, if a Navy option for all-weather, sea-surface temperature is adopted, radiometers at 5 and 10 GHz with resolutions of 10 and 25 km are likely to be incorporated. This instrument would allow the rain-filled regions of storms to be sensed for more accurate windspeeds, since the microwave radiation at these frequencies is not as affected by the water content of the atmosphere above the ocean surface as is the SSM/I.

Acknowledgments: The authors thank Mrs. Dawn Conway, Mr. Paul Doupont, and Mr. David Spangler, of Bendix Field Corporation, for their contributions to the software development of SSM/I imagery.

THE AUTHORS

JAMES P. HOLLINGER received his B.S. degree in physics from the New Mexico Institute of Mining and Technology, Socorro, in 1956 and his M.S. degree in physics from the University of Virginia, Charlottesville, in 1958. After attending Cambridge University in England on a Fulbright scholarship for one year, he returned to the University of Virginia and received his Ph.D. degree in physics in 1961.

After teaching physics at the George Washington University, Washington, DC, for one year, he joined the Radio Astronomy Branch at NRL. Until 1969, he was principally concerned with research on the polarization and variability of radio sources and on pulsars. For the past 20 years, he has worked in the area of passive microwave remote sensing. During this time, he has conducted measurements from ocean towers, aircraft, and spaceborne platforms at frequencies ranging from 1.4 to 220 GHz and has published over 50 papers on microwave remote sensing. He has done extensive experiments on the microwave emission of ocean surface waves and white caps, on the quantification of marine oil spills, on the microwave properties of sea ice, and on the absorption of atmospheric molecules and hydrometeors. He participated in the specification and source evaluation boards of S-193 and S-194 flown on SKYLAB, on LAMMR (which was planned for NOSS), and on the SSM/I and SSM/IS, flying and to be flown on DMSP. He was the technical manager of the LFMR instrument that was planned for N-ROSS. He led the DMSO calibration and validation of the SSM/I instrument and its geophysical retrieval algorithms and has been involved in every phase of its specification, development, and operation. He has conducted extensive airborne millimeter wave imaging measurements at 90, 140, and 220 GHz of terrain, cultural features, ships wakes, sea ice, and precipitating clouds. He has conducted studies and microwave measurements of target signatures and background clutter. He is currently head of the Passive Microwave Section at NRL.

GLENN D. SANDLIN graduated with honors from the University of Arkansas with a B.S. in physics and mathematics in 1962. For his honors thesis, he rebuilt an X-ray diffractometer and analyzed the atomic structure of liquid metals. He received his M.S. in astronomy and physics in 1964 from the University of Michigan, where he was the University Observing Fellow for novae and variable stars. From 1964 to 1966, he was an Instructor of Astronomy at the University of Michigan while he did postgraduate work in solar physics and geophysics at the McMath-Hulbert Solar Observatory, as an IGY investigator.

Mr. Sandlin came to NRL as a solar physicist in 1966 and worked in the Rocket Solar Spectroscopy and Skylab Programs until 1985. He has contributed original papers in X-ray and ultraviolet spectroscopy, radiation transfer, solar coronal physics, flares, and sunspots. In 1985, he joined the Remote Sensing Branch, where he has contributed to the Passive Microwave Program and especially to the SSM/I algorithm development and storm tracking. He has expertise in solar and geophysical research across the full spectrum of X-ray, ultraviolet, visual, and microwave radiations. His current work is in the remote sensing of atmospheric and oceanic physics of Earth.

Parallel Algorithms for Real-Time Tracking

Jay P. Boris and Ronald L. Kolbe
Laboratory for Computational Physics and Fluid Dynamics

Introduction

The world of large-scale computing has seen a number of major advances in the last 10 years. Today's supercomputers, for example the Cray, the BBN Butterfly, and the TMC Connection Machine (CM), can perform calculations 100 times faster than yesterday's computers. Tomorrow's computers promise the same increase in speed over today's. Not only has the speed increased, but the memory and hence the size of the problems that can be solved has also increased proportionally. The Butterfly and CM are two highly parallel computers employing a large number of distinct, rather inexpensive processors working together to solve a big problem while the Cray is a vector computer, getting its high performance from a few expensive, but very powerful processors. The Butterfly is a MIMD computer; its processors execute Multiple Instructions on Multiple Data, while the CM is a SIMD computer, broadcasting to all the processors a Single Instruction to operate on Multiple Data. These supercomputers require software and special algorithms customized for their architectures to obtain performance near the high maximum speeds.

In addition, heterogeneous element supercomputer systems are being developed to allow simultaneous execution of several different computational tasks, giving higher performance by exploiting parallelism at several levels simultaneously. A heterogeneous system consists of several supercomputers with different architectures linked by a fast communication network. The system work load, often a single complex problem with many different parts, is divided among the computers, taking advantage of the particular computer architecture best suited to each part of the problem. The necessary software is difficult to write and maintain, since synchronization of computers and communications is a major problem. Software tools, such as **Linda**, a portable, high-level, parallel programming environment conceived at Yale University, are being developed to simplify the software development process and to organize and monitor the necessary interprocessor exchanges of information during computation.

In 1983, the Strategic Defense Initiative (SDI) was proposed to conduct the research and development necessary to provide a system for intercepting and destroying ballistic missiles in flight. A major stumbling block of this program has been the enormous amount of real-time data processing needed to track all the objects in space, to discriminate among them, to assign them as targets to the available defensive weapons systems, and to evaluate the threats posed and the effectiveness of actions taken against these threats. The Strategic Defense Initiative Organization (SDIO) has funded extensive work in the development of Battle Management, Command, Control and Communication (BM/C^3) systems needed for this task. At the Naval Research Laboratory (NRL), several divisions including the Information Technology Division (ITD), Tactical Electronic Warfare Division (TEW), and the Laboratory for Computational Physics and Fluid Dynamics (LCPFD) have tackled various aspects of battle management computation. Using heterogeneous element systems consisting of several architectures of vector and parallel processing supercomputers seems a natural and

most cost-effective way to achieve the necessary computatonal power. Further, since any system actually implemented is likely to involve information processing spread across a number of different autonomous satellite battle managers, the use of parallelism in the context of distributed, networked computers is definitely required.

In an actual battle, data describing approximately 10^4 to 10^6 objects will have to be analyzed by the battle management system. These objects include boosters, satellites, reentry vehicles, decoys, and debris. To develop and test the battle management codes, imaginary engagements called "scenarios" have to be constructed in a computer, providing input data to the battle manager programs as if a suite of orbiting and ground-based sensors were actually seeing an engagement develop in space. Such "scenario generators" must calculate the locations, velocities, apparent brightnesses, and other related properties sensed for each of the objects. For passive sensors such as optical and infrared cameras, these properties include the target's temperature, cross-sectional area, and emissivity, but the range to the object can only be determined from correlating the simultaneous observations of two or more sensors. For active sensors such as radar and lidar, the field of view may be quite small, but the range is usually available directly.

Scenario generation is not even the most computationally intensive part of battle management data processing. Several other aspects, for example tracking and correlation, require much more computer time and memory. An object's computed track has three-dimensional positions and velocity components and other kinematic data derived from the sensor observations. These data must be kept current by continually correlating fresh observations about the object, generally called sensor contact reports, with the evolving, previously computed track. At the present time, most computers—VAX, Butterfly, or even Cray—cannot generate a scenario and perform the necessary tracking computations in real time for a realistically large number of objects. The existing scalar-algorithm tracking and correlation codes on these computers can only analyze a few hundred objects in real time, i.e., fast enough to keep up with an actual engagement of the same size. This problem is caused not only by the shear bulk of calculations and storage required but also by the use of inefficient algorithms whose cost scales quadratically with the number of objects, the "scaling problem." Also, these algorithms were never programmed with vector or parallel supercomputers in mind, i.e., the so-called "dusty deck conversion" problem.

To understand the scaling problem, consider more closely the conversion of sensor data to computed tracks. The sensors used for detection generally make observations in distinct frames or sequential scans separated by a small time difference. A frame (or scan) can be thought of as a picture of the objects in a region of space. To generate a new track, two different frames must be compared and the objects in each frame must be correlated with those in the other. Only after this correlation assignment is made can the velocity be determined by dividing the change in position by the corresponding time difference. The result is a set of short track segments for those objects in the sensor's field of view. To extend the existing computed tracks, one or more frames of track segments must be correlated with the computed tracks computed to be in the same region from which the frame of data was taken.

If two frames each contain 1000 objects, there exist roughly $1000^2 = 1$ million possible pairs of correspondences for new track generation or extension of existing tracks. This is an example of relatively disasterous quadratic scaling because roughly N^2 correlation pair evaluations would be required to isolate track data for N objects. Actually the scaling can be much worse because these correspondences are all coupled. Correlating two contact reports in successive frames precludes making a number of other assignments—even if those other assignments look just as likely as the one actually chosen. This aspect of correlation and

tracking is called the "constrained assignment" problem. Efficiently reducing the number of possible correspondence pairs that have to be considered to only those for which assignment is likely is called "gating." Without one or more very efficient gating steps, the tracking and correlation components of SDI battle management programs cannot run in real time for the numbers of objects required. To obtain real-time performance, massively parallel processing and concurrent programs will be required for most parts of BM/C^3. A heterogeneous computer system seems indicated with different architectures performing different tasks.

Scientists working in the LCPFD, have developed a number of parallel models for computational fluid dynamics and manybody dynamics by using different vector computers, parallel computers, and heterogeneous systems. This experience is also a valuable springboard for improving the performance of battle management algorithms and programs. Near-neighbor gating algorithms have been successfully developed for a working correlator-tracker on scalar hardware, with a break-even point of less than 100 objects. This means that for more than 100 objects, the new near-neighbor gating algorithms will provide an increase in computing speed proportional to $N/\log N$. For N = 10,000 objects, the speed increases by a factor of 50 when using our near-neighbor algorithms on a scalar computer like a SUN workstation [1]. Using new, highly parallel algorithms on NRL's CM [2], faster-than-real-time tracker-correlator performance has been demonstrated for scenarios with up to 32,768 objects, as will be described next. Using a full 64K-processor CM, this could be extended perhaps to 100,000 objects.

Thinking Parallel from the "Ground Up"

Funded by SDIO and the Defense Advanced Research Projects Agency (DARPA), a bare bones but real-time space battle management simulator called the Battle Engagement Area Simulator/ Tracker (BEAST) is under continuing development in the LCPFD [2,3]. The BEAST is a massively parallel model using our new monotonic Lagrangian grid (MLG) parallel data structure [4]. An MLG data structure arranges data by location into an organized grid, thus allowing full use of massively parallel computer architectures such as the CM, thereby considerably simplifying parallel programming [5].

The present BEAST model performs five operations: (1) the generation of model scenarios, (2) the simulation of primitive sensor observations, (3) the construction and maintenance of multiple sensor contact report data sets and fusing these observations frame by frame into track segment data structures, (4) the generation of new computed track "candidates" and the extension of existing computed tracks, and (5) the modeling of simple battle management decisions for sensor control and coordination. As with any of the various supercomputer options, realizing the potential of the CM requires customization of software and algorithms to its architecture.

The numerical simulations presently can follow the evolution of up to 32K (32,768) objects. The simulations include sensors, satellites, and missiles in minimum energy trajectories from one selected region of Earth to another. Up to 64 sensors observe the space in user-specified Earth orbits. The present programs currently model the tracking process at a "systems integration" level. The current model does not correlate pairs of frames or scan reports (pictures) seen from different sensors to generate the complete contact report files. These computations, which would be performed in an operational system by separate and distributed preprocessing computers, have been demonstrated in earlier work [6]. Instead, we assume that the sensors produce track segment reports as their contact reports, which include range and approximate velocity information for the objects in their field of view. These reports, generated from the suite of sensors all acting in parallel, are combined by a parallel multisensor data fusion algorithm that results in a single data structure containing all the track segments

observed in a short interval of time. After this composite track segment data structure or "file" is combined into a single MLG data structure with obvious redundancies removed, it is integrated with the computed track data, again organized as an MLG and also loosely called a "file," using a fully parallel correlation and tracking algorithm. These computational activities are performed at least as fast as would be required for a real-time operational system.

Figure 1 is a flow diagram of the BEAST code. The blocks represent the functional sections of the code. The block labels beginning with the task *Initialize* describe the necessary housekeeping functions of the code. *Initialize Program Control* reads the input data telling how many of what objects are to be considered, the types of output, orbital information, etc. *Initialize Scenario* uses the input data to create the physical starting conditions for the simulation. *Initialize Data Sets*

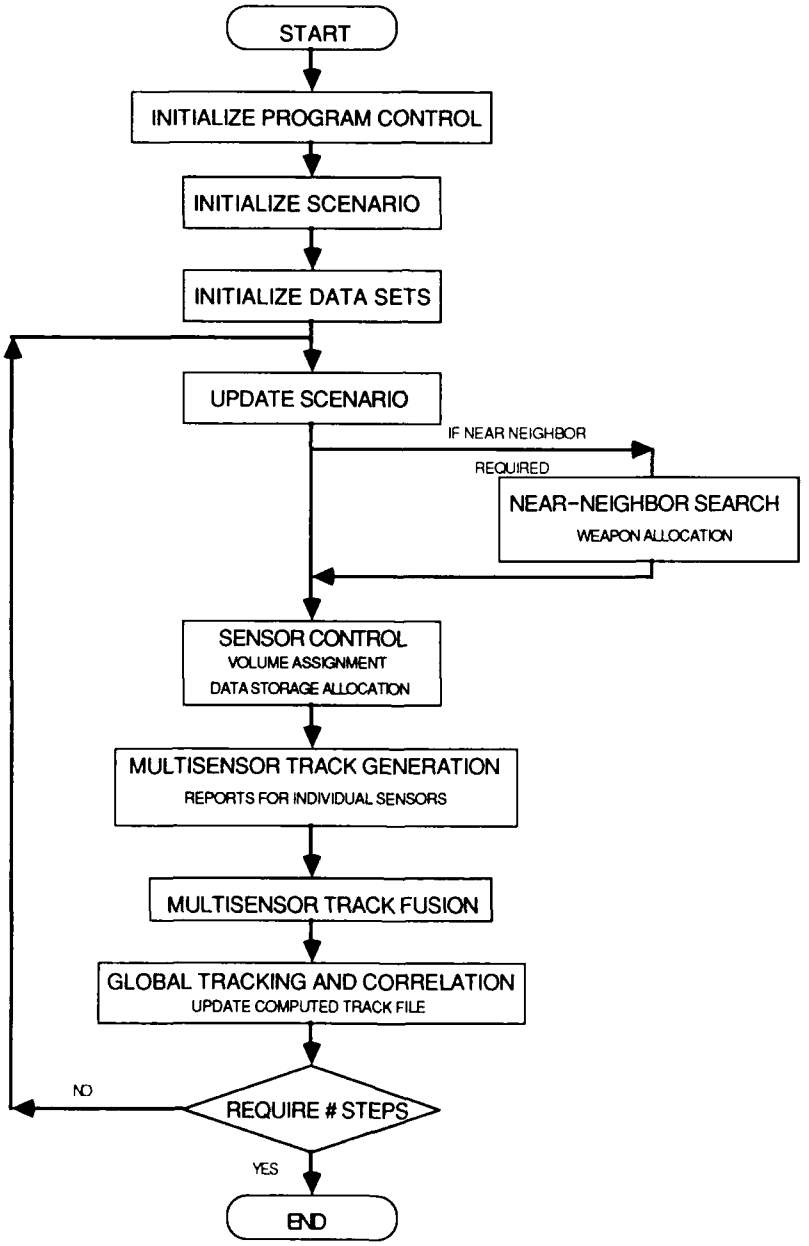

Fig. 1 — Block diagram of the BEAST code

creates the necessary files for the remainder of the code.

The code marches forward in time by continually repeating a sequence of tasks and functions, each of which is computed fully in parallel on the CM. Within this loop, the five operations of BEAST are conducted. Th functions shown within this loop are not performed at every step but only as needed. Operation 1, modeling scenarios, is achieved in the *Update Scenario* function. Positions and velocities are determined for the objects. Operation 2, simulating sensors, is performed by *Sensor Control* and *Multisensor Track Generator*. The *Sensor Control* function tells the suite of 64 sensors where to look. The *Multisensor Track Generation* function produces the individual candidate tracks for each sensor. Operations 3 and 4, the construction, maintenance, generation, and fusion of tracks are accomplished in *Multisensor Track Fusion* and *Global Tracking and Correlation*. The *Multisensor Track Fusion* function compares track segments from every sensor and produces a single track segment data set. The Global Tracking and Correlation function relates the new track segment data from the present time frame to the tracks computed from past time frames. By using information from all sightings, the best prediction can be made about an object's trajectory. Operation 5, modeling battle management, is cursorily treated in *Near-Neighbor Search*. The *Near-Neighbor Search* is a gating algorithm to identify objects within a critical distance of each other. This information would be used for weapons allocation.

The Connection Machine

The CM is a front-end scalar computer (host) that controls up to 65,536 processors operating in parallel [7]. The program instruction sequence is stored on the host, and each instruction is broadcast simultaneously to all the processors. Thus redundant instruction storage and execution hardware for multiple copies of the program are eliminated. Each processor is smaller and less powerful than a personal computer but, under the control of the host, each processor can store individual data sets and perform all of the required arithmetic and logical calculations. Based on local context flags computed in parallel in each processor, that processor will perform or ignore the generally broadcast instruction. Thus complicated logic is easy to implement. The CM, unlike other parallel processing systems, was particularly designed for fast interchange of small data packets between processors.

NRL has two CMs, each having two sections, and two host computers, a VAX and SUN. One CM has 4K (4096) physical processors per section, and the other has 8K (8192) physical processors per section. Each host can control either CM. The CM sections can be run either independently or together. To run a program, a user who is logged in on a host computer requests a particular CM and the required number of sections. An additional CM feature is its use of virtual processors. The physical processors can have their memory divided into regions and thereby act logically as several distinct processors. The processors can be arranged logically in an n-dimensional grid. Data exchange between processors is fastest along the axes between near-neighbor processors.

Figure 2 shows NRL's CM facilities. Because of its architecture, the CM has two additional hardware features. For data storage, it has a DataVault [8], and for graphics it has a Framebuffer [9] that is discussed in the section on graphics. The DataVault consists of a file server computer, DataVault disk controller, and 42 small independent disk drives that act together to give the CM the equivalent performance of a very large, very fast disk. The DataVault is connected to one of the CM's 8K processor sections by its controller and provides the high-speed data transfer necessary for the CM.

Parallel Scenario Generation

The contact report-track correlation tasks are the most computationally expensive part of the BEAST model. However, to model real-time

Fig. 2 — NRL's Connection Machine's facilities. On the left-hand side is the DataVault, in the center is the CM, on the right-hand side is the VAX hose computer, and in the background is the user's room.

battle management, a much faster-than-real-time interactive driver program called a scenario generator is required to provide the evolving data on the orbits and trajectories of all objects in the simulated scenario. Reading precomputed scenarios from either conventional disk storage or from tapes is much too slow for a massively parallel processor such as the CM. The CM DataVault could be used for storage of a precomputed scenario but its capacity is limited, even if fast enough, and prerecorded scenarios do not allow for interactive real-time modifications of the evolving scenario such as destroying a target or changing an object's orbit.

In modeling a scenario on the CM, each processor is assigned an object or designated as a "hole" in the MLG data structure. A hole has a positional value for the MLG data structure but has no other related object data. A new object, report, or track can subsequently be placed in one of the holes of the MLG structure if needed. The initial object positions and velocities are calculated in a separate initialization program section for both satellites and missiles. The current generator updates the scenario every 10 seconds to match the processing rate of the sensor, multisensor fusion, and track correlation algorithms. This rate is also sufficient to maintain adequately accurate orbits, but it could be increased substantially since the generator runs about 40 times faster than real time.

Figure 3 shows a 32,000 object scenario as a wave of defensive missiles (blue) and a wave of offensive missiles (red) pass through each other over the North Pole. The yellow points flag the instantaneous near-neighbors for possible weapon allocation operations or other defensive measures. The red and blue nodes are colored yellow when they pass within 200 km of each other in the figure. For the scenario pictured, the localized waves contain approximately 6000 red and 2000 blue objects.

The MLG data structure controls which objects are assigned to which processor. Since real space is three dimensional, the CM's processors are arranged in a $32 \times 32 \times 32$ three-dimensional MLG data structure. The MLG dynamically assigns objects to processors such that adjacent objects in real space are assigned near-neighbor

Fig. 3 — 32,000 objects passing over North Pole at 17 min. after launch

processors in three-dimensional grid space. This arrangement results in reduced communication distance and time for near-neighbor comparisons on the CM. When two objects pass each other in space, the data describing them are swapped between adjacent processors to ensure that the MLG structure in the CM accurately reflects the relative positioning of the objects in actual space. Thus the MLG assignment of objects to processors is the first and foremost gating function in the BEAST model. The MLG automatically allows faraway data to be ignored, as only nearby processors in the CM contain related data. Note that one processor contains information only about a single object, sensor contact report, track segment, or computed track assigned to it in a given data structure. To know about data in another processor, the processor must either receive that information or request it, implying communication between the CM nodes.

Parallel Sensor Modeling

In the scenarios considered, the 64 sensor satellites are assigned to circular orbits in both polar and inclined orbital planes. First, 54 of the sensor satellites are assigned, nine at a time, to six orbital planes equally spaced around the equator and inclined to the equator at an angle of 75°. The remaining ten sensor satellites are assigned to a polar orbit. We generally refer to these simulated sensor sateilites as simply the "sensors." Within each of the ten orbital planes, the sensors are equally spaced at an altitude 400 km about Earth.

The CM's maximum speed is obtained by using all its processors to perform calculations. To generate sensor contact reports using all the processors requires assigning a different contact report to each processor. Only 64 of the processors would be used if they were assigned to the sensors. Thus each processor is assigned to a contact report from one of the 64 sensors and then the processor performs a separate computation to determine which object in that sensor's field of view this contact report represents. This approach allows 32,768 contact reports to be developed simultaneously, including some objects that are sensed more than once by separate sensors and is an example of one of the major tricks used to enable highly parallel computation.

The processors generating sensor contact reports actually generate provisional track segments from the evolving scenario as if range data and approximate velocity data were available. This reflects the supposed presence of independent input preprocessors in an operational system to carry out this function. The BEAST program alternates the sensor's viewing volume. For the even frames (scans), the sensors look away from Earth. For the odd frames, the sensors look toward Earth. This alternation in sensor field of view results in almost complete coverage of all objects in space. In an operational system, much more complex patterns of cooperative sensing would undoubtedly be used, again controlled by different computers in the overall heterogeneous system.

Objects can be viewed by more than one sensor and therefore can generate multiple track segment reports. The parallel algorithm for arranging all of these track segment reports in data storage is critical for the next step of combining the

redundant track segment reports. The code then organizes the resulting track segments for subsequent correlation with computed tracks. In BEAST, the 64 distinct sets of sensor observations are collected as blocks of 512 track segment reports per sensor. Each of these blocks is constructed in MLG order. To generate the composite track segment data set, therefore, these separate MLG blocks are stacked into a single data structure in the order of the 64 sensors in their own $4 \times 4 \times 4$ sensor MLG. A sort of all the multiple sensor track segments reports to establish a global MLG order would require more time if the data are not in approximate order to start. The real-time performance objective would then suffer.

Parallel Multisensor Data Fusion

Once the individual blocks of sensor contact reports have been merged into a single data structure and the MLG order has been established globally, another new parallel algorithm is used to remove redundant reports. The composite report file is copied, and the copy is transferred along the MLG and CM grid axes from processor to processor in a sequence of neighboring processor communications called a "tour." As this tour passes through all of the neighboring processors, the local contact report and the touring contact report are compared and reports on the same object are marked. The replica data set returns to the starting processor with its collected information. This data transfer can be pictured as two initially coinciding cubes. As the data set is moved, the two cubes are offset. By use of this method, all the processors can be used to obtain maximum speed.

Finally, when the data set has returned home, the two cubes again coincide. Now, action can be taken to eliminate duplicate tracks or fuse the multiple sensor tracks. This results in a fused track segment data structure, or file, containing information about all objects scanned by the sensors in a single frame. The result is a single MLG data structure of verified track segments. This process takes advantage of the MLG data structure and the fast data exchange along MLG grid axes on the CM to obtain real-time performance. The current tour allows a given report to be compared with reports within two grid positions on all sides. A comparison with all reports is not required since the MLG data structure has automatically located multiple reports in processors near each other.

Figure 4 shows the relationships between multiple sensor contact reports, fused track segments, and the computed tracks. In a given frame, each sensor has a set of sensor contact reports associated with it, given here in the form of candidate track segments. A particular object can have track segment reports in several sensor's contact report blocks. In the case shown, object **a** is reported by sensors 1 and 3 but not be sensor 2. These redundant multiple sensor reports must be fused into track segments. The track segment 12 for scan period t_p is the composite track segment for object **a** from sensors 1 and 3. The track segment file contains the track segment information from all sensors during the frame. The computed track is the connected sequence of track segments as determined from the sensor measurements for all previous frames.The computed track points to the fused track segments for the present and previous scan periods. Computed track **A** points to track segment 12 for the frame period t_p and track segment 34 for frame period t_{p-1}. The computed track has no pointer to a track segment for frame period t_{p-2}.

Parallel Tracking and Correlation

Once the newly sensed track segments have been fused into a single track segment file, the computed track file can be updated. An object's track can be thought of as a string passing through an ordered sequence of beads, where the beads are the progressively newer track segments that belong to that track. The computed track file connects the new track segments to previously computed tracks. Each processor containing a computed track projects forward its track properties and matches them to the most likely new track segments in the vicinity. If any new track segments are unclaimed,

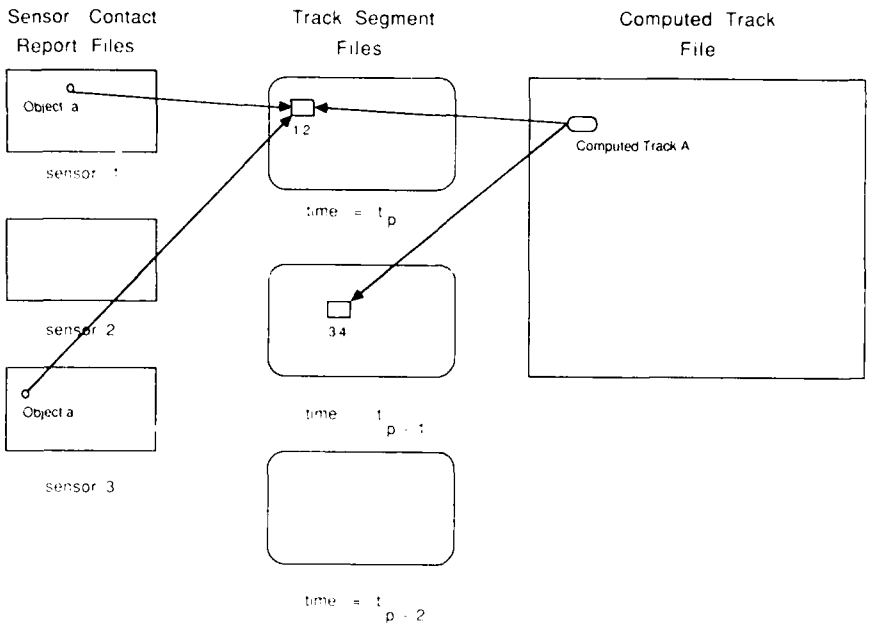

Fig. 4 — The sensor contact reports, track segment, and computed track relationships

they become candidate computed tracks. If a computed track has not claimed any new track segments during a specified number of sensor scans, it is eliminated from the computed track file.

The MLG data structure is used to assign computed tracks to processors and serves as an automatic parallel gating algorithm between the new tracks segments and the computed tracks. This gating results in two data sets, a fused track segment file and a computed track file in processors having near-neighbor communication links. Unlike the multisensor fusion computations described above, a replica data set cannot be constructed and taken "on tour" here. Since all the objects are not seen by the sensors in each scan period, a larger search pattern is required and potentially starts at a different location in the track segment file for each computed track. Each processor containing a computed track requests information from the other nearby processors about their new track segments. While the operations are performed with a single stream of broadcast instruction, each individual processor calculates which other processor to collect the necessary information from. At this point, comparisons are made to assign new track segments to computed tracks. In addition, checking is performed for any remaining duplicate track segments and computed tracks. Any unclaimed track segments are converted to candidate computed tracks that will be deleted if they are not reinforced after a few scans. Finally the new computed track file is sorted by the fully parallel swapping algorithm to restore MLG order, making the $N \ln N$ scaling of the overall algorithm possible.

Graphics

One difficult problem with using a massively parallel computer is that of analyzing the huge volume of information produced. A simple print request can result in thousands of lines of output. Graphical output is one way to format information and results for rapid human perception and comprehension. To permit convenient graphics to be computed during a running CM simulation, a hardware Framebuffer resides in each of the CM's 4K or 8K processor sections. It is controlled by a sequencer, which also controls the processors and DataVault controller. The Framebuffer contains a 7-Mbyte display memory into which pixel values

computed by the CM's virtual processors are written and can be stored.

Several graphical displays have been developed to diagnose the real-time tracking codes. The graphical displays use the online CM Framebuffer directly or produce related numerical output files that can be plotted by use of the interactive VOYEUR system on the LCPFD's GAPS computers. The Framebuffer displays can also be broadcast throughout NRL on NICENET for viewing on remote TV monitors. Four graphical displays are presently available on the CM. The first display shows the simulated scenario (Fig. 3). This display allows the instantaneous locations of all the objects to be seen as viewed from an arbitrary direction far away in space. The second display overlays the sensed objects on top of the actual object locations. This display shows which objects were actually detected in the current frame and conversely which objects avoided detection. The third display overlays the objects sensed, colored coded by the sensor that detects them, on top of the scenario. This display allows the fields of view of the individual sensors to be seen. The fourth display shows only the sensor locations without the confusion of the other objects.

Summary

The first generation BEAST model has been implemented by using fully parallel algorithms on the CM at NRL. The success of this model, though still in an early stage of development, shows that (1) real-time battle management with tens of thousands of targets is possible now, and (2) wholly new parallel approaches to the compute-intensive parts of battle management exist and are practical. To accomplish this, each CM node handles a single object, sensor contact report, new track segment, or computed track. The CM's full speed, up to 40 times a Cray X-MP processor in some cases, can only be obtained if all processors are used in performing a task. Thus scenarios with many fewer objects than processors will run no faster than those where the MLG data structures are full.

Using a single SIMD computer to perform all aspects of the BEAST computations has its advantages and disadvantages. The advantages are (1) only having to deal with a single computer system; (2) no communications required between heterogeneous architectures and operating systems; (3) concentration on efficient implementations; and (4) the very high performance currently available at moderate cost using SIMD. The disadvantages are (1) a SIMD architecture is not optimal for all tasks that have to be performed; (2) the different tasks have to be executed sequentially in BEAST instead of being performed simultaneously, as they would on heterogeneous systems; and (3) the enormous resistance there is in SDIO and the battle management community to the qualitative changes in algorithms and approaches needs to take full advantage of massive parallelism.

The current BEAST model is just a beginning; many improvements and refinements are possible. For example, the scenario generator could also be used to maintain a defensive track file. In an operational system, this known information would be used to remove contact reports associated with friendly objects, thus reducing the processing load on the tracker-correlator significantly. Multisensor contact report generation and fusion were most difficult tasks on our SIMD computer even when each sensor generates the same number of reports. In reality, each satellite will generally report a different number of objects and look in a different direction. A SIMD computer architecture does not easily allow for individual variations. To make progress, we chose a simple approach involving similar viewing volumes and equal numbers of tracks.

For this multisensor data preparation and fusion operation, it might make more sense to use a Hypercube or Butterfly with one processor per sensor to carry out track segment generation and to construct the local MLG blocks of contact reports. The data storage allocation of these relatively few blocks to one large MLG could then be performed

on a powerful scalar processor. The track segment-computed track correlation stage of the algorithm proved somewhat difficult on the CM but is probably among the most efficient uses of the architecture. The success of the current model is largely due to the fact that this aspect of the computations is the most compute intensive. Thus the CM and the problem are well matched for the most expensive part of the computation.

We have found that the major consideration for CM implementation of the BEAST is the cost of communications between processors. Even though the CM was designed to make the transfer of small data packets throughout the CM as fast as possible, communication still seems to occupy most of the running time of the programs. Thus the use of MIMD architectures, which expect fewer communications of larger size between processors, may cause the programs to run even slower and less efficiently for these parallel algorithms. Communication within a processor or between processors that share the same memory chips is nearly instantaneous on the CM. Within a processor, the floating point computations seem to use much more time than the operations for moving data.

Near-neighbor communication between adjacent processors—about ten times slower than intraprocessor data transfers—is the mode of communication used to maintain the various MLG data structures in the BEAST model. The MLG places near-neighbor objects, sensor tracks, fused tracks, and computed tracks into processors that are also near neighbors. Thus the necessary speed is obtained to run in real time. Communication between arbitrary distant processors is yet another factor of ten slower. This is the mode of communication needed for combining the track segment file at a given frame with the existing computed track file. Notwithstanding these progressive factors of ten reduction in speed as the communications must extend further, the CM is still faster than competing computers in exchanging these small data packets. Thus real-time data processing for realistically sized engagements is possible.

Acknowledgments

The authors thank Mike Picone and William Sandberg of the LCPFD for helpful suggestions in preparing this article and Bruce Wald and Steve McBurnett of NRL for introducing us to the battle management problem and for their encouragement and support of our efforts. Discussions and work on related research topics with Sam Lambrakos, Mike Picone, Miguel Zuniga, Felix Rosenthal, John Reynders, Jeff Uhlmann, and Joe Collins have played an important part in our being able to carry out this work. Special thanks to Robert Whaley of the Thinking Machines Corporation for his support and advice and for the CM support programs he has written, which are components of the current BEAST project. This work was supported by the Office of Naval Research through NRL, by DARPA, and by SDIO.

References

[1] M.R. Zuniga, J.M. Picone and J. Uhlmann, "Algorithms for Improved Gating Combinatorics in Multiple-Target Tracking," *Proc. IEEE*, submitted 1990.

[2] R.L. Kolbe and J.P. Boris, "Battle Engagement Area Simulator/Tracker," NRL Memorandum Report in press (1990).

[3] J.P. Boris, J.M. Picone, and S.G. Lambrakos, "Beast: A High-Performance Battle Engagement Area Simulator/Tracker," NRL Memorandum Report 5908, Dec. 1986.

[4] J.P. Boris, "A Vectorized Near Neighbors Algorithm of Order N Using a Monotonic Lagrangian Grid," *J. Comput. Phys.* **66** (1), 1-20, (1986).

[5] J.P. Boris and S.G. Lambrakos, "A Highly Efficient Algorithm for Tracking Objects," 1985 *NRL Review*.

[6] J.M. Picone, J.P. Boris, S.G. Lambrakos, J. Uhlmann, and M. Zuniga, "Near-Neighbor Algorithms for Processing Bearing Data," NRL Memorandum Report 6456, May 1989.

[7] D. Hillis, "The Connection Machine," *Sci. Am.* **256**, 108–115 (1987).

[8] *DataVault Reference Manual* (Thinking Machine Corporation, Cambridge, Mass., 1988).

[9] *Display Operations Reference Manual*, (Thinking Machine Corporation, Cambridge, Mass., 1988).

THE AUTHORS

JAY P. BORIS received his B.A degree in physics in 1964, his M.A. in astrophysical sciences in 1966, and his Ph.D., also in astrophysical sciences in 1968, all from Princeton University. Dr. Boris was a research physicist at Princeton from 1968 to 1970, joining NRL in 1969 first as a consultant. He is currently Chief Scientist and Director of the Laboratory for Computational Physics and Fluid Dynamics (LCPFD). Dr Boris plans, directs, and technically leads the LCPFD's mathematical and computational research programs in computational physics, fluid dynamics, chemically reactive flows, and large-scale scientific computing for military applications.

This year Dr. Boris was selected to receive the Navy's Captain Robert Dexter Conrad Award for Scientific Achievement. In 1988, he was awarded the Presidential Rank of Meritorious Executive in the Senior Executive Service by former President Reagan. He received the Navy Award for Distinguished Achievement in Science in 1980, the NRL Chair of Science in 1978, the Author S. Flemming Award in 1976, and the Navy Superior Civilian Service Award in 1975. He is a Fellow of the American Physical Society, where he chairs the APS Topical Group in Computational Physics and is a member of the American Institute of Aeronautics and Astronautics, the Combustion Institute, and Sigma Xi. He has recently coauthored a book with Dr. Elaine Oran of NRL entitled *Numerical Simulation of Reactive Flow*, published by Elsevier.

RONALD L. KOLBE graduated from the University of Maryland with a B.S. in mechanical engineering in 1973. He received his M.S. in nuclear engineering from Purdue University in 1976 and a Ph.D in mechanical engineering from the University of Tennessee in 1986. He has taught undergraduate engineering courses at the U.S. Merchant Marine Academy and at Shepherd College, where he was Director of Engineering. He has worked as a mechanical engineer for Burns and Roe, Inc., where he performed engineering studies related to advanced and conventional power plant design.

Present research activities focus on the parallel tracking and correlation program using the Connection Machine, as discussed here. His past areas of research include computational fluid dynamics, advanced energy conversion through MHD and fluidized bed systems, and thermal sciences. He is a member of the American Society of Mechanical Engineers, the American Institute of Astronautics and Aeronautics, the American Society of Engineering Educators, and Sigma Xi.

Behavior and Properties of Materials

BEHAVIOR AND PROPERTIES OF MATERIALS

The operating Navy is constructed from a vast array of materials that must withstand the rigors of the harshest of environments—the sea and space. Much of the research at NRL relates to the development of new materials—composites, ceramics, alloys, and metals, to name a few—and the determination of their properties, service performance, and reliability. Reported in this chapter is work on polycrystalline Fe–C alloys, glass fibers, material behavior under dynamic loading, oxide superconductors, and silicon carbide crystals.

Contributing to this work are the Materials Science and Technology Division (6300) and the Electronics Science and Technology Division (6800).

Other current research in materials includes:

- Metallic fracture surface characterization
- Epitaxially grown cobalt on GaAs
- Fabricating phase separated materials
- Low temperature charge density wave dynamics
- Superconducting current leads
- Low angle, oblique impact spall fractures
- SiC fiber/$ZrTiO_4$ composites
- Aligned composites

Ferrous Alloy Phase Transformations

R. A. Vandermeer
Materials Science and Technology Division

The ability to manipulate and control solid-state phase transformations during processing remains a most powerful and flexible way to develop useful mechanical properties in metals and alloys. This is especially true in the case of high-strength, low-alloy steels where control of the austenite (the stable phase at high temperatures) decomposition mechanism is crucial to obtain a fine-grained ferrite (one of the stable low-temperature phases) while avoiding decomposition to other undesirable microstructural states. A fine-grained ferrite microstructure is required to achieve both a high yield strength and a high toughness for naval ship structures.

Austenite decomposition diagrams called isothermal transformation (I-T) and continuous cooling transformation (C-T) diagrams are complex functions of many variables but especially of austenite grain-size and composition. Heat treaters and welders are among the processing engineers who find these diagrams extremely valuable. In the past, such diagrams have been determined experimentally at considerable time and expense. Our long-range research effort seeks to develop microstructural models of austenite decomposition in iron-carbon alloys based on known atomic mechanistic principles with the aim of calculating the I-T and C-T diagrams from these models. The ultimate success of this program is expected to reduce the work required to provide these diagrams to the engineer.

Our initial progress focuses on modeling the effects of austenite grain size, composition, and temperature on the decomposition of austenite to ferrite. The method allows partial I-T and C-T diagrams to be calculated for polycrystalline alloys of known composition and grain size. In the work, we discovered and experimentally verified a grain size scaling relationship that allows the austenite to ferrite portion of I-T and C-T diagrams to be calculated for any grain size once data are available for one grain size. Thus the diagrams do not need to be determined experimentally for each grain size of interest.

Model: The model is strictly applicable to any iron-carbon alloy undergoing austenite decomposition to proeutectoid, polygonal ferrite. The parent austenite grains are modeled as spheres. The polycrystalline solid is considered to consist of a log-normal distribution of contiguous spheres. Initially, the austenite grains contain a given uniform carbon concentration. Nucleation of ferrite is assumed to be site-saturated, occurring at the parent grain boundaries that are assumed to be covered fully with an infinitesimally thin ferrite layer immediately after nucleation. With increasing isothermal reaction time, the ferrite layer thickens as the austenite/ferrite interfaces move toward the centers of the austenite grains. Local thermodynamic equilibrium is assumed at the interfaces. The concentration of carbon in the untransformed austenite is given by a quasi-static, approximate solution of Fick's second law of diffusion with a constant, average diffusivity. Effects of temperature, composition, volume change, austenite grain size, and carbon build-up ahead of the advancing interfaces are incorporated in the treatment.

The I-T Diagram: The fraction of austenite transformed isothermally to ferrite at any instant is calculated from a carbon atom material balance. The time-dependence of the transformation fraction is computed numerically by summing up over all the grains in the microstructure. The I-T diagram is mapped out when the transformation kinetics are determined for a whole supercooled range of temperatures.

The C-T Diagram: Continuous cooling behavior is approximated as a series of small incremented isothermal steps. By applying the additivity principle, the I-T diagram data can be converted to a C-T diagram for any specified

cooling behavior by using numerical integration. Figure 1 is a representative C–T diagram for austenite decomposition to ferrite by a diffusional mechanism under constant cooling rate conditions for an iron +0.036 wt.% carbon alloy having an average mean grain size of 100 μm.

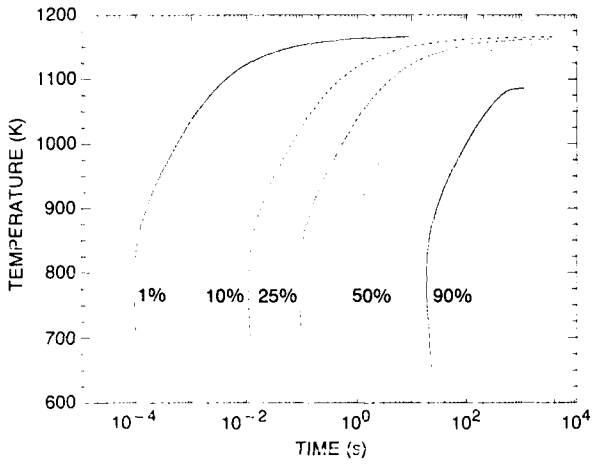

Fig. 1 — A C–T diagram for austenite decomposition to ferrite by a diffusional growth mechanism for an iron +0.036 wt.% carbon alloy under constant cooling rate conditions. The prior austenite grain size was 100 μm.

Effect of Austenite Grain Size: From the modeling studies it was noted that the reaction time needed to achieve a given fraction transformed was proportional to the square of the austenite grain size. From this observation, a scaling relationship is proposed to enable the effect of austenite grain size on transformation kinetics to be characterized for any grain size provided kinetic data are available for one grain size. This scaling relationship is in contrast to other suggested inferences in the literature of a linear grain size dependence. The newly proposed grain size relationship was tested and verified experimentally (Fig. 2) by using dilatometry and optical metallography. The test consisted of applying the scaling relationship to C–T diagram data from a fine-grained material (22.3 μm) and calculating the transformation times that would be obtained if the same material were coarse grained (68.5 μm). The predicted times are then compared to actual experimental data on the coarse-grained material.

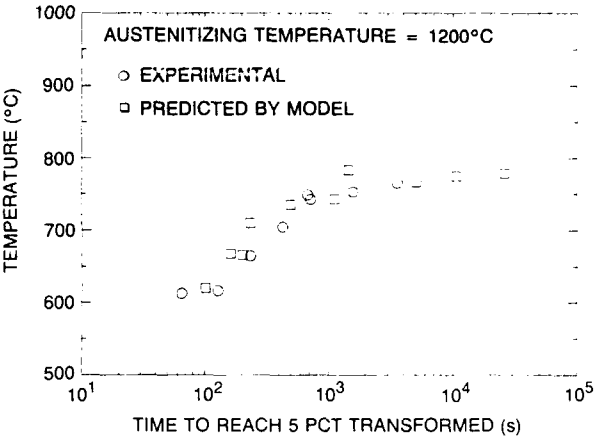

Fig. 2 — Comparison of model derived grain size scaling predictions with experiment in a laboratory ferrous alloy at 1200°C

Acknowledgment: NRL employees Carl L. Vold and William E. King, Jr. assisted with the experimental phase of this study while Robert A. Masamura helped with the modeling effort.

[Sponsored by ONR] ■

Glass Fibers with Metallic Cores

J. D. Ayers
Materials Science and Technology Division

Studies are under way of processes for producing glass fibers containing embedded single or multiple metallic filaments. The glass fibers have diameters ranging from approximately 10 to more than 100 μm, while the filaments have diameters varying from about 0.1 up to 50 μm or more. A method for making such fibers was first described in 1924 by G.F. Taylor [1], and such fibers have come to be known as Taylor wires. Taylor's method consisted of melting a small amount of metal within a glass capillary and of then drawing a fiber from the softened glass. Such fibers are restricted in length because of the small amount of metal enclosed, the softened glass generally being able to support only a gram or so of melt. One method for making long lengths of Taylor wires [2] maintains a constant melt pool size by feeding a small wire into it while simultaneously advancing the glass tube that

contains it. The previously unreported methods described here are far easier to control than the earlier technique, and they make possible the drawing of fibers containing multiple metallic or semiconducting filaments.

Processing Methods: Several new methods have been developed, each of them having advantages and disadvantages. One of the most versatile of these consists of simply closing one end of a capillary, filling it with powdered metal, evacuating it, and feeding it at a constant rate into a short hot zone while simultaneously drawing a fiber from the heated tip. Figure 3 schematically shows this process variant. Keys to the success of this approach are that the geometry naturally assures that only a small amount of the charge is molten at any time, and that the applied vacuum removes undesired gases from the melt zone, making it possible for the pressure of the atmosphere to collapse the glass around the charge and thus eliminate the free volume that would otherwise develop as the charge melts. The process is most successful with charge materials that melt at temperatures no more than a few hundred degrees below the working temperature of the glass, because the glass begins to constrict around the powder before it melts, and this constriction prevents the charge from settling and creating gaps as it fuses into the more dense melt pool. With properly selected materials, this process can produce very long lengths of fiber.

Figure 4 shows one of several possible variants of this process. This variant differs from that illustrated in Fig. 3 only in that the powder fill is a blend of metal, semiconductor, or crystalline ceramic powder and crushed glass powder. When a fiber is drawn under appropriate processing conditions from a glass tube containing this blended powder, the powdered glass particles fuse into a nearly continuous matrix phase. The individual metal (or other fill material) powder particles are each drawn out into fine filaments whose diameter depends on the initial particle size and the diameter reduction produced by the fiber

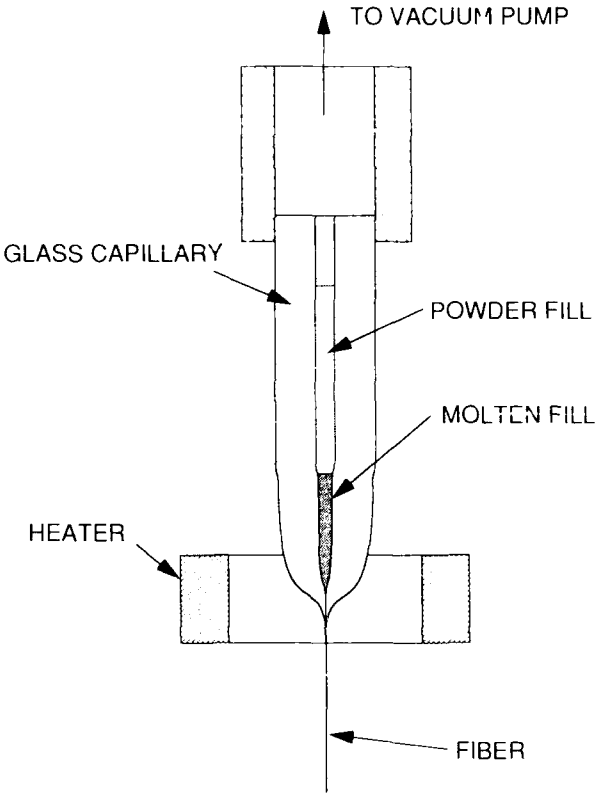

Fig. 3 — Fiber drawing process employing a powder fill. The glass capillary shown is greatly shortened and does not illustrate the mechanisms for advancing the glass and spooling the fiber.

drawing process. As an example of the possibilities with this process, if a 200-μm diameter metal droplet is drawn into a filament by using processing conditions that produce an overall diameter reduction ratio of 200 to 1, the filament will have a maximum diameter of 1 μm and a length of approximately 8 m. The long filaments that are generated from randomly spaced powder particles are randomly positioned within the fiber, but in any short section of the fiber most of the filaments are continuous (Fig. 5). Figure 5 shows the cut end of a fiber drawn from a Pyrex tube filled with a mix of Pyrex and high-purity germanium powders. The fiber was etched to remove the outer sheath of glass and most of the glass matrix between the Ge filaments, leaving them exposed.

Materials and Applications: A wide variety of metal types is investigated, though all must be

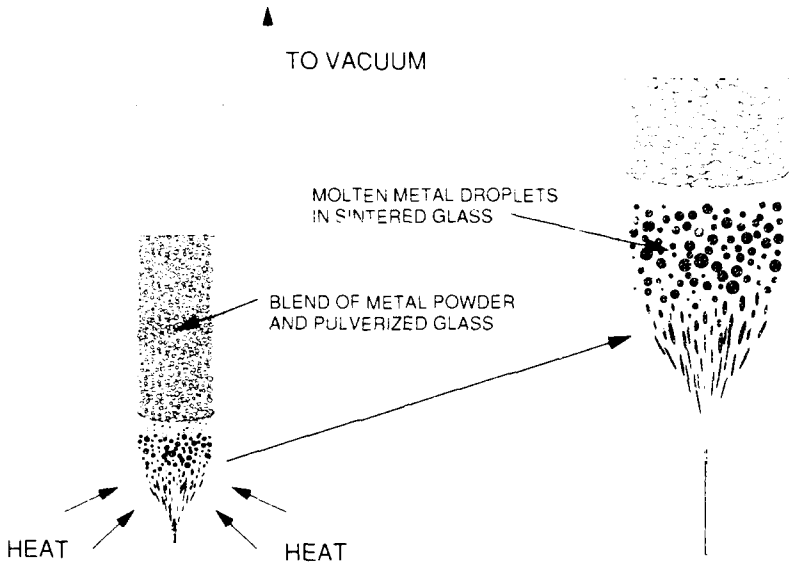

Fig. 4 — Process for drawing a glass fiber containing many fine filaments

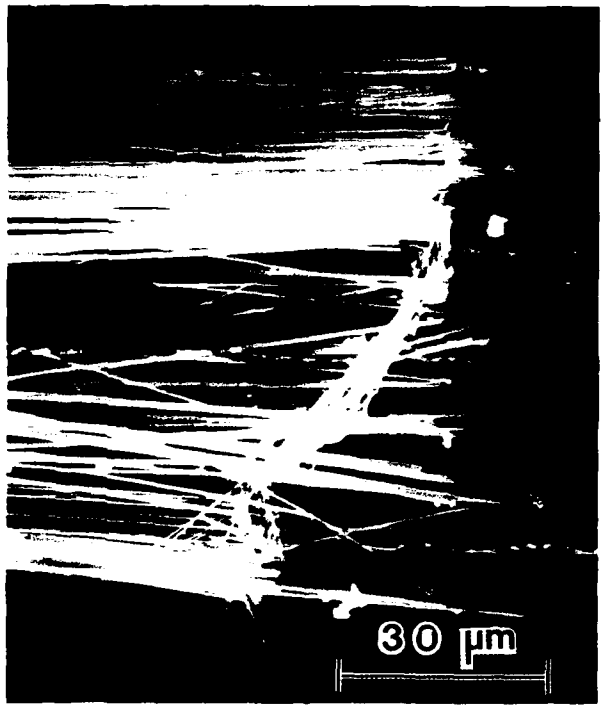

Fig. 5 — End of fiber that contains many germanium filaments. The fiber was deeply etched to remove much of the glass and expose the filaments.

compatible with the oxide glasses used. For this reason, metallic alloys with significant concentrations of reactive elements like Al, Ti, and Cr cannot be used, and filament materials must have melting temperatures below approximately 2000°C, the working temperature of fused silica, which is the most refractory of all glasses. This leaves a wide range of materials from which to choose.

We believe that these studies will lead to the development of materials that will find use in diverse electrical and magnetic applications. Work is under way to explore the potential of the Ge filamentary composites for use in high-current field emission arrays, and a study has begun of high-permeability composites containing soft magnetic filaments. Other possibilities include improved artificial dielectrics, magneto-optical sensors, electromagnetic emission control materials, and high-temperature superconducting wires. Studies of any of these materials should prove fruitful.

[Sponsored by ONR]

References

1. G.F. Taylor, "A Method for Drawing Metallic Filaments and a Discussion of Their Properties and Uses," *Phys Rev.* **23**, 655 (1924).

2. V.N. Parkhachev, U.S. Patent 3256584 (1966). ■

Impact Angle Effects on Fracture

V. Gensheimer DeGiorgi
Materials Science and Technology Division

Dynamic material response is a complex phenomenon influenced by component geometry and loading history. Cracks have significant effects on load-carrying capability and add complications to structural integrity predictions. Often, a component contains a crack that is subjected to dynamically applied loads. In such a situation, the difficulties of dynamic material response are combined with those of fracture mechanics. Understanding how a component with a crack responds to a dynamically applied load is essential for the development of a rational and scientifically based structural integrity methodology and acceptance criteria.

Details of dynamic load application may significantly affect dynamic fracture. In the work described, the effect of the impact angle on stress field patterns and time to fracture is examined for a simply supported beam with a crack.

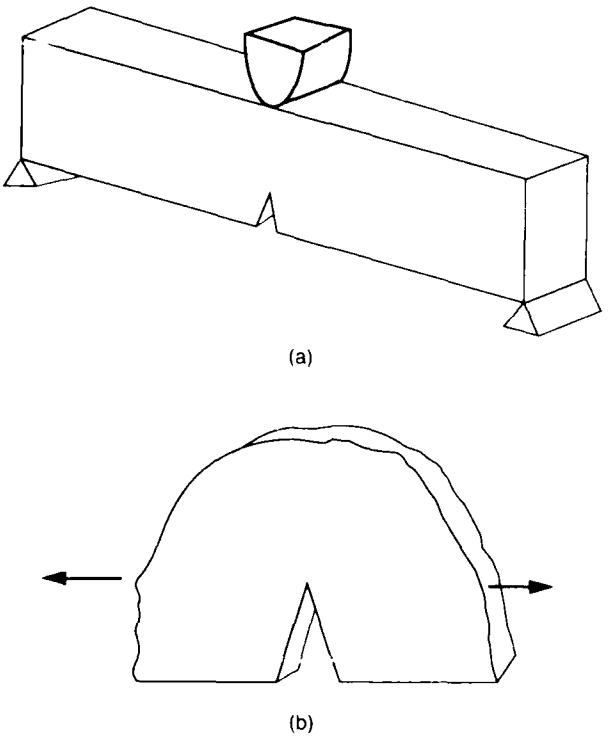

Fig. 3 — (a) Test specimen geometry (b) Mode I crack opening

Numerical Simulation: A simple beam with a rectangular cross section (Fig. 6(a)) and a crack on the lower surface at the center of the beam span is subjected to a dynamically applied load. A hammer strikes the beam directly above the crack generating a Mode I crack opening. Figure 6(b) shows that the crack faces are pulled apart in a Mode I crack opening. The stress fields that result from the dynamically applied load change with

time and are a combination of refractive and reflective stress waves.

In one numerical simulation, the dynamic load is applied so that the impact direction and beam surface form a 90° angle (Fig. 7(a)). In the second numerical simulation, the dynamic load is applied along a 45° angle (Fig. 7(b)). A load-time history obtained from a laboratory experiment is used to define the dynamically applied load in the numerical simulations [1].

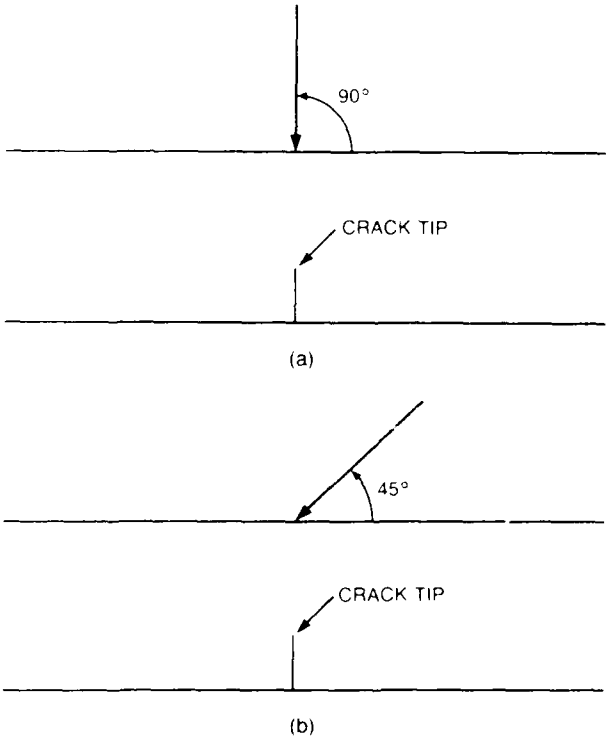

Fig. 7 — Impact angles

The numerical simulations are performed by using the commercial finite element code ABAQUS and NRL's Cray-XMP supercomputer. In both simulations, 276 time steps of 0.33×10^{-6} s each are performed for a total analyzed time of 81.2×10^{-6} s. Finite element results for the 90° impact load are used for verification of the model and solution procedures. Stress components from an analytical solution that does not include reflective stress waves are compared with finite element generated values [2]. The differences in the stress components prior to the arrival of the first reflective stress wave are negligible.

The Mode 1 linear elastic stress intensity factor is determined from the finite element results at an experimentally observed time to fracture for a 90° impact loading [1]. This value compares favorably with experimentally determined values, indicating that the finite element model accurately predicts the stress field magnitude at the fracture time [2]. The fracture time for the 45° impact loading is determined by comparing stress magnitudes with those for the 90° loading at the experimentally observed time to fracture. The fracture times are 66.0×10^{-6} and 60.0×10^{-6} s for the 90° and 45° loadings, respectively.

Stress Field Patterns: Fracture initiation is typically characterized by a comparison of point values, i.e., stress, strain, or energy values are compared with critical values. However, the path taken by a growing crack will be in part determined by the stress fields ahead of the crack tip. Therefore, the changes in time of the stress fields are of interest. Early in the dynamic stress history, the impact angle has a dramatic effect on the Mode I opening mode stress field near the crack tip (Fig. 8(a) and (b)). However, at 21.1×10^{-6} s, the opening mode stress field becomes symmetric about the crack tip despite the 45° impact angle (Fig. 8(c)). No significant differences exist between the stress patterns for the 90° and 45° impact angle loads past this time. The stress patterns for the two impact angles become similar well before the fracture times.

Summary: By comparing finite element results with analytical and experimental values, the model and procedures used accurately predict the stress fields caused by dynamically applied loads.

The impact angle affects the fracture time for the given material and geometry combination. A 45° difference in impact angles results in a 10% difference in fracture times. The most noticeable effect of impact angle is its influence on the stress fields that develop shortly after impact. However,

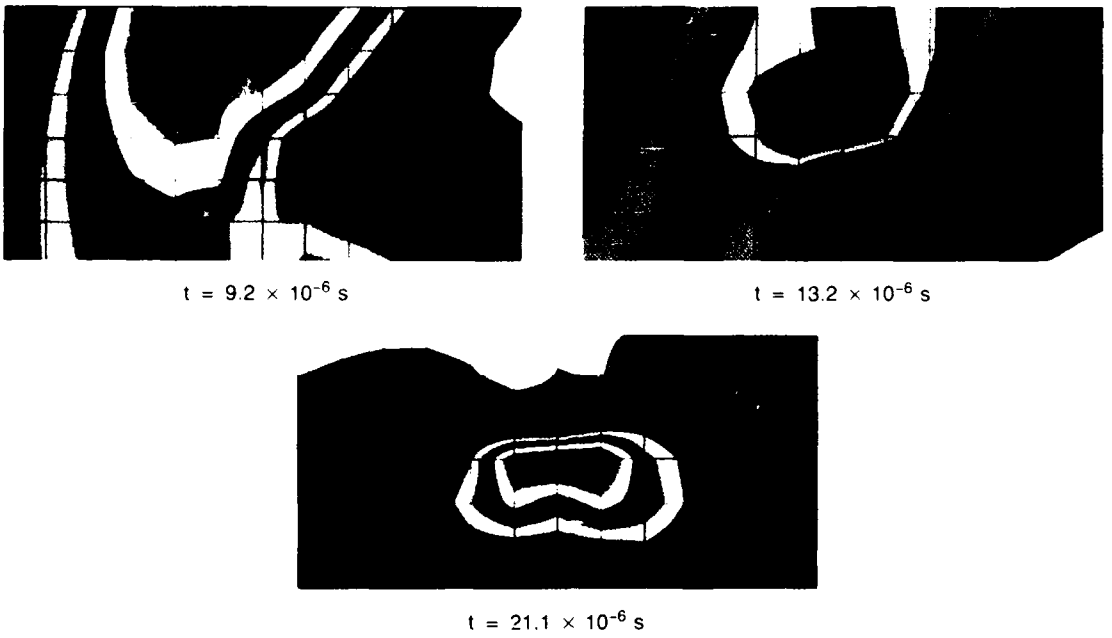

Fig. 8 — Mode I opening stress field in the near crack tip region

no significant differences in stress fields remain by the time fracture occurs.

[Sponsored by NRL]

References

1. G.E. Nash and E.A. Lange, "Mechanical Aspects of the Dynamic Tear Test," *ASME J. of Basic Engineering* **91** (1969).

2. V.M. Gensheimer, L.M. Brock, and M.I. Jolles, "The Effect of First Reflections in the Dynamic Tear Test," NRL Memorandum Report 6232 (1988). ■

Indicator of High-Temperature Oxide Superconductors

H. A. Hoff and M. S. Osofsky
Materials Science and Technology Division

The technological expectations for the new copper oxide high-temperature superconductors are tremendous. Using a technique discovered at NRL, these materials can be inspected for homogeneity and superconductivity at room temperature. This allows the materials to be processed into electronic devices quickly and efficiently. In any optical microscope equipped to view materials in reflected polarized light from a "daylight" source, the individual crystals that are the superconductors can be identified by their own characteristic color.

Processing Challenges: The copper oxide (cuprate) superconductors can be produced as thin films, polycrystalline bulk, or single crystals. Thin films for electronic components are one of the most important applications for the new cuprate superconductors; this is of interest to the Navy. Bulk materials are used to produce superconducting wires for magnets that can be used onboard Navy ships. Behind each of these efforts is a need to produce single crystals for basic research on the intrinsic properties of these unique materials. Stoichiometry and homogeneity impact critically on the proper electronic functioning of any component—thin film or wire—and local deviations within single crystals can lead to erroneous results.

Technique of Inspection: Many opaque, anisotropic materials have their own characteristic color when viewed in reflected polarized light through crossed polarizers (polarization color). If the structure or composition is changed, the color generally changes or disappears. For the high transition temperature T_c cuprate superconductors, a characteristic polarization color exists regardless of changes in structure or composition, as long as copper oxide is still the main component and the material is still superconducting [1]. Yet copper oxide (CuO or Cu_2O) itself does not have this color.

While color observation is not a replacement for resistivity, susceptibility, or magnetization measurements to determine the existence of superconductivity, the presence of a brownish yellow (golden) color always indicates which cuprate grains are superconductors. Any bench-top optical microscope equipped with a daylight source (color temperature 5400 K to 7000 K) can be used.

Figure 9 shows the golden color characteristic of all the cuprate superconductors; this is actually a bulk sample of a Bi-Sr-Ca-Cu-O (BiSCCO) superconductor. In one of the phases of the BiSCCO family, Bi can be partially replaced by Pb and to a limited extent by Sb. The golden color is found for both electron hole and electron cuprate superconductors. Included among those that are hole carrier superconductors, in addition to BiSCCO and $YBa_2Cu_3O_{7-}$type, are materials of the first family of cuprate superconductors discovered; for example, $La_{1.85}Sr_{0.15}CuO_4$ and the Tl-based superconductors, such as $Tl_2Ba_2Ca_2Cu_3O_{10}$. This latter superconductor has the highest T_c so far confirmed for any superconductor. The electron superconductors include materials such as $Nd_{1.85}Ce_{0.15}CuO_4$.

Thin films and single crystals can be examined in a nondestructive manner, as long as the grain size is at least within the range of resolution of an optical microscope (≥ 1 μm). A bulk material need only be polished to produce a clean, flat surface.

Fig. 9 — The characteristic golden color of polarization observable in all cuprate superconductors is shown here for a bulk sample of $Bi_2Sr_2CaCu_2O_8$

The presence of an intermediary color in the sequence gray→blue→brown→gold, seen upon observing the grains with an optical microscope, can point out a lack of metal ion or oxygen stoichiometry. Subsequent examination with energy dispersive X-ray spectroscopy can quantify the metal ion concentrations. For these superconductors, even when the metal ion concentrations are correct, the oxygen stoichiometry may be off so that individual grains are still insulators. Color analysis is a quick technique for indicating a possible oxygen deficiency. The presence of other colors, for example, green (usually Y_2BaCuO_5), red (Cu_2O), or bluish green (CuO), shows that inhomogeneities exist.

Significance of the Characteristic Color: The reflected region of the electromagnetic spectrum, which produces the golden color, contains significant information about the electronic structure and normal state properties of these materials. Specifically, it describes the electronic state of the copper oxygen (CuO_2) planes, where superconductivity originates, as they are affected by doping of either holes or excess electrons. The changes in color from

insulator to superconductor reflect the successive changes in the 3d orbitals and their ionic or metallic bonding combinations with the oxygen 2p states involved in superconductivity.

[Sponsored by ONR, ONT, SDIO/IST, and DARPA]

Reference

1. H.A. Hoff, M. Rubinstein, M.S. Osofsky, A.K. Singh, L.E. Richards, W.L. Lechter, L.E. Toth, B.N. Das, and C.S. Pande, *J. Superconduct.* **2**, 351 (1989). ■

An Hydroxide Etch for β-SiC

P. E. R. Nordquist, Jr., R. J. Gorman, and P. H. Klein
Electronics Science and Technology Division

Cubic, or beta, silicon carbide (β-SiC) is a *semiconductor* material currently under study for high power and high-temperature applications. β-SiC is most commonly grown by chemical vapor deposition (CVD) at 1350°C on (100) silicon from a gas stream containing propane (C_3H_8) and (SiH_4) in a flowing hydrogen ambient. Because of the difference in lattice constants between silicon (a_o = 5.43 Å) and β-SiC (a_o = 4.36 Å), CVD-grown SiC has a high incidence of crystalline defects, such as stacking faults, dislocations, and antiphase boundaries (APBs). APBs are reversals in polarity in the (111) direction of the β-SiC zinc blende lattice.

Crystalline defects degrade the performance of semiconductor devices. A rapid way to reveal and measure them is of paramount importance to the materials scientist who aspires to grow low defect materials. Defects in β-SiC can be revealed by transmission electron microscopy, but a quicker, more convenient method is by chemical etching.

Chemical etches, by selectively attacking areas of increased reactivity on crystal surfaces, offer a useful way of evaluating the crystalline quality of ordered materials. In etching, chemical attack occurs at points where crystalline defects in the bulk material intersect the surface. The shape of the etch figures and the etch pit density (EPD) measure crystal quality and provide a way to evaluate the effect of changes in crystal growth variables.

Defects in β-SiC can be revealed by etching with molten KOH at 600°C. The high etch temperature gives a rapid etch rate and a high background etch, leading to poorly developed etch pits. Lower temperatures cannot be used with pure KOH because of its high viscosity close to its melting point (380°C). We have found that etching with the NaOH-KOH eutectic (an equimolar mixture of NaOH and KOH melting at 170°C) reveals dislocations, stacking faults, and APBs after 75 min etching at only 350°C. Because of the lower etch temperature, etch figures are obtained with negligible background attack.

Figure 10 shows a typical surface of CVD β-SiC etched by the NaOH-KOH eutectic. Etch figures reveal the presence of APBs (A), stacking faults (B), and dislocations (C).

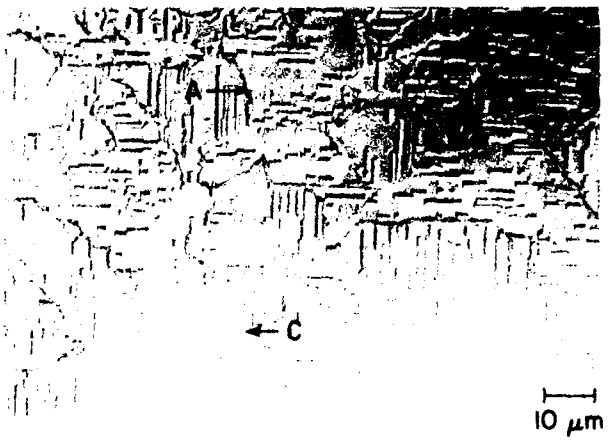

Fig. 10 — Etched β-SiC grown on (100) Si; layer thickness is 19 μm

We have used the NaOH-KOH eutectic etch to study the effect of crystal thickness, carbon-to-silicon ratio (C/Si) in the reactant gas stream, and substrate orientation on the EPD and

on the formation of APBs. We find that both EPD and the density of APBs decline by about 50% as layer thickness increases from 8 to 16 μm. EPD in 16 μm layers is approximately $8 \times 10^6/cm^{-2}$ for a C/Si of 2.4.

At constant layer thickness (10 μm), we find that increasing the C/Si in the reactant gases, at constant ([C] + [Si]) and total flow rate, diminishes the APB density from 1200 APB/cm at C/Si = 1.2 to 610 APB/cm at C/Si = 4.0. EPD, however, declines only slightly with increasing C/Si in the same range from $2.4 \times 10^7/cm^2$ to $2.0 \times 10^7/cm^2$. Our use of the NaOH–KOH etch also confirms that APBs are dramatically reduced but not completely eliminated by CVD growth of β-SiC on off-axis silicon (e.g., (100) oriented 4° toward the (110)).

The NaOH–KOH eutectic etch allows rapid and simple characterization of the crystalline quality of β-SiC and permits selection of optimum growth conditions for the CVD of β-SiC.

[Sponsored by ONR]

References

1. P.E.R. Nordquist, Jr., H. Lessoff, R.J. Gorman, and M.L. Gipe, *Materials Letters* 7, 316 (1989).

2. P.E.R. Nordquist, Jr., M.L. Gipe, G. Kelner, P.H. Klein, and R.J. Gorman, *Materials Letters*, in press. ■

Chemical Research and Biotechnology

CHEMICAL RESEARCH AND BIOTECHNOLOGY

Chemistry has played an important role in solving many of the Navy's problems relating to polymeric materials, coatings, fuels and combustion, synthesis of materials, firefighting, and surface chemistry; biomolecular engineering holds much promise. Reported in this chapter is work on membrane-active peptides, fuel availability and performance, high-temperature combustion, epoxy coatings for shipboard piping, and polymerized vesicles.

Contributing to this work are the Laboratory for Structure of Matter (6030), the Center for Bio/Molecular Science and Engineering (6090), and the Chemistry Division (6100).

Other current research in chemistry includes:

- Membrane biosensors
- Polymer microlithography
- Surface mechanics and adhesion
- Cold fusion theories

Assembly of Membrane-Active Peptides

I.L. Karle and J.L. Flippen-Anderson
Laboratory for Structure of Matter

Naval personnel are exposed to diseases in their tours of duty, as well as to shock and trauma in extreme circumstances. The transport of ions through cell membranes plays a vital role in the above conditions. Antibiotic peptides such as gramicidins, antiamoebins, and zervamicins insert themselves into biological membranes and mediate ion transport. The general objective of the present study is to try to determine the nature of the pores or channels that such peptides form in membranes and the mechanism by which the ions are transported.

Mode of Investigation: X-ray diffraction analyses of single crystals yield information in the form of coordinates of each atom in the crystal. Hence accurate pictures of the shapes and dimensions of molecules that compose the crystal are obtained. An ideal situation would be to cocrystallize a component material of a membrane with a membrane-active peptide. Since such cocrystallizations have not yielded suitable crystals yet, the practical alternative has been to examine single crystals of a large number of peptides. The immediate objective has been to establish the mode or modes of assembly of helical peptides that should give information about pore formation.

Materials: Apolar, membrane-active peptides with 10 to 20 amino acid residues are synthesized (by P. Balaram and students at the Indian Institute of Science, Bangalore, India) with a variety of sequences of amino acid residues that contain different hydrocarbon side chains. Single crystals are grown from solvents having varying hydrophobic or hydrophilic properties and are analyzed by X-ray diffraction. Often peptides with the same sequence produce crystals from different solvents that have a different arrangement of molecules in the crystal.

Experimental Results: All of these peptides form alpha-helices (Fig. 1). The backbone of an alpha-helix is wound much too tightly for an ion to travel down the core. Accordingly, the present ideas are that a number of helices must aggregate in

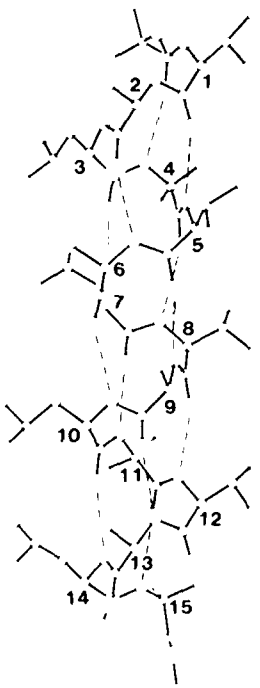

Fig. 1 — A 15-residue alpha-helix. The C^{α} atoms are labeled 1-15. All carbonyl groups (O atoms have the largest circles) are directed downwards. All NH groups (N atoms have medium circles; H atoms have been omitted) are directed upwards. Dashed lines represent the intramolecular hydrogen bonds.

some fashion to form a pore or channel in a membrane.

Figure 2 summarizes the mode of assembly of helices found in 25 crystals. All the helical peptides form continuous columns by head-to-tail NH···OC hydrogen bonding (Fig. 2 (a)). As Fig. 1 shows, for every helical molecule, three NH groups at the top of the helix and three C=0 groups at the bottom are not involved in *intra*molecular hydrogen bonding. These moieties participate in the head-to-tail hydrogen bonding. Laterally, the sidegroups of this group of peptides are all apolar and hydrophobic. Assembly is by van der Waals' attraction. In all the crystals studied, the columns of peptides assemble into sheets with *all* the helix axes pointed in the same, or nearly the same direction (Fig. 2(b)). If two conformers are present in the same crystal, each conformer assembles into a separate sheet, each with parallel packing of helices. The column and sheet motif appears to be common to all the helical peptides studied so far.

The differences in aggregation of the peptides are the manner in which sheets assemble: parallel, antiparallel, or skewed. Peptides with nearly identical sequences have been found to exhibit all three modes of assembling sheets. In several cases, for two polymorphs (crystal forms) of the same peptide, the sheets in one polymorph assemble in the parallel mode, with all helix axes pointed in the same direction (Fig. 2(c) parallel), while the sheets in the other polymorph assemble in the antiparallel mode (Fig. 2(c) antiparallel). The third mode with skewed helix assemblies (Fig. 2(c) skewed and

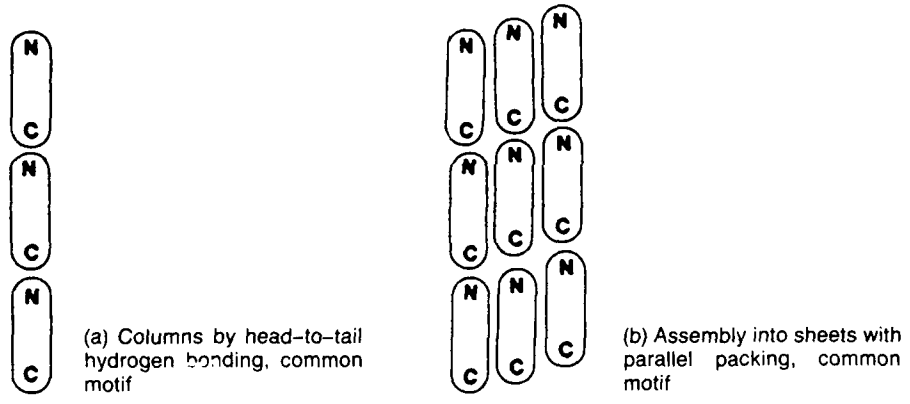

(a) Columns by head-to-tail hydrogen bonding, common motif

(b) Assembly into sheets with parallel packing, common motif

(c) Assembly of sheets with parallel packing, varying motifs

Fig. 2 — Elements of aggregation of helices

Fig. 3) has occurred only once so far. In that crystal, adjacent sheets were rotated by 40° or 180° ± 40° with respect to each other.

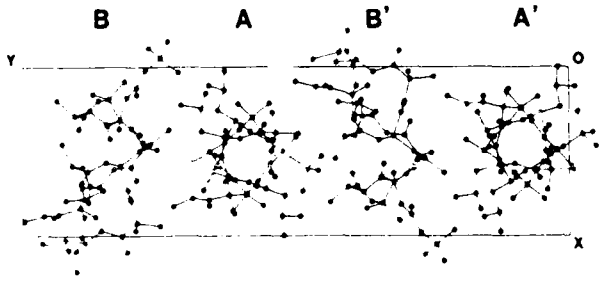

Fig. 3 — Crystal packing of a helical peptide with adjacent helices meeting at an oblique angle, 40°. Each of the molecules lies in a sheet, perpendicular to the view shown, in a parallel sheet motif as shown in Fig. 2(b).

Conclusions: These results show that for apolar helices no particular correlation exists between the type of side chain and the mode of three-dimensional assembly. Furthermore, in many of the crystals, the packing of the side chains is quite inefficient and creates voids between the molecules. These facts may indicate why considerable compatibility exists between membranes of various composition and peptides of various sequences.

Antiparallel assembly of helices was expected *a priori* because helices in protein molecules have been observed to associate either in the antiparallel or skewed mode [1]. In addition, alpha-helices possess a considerable dipole moment since all the C=O groups are aligned in one direction—parallel to the helix axis—whereas all the NH groups are aligned in the opposite direction. The strong dipole moment was shown theoretically to prevent parallel assembly [2]. However, structure analyses at NRL show that nearly as many crystals exist with parallel association of peptides as with antiparallel association. Obviously, the dipole moment is not a factor.

New directions being pursued involve peptides with a small number of polar side chains on one side of the helix, which may orient the helices toward pore-forming assemblies. A positive indication has been a polar channel formed by an assembly of apolar helices in which water molecules have insinuated themselves into one side of the backbone of the helix [3].

[Sponsored by NIH and ONR]

References

1. J.S. Richarson, in *Advances in Protein Chemistry*, C.B. Anfinson, M.L Anson, J.T. Edsall, and F.M. Richards, eds. (Academic, New York, 1981), pp. 169-339.

2. W.G.J. Hol and M.C.H. de Maeyer, *Biopolymers* **23** 809-817 (1984).

3. I.L. Karle, J.L. Flippen-Anderson, K. Uma, and P. Balaram, *Proc. Natl. Acad. Sci. USA* **85** 299-304 (1988) and I.L. Karle, *1987 NRL Review*, pp. 75-77 (July 1988). ■

Polymerized Vesicles Revisited

A. Singh
Center for Bio/Molecular Science and Engineering

Introduction: Nature provides excellent working models for the development of technological marvels. Our current research is aimed at identifying and understanding some of those biological systems that might provide significant aid in solving material problems for the Navy. Phospholipid membranes constitute one such biological system and have been used for encapsulation, transport, and delivery of substances, target recognition, and catalytic reactions to name a few.

Structurally, phospholipids are simple molecules that, because of their amphiphilic characters (i.e., being hydrophobic at one end and hydrophilic at the other), are one of the most versatile classes of organic compounds of biological origin. Phospholipids (natural, synthetic, or modified), upon coming in contact with water, spontaneously self-organize in a manner that keeps their hydrophilic regions (polar

headgroups) facing water. This leads to the formation of closed, hollow, concentric bilayer structures called vesicles. Figure 4 illustrates the versatility of these microstructures.

Background: Polymerized vesicles were first synthesized in 1980 [1] mainly for the purpose of retaining their structural integrity and function under harsh environments. Studies on polymerizable diacetylenic phosphatidylcholines (PC), a precursor of polymerized vesicles, have also led to the discovery of "tubules" (see Schnur, *NRL Review* 1987). As a result of our ongoing studies, we now believe that polymerized vesicles, with the aid of planned molecular engineering, can be used in the development of stabilized microdevices that will be functional at higher temperatures and in adverse solvents. At NRL's Center for Bio/Molecular Science and Engineering, studies on polymerizable lipids and other synthetic self-assembling molecules are in progress to develop scientific understanding to meet the challenges needed for future technology [2].

In principle, any amphiphile with proper headgroup hydrocarbon chain volume ratio (usually 3) serves as material for constructing vesicles. At NRL, we have undertaken synthesis as an approach to make a variety of polymerizable amphiphiles not only to fulfill the material need for advanced applications but also to enhance the basic understanding towards self-organization of molecules. Synthetic strategies consist of chemical modifications on both segments of the molecules, the polar headgroup and hydrocarbon chains. Our efforts are summarized in Fig. 5.

Ongoing Research: In our laboratory, only the hydrocarbon chains are modified by introducing polymerizable moieties such as diacetylenes (conjugated and nonconjugated), acetylene, olefin, and methacrylate. Polymerization in vesicles is initiated by ultraviolet or gamma radiation, as well as by using radical initiators. Preliminary studies on headgroup–modified lipids have demonstrated the influence of size and/or charge of the headgroup on the morphologies of resultant microstructures, and on polymerization efficiency in bilayers. We have

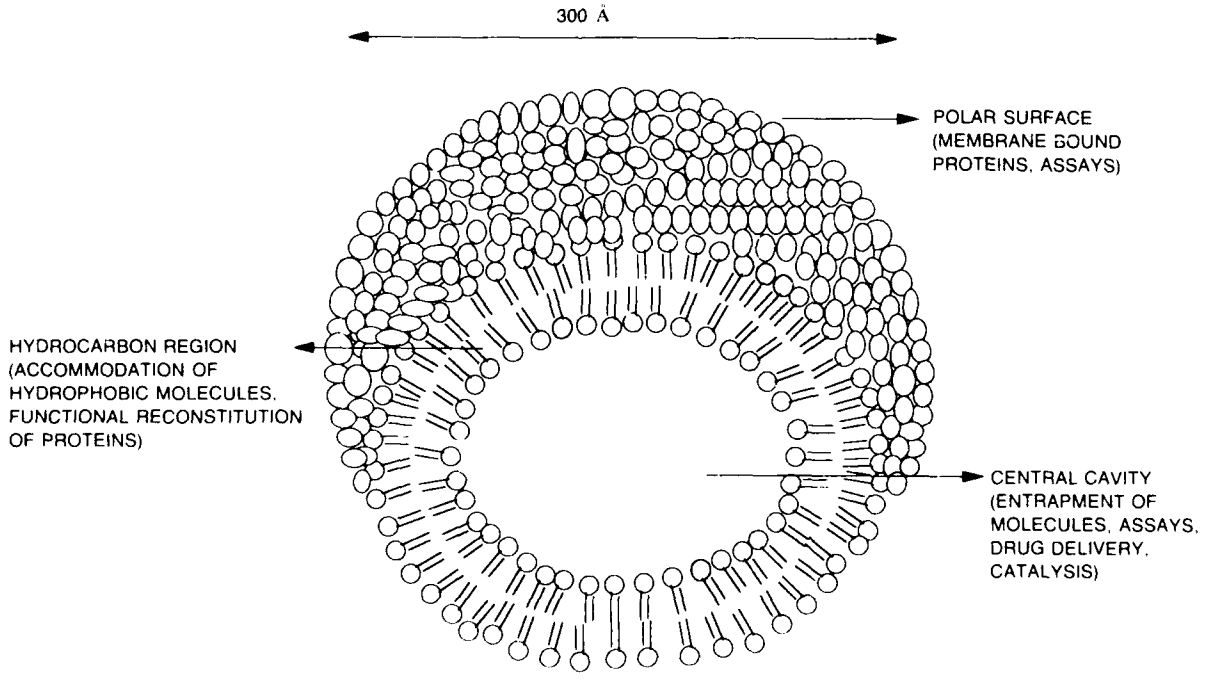

Fig. 4 — Each site in a vesicle offers potential for application

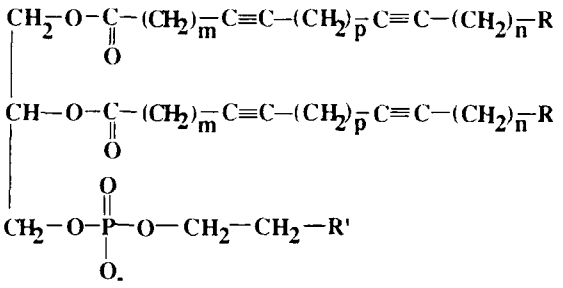

m	n	p	R	R'
5 - 15	6 - 16	0	CH_3	$\overset{+}{N}Me_3$
4,8	13,9	1	CH_3	$\overset{+}{N}Me_3$
8	8	0	$CH{=}CH_2$	$\overset{+}{N}Me_3$
8	9	0	CH_3	NHMe
8	9	0	CH_3	OH

Fig. 5 — Polymerizable phospholipids

also modified headgroups to create functionally reactive stabilized vesicle surfaces to which enzymes or other molecules of interest may be attached. This is achieved by introducing substituted ethanolamines and hydroxyalkanols. As a new approach, we are now investigating the use of two single-chain amphiphiles consisting of identical chains but different headgroups. This strategy will allow us to functionalize vesicle surfaces with two chemically different molecules.

For our studies, we have fabricated vesicles by hydrating a thin film of an amphiphile above its chain-melting temperature followed by intermittent vortex mixing (from 1 to 5 minutes) to produce multilamellar vesicles (MLVs, diameter up to 5 μm) and extensive sonication of MLVs to produce small unilamellar vesicles (from 200 to 500 Å). We have studied vesicles before and after polymerization for their entrapment efficiency and leak rates to develop controlled release carriers.

Currently, we are exploring the potential of vesicles constructed from a mixture of polymerizable diacetylenic PC and a nonpolymerizable PC in which the acyl chain length of the nonpolymerizable PC is similar to the upper segment (m) of diacetylenic PC [3]. We have made two observations. First, the polymerization of diacetylenes in vesicle bilayers is fast (seconds as compared to minutes) and extensive, which is evident with the production of deep blue color and the presence of a small amount of unreacted monomer. Second, nonpolymerizable lipid could be removed from the vesicles by detergent dialysis leaving a void in vesicles. We have successfully used detergent dialysis technique to incorporate bacteriorhodopsin, a membrane protein, in the vacated space. This result clears the way to fill the void left by a nonpolymerizable lipid with a molecule or molecular assembly assigned to perform a specific function (e.g., molecular recognition, metal detection, and recovery). Figure 6 illustrates the general working scheme of this system.

Significance and Future Goals: Applicability of conventional vesicles in complement-mediated ultrasensitive detection, immunosensors, and heme encapsulation is well demonstrated. Polymerized vesicle systems have been used to develop receptor-based biosensors [4]. These systems have also been used in membrane protein incorporation. We are now exploring mixed lipid systems consisting of polymerizable lipids to achieve molecular recognition, triggered release of encapsulant (decorking), and metal-ion transport (ionophore incorporation). We are also exploring polymerizable vesicles constructed by mixing neutral lipid and surface modified lipids in the development of rugged, ultrasensitive detection devices. Flexible membranes may be produced from allenic, dienic, methacrylic, or sulfhydryl lipids, which may attract the attention of scientists and engineers.

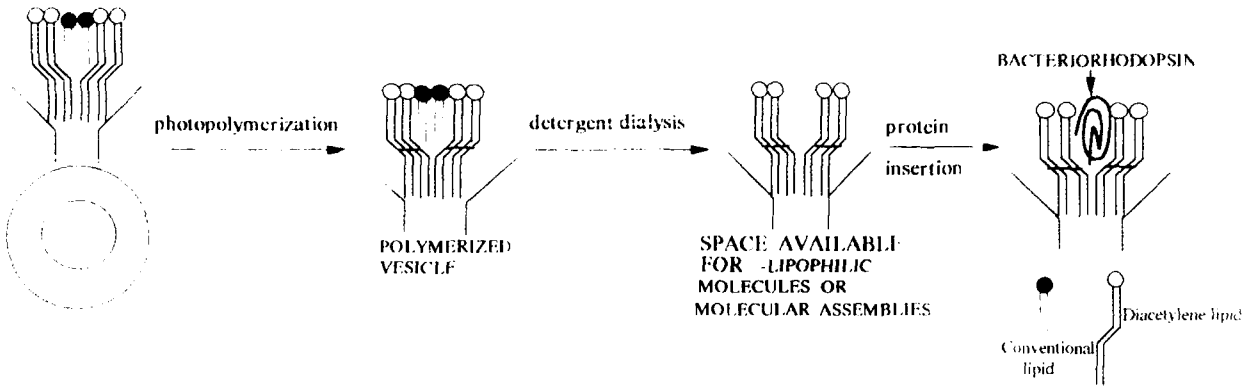

Fig. 6 — Vesicles from mixed lipid system

Acknowledgment: I wish to thank Drs. Joel M. Schnur and Bruce P. Gaber for their comments and suggestions.

[Sponsored by ONR]

References

1. S.L. Regen, B. Czech, and A. Singh, "Polymerized Vesicles," *J. Am. Chem. Soc.*, **102**, 6638-6640 (1980).

2. J.M. Schnur, B.P. Gaber, and D. Chapman, *Biotechnological Applications of Lipid Microstructures* (Plenum Press, New York, 1988).

3. A. Singh and B.P. Gaber, in *Applied Bioactive Polymeric Materials*, C.G. Gebelein, C.E. Carraher, and V.R. Foster, eds. (Plenum Press New York, 1988), pp. 239-249.

4. F.S. Ligler, T.L. Fare, K.D. Seib, J.W. Smuda, A. Singh, P. Ahl, M.E. Ayers, A. Dalziel, and P. Yager, "Fabrication of Key Components of a Receptor-based Biosensor," *Med. Inst.*, **22**, 247-250 (1988). ■

Ensuring Navy Fuel Availability and Performance

D. R. Hardy
Chemistry Division

Ensuring an adequate global supply of quality, liquid mobility fuels wherever the Navy needs them and maintaining the Navy's critical engine performance requirements for such fuels are goals of the NRL fuel technology program. This includes research aimed at precluding fuel-related problems and solving unanticipated problems in the Fleet and ashore. Fleet needs and problems normally fall within several categories, many of which are currently under investigation. Two that have a great potential impact are described as examples of recent advances in fuel technology.

Development of a New Diesel Fuel Shelf Life Test: The Navy procures about 20 million barrels of diesel fuel annually, primarily for ship propulsion. In the last 10 years, more strict refinery processing regulations have been implemented to increase middle distillate fuel production. One major adverse effect has been a substantial decrease in the shelf life of vast quantities of strategically stored diesel fuel. Shelf life is measured by the stability of a diesel fuel in ambient storage to oxidative degradation leading to insoluble sludge-like material. In severe cases, this sludge makes subsequent fuel handling and use in gas turbine, diesel, and pressure-fired boilers impossible. Efforts to screen fuels at procurement time to predict their shelf life have been hampered by the lack of a rapid, realistic test method.

A simple test method has been developed as a spin-off from related programs that assesses sludge-preventing additives and investigates the chemical causes of fuel degradation. The test

involves heating a small sample of diesel fuel for a short time under moderate oxygen pressures. The amount of solids formed within 24 hours of the test accurately predicts the fuel shelf life (up to three years) at ambient conditions.

Fuel degradation can be rapid and severe at any time during its storage life up to the time of its combustion in a ship. The consequences of this degradation can impact naval operations at the most basic level—ship mobility—through filter blockage and servo systems malfunction. The logistics of interrupting fuel movement worldwide negatively impact combat readiness. This new predictive test minimizes these problems.

Improved Understanding of Jet Fuel as a Heat Sink: Improved jet-turbine efficiency, which is accomplished by increasing combustor temperatures and pressures, is currently being developed for future Navy engine designs. This places greater burdens on Navy jet fuel as a heat sink (for avionic and oil cooling) before final combustion. The higher operating temperatures to which the fuel is subjected cause trace levels of solids (0.1 to 1.0 ppm) to form in the fuel. This material then deposits or adheres to the heat exchanger surfaces and acts as an insulator for heat exchange. In addition, the solids may clog fine fuel filters or deposit on engine nozzles and interfere with proper fuel spray patterns in combustors. This tendency of jet fuel to degrade is called its thermal stability. It is assessed at the time of procurement by a simulated flow test of fuel over a hot metal surface (the Jet Fuel Total Oxidation Test, JFTOT) and by measuring the amount of deposit formed. A metal deactivator additive (MDA) can be added to jet fuels to greatly improve the fuel stability measured by JFTOT.

It had been postulated that the actual mode of action for MDA is for this additive to attach to the surface of the hot metal, thus passivating it and preventing fuel deposit from adhering. By using model fuels with and without the MDA in the JFTOT and, subsequently, by using sensitive metal surface examination techniques, it was found that fuel solids quickly adhere in multiple layers. Further surface analysis identified the major initial surface material as acidic components present in the fuels at 1 to 2 ppm levels.

As a result, a new model has been proposed to explain the effectiveness of MDA for improving jet fuel thermal stability. The MDA, which is both a divalent metal chelator and an organic base, interacts with acidic fuel components deposited on the surface to effectively strip them off and back into the bulk fuel. The acidic components, if left on the hot metal surface, are probably the precursors of the subsequent multilayer deposit formed on the tube surface. An understanding of the correct model for this complex process will greatly impact the capability of high performance Navy combat aircraft to use lower thermal stability fuels because of additives like MDA.

[Sponsored by ONR, DTRC, and NACP] ■

Combustion Chemistry Studied at High Temperature

N. L. Garland, J. W. Fleming, and H. H. Nelson
Chemistry Division

A knowledge of the kinetics and mechanisms of the reactions of gas phase molecules is needed to understand chemical behavior in combustion environments that vary from hydrocarbon flames to novel fuels and propellants. Such information is needed as input to model different combustion problems. The necessary kinetic information includes rate constants, which tell us how fast chemical species react, and the mechanism, which tells us what the products of chemical reactions are. Many of the kinetic studies in the past were carried out at room temperature; however, those results are often not applicable to real combustion problems. To gain a more complete understanding of combustion chemistry, we must measure the temperature and pressure dependence of rate constants and product channels at conditions close to those encountered in combustion.

Kinetic measurements at combustion temperatures are difficult to make in the laboratory because of materials incompatibility (e.g., glass cells melt at 1100 K) coupled with the problem of obtaining a steady, reproducible temperature environment. We have overcome some of these problems by combining laser-based spectroscopic techniques with a newly constructed high-temperature reactor. Figure 7 shows a schematic of this reactor, which is capable of operating up to 1500 K and enables us to study species that are highly reactive and/or thermally unstable.

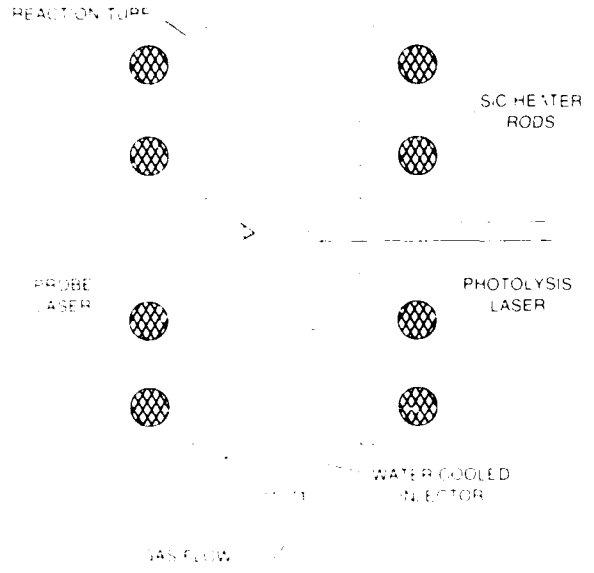

Fig. 7 — Schematic diagram of the reaction zone of the NRL high-temperature reactor

Kinetic Measurements: We slowly flow a gas mixture of the radical precursor, reactant, and a buffer gas through the resistively heated reactor cell. The combustion species to be studied—generally radicals—are generated by excimer laser photolysis of the precursor and are detected by laser induced fluorescence. Rate constants are determined by measuring the chemical lifetime of the radical as a function of reactant partial pressure. We measure these rate constants at different temperatures and total pressures. In certain cases, detection of the reaction product can confirm the chemical mechanism.

Boron Combustion: Because of the potential for extremely large energy release during the combustion of boron and boron compounds, there is renewed interest in the chemistry of these species. As part of this effort, we have studied the kinetics of reactive intermediates such as BH and BH_3 at room temperature. With our new reactor [1], we measured the rate constants of BH radical reactions with molecules such as O_2, H_2O, and C_3H_8, which would be important in boron combustion. Figure 8 illustrates an example of the data. We measured the pressure dependence of the reactions and the temperature dependence from 300 to 750 K. Several reactions showed little temperature dependence (BH with NO, C_2H_4, or H_2O); these reactions probably involve formation of complexes. Reactions that showed a stronger temperature dependence (BH with O_2 or C_3H_8 may involve abstraction.

Recent theoretical calculations from the Laboratory for Computational Physics and Fluid Dynamics at NRL show that the reaction of BH with D_2 proceeds by formation of a complex, BHD_2, followed by either fragmentation into the diatomic products or collisional stabilization of the complex. We have measured the temperature dependence of this reaction between 300 and 600 K and found excellent agreement with the calculated rate constants [2].

Hydrocarbon Combustion: We have shown in our flame studies that considerable uncertainty exists in the kinetics of the CH radical. As part of our continued study of CH radical kinetics, the temperature and pressure dependence of the reaction of CH and D_2 were studied in the high-temperature reactor. Preliminary results show that the reaction is very fast and pressure independent at room temperature. These results compare favorably with the recent theoretical results from the Argonne National Laboratory.

Summary: The combination of laser techniques with the high-temperature reactor makes it possible to acquire previously

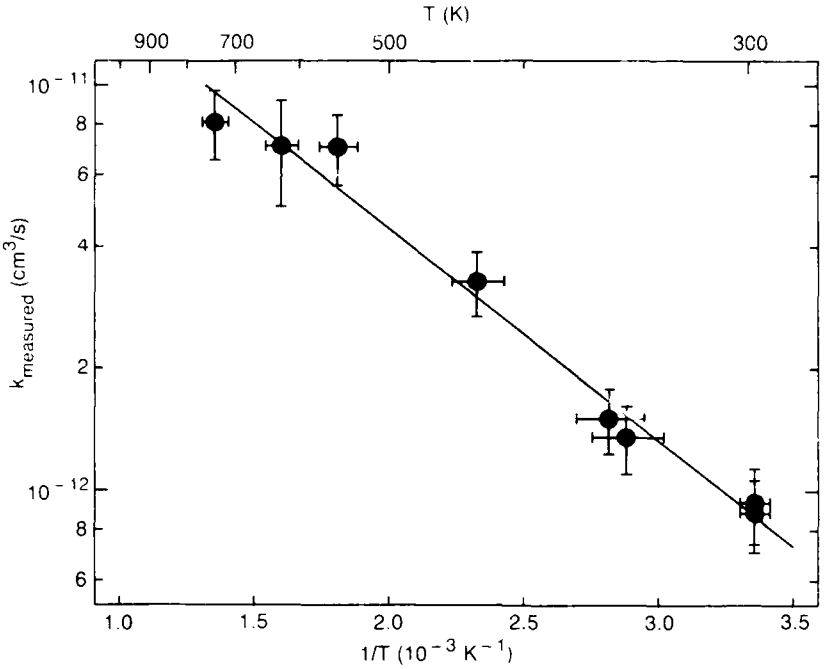

Fig. 8 — Arrhenius plot of the measured bimolecular rate constants for the reaction BH + O_2.The solid line is the result of a linear least squares fit to the uata.

unobtainable kinetic information. These data have allowed us to construct a more realistic model of boron combustion.

(Sponsored by ONR]

References

1. N. L. Garland, C. T. Stanton, J. W. Fleming, A. P. Baronavski, and H. H. Nelson, submitted to *J. Phys. Chem.*

2. N. J. Caldwell, J. K. Rice, H. H. Nelson, G. F. Adams, and M. Page, *J. Chem. Phys.*, in press. ■

Epoxy Coatings for Shipboard Copper-Nickel Piping

R. F. Brady, Jr.
Chemistry Division

Discharge piping in shipboard sanitary systems corrodes rapidly and must be replaced frequently. Made from an alloy of copper and nickel, the pipe is corroded both by sulfuric acid from aerobic bacteria and by sulfides from anaerobic bacteria. In some cases, new pipe has failed within six months of installation. Piping systems aboard aircraft carriers are now being preserved from corrosion by a chemically resistant epoxy lir ing developed in the Chemistry Division.

Application Process: The lining is applied to the inside of pipes by either of two methods. In the "air-sand" method, compressed air propels an abrasive grit through the pipe, which cleans the metal surface and prepares it for lining. A spray of paint is then blown through the pipe, and all surfaces of the pipe are coated uniformly by the turbulence of the spray. In the second method, the metal surface is prepared for painting as above, but the paint is contained between two tightly fitting rubber balls and is squeezed onto the surface as the pair of balls is moved by compressed nitrogen. In either method, the paint must dry for 72 hours before the pipe is returned to service. Figure 9 shows a pipe treated with the coating.

Shipboard sanitary systems, known as collection-holding-and-transfer (CHT) systems, were the first to receive the epoxy lining. It was

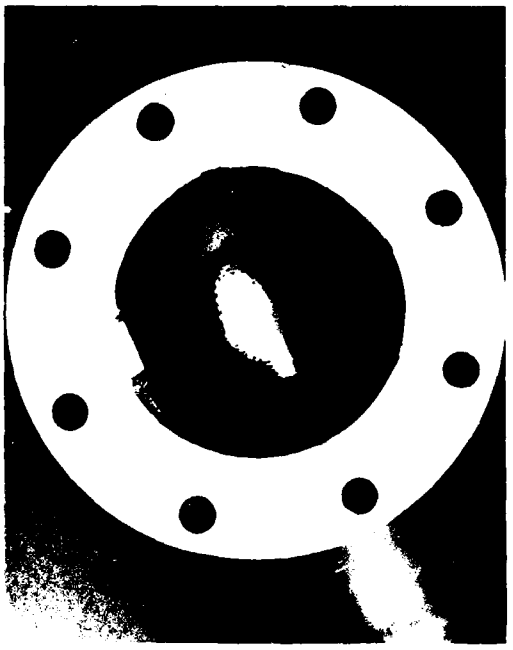

Fig. 9 — The chemically-resistant epoxy coating can be seen in an elbow of a 4.in. copper-nickel pipe removed from the USS *America* (CV 66)

installed in discharge piping in the USS *America* (CV 66) in November, 1988, and since then in six more carriers: USS *John F Kennedy* (CV 67), USS *Carl Vinson* (CVN 70), USS *Forrestal* (CV 59), USS *Saratoga* (CV 60), USS *Eisenhower* (CVN 69), and USS *Ranger* (CV 63). The eight remaining carriers will receive the same treatment in 1990.

Savings: The lining costs about $280,000 per carrier to install, and this amount grows smaller with experience. This can be compared with the $500,000 now spent per carrier per year to replace corroded piping. Tangible savings will be realized for each of the 15 carriers, and intangibles such as reduced maintenance and avoidance of unsanitary conditions will boost the morale of the ships' forces. The lining is expected to last at least six years.

A military standard governing the pipelining process and a military specification stipulating the ingredients and properties of the epoxy coating were drafted and submitted to the Naval Sea Systems Command to be issued. These documents will regulate the process in the future.

Other Uses: This process is likely to be used on ships other than carriers. In addition, the Naval Medical Command is evaluating the epoxy lining for use in shore and shipboard drinking water systems. The ingredients of the paint are approved by the Food and Drug Administration for contact with drinking water, and the cured paint contains no extractable materials. It is easy to think of numerous applications for this lining in municipal utilities, merchant vessels, and civil engineering situations. It is important to note, however, that this process is suitable for cathodic pipes only and cannot be used on such anodic metals as iron alloys.

Acknowledgments: Dr. James D. Adkins (Sachs/Freeman Associates, Inc.) and Jeffrey Breidenstein (Geocenters, Inc.) made important contributions to the development and testing of this coating.

[Sponsored by NAVSEA] ■

Electromagnetic Systems

ELECTROMAGNETIC SYSTEMS

Radar commands an important position as a major sensor and detection system for the Navy, and radar research continuously focuses on advanced sensor concepts to upgrade this technology. Electromagnetic radiation is also used for applications in the areas of countermeasures, signal simulation, jamming, and decoys. Reported in this chapter is work on wide-band radar for surveillance, improvements to air-surveillance radar, airborne infrared ship signature measurements, and an odd-ratio frequency divider.

This work was performed by the Radar Division (5300), the Tactical Electronic Warfare Division (5700) and the Space Systems Development Department (8100).

Other current research in electromagnetic systems includes:

- Parallel plate waveguides
- Testing and validation of VHDL models
- Radar electromagnetic interference

High-Resolution Waveforms in Radar Surveillance

G. J. Linde
Radar Division

Recent events have emphasized the need to obtain more information about objects that are detected by surveillance radar systems. One approach to improved radar information is to employ wideband waveforms that provide high-range resolution data. These types of waveforms are not new to radar but have not been used in air surveillance systems because of cost considerations and technology limitations. Air surveillance radar systems need to search a large volume in a short time. Therefore, high-power transmitters are used at relatively low radar frequencies that make large bandwidth signals difficult to achieve. Improvements in transmitter and signal processing technology make it practical to use greater signal bandwidths to obtain new capabilities while still performing the basic surveillance functions. The objective of this task is to develop and test wideband waveforms and processing techniques to improve radar surveillance and long-range target identification.

Benefits of High Resolution Waveforms: When the bandwidth of a radar pulse is large enough to resolve a complex object into many individual scatterers, then the received echo signal is a characteristic signature that can be used to distinguish one object from another or to determine the target's size. If sea-surface multipath is present and the reflected signal is resolved from the direct signal, fading of the signal is eliminated. The measured range difference can then be used to estimate the height of the object above the sea surface. High-range resolution can be used to measure target velocity in a short radar dwell with no ambiguity. Detection of targets in clutter from rain or chaff is improved with increased bandwidth because of the reduced volume of clutter in a resolution cell.

Increased Resolution for Improved Detection: Wideband radar signals are usually implemented by frequency or phase modulation of a long pulse. A simple, short pulse has the disadvantage of needing very high peak transmitted power to attain high energy for target detection. The modulated long pulses are compressed in a matched filter to obtain signals with high-range resolution. One common modulation format is a linear frequency modulation (LFM) where frequency changes linearly during the pulse. A dispersive filter, one in which propagation time is a linear function of frequency, is used to compress these pulses. An example of potential benefits of increased signal bandwidth is shown by the two radar maps in Fig. 1 where radar echoes from a portion of Tilghman Island are displayed with two waveforms that have different bandwidths. Fig. 1(a) shows the results of a 10 μs pulse with a 2 MHz LFM compressed to 0.7 μs; Fig. 1(b) is from a 5 μs, 14 MHz pulse compressed to 0.1 μs. Signal amplitude variations are shown by color differences. Greater details about the island, such as the cove near the center, are apparent with increased resolution. The higher resolution map also shows more amplitude variation and has regions of low amplitude areas between high peaks where it would be possible to detect some airborne targets.

Wideband Waveforms for Target Classification: High resolution data are not needed for target classification in the entire search volume but only for objects already detected. Thus the range is known and the range extent can be limited. In these situations, a technique known as "stretch" [1] can be used to obtain high-range resolution without the need for a wideband matched filter or wideband data processing. There are few restrictions on the maximum pulse width that can be processed. Figure 2 illustrates the processing involved in "stretch." A linear FM pulse is transmitted and received conventionally. It is then mixed with a linear FM pulse with a slope that transforms the time scale so that it can be

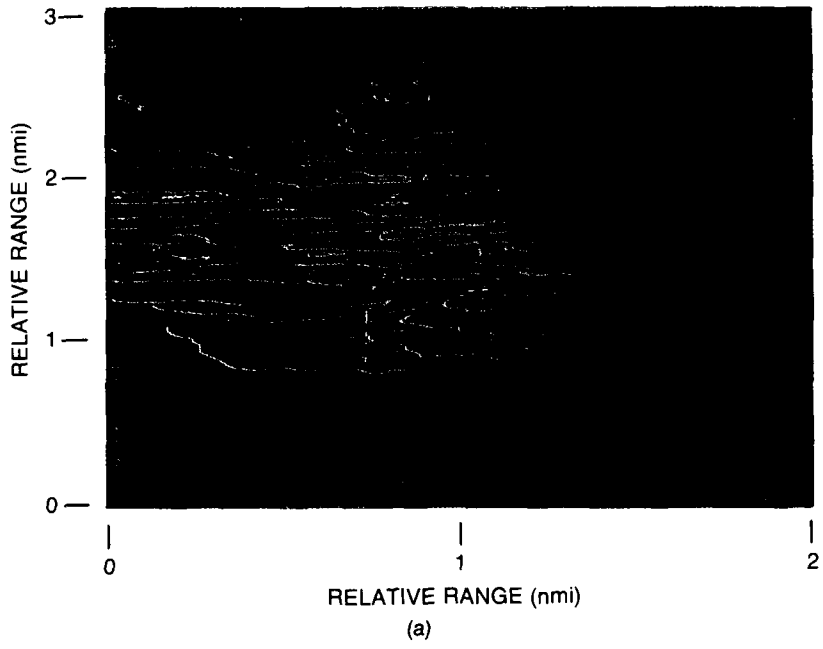

(a)

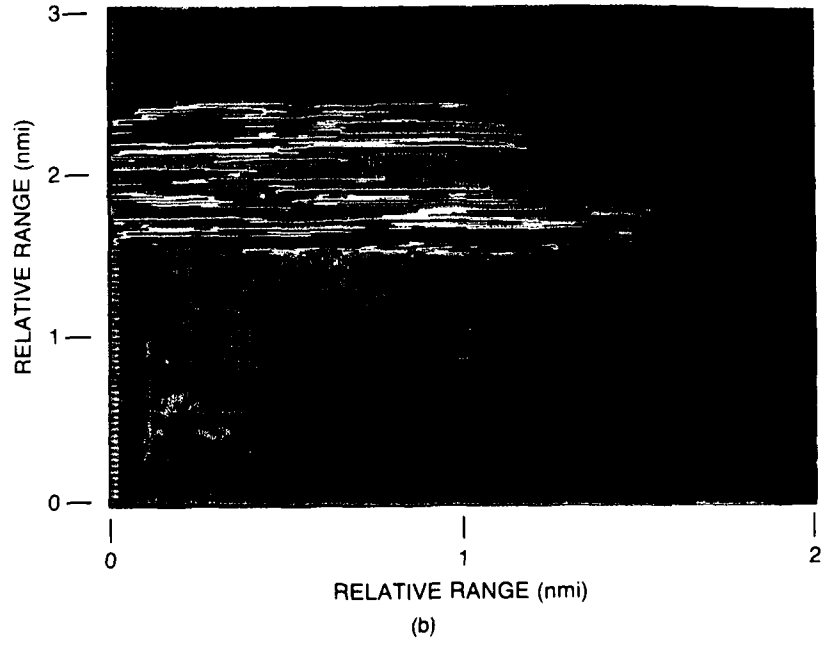

(b)

Fig. 1 — Radar maps of southern tip of Tilghman Island, comparing two waveforms (a) 10 μs pulse compressed to 0.7 μs and (b) 5 μs pulse compressed to 0.1 μs

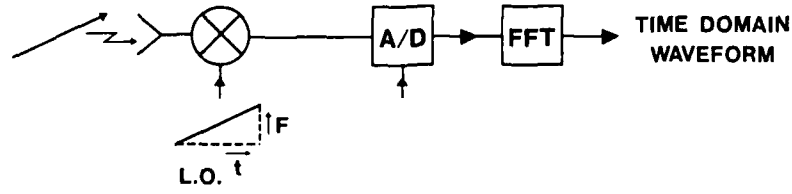

Fig. 2 — Stretch processing of a linear FM waveform

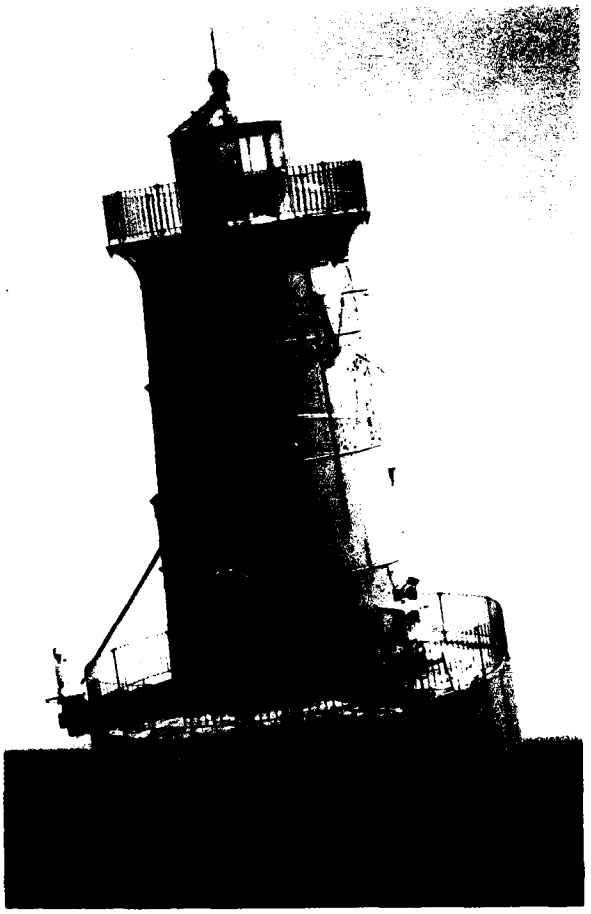

(a)

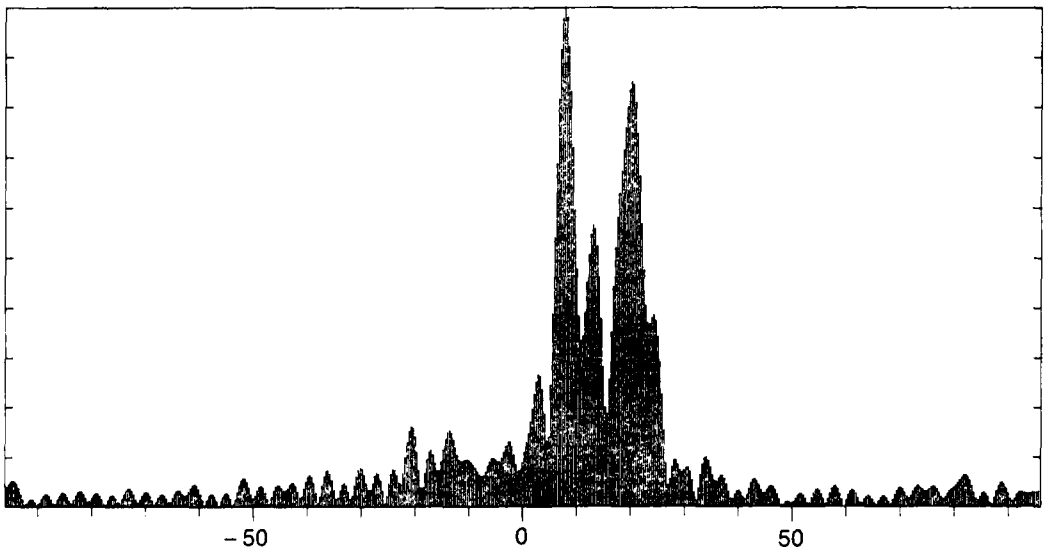

(b)

Fig. 3 — (a) Photograph of Sharps Island lighthouse; (b) amplitude response of lighthouse using a 185 MHz bandwidth waveform and stretch processing

processed in a low bandwidth matched filter. One option is to exactly match the slope of the transmitted signal. Then the output signal has a frequency proportional to the range of target scattering centers and a time domain presentation is obtained with a Fast Fourier Transform (FFT). Figure 3 shows the results of "stretch" processing that has enough resolution for target classification. Figure (3a) shows Sharps Island and lighthouse, and Fig. 3(b) shows the range profile using a 185 MHz linear FM pulse. Several prominent scatterers are present; they correspond to radar echoes from the upper part of the lighthouse.

Plans: High-range resolution airborne target signatures will be measured and evaluated for their suitability in identification and height finding. An increase in surveillance bandwidth shows promise for improved detection of air targets over land. Further increases in bandwidth will be evaluated for utility.

[Sponsored by ONT]

Reference

1. W. J. Caputi, "Stretch: A Time-Transformation Technique," *IEEE Transactions on Aerospace and Electronic Systems* **AES-7**, No. 2 (1971). ■

At-Sea Support for SPS-49 Radar Improvements

R. M. Crisler, J. L. Walters, and J. P. Barry
Radar Division

The AN/SPS-49(V)5 is the Navy's most capable shipboard long-range, two-dimensional (range and bearing) air surveillance radar. Figure 4 shows the radar antenna. Under direction of the Naval Sea Systems Command (NAVSEA 62X2), improvements are continually being implemented on the Raytheon-built radar. NRL provides technical guidance to NAVSEA by participating in

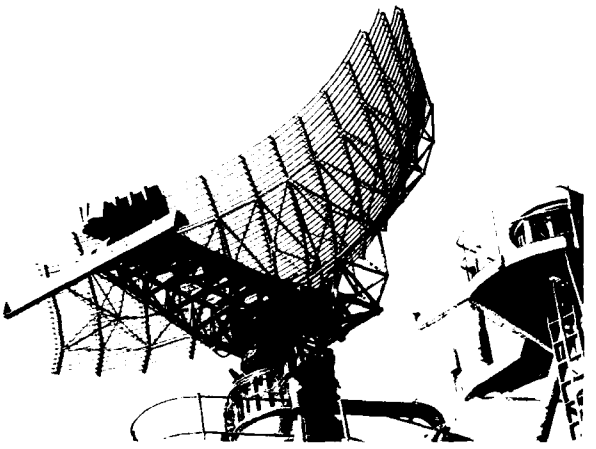

Fig. 4 — AN/SPS-49(V)5 antenna

design reviews and by planning and conducting detailed performance tests of the improvements at land-based test sites and aboard ship.

Automatic Target Detection: Automatic detection of targets has now been added to the radar as part of the New Threat Upgrade (NTU) program to upgrade cruiser combat systems to counter high-speed, high-altitude, antiship missiles.

Test Program: To provide automatic detection of desired targets while maintaining an acceptable false alarm rate in severe jamming, radio frequency interference, and clutter environments, the SPS-49 radar was extensively modified. Detailed evaluation of the performance in these environments required that we specify and aid in the development of a computer-driven specialized Radar Test Unit (RTU) capable of injecting carefully controlled test signals for detailed bench tests and of recording target, clutter, and jamming data aboard ship during missile firing exercises. Examples are given of data collected on USS *Biddle*, CG-34.

Test Result Examples: A most important measure of the effectiveness of the radar's signal processing chain is the least (single pulse) signal-to-noise ratio required for detection. Since the noise is fluctuating, one must specify the probability of detecting a true target as well as the

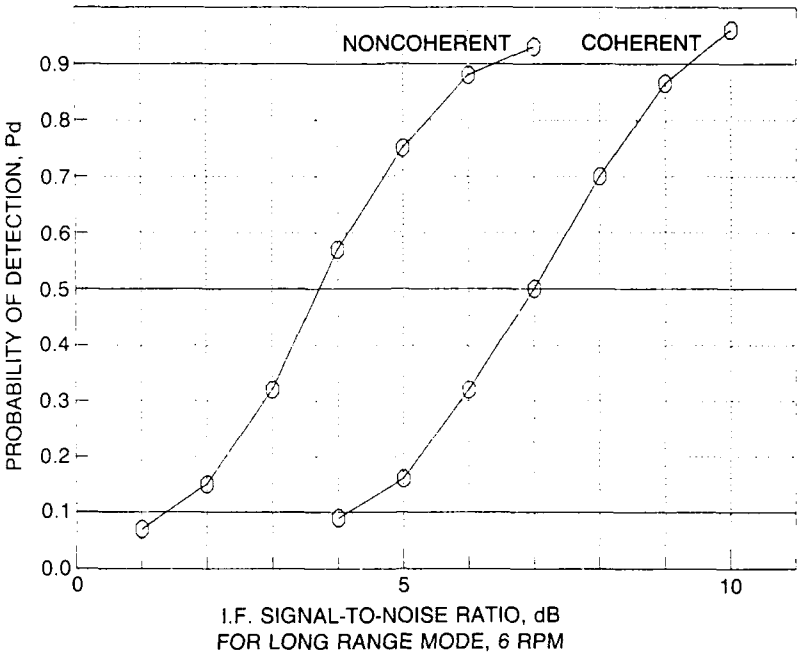

Fig. 5 — Probability of detection curves measured with calibrated test targets

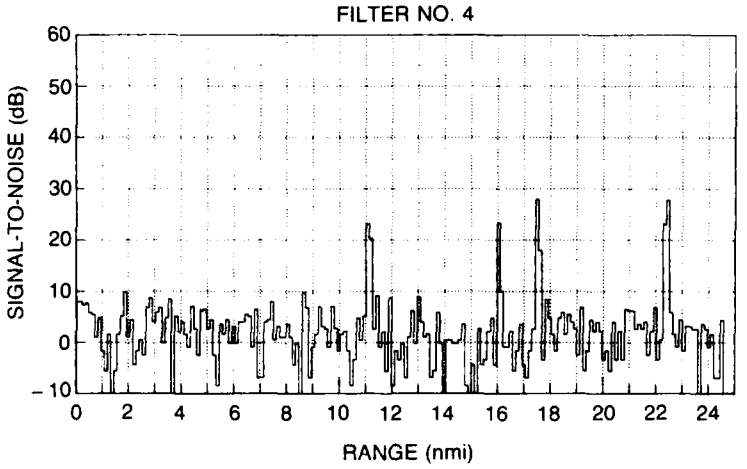

Fig. 6 — Target returns recorded with the radar test unit

time rate of false alarms or the equivalent probability of getting a false detection in one range resolution cell. Figure 5 shows curves of Pd for two channels of the signal processing. These were taken by using pulses of controlled amplitudes from the RTU and counting the numbers of detections. Such curves allow precise prediction of radar range performance. It is seen that the coherent processing, which discriminates against fixed clutter targets, does require 3 dB more power.

Figure 6 shows the video, digital-to-analog signal output from one of the Doppler filters. Aircraft targets are shown at 11, 16, 17.5, and

22.5 miles. The digital range cells are 1/8-mi long. At 11 mi, the target has straddled two adjacent cells. The data acquisition system enables the capture and display of these fine-grained results, which permit detailed diagnoses.

Figure 7 shows a time history of reported target positions from the automatic detection system, which were digitally recorded. It is equivalent to a long-time exposure of a radar display except that the data are of immensely better quality. Each square represents a target of which azimuth, range, and time are known with precision as well as a signal-to-noise value.

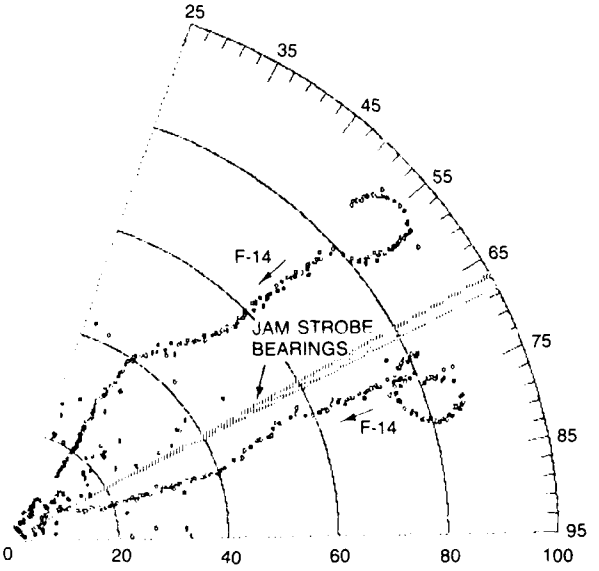

Fig. 7 — Range-bearing plot of F-14 A/C detections in barrage noise standoff jamming. Long range mode, 12 rpm

Test Summary: The testing program involving the use of the RTU has permitted performance evaluation to levels not normally achieved in at-sea tests. This has resulted in several design changes to the radar enhancing its capability in severe at-sea environments. At the conclusion of the test program, the radar received Navy approval for full production.

[Sponsored by NAVSEA] ■

Airborne Infrared Signature Measurement Facility

J. W. Dries, J. S. Price, and D. S. Fraedrich
Tactical Electronics Warfare Division

The continued need for quantifiable infrared signatures of naval surface ships has resulted in the Naval Research Laboratory (NRL) developing a comprehensive airborne infrared ship signature measurement facility that has been flown aboard an NRL P-3 aircraft (Fig. 8) and a Naval Air Test Center CH-53 helicopter (Fig. 9).

Fig. 8 — NRL P-3 607

Fig. 9 — CH-53 helicopter

During the measurement, the aircraft is flown in circles around the ship at various altitudes and ranges. The ship is in direct communication with the aircraft thereby ensuring that all operational conditions are monitored.

Fig. 10 — IR ship gimbal assembly

The advantages of an airborne measurement facility are significant. In particular, the ability of this system to measure the vessels in their at-sea environment under different operational conditions enables the researchers more detailed technical information than has been previously available.

The system incorporates two calibrated imaging radiometers spanning the 2 to 12 μm region. An eye-safe laser rangefinder and a CCD visual camera are also used in the integrated system to determine range to the vessel and to provide optical referencing of the sensors. The various components are installed in a two-axis dynamically stabilized gimbal assembly (Fig. 10) that provides a significant enhancement to its measurement capability. The gimbal can be manually controlled by an operator through a joystick or can be automatically positioned by a video tracking system. The video tracking system will direct the position of the gimbal system in azimuth and elevation from the output video signals of the infrared or visual cameras.

The 3-year engineering effort has resulted in the development of advanced imaging radiometric sensors. The Inframetrics 2100 radiometer is a dual-band system that simultaneously measures radiation in the 3 to 5 μm and 8 to 12 μm regions. A common 4X afocal telescope and scanner are used for both channels. At the exit of the scanner, a dichroic mirror splits the radiation into the 3 to 5 μm and 8 to 12 μm components. Each of the two beams is independently focused on two-element HgCdTe detectors with an aspheric germanium lens. Radiometric stabilization is accomplished by using separate gain and offset stabilization techniques. Gain stability is achieved by tuning the feedback of the postamplifier with various combinations of resistors and sensistors. Offset stability is achieved by sampling the radiance of an internal mechanical chopper after every video field. The temperature of the chopper is measured independently, and this value is used with calibration data stored on EPROMS to compensate the video signal. In addition to the 2100 imager, the system is installed with an Agema 870 imager that is sensitive to energy within the 2 to 5 μm region. The Agema imager is a SPRITE detector based system that accomplishes radiometric stabilization by sampling two internal blackbody sources. These measured signal levels are used to adjust preamplifier gain and offset level every 400 μs.

The imagery from these radiometers is stored on standard video tapes. These tapes are later played back into image analysis computers (Fig. 4). Each selected image is processed by using image analysis software that facilitates the calculation of radiance maps and integrated radiant intensities (Figs. 11 and 12). Hardcopy black and white or color reproductions are easily obtained by enhanced resolution on-line printers (Fig. 12).

Since its completion, the airborne ship signature facility has performed numerous ship signature trials. This includes a very extensive NATO sponsored exercise off the coast of Italy with multinational ship participation. ■

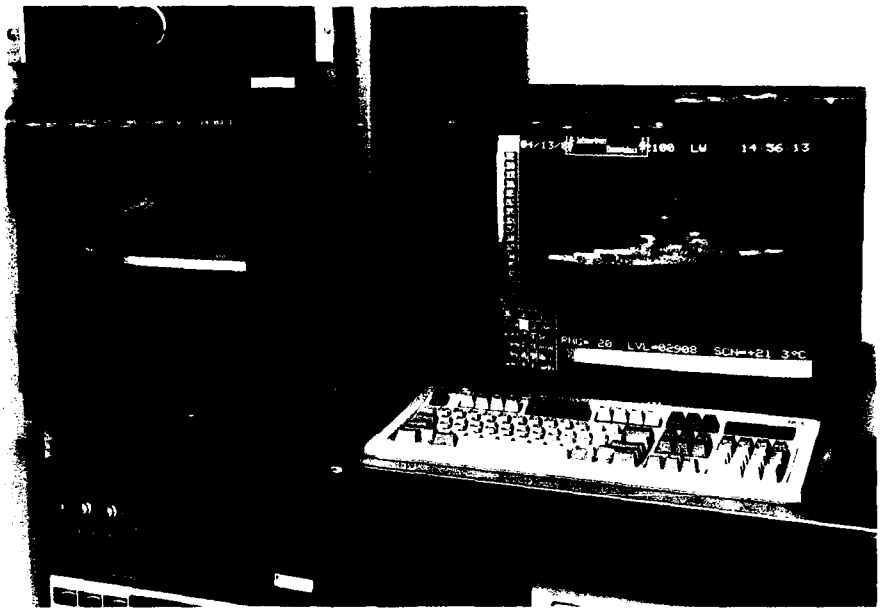

Fig. 11— Image analysis computer

Fig. 12 — Computerized thermal image with pseudocolor

A Novel Design of a 1.8 GHz Input Odd Ratio Frequency Divider

D. S. Korn
Space Systems Development Department

Introduction and Background Perspective: A new technique is presented for building an odd ratio, fixed frequency divider at a demonstrated 1.8 GHz maximum input frequency. The author and Carl Deierling of GigaBit Logic, Newbury Park, CA, conceived, designed, tested, and built the divider. In this article, the word "odd" is used as a mnemonic for a non-2^n integer rather than a noneven number. This divider, which was necessitated by and is intended for radio frequency (RF) synthesizer applications, can divide by any integer; however, its novelty is most useful when

the integer chosen is a non-2^n number, namely 3, 5, 6, 7, etc., as there are many multi-GHz input 2^n (2, 4, 8, 16, etc.) dividers presently available. Both the circuit itself and its intended function, non-2^n ratio multi-GHz input frequency division, appear to be novel and are certainly useful. No dividers appear to be available based on this circuit concept, and the few dividers that are available with input frequencies above 1 GHz cannot divide by any integer. Consequently it gives the frequency synthesizer designer another design option not currently available. The circuit concept is based on a *D* flip-flop with a delay Tau fed back from the inverted *Q* output to the flip-flop clear input with the *D* input tied high; the divide ratio *N* is controlled by selecting the delay Tau. The input frequency is applied to the clock input, and the output frequency is the *Q* output. Since this RF circuit is based on a digital IC, its features are directly coupled to the anticipated advances in high-speed digital integrated circuits, namely increasing maximum input clock frequency and minimizing the residual (additive) phase noise, physical size, and DC power consumption. The most important measured inherent characteristics of this divider technique from a frequency synthesis point of view are lack of measurable spurious oscillations as the input RF, RF power, DC voltage, and ambient temperature are changed—all dependently or independently of one another; a scarcity of undesired subharmonics; low residual phase noise; very small size; low DC power consumption; low input RF drive; and moderate RF power output delivery.

Concept and Analysis: The concept of this novel divider technique is based on a *D* flip-flop and a delay Tau fed back from the inverted *Q* (*Q* bar) output to the asynchronous clear (CLR) input with the *D* input tied high as shown in the schematic, Fig. 13. The maximum input frequency is limited by the maximum clock (CK) frequency of *D* flip-flops on the market, and the divide ratio is controlled by setting the propagation delay Tau of the feedback circuit. The *D* flip-flop must have an asynchronous CLR input. The circuit analysis, including real-world propagation delays, is most clearly visualized by referring to the timing diagram of the built divider, Fig. 14. The input frequency is 1.4 GHz (714 ps), the flip-flop is GigaBit Logic's 10G021A, and the desired divide ratio *N* is 3. The cause and consequence of each change of state in either CK, *Q*, *Q*bar, or CLR with respect to time is marked by a number in Fig. 14 and verbally explained as follows:

-1- On the clock falling edge, the *D* input is strobed into the flip-flop. *D* is hard-wired logic high, and the particular flip-flop is negative edge triggered. Whether the particular flip-flop used is negative or positive edge triggered is inconsequential. The state of *Q* prior to event -1- is irrelevant.

-2- As a result of event -1-, the *Q* and *Q*bar outputs go high and low respectively after the CK-to-*Q* delay, in this case 525 ps.

-3- Since the *Q*bar output is fed back by a delay Tau to the CLR input, a time delay Tau after event -2- *Q*bar low appears at the CLR input. No changes occur in *Q* because of any clock falling edges that might occur between events -2- and -3-, since the *D* input is hard-wired high and *Q* is already high.

-4- As a result of event -3-, the *Q* and *Q*bar outputs go low and high respectively after the CLR to *Q* and *Q*bar delay, in this case 625 ps.

-5- Since the CLR input is merely the delayed *Q*bar output, a time delay Tau after event -4-, the CLR port goes high (deactivated). Remember that between events -3- and -5-, when the CLR input is low, the clock input has no effect on the state of either outputs.

-6- Event -6- is a repeat of event -1-, at that time the *D* input is strobed into the flip-flop. *Q* is low at this time.

-7- As a result of event -6-, *Q* changes state and goes high after the CK-to-*Q* delay, thus completing one frequency division cycle.

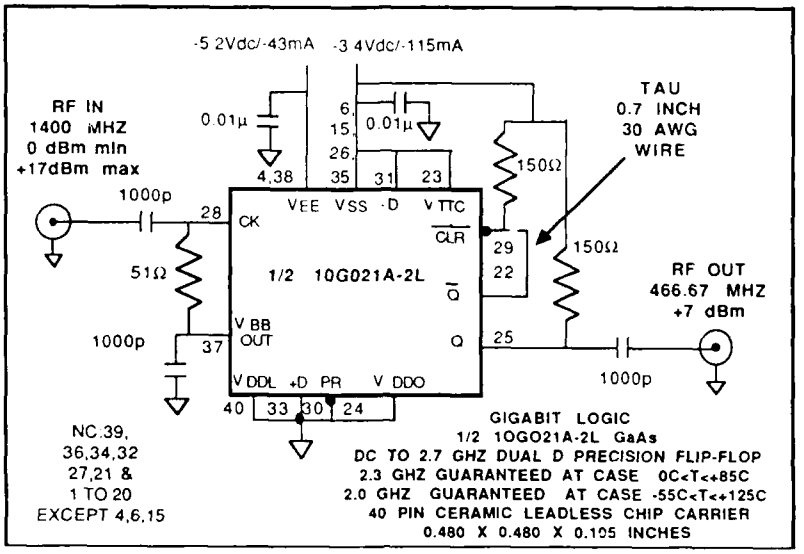

Fig. 13 — Schematic

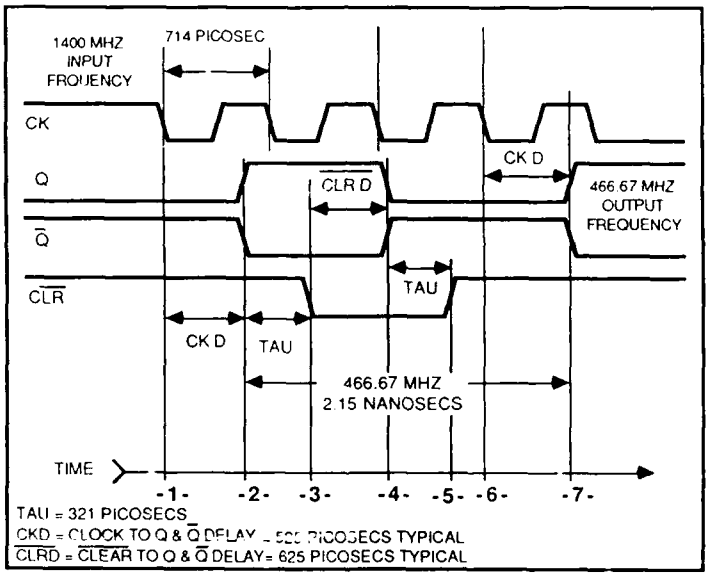

Fig. 14 — Timing diagram

Given the preceding explanation, one can realize the following. The value of Tau is chosen such that 2 Tau plus both CK-to-Q and CLR-to-Q delays is greater than N 1 input clock cycles and less than N clock cycles where N is the desired divide ratio; this would be stated in equation form as:

$$(1\text{CK cycle})(N - 1) < 2\ \text{Tau} + \text{CK-to-}Q + \text{CLR-to-}Q < (1\text{CK cycle})(N)\ \text{s}.$$

The objective is to solve for Tau given a known (desired) value of N. This is the only pertinent design equation. Note that a dual modulus divider can be designed with this technique by merely placing two delay lines in parallel, one for each divide ratio N and $N + 1$, and switching between the two with a high-speed multiplexer such as the GigaBit Logic 10G004.

Measured Results: The schematic (Fig. 13) was built and measured. The system imposed objective is to divide 1.4 GHz by 3. The required delay Tau for $N = 3$ was calculated by the preceding equation to be between 140 and 496 ps.

The predominating inherent delay is due to the CLR port input capacitance and delay line characteristic impedance; this was calculated to be 261 ps. The additional delay that the designer can control is the physical length of the delay line Tau. A length corresponding to 60 ps places the total delay at 321 ps; this 60 ps is realized with a 0.7-in. length of 30 AWG wire.

The circuit is 0.8 by 0.8 by 0.2 in. excluding SMA connectors, consumes 615 mW DC power, requires at least 0 dBm input power, and delivers +7 dBm into a 50Ω load. The input frequency F can be varied from 1.2 to 1.8 GHz before the divide ratio changes, a wide dynamic frequency range. All integer multiple frequencies of $F/3$ are 15 dBc or lower, and the only other subharmonic frequencies of F are $F/2$ and $F/6$, both about −70 dBc. The divider output spectrum and residual phase noise were measured on a Hewlett Packard 8566B spectrum analyzer and 3047A phase noise test set, respectively. Spurious frequencies are defined as frequencies not harmonically or subharmonically related to the input frequency F. No spurious frequencies between 100 Hz and 1 GHz are visible above the spectrum analyzer noise floor of −85 dB below carrier (dBc) with the carrier at +7 dBm. The phase noise measurement from 10 Hz to 40 MHz offset reveals no divider-generated spurs except a 30 MHz offset spur at −120 dBc; however, because of the subtlety of this measurement, it cannot be concluded that the divider generates this spur. The method used to measure divider residual phase noise is to use one signal source and measure the phase noise, thereby eliminating the signal source phase noise then to insert one divider in each signal path and repeat the measurement. The degradation between the two measurements is due to the dividers. The measurement system phase noise is not degraded when the dividers are inserted; therefore one can conclude that the divider residual phase noise is lower than the measurement system phase noise. Figure 15 is a plot of the measurement system phase noise with the dividers; it is between 0 and 5 dB lower than the phase noise without the dividers. The fact that it is lower is due to the subtlety of the measurement. All of the above measurements were made at +22°C except for the spurious search, input frequency range, and output power, which were measured at −55°, +22°, and +85°C. The degradations at −55°C and +85°C are a slight decrease in output power and input frequency range.

[Sponsored by MATT] ■

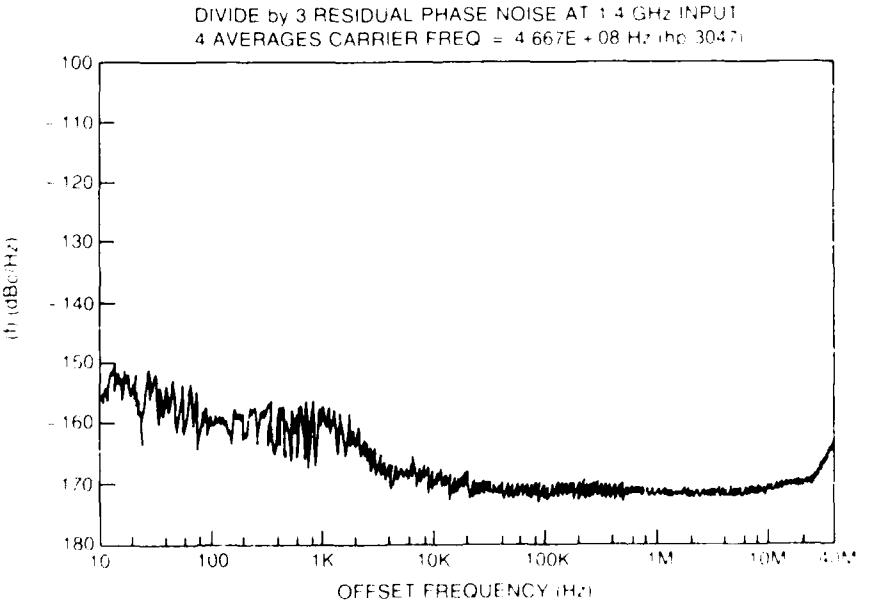

Fig. 15 — Divider residual phase noise

Electronics Research

ELECTRONICS RESEARCH

Electronics research embraces, in part, work on microwave techniques; thin films; semiconductor microstructure, interfaces, and surfaces; vacuum electronics; and solid state circuitry and sensors. Reported in this chapter is work on electronic warfare, hazardous gas storage, atomic layer electronics, microelectronics, and resistance switching.

The Tactical Electronics Warfare Division (5700) and the Electronics Science and Technology Division (6800) contributed to these research efforts.

Other current research in electronics includes:

- Thermionic cathodes
- Microwave and optoelectronic applications
- Single crystal germanium grown on sapphire
- MBE silicon on sapphire
- Vertical zone melt growth of GaAs
- Dark current in IR detectors

EWCM Prototype Readied for Deployment

G. E. Layman
Tactical Electronic Warfare Division

Electronic warfare (EW) has been widely employed in combat since the early stages of World War II. One component of EW is to collect emission information on the enemy's use of electronic devices such as radars, radios, and missile seekers. This information is used to identify and locate hostile forces and to determine the nature of their activities. A second component of EW is to jam or deceive these same devices in a manner that causes the enemy to position and use its forces unwisely and to reduce the effects of its weapons. A final component of EW, counter-countermeasures, is to prevent the enemy from degrading our systems.

In many uses, EW tactics are understood and committed to doctrine such as self-defense of an aircraft or a ship. However, the command problem gets very difficult in broad applications such as coordinating EW across multiple forces in concert with other warfare activities. This requires critical and timely decisions and precise timing of actions.

Electronic Warfare Coordination Module: The Electronic Warfare Coordination Module (EWCM) is a force level command support system that will provide a battle group commander, or Fleet commander, with the capability to plan and supervise the optimum employment of EW assets.

The EWCM prototype was deployed for the first time in October 1989, aboard the USS *Dwight D. Eisenhower* (CVAN-69) in support of Commander, Carrier Group Four.

Figures 1 and 2 are typical of the types of displays that the system uses to provide

Fig. 1 — Composite coverages of battle group sensors

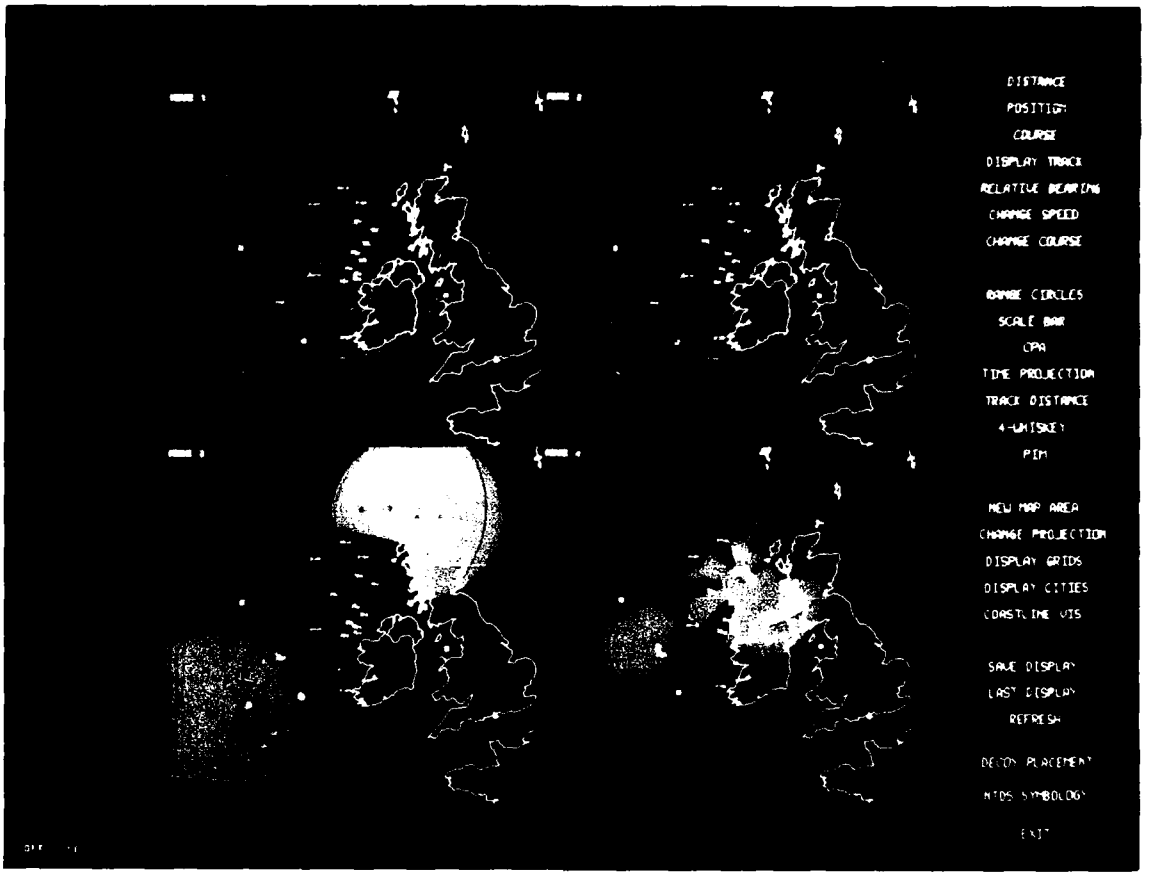

Fig. 2 – Multiple displays showing the effects of alternate dispositions and time projections

information to a tactical decision-maker. The system is menu-driven for ease of learning and operating. Much of the information is provided through geographic displays consistent with the centuries old method of using maps to plan and conduct warfare.

Figure 1 shows a display of a deployed U.S. Navy carrier battle group and some potentially hostile forces. Friendly forces are blue, and hostile forces are red. The positions may be actual, driven from real-time information, or postulated for planning potential actions. The lines simulate representative coverages using sensors aboard U.S. ships and aircraft. In this figure, the operator has chosen to evaluate shipboard radar coverage (outer solid blue line) against a specified aircraft type and passive detection coverage (dotted and solid green lines) against some specified emitters. The inner line, shaped like a number eight, represents the burnthrough range of a simulated enemy radar being jammed.

The top of Fig. 2 shows side-by-side comparisons of sensor coverages for alternate dispositions that may be evaluated in the planning phase.

The lower left display simulates the effects of jamming a hostile airborne radar. The pink area is where a radar remains effective in detecting a specified sized target. The lower right figure again depicts the effects of jamming a hostile airborne radar, but this time after a time projection that allows the evaluation of the dynamic effects of jamming and indicates multiple jammer effectiveness.

Other Capabilities: These are examples of simple analysis. In an actual analysis the decision-maker may include the coverages of

many other systems and weapons. For example, the decision-maker might assess the same sorts of coverages for the enemy superimposed on the display.

The operator is free to evaluate many other factors. For example, aids exist to select power of transmission, communication frequencies to reduce the probability of detection by hostile forces, analytical tools to determine the effectiveness of the placement of decoys, aids in generating plans and directives, time projections, reconstruction of events, and many other capabilities.

Most important is the flexibility that the operator has in using these decision support aids to analyze EW in conjunction with other warfare areas.

The system also provides the operator with the command and control means to supervise actions. Supervision is aided through the use of the tools embedded within the EWCM to analyze real-time conditions and, through connectivity to other command and control systems, to exchange information and directives.

Technologies: A number of technologies were advanced in this development. The most significant was the development of a new software architecture for modern command and control systems [1,2]. This architecture features software reusability and ease of modification. It is based on a hierarchical control structure and provides multilevel modularity, factorization of operative and control software, libraries of reusable software modules, independently specified subsystems, distributed processing, simplified communications, and traceability between requirements and software.

Other technologies used include decision aids, artificial intelligence applications, distributed systems, embedded database management subsystems, networking, optimized man-machine-interfaces, and computer graphics.

Summary: The EWCM prototype provides a commander with the means to rapidly and accurately assimulate and analyze information. These capabilities facilitate a better understanding of the military situation. This will permit the commander to improve the quality and timeliness of decisions in planning and implementing warfare actions.

The EWCM prototype will continue to be deployed as a research vehicle to refine decision support technologies and to enable the Fleet to develop doctrine and procedures for the use of modern command and control systems such as the EWCM. Three more deployments are planned for FY 90.

Acknowledgments: Dr. J. Egan, B. Weber, and D. McGroder of NRL and J. Robins, S. Hellstrom, and L. Miller of Locus, Inc. contributed to this research and development.

[Sponsored by ONT and SPAWAR]

References

1. G.E. Layman and J.R. Robins, "Open Architecture for Modern Command and Control Systems," *Signal*, Aug. 1988.

2. G.E. Layman and J.T. Egan, "Organizing Software for Distributed Military Command and Control Systems," Proc. 26th Annual Symposium, Washington, DC Chapter of ACM, 1987. ■

A Safe Storage and Delivery System for Hazardous Gases

R. S. Sillmon
Electronics Science and Technology Division

In recent years, the increased use of hazardous gases, especially arsine (AsH_3), phosphine (PH_3), and silane (SiH_4) by semiconductor research and manufacturing facilities has drawn much attention to the safety

issues associated with the transport and use of these gases, which are among the most lethal gases known to man even at very low concentrations. The Department of Defense has invested millions of dollars in developing the technology to mass produce electronic components from materials such as gallium arsenide and indium phosphide. Programs such as the Microwave and Millimeterwave Integrated Circuits have targeted organometallic vapor phase epitaxy (OMVPE), which uses AsH_3 and PH_3, as the technology for producing such devices. The use of these compressed or liquified hazardous gases has a large impact on the final cost, and even realization, of devices because the production facilities must comply with strict state and federal regulations in handling such gases to safeguard workers in a production environment. Since a sudden release of a hazardous gas from a supply cylinder may constitute a major catastrophe, it is imperative to find safer forms of storage for these gases. The Electronics Materials Branch of NRL has developed and tested a new storage and on-demand delivery system for hazardous hydride gases such as AsH_3, PH_3, and SiH_4. The system is based on gas adsorption into the microcavities of synthetic zeolites [1] at room temperature then subsequent desorption at higher temperatures to provide supply pressures from 1 atmosphere to several atmospheres on demand. The new system's storage vessel can be filled to a gas pressure just below 1 atmosphere, thus drastically reducing the leakage or sudden release hazard during a transportation mishap. Here we describe the measured adsorption/desorption properties of AsH_3 on zeolite and the preliminary results of operating a prototype AsH_3-zeolite system connected to an OMVPE reactor for the growth of GaAs and AlGaAs thin films.

Adsorption Measurements: The adsorption isotherm and isobar measurements were made by using 100% AsH_3 and a 150-cc stainless steel cylinder packed with zeolite beads (Linde NaA or CaA with a 20% clay binder). Figure 3 shows

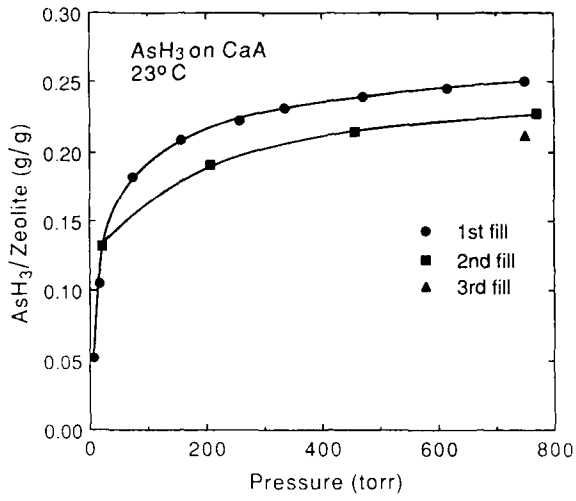

Fig. 3— Adsorption isotherms for AsH_3 on CaA zeolite at 23°C for three separate fills on the same zeolite (weight of zeolite does not include clay binder)

adsorption isotherm for AsH_3 on CaA zeolite. An adsorption capacity (AsH_3/zeolite, g/g) of 25% at 760 torr was measured for the first fill with about a 10% reduction in capacity for each of two subsequent refills. The adsorption rate of AsH_3 on CaA zeolite was fast, being limited to 100 cc/min by the mass flow controller used in these experiments. The zeolite beads used have a packing density of about 0.65 kg/l, therefore a cylinder size of only 6 l is needed to store 1 kg of AsH_3 on CaA zeolite. Therefore, large quantities of gas can be stored in vessels that can fit into conventional gas cabinets without size modifications. The adsorbed phase of AsH_3 is very stable. The adsorption capacity of a CaA zeolite system filled to 760 torr AsH_3 pressure varied only 1% over a period of 36 days at room temperature. No flow of AsH_3 out of the cylinder was observed until the temperature of the zeolite was increased. Figure 4 shows the adsorption isobars of AsH_3 on CaA zeolite at a pressure of 860 torr. Temperatures well below the decomposition temperature of AsH_3 are needed to desorbed and thus use the AsH_3. About 100% of the adsorbed AsH_3 was recovered on demand at a pressure and flow rate commonly used in OMVPE systems.

Prototype Testing: To test the purity of the AsH_3 desorbed from CaA zeolite, a 500-cc

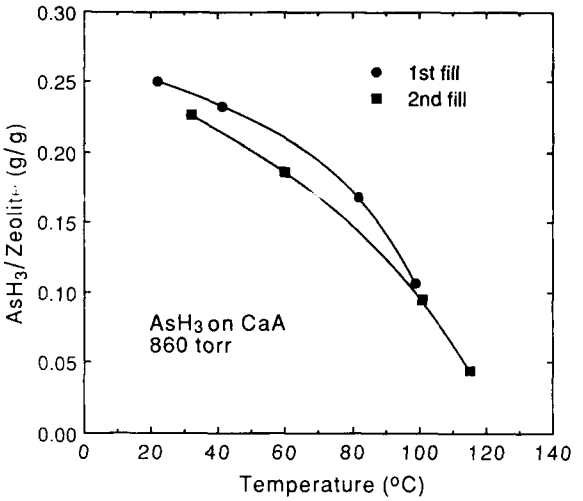

Fig. 4 — Adsorption isobars for AsH_3 on CaA zeolite at 860 torr for two separate fills on the same zeolite (weight of zeolite does not include clay binder)

Table 1 — Hall Data for Three Types of Epitaxial Layers Grown with a Conventional 100% AsH_3 Source and the AsH_3-Zeolite Source (source AsH_3-Z)

Material	AsH_3 type	293 K		77 K	
		n,p (cm^{-3})	Mobility ($cm^2V \times s$)	n,p (cm^{-3})	Mobility ($cm^2V \times s$)
GaAs	AsH_3	$+1.6 \times 10^{14}$	0431	$+1.4 \times 10^{14}$	04320
	AsH_3-Z	insulating			
GaAs(si)	AsH_3	-1.5×10^{16}	5880	-1.1×10^{16}	16900
	AsH_3-Z	-1.6×10^{16}	5440	-1.1×10^{16}	16100
$Al_{0.28}Ga_{0.72}As$	AsH_3	$+2.6 \times 10^{16}$	0155	$+1.0 \times 10^{16}$	00498
	AsH_3-Z	$+5.6 \times 10^{16}$	0147	$+1.8 \times 10^{16}$	00432

prototype system was constructed and installed at the AsH_3 supply line of our OMVPE system. The zeolite system was filled at room temperature to an AsH_3 pressure of 760 torr from our conventional 100% AsH_3 source. Supply pressure was easily maintained by manual temperature control during runs lasting up to 5 hours. Several epitaxial layers were grown under identical conditions except for the AsH_3 source. Table 1 summarizes the electrical data of three types of layers grown by using the conventional 100% AsH_3 source and the AsH_3-zeolite source (source AsH_3-Z). We were unable to make ohmic contacts to the 6.5-μm thick undoped GaAs layer grown from the AsH_3-Z source. A comparison of the electrical data of two intentionally Si-doped GaAs layers shows little difference between the two AsH_3 sources. The difference in hole concentration of the two $Al_{0.28}Ga_{0.72}As$ is within the variance of background carrier concentration from run to run for AlGaAs grown in our reactor by using the conventional AsH_3 source.

Optical spectroscopy, such as photoreflectance (PR) and photoluminescence (PL), were also used to compare the quality of the epitaxial layers. A comparison of the PR and PL spectra of

the epitaxial layers grown by using the two different AsH_3 sources shows that the layers are virtually identical. Figure 5 shows an example of low-temperature (6 K) PL of the two undoped GaAs layers. The peaks are due to optical transitions involving free and impurity-bound excitons and a transition at 1.5134 eV caused by recombination of a free hole and an electron bound to a donor (h,D°). A close examination of the PL shows that the peak intensity ratio of donor-bound excitons to acceptor-bound excitons is slightly higher for the AsH_3-Z grown layer. This implies that the AsH_3-Z grown layer is more compensated and may explain the insulating electrical properties of this layer. In general, the PR and PL spectra of these two GaAs layers indicate that both are of high quality with total impurity concentrations in the low 10^{14} cm^{-3} (10 ppb).

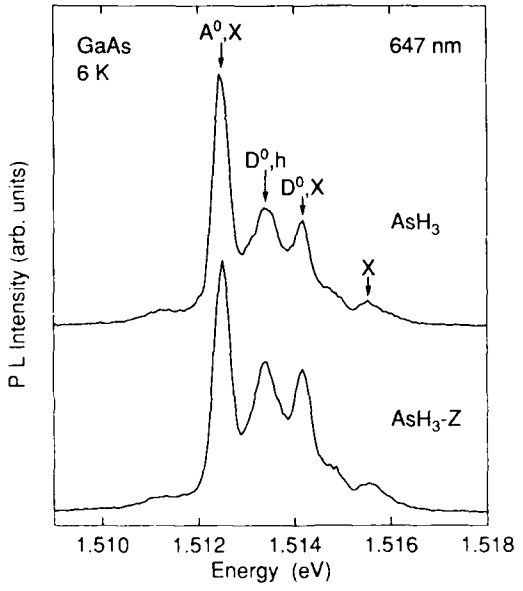

Fig. 5 — Photoluminescence spectra at 6 K in the exciton region of two undoped GaAs layers grown with a conventional AsH_3 source (AsH_3) and the AsH_3-zeolite source (AsH_3-Z)

Conclusions: We have demonstrated the growth by OMVPE of GaAs and AlGaAs by using an AsH_3 on-demand atmospheric pressure storage system that is based on gas adsorption into the microcavities of CaA zeolite and subsequent controlled desorption. The purity of these epitaxial layers compares favorably with those grown by use of a conventional 100% AsH_3 source. The storage system eliminates the sudden release hazard associated with compressed or liquified hazardous gases and is a simple and direct replacement for existing gas storage cylinders.

Acknowledgment: The authors acknowledge J.A. Freitas, Jr., for the PL work and A.D. Berry, D.K. Gaskill, and N. Bottka for helpful discussions.

[Sponsored by ONR and ONT]

Reference

1. D.W. Breck, *Zeolite Molecular Sieves—Structure, Chemistry, and Use* (John Wiley & Sons, New York, 1974). ■

Atomic Layer Electronics

W. E. Carlos, D. G. Gammon, S. M. Prokes, and B. V. Shanabrook
Electronics Science and Technology Division

Tomorrow's electronics will require nanometer-scale devices that exhibit novel optoelectronic properties caused by the confinement of electrons and holes in very small low-dimensional quantum structures. Unfortunately, growth and processing procedures encounter problems such as interdiffusion, point defects, and inhomogeneities that limit our ability to turn ideas into reality. Conventional growth techniques such as molecular beam epitaxy (MBE) only control interfacial regions to about two or three monolayers. Our atomic layer electronics (ALE) program strives to achieve submonolayer control of the interfacial region. Several procedures are used to form sharper interfaces than those formed with conventional growth methods. In one technique, growth is interrupted at the interfaces to allow atomic diffusion and form a smoother surface layer and therefore a sharper interface. In another, migration-enhanced epitaxy, the atomic species are deposited alternately rather than concurrently, leading to

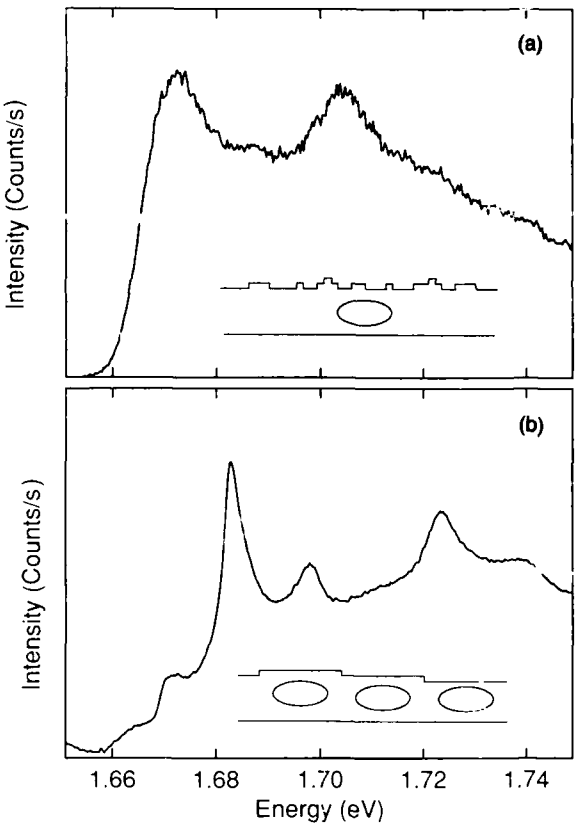

Fig. 6 — The PLE spectra of two GaAs/AlAs superlattices (a) with no growth interruption between layers and (b) with a growth interruption between GaAs and AlAs layer

sharper interfaces at lower temperatures. These techniques are currently being used to grow GaAs/AlAs superlattices, with GaAs/InAs structures and lateral superlattices planned for early 1990. Characterization of materials grown by these methods requires development or refinement of novel optical and X-ray techniques for evaluation of interfacial sharpness.

One exceptionally useful technique is photoluminescence excitation spectroscopy (PLE) in which the band-edge photoluminescence intensity is monitored as a function of excitation energy, essentially providing a measurement of optical absorption. The excitation process produces an electron-hole pair loosely bound into a hydrogen atom-like exciton. Because the effective mass of the electron in the conduction band of a semiconductor is much less than the mass of a free electron and because the dielectric constant of semiconductors such as GaAs is relatively high, the exciton is much larger than a hydrogen atom (on the order of 100 Å vs 0.5 Å for hydrogen). Because the electron and hole are confined to a thin GaAs layer, the PLE absorption energy of an electron-hole pair includes a confinement energy, which depends inversely on the layer thickness. If the interfaces are rough, as shown in Fig. 6(a), there are many different layer thicknesses and the PLE is broad, measuring the confinement energy for an average layer thickness. If we make one of the interfaces smooth (roughness larger than exciton), then the PLE will split into two or three lines, each associated with a single exciton diameter as shown in Fig. 6(b).

In addition to the optical studies, X-ray diffraction is used to characterize the superlattices as shown in Fig. 7(a). The magnitudes of the satellite peaks around the central GaAs(002) diffraction peak are proportional to the squares of the Fourier transform components of the atomic distribution. A very sharp distribution function

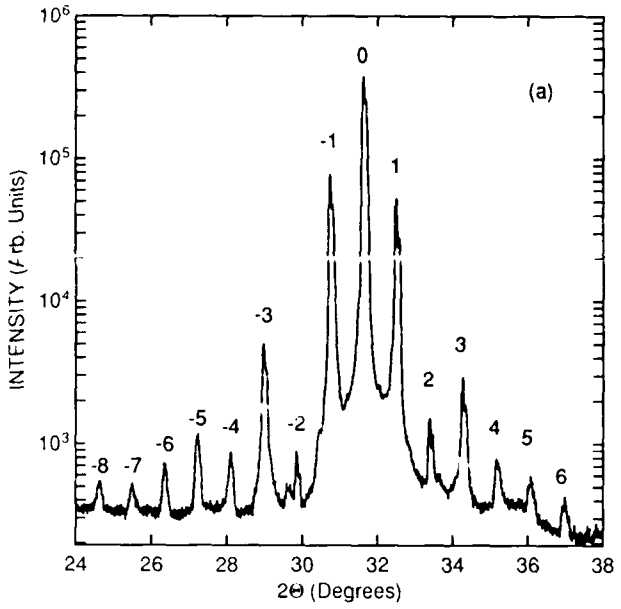

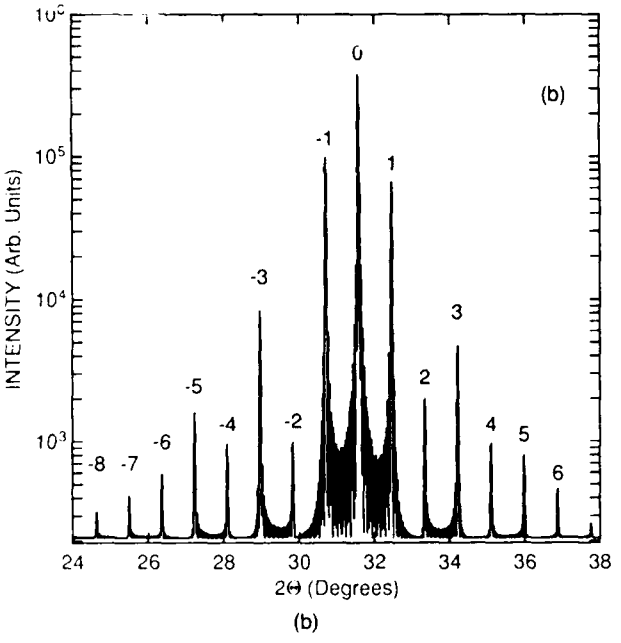

Fig. 7 — X-ray diffraction spectra (a) around the GaAs(002) peak for the GaAs/AlAs sample with growth interruption, and a computer simulation (b) of the diffraction spectra, including a two-monolayer-thick interfacial layer. The numbers indicate the order of the satellite peaks.

requires many Fourier terms to accurately model the abrupt change at the interface. The intensities of the higher satellites are then a measure of the sharpness of the interfaces. Figure 7(b) shows a simulation of the diffraction scan 2a, which includes an interfacial broadening of two monolayers.

Much of the growth of materials used in this project was performed by D.S. Katzer, an ONT postdoctoral fellow. In addition to the two measurements mentioned here, Raman spectroscopy, magnetic resonance, and photoreflectance are being used to probe the physics of the interfaces. The ongoing collaborations of the several scientists working on these measurements are crucial to our efforts to turn today's conceptual models into tomorrow's electronic materials.

[Sponsored by ONR] ■

Vacuum Microelectronics

H. F. Gray and R. K. Parker
Electronics Science and Technology Division

Vacuum microelectronics is an emerging electronics science and technology that exploits the advantages of solid-state microelectronics and vacuum ballistic charge transport. Solid-state fabrication techniques have made possible 3-D nanostructures, large integrated circuits, and economical batch processing, while vacuum electronics has attractive properties that include high electron velocities, voltage isolation, temperature insensitivity, and radiation hardness.

Background: The concept of vacuum microelectronics is not new. More than 30 years ago, Shoulders [1] suggested the possibility of small vacuum triodes based on field emission. His efforts initiated a program at SRI International that led to the development of a thin-film field-emission cathode (TFFEC) [2]. These TFFECs were developed for high-brightness cold cathodes to be used in high-power microwave tubes and CRTs. However, the TFFEC fabrication and processing approach was based on a unique "fly's-eye" e-beam lithographic process and a complicated multiple-source e-beam deposition process—techniques not extensively used by the

solid-state community. At that time, little interest was expressed for vacuum microelectronic devices because the limitations in solid-state electronics had not yet been reached. Solid-state scientists were intensely interested in modifying semiconductor bandgaps, creating precise doping profiles, fabricating heterojunction superlattices with molecular beam epitaxy, and developing batch processing techniques for solid-state integrated circuits.

Field Emitter Arrays: Recognizing the uniqueness of the SRI fabrication process, NRL researchers attempted to demonstrate that standard solid-state processes could be used to fabricate field emitter arrays (FEAs) similar to the TFFECs. This was accomplished by using standard 3-D micromachining techniques and optical lithography to create sharp nanostructure pyramids in bulk silicon [3] and sharp metal pyramids by use of a silicon "mold" process [4]. Integral extraction gates were fabricated with a simple one-mask self-aligned deposition process. Figure 8 is a scanning electron micrograph of a silicon FEA designed and fabricated at NRL. This array is composed of pointlike silicon field emitters that have an average radius of curvature of ~ 50 nm; the average aperture diameter in the extraction gate is slightly > 1 μm. We have also made FEAs from wedgelike field emitters to obtain greater emitting area per tip.

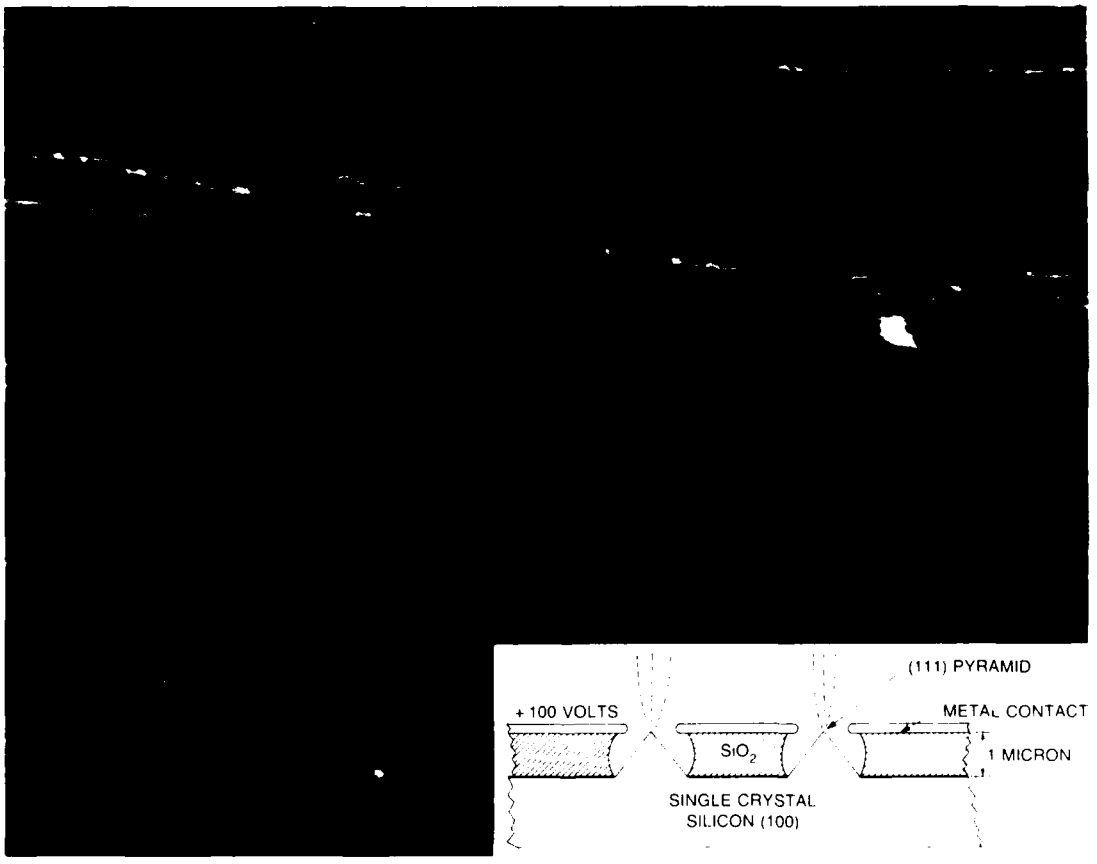

Fig. 8 — A colorized scanning electron micrograph of a silicon FEA, and an insert line drawing designed and fabricated at NRL. The spacing between cells is about 10 μm, the average diameter of the extraction gate aperture is about 1 μm, and the average radius of curvature of the silicon field tips is about 50 nm.

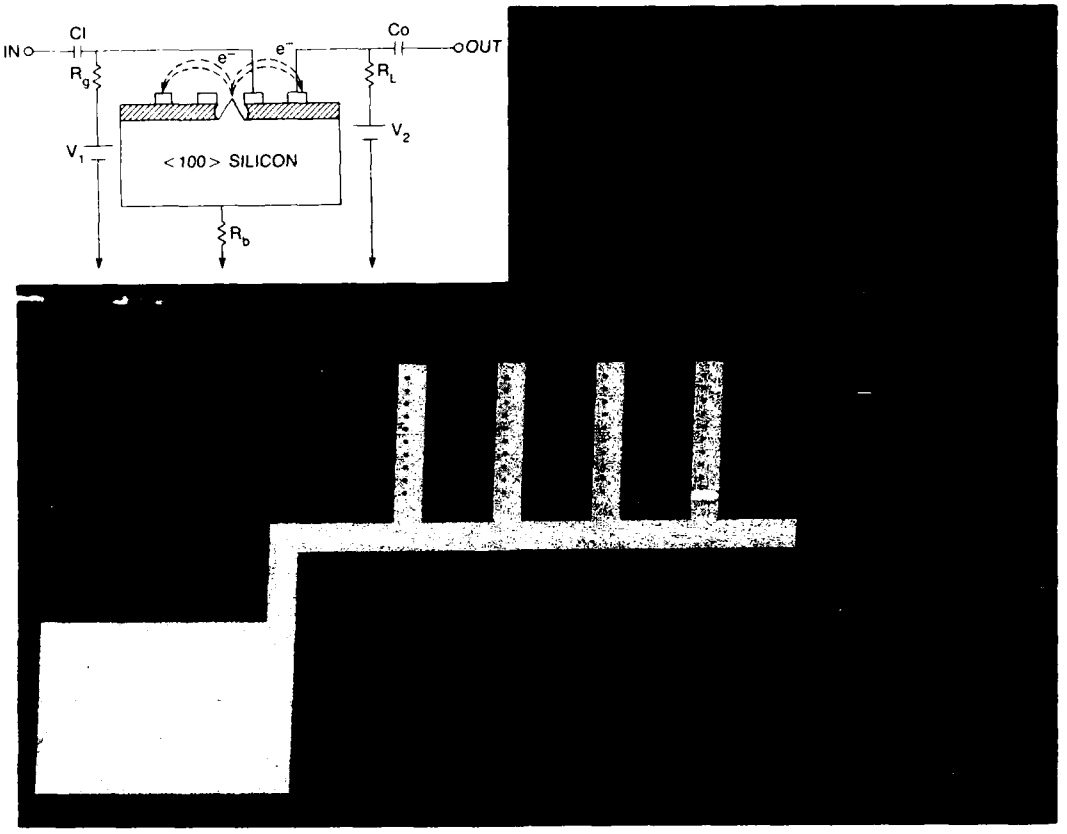

Fig. 9 — A colorized scanning electron micrograph of the first planar silicon vacuum FET and an insert schematic diagram. The orange pad in the lower left-hand corner connects to the gate; the red pad in the upper right-hand corner connects to the drain; the silicon field emitters that can be seen inside the holes in the gate fingers make up the source. Electrons tunnel from the source (field emitters) and travel in vacuum to the drain where they are collected. The fingers are about 20 μm wide and are separated by about 10 μm. The transit time from source to drain is estimated to be a few picoseconds.

Vacuum Microelectronics: Figure 9 is a scanning electron microscope picture of the first vacuum transistor, a planar silicon vacuum field effect transistor (FET) based on our silicon FEA ideas [5]. We measured both current and voltage gain from this device. Although this device has large dimensions, 20-μm finger widths, and 10-μm spacings between fingers, the calculated total transit time for electrons traveling from source to drain is only a few picoseconds.

Figure 10 is a modified Fowler-Nordheim plot of the current-voltage characteristics of the vacuum transistor shown in Fig. 9. This curve shows that the emitted current saturates at very high electric fields thereby preventing tip blowup, which is a serious reliability problem with metal FEAs. This current saturation, which we believe is due to charge carrier velocity saturation in the near-surface region inside the field tip, can be controlled by doping and by modifying the surface layer with metal and dielectric thin films. This phenomena requires an understanding of the physics of nonequilibrium electron transport in very high electric fields, particularly in the near-surface region of 3-D nanostructures. It also requires an understanding of the physics that controls tunneling through metal, semiconductor, and dielectric surface films, which are thin compared to the inelastic scattering length of electrons. Furthermore, it requires an understanding of the dynamics of "hot" electron

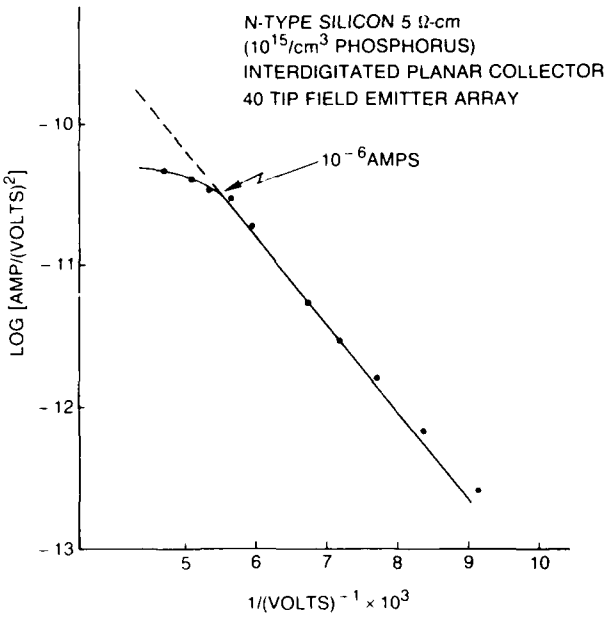

Fig. 10 — A modified Fowler-Nordheim plot that shows the current-voltage characteristic of the first vacuum FET. Note that current saturation in semiconductors prevents tip blowup, which is a serious problem in metal FEAs.

generation and annihilation under these conditions. Theoretical and experimental investigations into these questions are just beginning to be addressed. Fundamental physical questions of this type can be addressed today because we have the fabrication tools and processes to make reproducible 3-D nanostructures.

In addition to fundamental physical questions, we are interested in applications of these nanostructures. We are now investigating new theoretical device concepts, including one called a nondiscrete distributed amplifier that might be useful for wide-bandwidth millimeter wave applications [6,7]. We are also investigating a variety of new fabrication approaches to generate novel structures such as those composed of multilevel thin-conducting films for edge-emission devices [8].

The demonstration of the NRL vacuum transistor, along with the field emission results reported recently by researchers throughout the world by using other types of structures, indicates that FEAs promise to be the basis of an interesting microelectronics technology that exploits the ballistic transport properties of vacuum. It promises to address military applications such as low- and medium-power microwave and millimeter power amplifiers, electronic warfare applications, radar, and possibly signal processing. It might also address a variety of commercial applications, such as analog and digital communications, high temperature electronics, flat-panel displays, and high-definition television (HDTV).

[Sponsored by ONR]

References

1. K. Shoulders, "Microelectronics Using Electron-Beam-Activated Machining Techniques," in *Advances in Computers*, F. L. Alt, ed. (Academic Press, New York, 1961), Vol. 2, pp. 135-293.

2. C. A. Spindt, I. Brodie, L. Humphrey, and E. R. Westerberg, "Physical Properties of Thin-film Emission Cathodes with Molybdenum Cones," *J. Appl. Phys.* **47**, 5248-5263 (1976).

3. H. F. Gray, "Silicon Field Emitter Array Technology," Proceedings of the 29th International Field Emission Symposium, H.O. Andren and H. Orden, eds. (Almqvist and Wiksel International, Stockholm, 1982), pp. 111-118.

4. H. F. Gray and R. F. Greene, "Method of Manufacturing a Field-Emission Cathode Structure," U.S. Patent No. 4,307,507.

5. H. F. Gray and G. J. Campisi, "A Silicon Field Emitter Array Planar Vacuum FET Fabricated with Microfabrication Techniques," *Mat. Res. Soc. Proc.* **76**, 25 (1987); H. F. Gray and R. F. Greene, "Ultra-Fast Field Emitter Array Vacuum Integrated Circuit Switching Device," U.S. Patent No. 4,578,614.

6. A. K. Ganguly, P. M. Phillips, and H. F. Gray, "Linear Theory of a Field Emitter

Array Distributed Amplifier," *J. Appl. Phys.*, (accepted for publication) (1990).

7. Z. H. Huang, P. H. Cutler, T. E. Feuchtwang, and H. F. Gray, "Theoretical Study of a Vacuum Field Effect Transistor," Proceedings of the Second International Conference on Vacuum Microelectronics in Bath, England, 24–26 July 1989; *Vacuum Microelectronics 1989*, R. E. Turner, ed., Institute of Physics Conference Series Number 99; Section 7 (Institute of Physics, Bristol and New York, 1989), pp. 223–230.

8. H. F. Gray, "Symmetrical Layered Thin-Film Manufacturing Method of Making Field Emitter Arrays," Invention Disclosure Navy Case No. 70526 (patent application in preparation (1990). ■

Light-Activated Resistance Switching: An Extremely Sensitive Solid-State Photodetector

E. S. Snow and P. M. Campbell
Electronics Science and Technology Division

A basic goal of solid-state electronics has been the reduction in size of electronic devices. It is now possible to fabricate devices that have dimensions on the order of a few hundred atoms. In this size regime, changes in the charge state of single defects are expected to have measurable effects on device conduction properties. Noise measurements in submicrometer metal-oxide-semiconductor field-effect transistors have detected discrete changes in electrical resistance [1]. This resistance switching arises from the capture and release of electrons from single defects, and that a large ensemble of defect-mediated resistance switching is a fundamental source of $1/f$ noise. $1/f$ noise is a limitation in many semiconductor devices, although no complete explanation for the source of the noise exists. If the defect model of the resistance switching is correct, then it should be possible to activate the resistance switching optically. This effect had never been observed.

Recent experiments at NRL have detected optically activated resistance switching in the tunneling current of GaAs/AlGaAs single-barrier tunneling devices. These measurements confirm the defect origin of discrete resistance switching in this system. In one case the optical sensitivity of the switching outperforms the best commercial near-infrared photodetectors, which suggests that optically activated resistance switching may provide a novel, extremely sensitive mechanism for photodetection.

Light-Activated Resistance Switching: Noise measurements on GaAs/AlGaAs heterostructure tunnel barriers at NRL indicate that under constant bias the current switches between a few discrete levels. Analysis of the temperature and voltage dependence of the resistance switching suggests that the origin of the noise may be defect related. The frequency spectra of the noise indicate that the resistance switching is a fundamental source of $1/f$ noise in tunnel barriers. The conduction and noise properties of heterostructure tunnel barriers are important because the barriers constitute the fundamental building blocks of modern electronic and electro-optic devices. Subsequent optical studies have shown that the resistance switching in some of the devices is light-active [2]. The optical studies represent the first observation of light-activated resistance switching. The optical data also provide the first proof that resistance switching can originate from the capture of a single electron by a single trap. Figure 11 is a current vs time trace of a light-active tunnel barrier exposed to weak light. The current pulses represent the capture of optically created holes by a single electrically active defect resident in the tunnel barrier. The ability to observe the effects of single defects allows us the unique opportunity to study defect-mediated transport phenomena on the single defect level.

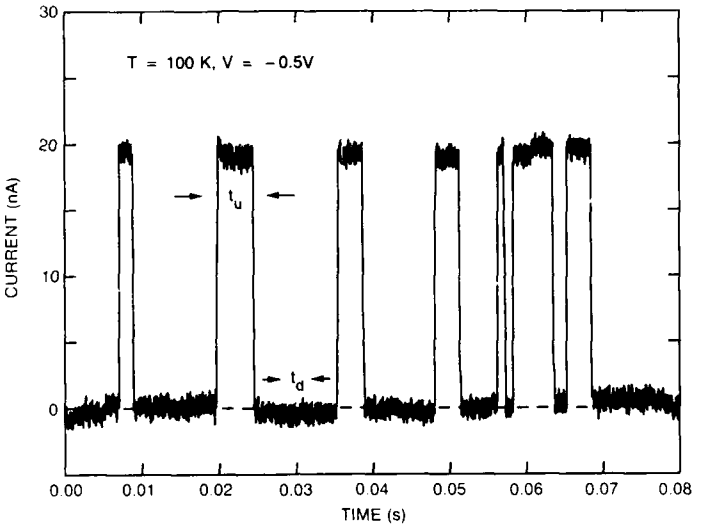

Fig. 11 — Current vs time trace of a single-barrier tunneling device exposed to weak light. Each current pulse signifies the capture of a photoinjected hole by the defect. The time between pulses t_d, represents the time between detection of photons, and t_u represents the time the hole is localized in the trap.

A Novel Photodetection System: In addition to the unique research opportunities afforded by this system, the light-activated resistance switching shows remarkable technological promise. The optical sensitivity of one of our devices surpasses that of the best commercial near-infrared detectors. The device can detect photons (wavelength = 8200 Å) at a flux of less than one photon per hour. The optically sensitive area of the device is larger than 100 μm^2. The extreme sensitivity of this device owes itself to the unique electronic properties of defects resident in the semiconductor structure. Reliable reproduction of these defects through defect engineering could result in extremely sensitive photodetector arrays. Alternatively, a combination of band-gap engineering and submicrometer lithography could replace the defects. Both of these options are being pursued at NRL.

Acknowledgments: Drs. S. W. Kirchoefer, O. J. Glembocki, and W. J. Moore have made significant contributions to this research.

[Sponsored by ONR]

References

1. K. S. Ralls, W. J. Skocpol, L. D. Jackel, R. E. Howard, L. A. Fetter, R. W. Epworth, and D. M. Tennant, *Phys. Rev. Lett.* **52**, 228 (1984).

2. E. S. Snow, P. M. Campbell, O. J. Glembocki, W. J. Moore, and S. W. Kirchoefer, *Appl. Phys. Lett.*, in press. ■

Energetic Particles and Beams

ENERGETIC PARTICLES AND BEAMS

More compact energetic beam sources with a higher energy output continue to be developed at NRL where research is performed in the areas of plasma, laser, and advanced beam technology.The ways in which energetic beams react with, and affect, matter are also studied. Reported in this chapter is work on electron beam deposition in metals and charged particle beam propagation.

The Condensed Matter and Radiation Sciences Division (4600) and the Plasma Physics Division (4700) contributed to this work.

Other current research in energetic particles includes:

- Damage to microcircuits by energetic electrons from space radiation or weapons
- X-ray studies on Cr activated charcoal
- Modified betatron accelerator

Anomalous Intense Electron Beam Deposition in Metals

A. Stolovy, J. M. Kidd, and A. I. Namenson
Condensed Matter and
Radiation Sciences Division

Electron beam weapons are being proposed to protect ships from missile attack. Such a weapon would require intense short pulses of high-energy electrons to allow propagation through the atmosphere. The beam can penetrate deep into the target and deposit enough energy to disrupt electronic guidance controls or to ignite the high-explosive warhead. The energy deposited by such a beam may be distributed differently from that for a sum of single electrons, however, because of collective effects when the intense pulse of electrons interacts with the solid target. To test this hypothesis, we have performed a series of experiments to measure how energy is deposited in targets of Al, Ti, and W with both intense and weak electron beam pulses. Monte Carlo electron-photon shower codes were also calculated and were compared to both sets of experimental results.

Experiments with relatively intense beam pulses (8 kA/cm^2) were performed at the Los Alamos National Laboratory pulsed high-energy radiographic machine emitting X rays (PHERMEX). The low-intensity (5 A/cm^2) experiments were done at the NRL Linac. The average beam energy was set at 26 MeV at both facilities, and the energy spectra are very similar.

Energy Absorption Measurements: Since the energy absorbed by the target is rapidly thermalized, we have used a calorimetric technique to measure the deposited energy in metal targets. Three calorimeter assemblies were constructed, each of which has four disk sections, as shown in Fig. 1. The first assembly contains aluminum sections; the second contains titanium sections; and the third contains tungsten sections, to look for a possible Z dependence. In each case, the total thickness is about 20% greater than the

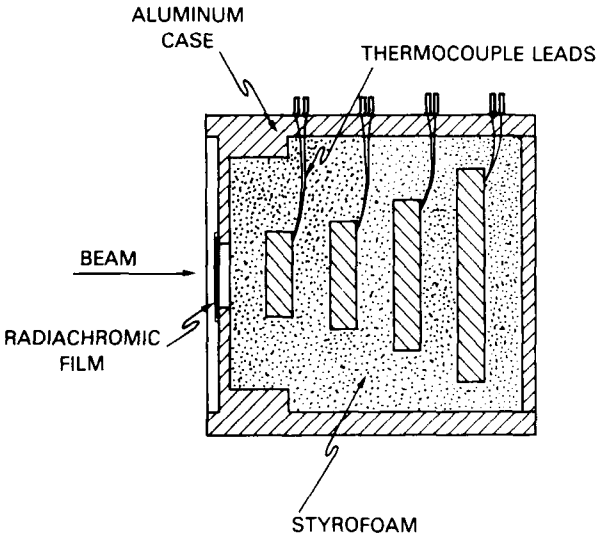

Fig. 1 — Calorimeter assembly consisting of four disks of the same metal, with attached thermocouples (cylindrical geometry)

maximum electron range, and the sections are tapered, to ensure that all of the electrons of the spreading beam are stopped. A portion of the electron energy is converted into electromagnetic radiation (bremsstrahlung), some of which is absorbed by the downstream sections, and some of which escapes. The sections are imbedded in Styrofoam for thermal insulation, and each has a Chromel-Alumel thermocouple attached near the edge. The energy deposited in each section is then easily calculated from the observed temperature rise, the mass, and the specific heat. Measurements were repeated many times for two separate observation periods at each accelerator, and the results were averaged. Thus, we are able to compare energy depth profiles for high-intensity and low-intensity beams with each other, and with Monte Carlo code calculations for these three metals.

Results: Figures 2 and 3 show the distribution of beam energy deposited in the four sections of the titanium and tungsten assemblies. The data for aluminum are similar. The Linac (low-intensity) data are in excellent agreement with the single-electron code calculations. The data taken at the PHERMEX (high intensity) consistently show anomalously strong energy deposition in the

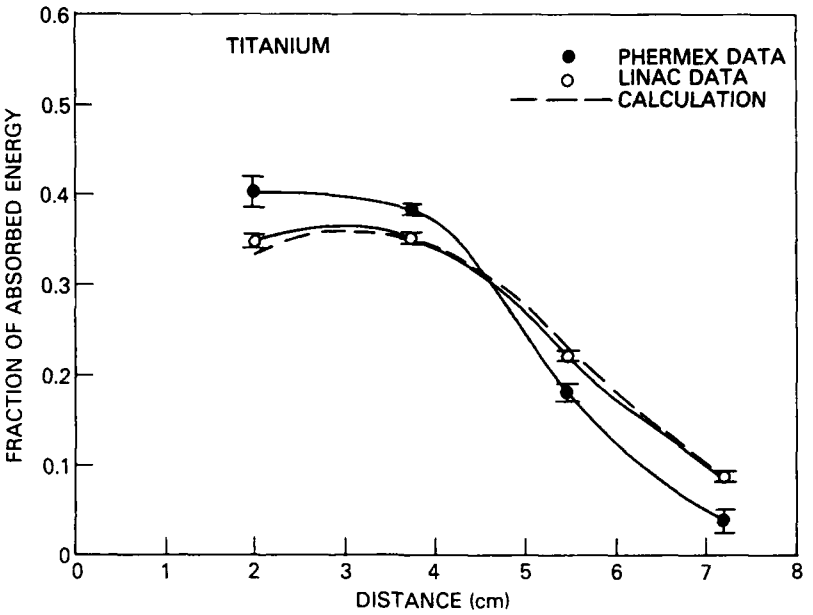

Fig. 2 — Comparison of distributions of deposited energy in the four-section Ti calorimeter as measured at the NRL Linac and the PHERMEX facility and as calculated with an electron-photon shower code. Distances are from the front face of the calorimeter assembly to the center of each section. Uncertainty in the calculated curve is about 5%.

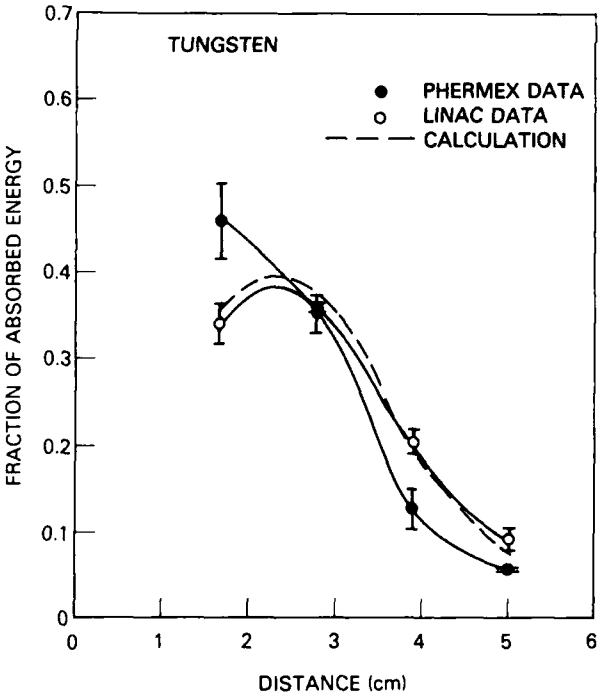

Fig. 3 — Comparison of distributions of deposited energy in the four-section W calorimeter as measured at the NRL Linac and the PHERMEX facility, and as calculated with an electron-photon shower code. Distances are from the front face of the calorimeter assembly to the center of each section. Uncertainty in the calculated curve is about 5%.

first section (upon which the beam is incident) and reduced deposition in the section farthest downstream. The largest effect is in the tungsten data, suggesting a Z dependence. A statistical analysis allows us to say with 99.9% confidence that the PHERMEX data do not agree with single-electron calculations. These results are somewhat surprising in that the PHERMEX beam intensity is two to three orders of magnitude lower than that required to produce plasma-related effects, where anomalously large energy deposition has been observed previously [1]. Thus, the explanation of the effect observed at intermediate beam intensity is not clear, but it may be related to magnetic or electric fields induced in the target by the beam. These results could have important consequences for the effectiveness of an electron beam weapon, since the energy deposited in the skin of the target is greater, and the energy deposited deep within the target is lower than expected from single-electron theory. The importance of this collective effect depends upon the weapon beam intensity and energy.

Acknowledgments: Drs. M. I. Haftel and G. H. Herling performed the electron-photon shower code calculations, and Dr. J. B. Aviles, Jr., made significant contributions to this work [2].

[Sponsored by the DEO]

References

1. K. Imasaki, S. Miyamoto, S. Higaki, S. Nakai, and C. Yamanaka, *Phys. Rev. Lett.* **43**, 1937 (1979).

2. A. Stolovy, J. M. Kidd, A. I. Namenson, M. I. Haftel, G. H. Herling, and J. B. Aviles, Jr., *Phys. Rev. A* **40**, 2558 (1989). ■

Charged Particle Beam Research for Directed Energy Applications: Experimental Program

R. A. Meger
Plasma Physics Division

Background: Antiship missiles (ASMs) represent a major threat to Navy ships. As missile technology improves and spreads throughout the world, this threat increases. Several technologies are available or are under development to counter this threat. These include counter missiles, gattling guns, rail guns, and directed energy weapons (DEWs). DEWs may be the ultimate solution with their promise of speed-of-light delivery, rapid retargeting, and magazine requiring only a large energy supply. They are inherently defensive because of their limited range but may offer a mobile umbrella against ASMs for ships of the future. Development of such weapons fits well with the Navy's plans for switching to all-electric ships in the early 2000s, since power from the ship's propulsion system could also power the defensive weapons systems. Three types of DEW systems are under development—high power microwaves, lasers, and charged particle beams (CPBs). Of these, CPBs have the greatest potential for a hard kill of incoming ASMs but are also the most technically challenging to develop. NRL has been in the forefront of this research effort for a decade.

A CPB DEW consists of a high-energy, high-current stream of electrons, traveling at near the speed of light. The advantage of using high-energy electrons is that they can penetrate into a target and damage internal components. To be viable as a DEW, a CPB must be able to propagate from the accelerator to the target in a stable and reproducible manner. Two problems associated with propagating electron beams in the atmosphere have been investigated at NRL—range extension and beam stability.

CPB Range Extension: In the first case, the distance that even a high-energy (relativistic) beam can travel in full density air at sea level is limited to several hundred meters by electron beam energy loss to the background gas. This is somewhat short for an ASM defensive system. The only way to extend the range is to lower the background density through which the beam propagates. It has been shown experimentally that a large fraction of the energy lost by the beam ends up heating the background gas. This results in a cylindrical channel of low density gas in pressure equilibrium with the surrounding air along the beam path. Such channels can have minimum densities of a small fraction of an atmosphere and are very stable, lasting for many milliseconds until turbulence sets in and destroys the channel. Thus the range of a CPB DEW could be extended if a burst of beam pulses is used rather than a single pulse. Each successive pulse in the burst would first have to follow (or track) the existing channel until it reaches the end and then either interact with a target or extend the channel (Fig. 4(a)). The tracking of such a preformed density channel is a key element to extending the range of a CPB DEW. NRL pioneered the experimental study of channel tracking and has demonstrated the existence of a theoretically predicted tracking force acting on the beam by a preformed density channel. This was accomplished by using a laser discharge channel

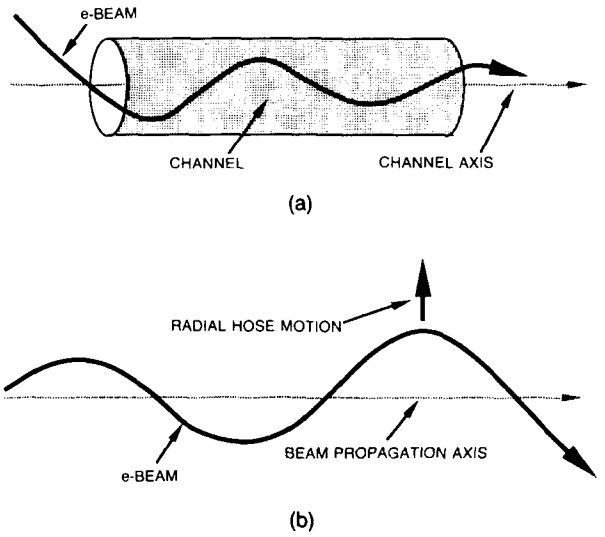

Fig. 4 — (a) A charged particle beam (e-beam) is pulled into and tracks a density channel formed by either previous electron beam pulses or a laser-initiated discharge. (b) The radial motion of an e-beam increases both with propagation distance and with distance from the front of the beam as it propagates; this is due to an interaction with return currents that are generated in the background. The hose motion eventually can result in disruption of the beam.

and a single pulse electron beam. Other experiments outside NRL using beam-produced channels have corroborated the existence of the tracking force. Investigation of the tracking phenomenon is continuing both experimentally and theoretically at NRL.

CPB Stability: The second major hurdle for CPB DEWs is beam-propagation stability. When a beam propagates in a neutral gas, it partially ionizes the background gas and produces a conducting plasma channel. Return currents are driven by the beam's magnetic field in this channel as it propagates. The interaction of the beam and these return currents can be unstable, resulting in the electron beam expanding up to a large radius or moving laterally after propagating only a few meters. One of the strongest instabilities that must be overcome is the resistive hose instability (Fig. 4(b)). This instability causes the beam to behave like a fire hose, snaking around at increasing amplitude as it propagates (Fig. 5). Techniques that involve manipulating the beam parameters within the beam pulse have been developed at NRL and elsewhere that can minimize the growth of this instability, allowing the beam to travel in a straight line. NRL is actively studying these techniques both experimentally and theoretically.

NRL Facilities: Much of the work discussed above has been carried out in a new CPB propagation laboratory, funded by NRL and completed in 1988. This new lab contains two high-power electron beam generators, a high-power laser system for producing channels, and a 20-m-long propagation range. The flagship beam generator is the SuperIBEX accelerator, which produces a 50-ns-long, 5-MV, 100-kA beam for injection into channels of uniform density gas. At present, propagation is studied in a 5-m-long, 2 m in diameter vacuum chamber with numerous ports for diagnostic access. Hardware to scale experiments up to 20 m in length is available for future experiments. Diagnostics include arrays of electromagnetic field, X ray, and optical diagnostics coupled to a computer controlled data analysis system.

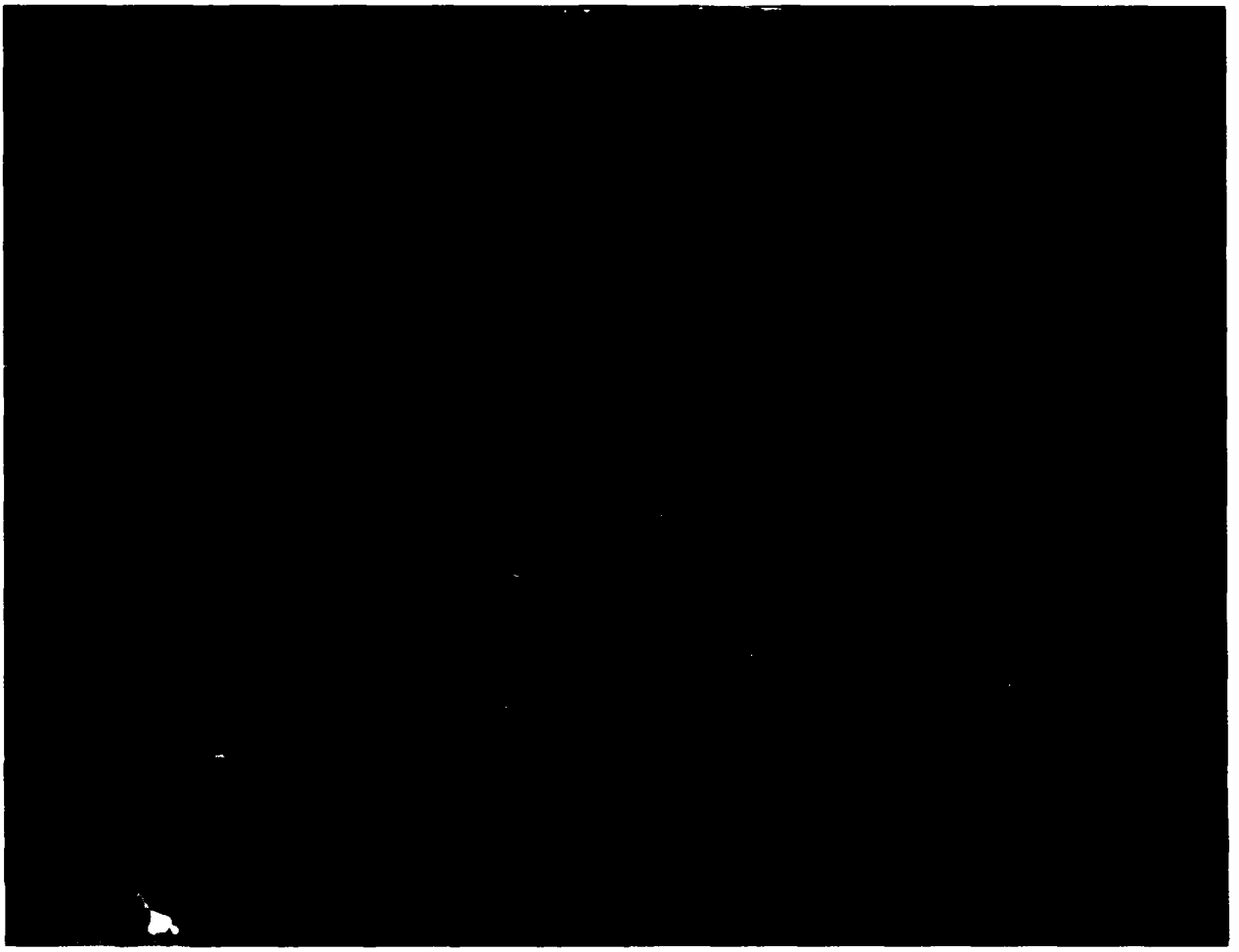

Fig. 5 — A high-current e-beam undergoing large-scale hose motion after 1 m of propagation resulting in the loss of the beam

Acknowledgments: This research is performed by members of the Charged Particle Beam Physics Section of the Charged Particle Physics Branch with theory support provided by members of the Beam Physics Branch. Other labs performing similar research include Sandia National Laboratories, Lawrence Livermore National Laboratory, and a number of private companies. With the research performed in the CPB propagation laboratory, NRL has made and will continue to make a significant contribution to the area of DEW research for Navy ship defense.

[Sponsored by ONR and DARPA]

Information Technology and Communications

INFORMATION TECHNOLOGY AND COMMUNICATIONS

Modern battle management is composed of a number of integrated components; one is communication. Secure transmission of battle information and its subsequent timely processing is paramount to battle success, and research addresses artificial intelligence, parallel computing, information security, and human-computer interactions. Reported in this chapter is work on analysis of key distribution protocols, certification methodology, and communications network research.

The Information Technology Division (5500) contributed to the work presented here.

Other current research in information technology and communication includes:

- Trustworthy communications systems
- Artificial intelligence in diagnosis
- Parallel interference performance evaluation and refinement (PIPER)
- Decision support shell
- Estimate/report correlations

Applying Formal Methods to the Analysis of Key Distribution Protocols

C. A. Meadows
Information Technology Division

It is difficult to be certain whether or not a cryptographic protocol, that is, the means by which a machine manages and distributes keys and authenticates itself to others, satisfies its requirements. Protocols have been designed with subtle security flaws, independent of the strengths or weaknesses or the cryptoalgorithm used, that were not discovered until some time after they had been published.

One approach to the problem of assuring correctness is to use machine-aided, formal verification techniques. The protocol and its desirable security properties are modeled in a formal specification language, and a machine verification system is used in an attempt to prove that these properties hold. If the attempt succeeds, one has gained greater assurance that the protocol satisfies its requirements. If it fails, examining the reasons for the failure may point out security flaws in the protocol.

Techniques like these have as yet found little application in analyzing cryptographic protocols, even though these same techniques are widely used in the related areas of communication protocols and secure computing systems. The reason for this may be that existing formal specification languages and machine verification systems do not emphasize the models and the theorem-proving techniques that would be the most useful in analyzing such protocols.

We have attempted to fill this gap by developing a formal model and specification language for cryptographic protocols and a software tool for their analysis. We have used them to specify and analyze a protocol developed at Sandia Laboratories [1]. The fact that the application of our techniques uncovered two previously unknown security flaws in the protocol shows that they promise to be useful. Simmons [2] gives a full report on the specification and analysis of this protocol.

The Model and Specification Language: The model we use is an adaptation of the public-key model of Dolev and Yao [3]. We consider a protocol as a set of rules for passing messages between the participants. A participant in the protocol who receives a message will, if accepting it as genuine, generate a new message by performing certain operations on it or other messages received earlier. Thus a cryptographic protocol may be thought of as a set of rules for generating words in some formal language. A penetrator who tries to break the protocol by intercepting messages, supplying false messages to the participants, and performing operations on messages to find out a secret word, may be thought of as attempting to determine whether a particular word belongs to that language.

In our model, a state in a protocol is specified by listing a set of words known by the penetrator and the values of the local state variables of the participants. Rules for moving from one state to the other are specified by describing the words that must be known by a penetrator, the values of the local state variables that must hold for the rule to be applicable, the words learned by the penetrator, and the new values of the local state variables after the rule has been applied.

For example, if the penetrator is able to encrypt data, we can represent this by a rule

$$\textit{if } \{X,Y\} \subset \mathbf{W}, \textit{ then } \mathbf{W} := \mathbf{W} \cup \{e(X,Y)\},$$

where e(X,Y) denotes the result of encrypting message Y with key X and **W** is the set of words known by the penetrator. On the other hand, if a participant in a protocol will encrypt all messages sent to it with the current session key and send them out, this may be described by the rule

$$\textit{if } \{Y\} \subset \mathbf{W}, \textit{ and } \text{KEYSTONE}(a) = X, \textit{ then } \mathbf{W} := \mathbf{W} \cup \{e(X,Y)\}.$$

We also specify a set of *reduction rules* relevant to the security of the protocol. Examples of such rules are:

d(X,e(X,Y)) → Y, where e(A,B) denotes encryption of word B with key A, and d(A,B) denotes decryption of word B with key A; and p(s(X)) → X, where s and p are the successor and predecessor operators, respectively.

Formal Analysis of Protocols: We begin analyzing a protocol in our system by identifying the insecure states. We identify all states that immediately precede the insecure states, the states that immediately precede those, and so on through several iterations. We then attempt to define a formal language that contains all these states and show that, to generate one term in this formal language, one must have already generated another term. If the language contains no initial states, then we have shown that the insecure states are unreachable.

To assist us in this analysis, we implement a program in Prolog that computes all states from which a given state is immediately reachable. It does this by using a modified version of the NARROWER algorithm of Rety et al., [4]. This algorithm matches the state description with all substitutions for the variables of the conclusion of a rule. This rule generates states that can be shown to be equal to the specified state after all possible reductions are applied. The states obtained by applying the same substitutions to the *if* part of the rule are the immediately preceding states.

Results of Applying the Analysis to a Protocol: We have applied our techniques to a protocol developed at Sandia Laboratories that employs a combination of encryption and tamperproof devices. These ensure that a participant can encrypt a message (for example, a cryptographic key or a computer program) so that it can be used only by a designated subset of the other participants and so that participants with the ability to use a message cannot learn the contents of the message or pass on this ability or the message to other participants.

We attempt to prove that a penetrator cannot learn the contents of an encrypted message, cannot gain the use of a message unless such use was granted by the originator, and cannot pass off a message as someone else's.

Our analysis found two security flaws in the protocol. One allowed a penetrator to take advantage of a system malfunction to gain the illegal use of a message, and the other allowed a penetrator to pass off a message as someone else's. Both flaws were easily correctable, but they were subtle and might not have been found in a less formal analysis.

Conclusion: We have developed a formal model for cryptographic protocols and a technique for applying this model to determining whether or not a protocol satisfied its security requirements. The fact that the application of these techniques uncovered two security flaws in an independently developed protocol shows that it is likely that they can be refined and developed into a useful tool for protocol analysis.

[Sponsored by ONR]

References

1. G.E. Simmons, "How to (Selectively) Broadcast a Secret," in *Proc. IEEE Symposium on Security and Privacy* (IEEE Computer Society Press, Washington, DC, 1985), pp. 108–113.

2. C.A. Meadows, "Applying Formal Methods to the Analysis of a Key Management Protocol," to appear as an NRL report.

3. D. Dolev and A. Yao, "On the Security of Public-Key Protocols," *IEEE Trans. Inf. Theory* **29**, 198–208 (1983).

4. P. Rety, C. Kirchner, H. Kirchner, and P. Lescanne, "NARROWER: a New Algorithm for Unification and its Application to Logic Programming," in *Rewriting Techniques and Applications, Lecture Notes in Computer Science* (Springer-Verlag, New York, 1985), Vol. 202. ■

Certification Methodology for Trusted Application Systems

J. N. Froscher and J. P. McDermott
Information Technology Division

Background: The Internet Worm incident of November 1988 and malicious attempts by German hackers to penetrate U.S. defense computer networks and systems have dramatized computer security problems of which the DoD has long been aware. DoD efforts in this area have centered on persuading manufacturers to improve security in their commercial computer system products by providing a set of security criteria (the Trusted Computer System Evaluation Criteria (TCSEC)) against which those systems can be evaluated. The National Computer Security Center (NCSC) uses these criteria to evaluate systems submitted voluntarily by manufacturers; the evaluation process is both lengthy and expensive.

In theory, the Navy can purchase these evaluated products and use them as the basis for secure application systems. In practice, the security policies enforced by the evaluated commercial products rarely satisfy the specific and complex needs of particular Navy applications. For example, in command and control systems, the evaluated product must be modified or augmented before it can be fielded. But changing an evaluated product normally invalidates the original evaluation, leaving the purchaser with a system whose security properties are open to question.

Certification Methodology: Because the Navy needs a sound basis for trusting its computer systems to input, process, and output classified information securely, NRL is developing a methodology for certifying that application systems satisfy stringent, application-dependent security requirements. By applying this methodology to an individual application system, the Navy will be able to determine to what degree that system can be trusted to enforce its security requirements.

The problem of determining whether a system can be trusted to enforce security requirements has much in common with the more general problem of determining whether any collection of computer programs behaves as its specifier intended. Since specifiers' intentions are inherently informal, there is no way to be certain that a collection of programs is absolutely correct in this sense. Recognizing this fact, the certification methodology defines a variety of tasks whose goals are to assure precise specification of intentions, careful and well-documented design and implementation of software to realize those intentions, extensive review of system design and implementation documents, and thorough testing of the delivered product, both to determine that it has the required security functions and that it is free of security holes.

The methodology is based on the TCSEC and controls the same kinds of documents and procedures the TCSEC requires. These include:

- the configuration management system
- formal security policy model
- descriptive top-level specification
- source code and implementation documentation
- system security documentation
- covert channel analysis
- security features testing
- penetration testing

The scope of these documents and procedures, however, is different for application systems than the commercial computer system products. NRL's contribution is to develop detailed interpretations of the TCSEC that can be used during the development of an application system and that will lead to a sound technical determination of its certifiability.

Certification Tasks: The certification activities are organized as a directed graph of tasks; each task is a collection of certification procedures to be performed in coordination with the application system development. This graph

has been designed so that it can be applied to system developments organized around the iterative or spiral models of the software life cycle as well as the traditional "waterfall" model.

The first certification task is to support the initial Navy procurement team. Because Navy application systems are usually developed under contract, both security requirements and the certification method must be considered in the initial contracting process. The procurement team is briefed on the latest computer security technology and on the application system certification method. This task also provides for consultation on the certification aspects of proposed contractual approaches.

The second certification task is to evaluate the system developer's configuration management system. Stringent configuration management is necessary for development of trusted systems for two reasons: 1) to guard against the introduction of malicious code and 2) to preserve the rigorous mappings between documentation and implementation that are required by the TCSEC. Since the mappings involve documents from the earliest phases of the project, an acceptable configuration management system must be in place before any documents or code are evaluated.

The third certification task is to evaluate the formal security policy model. This model must define precisely the meaning of security for the application system; it is evaluated both for internal consistency and for its relationship to the informally stated security policy.

For systems attempting to satisfy the higher classes of the TCSEC, a detailed top-level specification of the interface provided by the application system Trusted Computing Base (TCB) is required. (The TCB comprises all parts of the application system responsible for enforcing security.) The next certification tasks are to evaluate this specification and its relation to the formal security policy model for consistency and correctness.

The source code and the intermediate-level specifications used to design it must also be evaluated. When the top-level specification is completed, the detailed design and implementation of the TCB software can begin. Evaluation of this detailed design and development activity is partitioned to allow an iterative or spiral approach to design and implementation.

Mechanisms not intended for transferring information, but which could be exploited for this purpose by malicious code, are known as *covert channels*. A simple example is the locking and status information associated with a file: if a program operating at a higher security level can lock a sensitive file or modify its status information in a way that is visible to a program operating at a lower security level, information can be transferred between levels even though the contents of the file are not directly readable at the lower level.

Systems that aim for the higher classes of the TCSEC are analyzed for covert channels. The system developer is required to search for covert channels by using an approved technique. The associated evaluation determines the accuracy of the analysis and the acceptability of the measures used to limit the covert channels.

Both security features testing and penetration testing are included in the certification method. Security features testing is equivalent to conventional testing of the application system's security features, and it is performed by the application system developer. The developer's test plans, test design, and test results are evaluated and verified. When the features testing is complete, the certification team performs penetration testing. In penetration testing, the certification team attempts to bypass or tamper with the system security mechanisms or exploit an oversight in the system security policy.

Another task is evaluation of the system security documentation. Both user security

documentation and system administrator security documentation are required.

The final certification task is to prepare a report that describes the results of all of the assessments. This report is to be used by the certification authority when it certifies the TCSEC class of the completed application system.

Testing the Methodology: To test the certification methodology, NRL is currently participating in the security certification of two NATO command and control information systems currently under development. The security policies for these systems require two-man control of some operations, the ability to transfer control of a work position from one user to another, and the ability to authorize the downgrading of message classifications.

Technology Transfer: NRL is developing this methodology for use by the Naval Electronics System Security Engineering Command (NESSEC), and NESSEC personnel have been recruited to assist with the current experimental computer security certifications. In this way, the transfer of security certification technology to the operational component that will be responsible for conducting future certifications has already begun. NRL expects to remain in a supervisory/consultative role once the technology is fully transferred to NESSEC.

[Sponsored by SPAWAR, VSCINCLANT, and CEIOTAN] ■

Communication Network Research for SDI

E.L. Althouse and D.N. McGregor
Information Technology Division

A communication network simulator/emulator was developed to analyze the communication system performance for the proposed Strategic Defense Initiative (SDI) Phase I architecture. The software was implemented on a 128-node multiprocessor computer. The basic emulator structure is flexible enough to handle both space- and ground-based communication networks for SDI and is generally extensible to other large-scale network applications.

SDI Network Application: The physical architecture under consideration for Phase I consists of three constellations of space platforms connected to multiple ground-entry points within the United States. Figure 1 represents a generic version of this architecture for several rings of high-, medium-, and low-altitude satellite platforms. The high- and medium-altitude platforms provide many of the necessary surveillance, tracking, and information transfer functions used for SDI battle management. The low-altitude platforms carry the space-based interceptors and, upon receipt of weapon-targeting assignments from either space or ground elements, then attempt to destroy all incoming submarine launched and intercontinental ballistic missiles (ICBMs).

The SDI communication network represents a challenging and complex problem. Approximately 200 satellite platforms in varying orbits and inclinations have to be modeled in conjunction with certain rules for their connectivity. In addition, several types of communication traffic (for example, sensor tracking, command and control, health and status, and weapons targeting) have to be sent according to different levels of precedence and timeliness. The system operates in several frequency bands and has several independent transmissions per platform with varying degrees of data rates. Finally, a threat model must be incorporated into the network that represents the approaching ICBMs as a function of time. This threat model then acts as a stimulus for SDI message generation.

Communication Network Emulator: Our communication network simulator/emulator attempts to model this complex problem in its entirety. It is implemented on NRL's 128-node Butterfly Plus multiprocessor developed by the

Fig. 1 — Generic version of the physical architecture under consideration for Phase I for several rings of high–, medium–, and low–altitude satellite platform

Bolt, Beranek, and Newman Corporation. Each node (processor) on the Butterfly is capable of operating at 2.5 million instructions per second (MIPS) and has a local memory of 4 Mbytes. We have adopted the terminology of both network simulator and emulator. Since the SDI system is so large and complex, some parts of the problem are simulated (transmission delays, multiple transmission links per node, effects of noise errors, propagation effects, jamming, and nuclear weapons effects). However, we refer to it as a network emulator because we have established a one–to–one correspondence between real SDI network nodes and Butterfly processors in terms of running the same network management algorithms and developing similar platform local data bases.

The emulator provides the tools and experimental environment needed to perform sensitivity tradeoff studies to evaluate the performance of the Phase I SDI communication network. It currently provides information on platform sizing in terms of link capacity and buffer–size requirements. It is also used to estimate system responses that depend on the threat, network management design and resulting connectivity, and message delivery times. The performance of various network management algorithms for link assignment, routing, and flow and congestion control can also be assessed. We can examine the robustness of the SDI architecture by examining degraded mode operation that may be caused by losses of network resources (satellite and/or ground), jammed or nuclear disturbed links, node failure and destruction, and other perturbing factors. A series of experimental scenarios have been developed to examine the impact on such sizing requirements as throughput and delay.

Emulator Experiments: An experiment begins with network traffic being initiated by a threat and sensor model that computes a time line

of sightings of threat objects at each node based on computed trajectories for approaching ICBMs. Currently, our emulator can handle up to 10,000 threat objects. A threat-message generator and a response-message generator are combined to form the message generation process. Each is implemented on a sensor platform. The former provides the threat object data to the latter, which, in turn, uses this information and other user-specified criteria to develop two-dimensional messages based on initial threat object visibility, three-dimensional track messages, and finally, weapons target-assignment messages. Note that the exchange of sensor messages within the network creates additional classes of messages having different requirements for distribution in order to accomplish the battle management function.

In addition to developing the threat model and the emulator itself, algorithms that control or manage the primary functions of the network were designed. These algorithms include link assignment, routing, flow control, and congestion control. These factors influence the network connectivity, traffic distribution, timeliness of message receipt, and network reconstitution under adverse conditions.

This emulator is being used as a tool to provide guidance to SDIO on the effectiveness of the Phase I design. Our approach is to perform sensitivity tradeoffs of the physical architecture and the networking algorithms that control its operation. Our fundamental goal is to provide those system tradeoffs that will allow for the development of a robust Phase I SDI baseline architecture.

This emulator structure is flexible and easily extensible to other large-scale complex networks. Modifications to the emulator are underway to increase its capability to allow for larger threat sizes, MIRVing of ICBMs, and nuclear weapons and error effects. The emulator development is a joint effort between NRL and Harris Corporation.

[Sponsored by SDIO] ■

Numerical Simulating, Computing, and Modeling

NUMERICAL SIMULATING, COMPUTING, AND MODELING

Reflecting the age of computers, much fundamental and applied research is performed at NRL around the Cray X/MP supercomputer and the ubiquitous desktop personal computer. This research includes simulation and modeling to interface with the Navy's real-world problems. Reported in this chapter is work on vector computors, the strategic scene generator model, spectral simulations of the solar corona, the Connection Machine, monopulse radar simulation, large-scale scenario tracking/correlation, and shape functions techniques.

The work presented here was contributed by the Laboratory for Computational Physics and Fluid Dynamics (4400), the Chemistry Division (6100), the Acoustics Division (5100), the Radar Division (5300), the Information Technology Division (5500), and the Space Systems Technology Department (8300).

Other current research in numerical simulation includes:

- Battle engagement area simulator
- Parallel and supercomputer technology
- Modeling of ocean radar signatures
- Neural networks
- Properties of ordered intermetallic alloys

An Algorithm for Calculating Intramolecular Angle-Dependent Forces on Vector Computers

J. H. Dunn
Research Computation Division
and
S. G. Lambrakos
Materials Sciences and Technology Division

In molecular dynamics simulations of systems consisting of polyatomic molecules, e.g., polymers or lipids, modeling the energy transfer between intermolecular and intramolecular (internal) degrees of freedom is necessary if accurate molecular parameters are to be extracted. Such detailed simulations are important to diverse Navy research projects. These include studies of drag reduction for Navy submarines, biological membranes, and microencapsulation. The success of these studies hinges on the Navy's ability to model accurately large groups of macromolecules. The task, then, is to formulate these problems so that they are computationally tractable. The aspect of this problem addressed here is the calculation of intramolecular forces.

Force Calculation: In molecular dynamics simulations, the force calculation for a particle can be separated into two parts: intermolecular and intramolecular. Intermolecular, or nonbonded, forces act only between particles in different molecules or particles in the same molecule separated by four or more intervening particles, that is, nonbonded particles. In the classical representation [1], intramolecular degrees of freedom are decomposed into four general types of interactions for which both *ab initio* quantum mechanical data and experimental data can be obtained. These interactions are bond stretching; bond-angle bending; torsion, which acts on 2, 3, and 4 linearly linked particles, respectively; and out-of-plane wag (which we will not consider). Although the calculation of bond-stretching is easily vectorized, i.e., the equations may be translated into computer code that takes advantage of vector processors on modern supercomputers, the vectorization of angle-bending and torsional force evaluations are inherently limited. These are due to the many-body nature of the forces, as well as the multiple linkage between particles. Further, the computational cost of evaluating angle-dependent forces is relatively high since these forces are noncentral and, therefore, require additional operations to evaluate their direction cosines.

Typical procedures for calculating the direction cosines of angle-dependent forces involve cross products. Cross-product procedures can be vectorized by using *gather-scatter* operations, which addresses the linkage problem by using linked lists; however, projection methods are still more efficient. Projection methods require fewer high-cost operations, e.g., square roots and division, and incorporate efficient programming structures for vector computation. Initial tests show factors of 7 and 1.4 increase in speed for the calculation of angle-bending and torsional forces, respectively, relative to a comparable cross-product formulation on a Cray X-MP.

Projection and Torsion: The projection method entails calculating vectors that are orthogonal either to other vectors or to planes in 3-space. This is done by selecting a suitable vector and subtracting its components that lie in the direction of the vector or in the plane in question. For example, an arbitrary vector could be projected out of the x-y plane by simply setting its x and y components to zero. This method is especially well suited to the Cray X-MP as it takes advantage of machine-coded Basic Linear Algebra Subprograms (BLAS).

The torsional force acts on groups of four linearly linked particles (Fig. 1). The torsional forces on particles 1 and 4 must be perpendicular to the planes (1,2,3) and (2,3,4), respectively. Therefore, the force direction may be calculated either by taking cross products between two vectors in the plane, e.g., the vectors directed from 2 to 1 and 3 to 2, or by projecting components of a

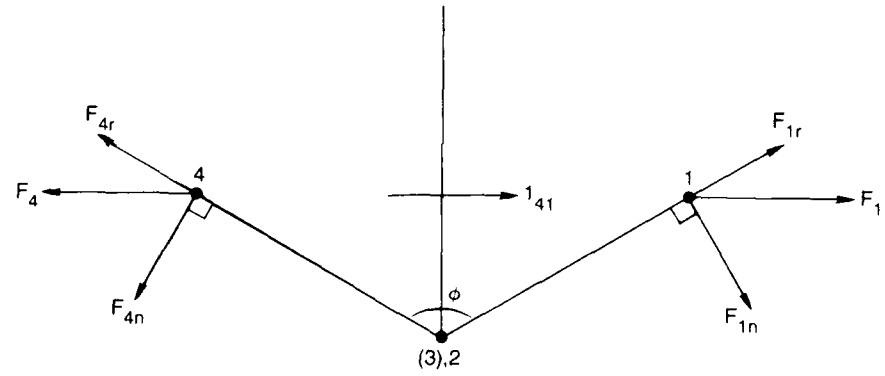

Fig. 1 — Four-body geometry for torsional force calculation

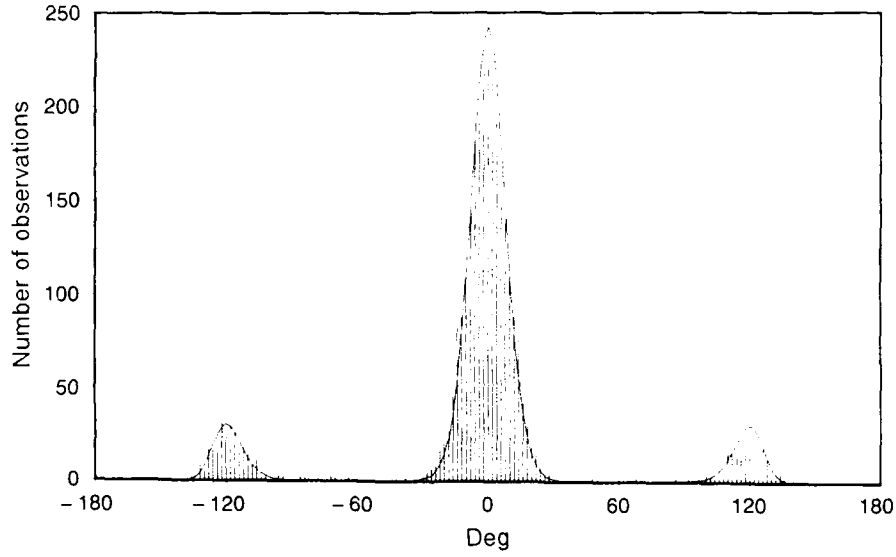

Fig. 2 — Dihedral angle distribution

suitably chosen vector out of the plane, such an $\mathbf{l}_{41}$, the vector pointing from particle 4 to particle 1 (Fig. 1). Thus the torsional force on particle 1 is

$$\mathbf{F}_{1n} + \mathbf{F}_1 - \mathbf{F}_{1r},$$

where $\mathbf{F}_1$ is the force magnitude times $\mathbf{l}_{41}$, and $\mathbf{F}_{1r}$ comprises the components of $\mathbf{F}_1$ that lie in the plane (1,2,3). The magnitude of the forces on the end particles, 1 and 4, is a function of the dihedral (torsion) angle ϕ between the planes defined by atoms (1,2,3) and (2,3,4) of the sequence (Fig. 1). Further, the forces on particles 2 and 3 are simple linear combinations of the forces on particles 1 and 4. It is fortuitous that the coefficients of these combinations are intermediate results of the projection calculation; therefore, these forces are very inexpensive to compute.

Molecular Dynamics Simulations: Two molecular dynamics simulations were conducted on a system representing the hydrocarbon C_4H_{10} (butane). The system comprised 144 butane molecules, and the bond angles and bond lengths were constrained by using the MSHAKE procedure [2]. The torsional potential was modeled by a cosine power expansion and is depicted, along with the dihedral angle distribution, in Fig. 2. The simulations were conducted to test the stability of the torsional force

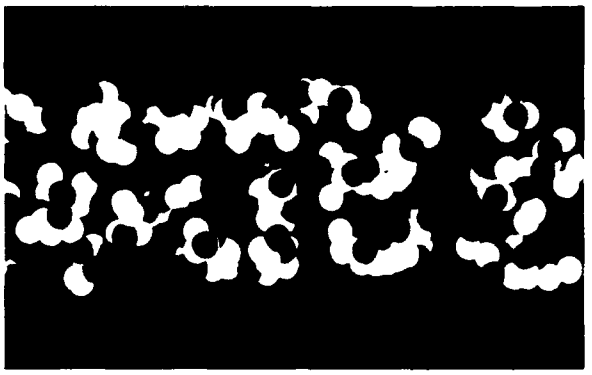

Fig. 3 — Simulated system configuration: green = CH_3 and yellow = CH_2

algorithm when used in conjunction with intermolecular potential and the constraint force algorithm. After an equilibration period, the dihedral angle distribution and total energy remained constant. Figure 3 shows the molecular configuration at 65,000 timesteps.

The development of new, fast algorithms represents a significant challenge to applied mathematicians. However, advances in numerical algorithms afford the Navy not only the ability to solve its present problems faster and more efficiently, but render previously unmanageable problems computationally tractable. The angle-dependent force algorithm is being incorporated into several molecular dynamics codes already on board at NRL, as well as serving as the basis for new simulation development. These codes will advance our understanding of microscopic systems as they apply to current Navy operational requirements.

[Sponsored by ONR]

References

1. E.B. Wilson, J.C. Decius, and P.C. Cross, *Molecular Vibrations* (McGraw-Hill, New York, 1955).

2. S.G. Lambrakos, J.P. Boris, E.S. Oran, I. Chandrasekhar, and M. Nagumo, *J. Comp. Phys.*, in press. ■

Strategic Scene Generation Model

H.M. Heckathorn, H. Gursky, and R.G. Groshans
Space Science Division

The Strategic Defense Initiative Organization (SDIO) needs to simulate the acquisition, discrimination, and tracking of targets and to predict the effect of natural and man-made background phenomena on optical sensor systems designed to perform these tasks. The Naval Research Laboratory (NRL) is developing such a capability, the Strategic Scene Generation Model (SSGM), that uses a computerized methodology to provide modeled data in the form of digital realizations of complex, dynamic scenes. The project supports research and development technology demonstrations and measurements programs by furnishing precomputed scenes and dynamic scene sequences for specific sensors, such as the Boost Surveillance and Tracking System. It also supports various hardware-in-the-loop system simulations of weapon systems by providing the software and databases needed by a user to specify and generate the digital images easily and rapidly. User-generated scenes represent large databases required by system test beds and development facilities for exercising and refining algorithms used in target acquisition, aim-point control, and defensive attack management.

The SSGM is designed to integrate databases and computerized phenomenological models to simulate strategic engagement scenarios and to support the design, development and test of advanced surveillance systems. Multiphenomenology scenes are produced from validated codes that are traceable to a consistent set of physical assumptions and conditions. The intent of SDIO, in part, is to use the SSGM to create traceable standards provided by the government to vendors for assessing system performance. NRL is, in fact, doing just that. We have provided scenes that are being used as part of the contractor selection process for an element of SDIO's Phase I

architecture. We are becoming a "Bureau of Standards" for SDIO test and evaluation.

Architecture: Viewer-perspective digital radiance maps, or scenes, are derived from the best available government standard models and databases through an interactive software system that selects the required input parameters and executes the pertinent models to generate the scenes specified by the user (Fig. 4). The multivariate output from these codes populates a run-time library that can be accessed quickly during frame generation. Run-time library files are subsequently cast into image elements that can be spatially and temporally resampled and combined to create multiphenomenology scenes. When the statistics of a random process can be specified from empirical data, the computed image elements can be modulated accordingly. Following frame generation, the composite scenes are stored as files in the scene library where they can be analyzed and displayed. When a user's purpose is to generate input databases for sensor or system models or for use in actual hardware simulations, certain features or events in a scene may trigger changes in the definition of subsequent frames. In this case the simulation interface feedback loop is invoked to modify the scenario library that drives the scene generation processes.

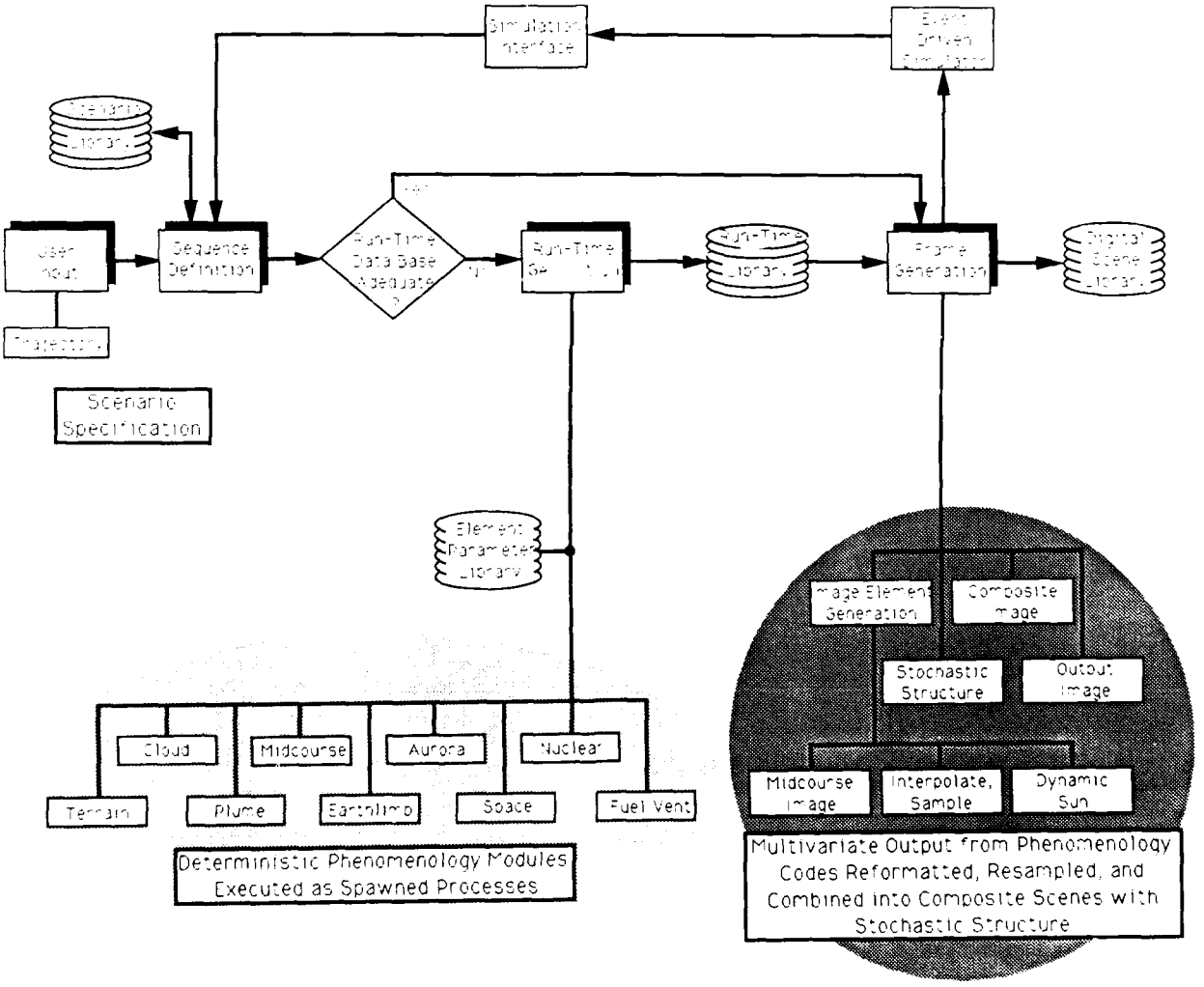

Fig. 4 — Strategic Scene Generation Model (SSGM) architecture

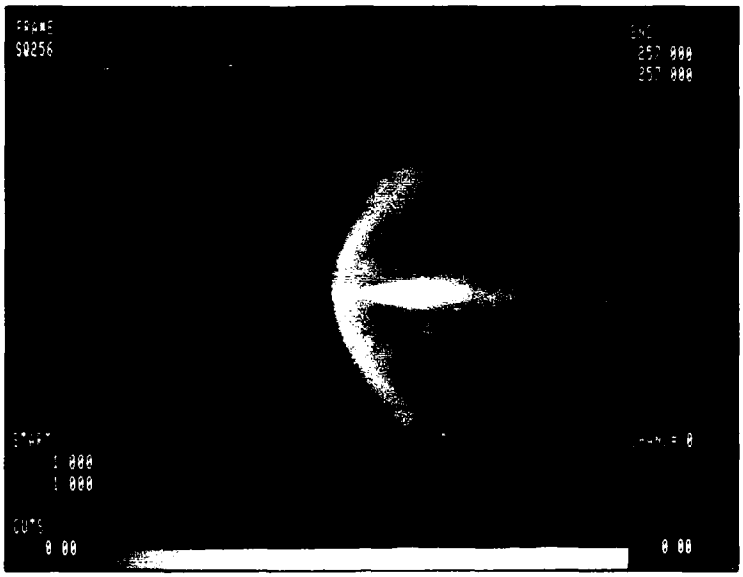

Fig. 5 — SSGM prototype output of a solid missile plume as seen from a space platform orbiting overhead. The background phenomenology includes ocean and altostratus clouds. The intensity scaling is logarithmic for this view in the short-wavelength infrared.

Phenomenology: The phenomenology consists of quiescent and enhanced natural backgrounds, and of perturbed backgrounds with imbedded targets and target-induced or related events. Backgrounds include earth terrain, opaque and semitransparent clouds, atmospheric scattering and molecular emission and absorption, quiescent atmospheric emission including airglow, the enhanced atmosphere with aurora and man-made nuclear perturbations, and celestial backgrounds. Target phenomena include missile bodies and plumes, fuel vents, postboost vehicles, decoys, satellites, etc. Endorsed and validated predictive models for these phenomena continue to be developed and refined by various government agencies such as NASA, DNA, AFGL, AFAL, and ASDC. NRL will rehost these standard codes or submodules within the SSGM architecture and will verify that the composite scene is an accurate rendition of that specified.

Within the limitations of the phenomenology models, the spatial, temporal, and spectral-sampling requirements are set by anticipated sensor system specifications and engagement scenarios. The SSGM architecture anticipates the use of active illumination of targets and missile plumes by lasers and allows limited interaction of phenomena where practical. Nuclear bursts, for example, illuminate terrain and clouds and may elevate earthlimb and auroral radiances by modifying atmospheric density.

Technical Challenges: An evolutionary approach is shown by the development of the SSGM that attempts, for the first time, to integrate the relevant phenomenology codes (which differ from each other in origin and level of sophistication) into a common architecture. The SSGM program must provide interim capabilities to meet current SDI requirements and simultaneously address configuration management issues relating to SSGM maintenance, augmentation, and traceability in an environment where the fundamental codes themselves are undergoing development. A prototype SSGM was completed and distributed to the SDI community in 1989. Figures 5 and 6 are sample output images generated with the prototype software that will evolve into a fully functional capability by 1992. The SSGM program also provides a basis for NRL

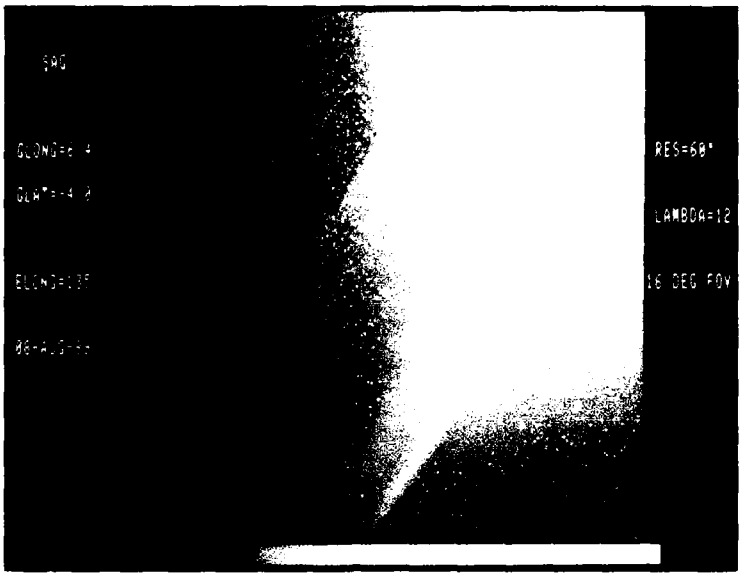

Fig. 6 — SSGM prototype output of a long-wavelength infrared celestial scene in Sagittarius. The modeled phenomenology includes galactic stars, galaxies, and the diffuse, banded emission from zodiacal dust within the solar system. The sun, 135° from the image center, is outside of the 16° x 16° field. The image resolution is a half-meter diffraction-limited optical system, and the intensity scaling is linear.

scientists to develop advanced techniques of image processing and analysis, and the management of large data sets.

[Sponsored by SDIO] ■

Three-Dimensional Spectral Simulations of the Solar Corona

R. B. Dahlburg
Laboratory for Computational Physics and Fluid Dynamics
and
S.K. Antiochos
Space Science Division

Background: One of the most challenging theoretical problems associated with the sun is the explanation of why the temperature of its corona is so much higher than that of the atmosphere immediately below it. Although several explanations have been given for this phenomenon, it is now generally believed that the high temperature of the solar corona is due to the transformation of magnetic energy into heat energy. The exact way in which this occurs is still a matter of dispute; theory and observation have suggested several likely candidates.

Numerical simulations play an important role unraveling this mystery, since they can be used to supplement observation and experiment. The relevant physical processes are postulated to occur on a spatial scale too fine to be resolved by the present generation of instruments. Furthermore, observations cannot provide simultaneous, pointwise measurements of important variables, such as the vector velocity field, the vector magnetic field, and the pressure and density fields. Theorists generally assume that the corona can be modeled as an electrically conducting fluid. The resulting nonlinear partial differential equations, called the magnetohydrodynamic (MHD) equations, are so complex that most problems are analytically intractable.

We are using numerical simulations to supplement the above activities. For simple geometries and somewhat restricted regions of parameter space, numerical simulations can

furnish information about the interaction of large and small spatial scales, provided the small scales are computed with as much exactness as the large spatial scales. Information about primitive variables and also derived quantities is available at every timestep. Furthermore, numerical simulation is the preferred tool for examining systems of equations that are too complex to integrate analytically. In this way, numerical simulations can serve as a check and guide for both theory and observation.

Model and Simulation: We have been pursuing a program of numerical simulation of electrically conducting fluids aimed at examining various coronal heating hypotheses. We have developed several new advanced numerical techniques that are applicable to many turbulence problems of interest to the Navy and the nation. To model numerically the processes involved in heating the corona, we developed *MHDCHAN*, the first fully spectral, three-dimensional channel code for magnetohydrodynamic problems. *MHDCHAN* extends a successful Navier-Stokes model to the case of electrically conducting fluids [1], and it is an improvement over our earlier *MHDBOX* model [2] by including boundary conditions more relevant to the solar atmosphere. The code simulates the stressing of the coronal magnetic field by underlying photospheric motions. Such processes are believed to be responsible not only for coronal heating but also for prominence formation.

Figure 7 shows the magnetic field lines that illustrate the results of a typical numerical simulation. We begin with a two-dimensional, infinite-dipole magnetic field subject to twisting by a smooth photospheric flow applied at the lower boundary. Figure 7(a) shows the system after one characteristic time. At this time the effect of the twisting on the magnetic field lines becomes apparent. Figure 7(b) shows the same system after

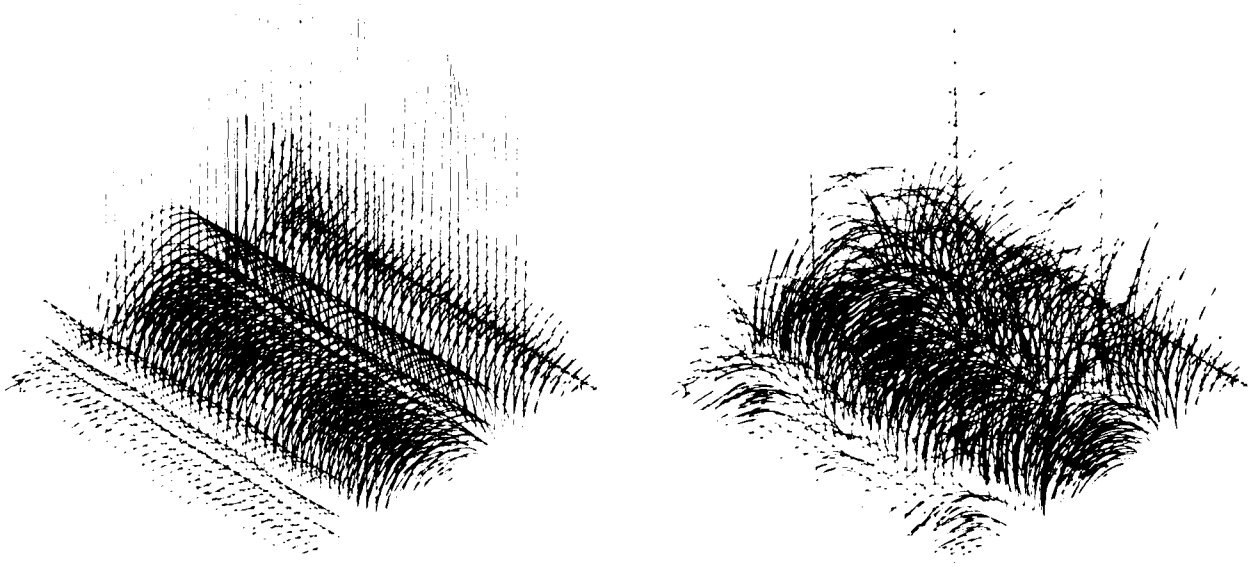

(a) (b)

Fig. 7 — These plots show magnetic field lines for a coronal heating calculation using our *MHDCHAN* code. (a) The field lines after one characteristic time, where the influence of the smooth photospheric flow pattern imposed at the lower boundary is beginning to be evident. (b) The magnetic field after 50 characteristic times. "Ballooning" and twisting of the field are evident. Most important, at no time do we see evidence of electric current sheets forming in the interior, implying that either more complex magnetic topologies or more complex photospheric flow patterns are required to heat the sun's corona.

50 characteristic times. Note that the field lines have "bowed out" in response to the applied twisting and also that we see no evidence of electric current sheet formation.

Implications: The study of solar MHD has led to discoveries with more widespread application. For example, magnetic reconnection and radiation-driven thermal instability, both identified in the solar context, have been applied to problems of interest in confined magnetic fusion. Hence solar physics is not only valuable for expanding our knowledge of the sun, but also because it gives us insight into important physical processes that are significant, albeit perhaps more concealed, in other systems. The same remarks apply to the development of new numerical technology for simulating bounded magnetofluids, as described in this article. Such techniques are useful for investigating, for example, confined magnetic fusion, MHD power generators, and MHD boundary layers.

[Sponsored by ONR and NASA]

References

1. T.A. Zang and M.Y. Hussaini, "On Spectral Multigrid Methods for the Time-Dependent Navier-Stokes Equations," *Appl. Math. Comp.* **19**, 359 (1986).

2. R.B. Dahlburg, J.P. Dahlburg, and J.T. Mariska, "Helical Magnetohydrodynamic Turbulence and the Coronal Heating Problem," *Astron. Astrophys.* **198**, 300 (1988). ■

Investigating the Potential of Parallel Processing

H. F. Webb
Acoustics Division

Two years ago, the Naval Research Laboratory (NRL) established the Connection Machine Facility to investigate the uses of parallel computing for scientific research and Navy signal processing applications. This facility, the first experiment of its kind in the Department of Defense, represents a major investment in this promising new approach to high-performance computing. Enthusiastically taken up by a wide variety of users, it is already allowing them to look at problems previously beyond their reach.

Large-scale computing needs, whether for theoretical science or operational Navy signal processing applications, continue to grow at a dazzling rate. One highly promising approach for fulfilling these needs is massively parallel computation, a technology still in its infancy. In 1987, NRL initiated a major thrust to investigate the potential of parallel computation by establishing a hands-on laboratory built around an advanced parallel computer, the Connection Machine.

The Connection Machine Facility: The Connection Machine is a massively parallel supercomputer consisting of up to 64K individual processing units that perform operations in unison on large data sets. In 1987, NRL collaborated with DARPA/ISTO to obtain a prototype CM-1 with 16K processors from the manufacturer, Thinking Machines Corporation. In March 1988, NRL, again with assistance from DARPA/ISTO, obtained a production CM-2 with hardware floating point and 16K processors. Both of these purchases were DoD firsts. The NRL Connection Machine Facility also consists of several serial front-end computers that provide the software interface to the Connection Machines. A team of NRL experts on parallel computation brought the facility on-line during the past year, networked the CMs for remote access in March 1988, well before the rest of the community, and is constantly improving the facility to make it more accessible to users. This includes hardware modifications, software tool development, and working with Thinking Machines Corporation on the implementation of a repertoire of programming languages. These languages range from Fortran

8x, which requires no special parallelization by the user, to C/PARIS (C, with a PARallel Instruction Set), which lets advanced parallel programmers control which processors act on which data sets.

Applications: A goal of the NRL team was to make the facility easily accessible to a wide variety of users nationwide. This provides some insight as to how parallel computing fares over the whole spectrum of computing requirements, and also provides the scientific communities with a self-bootstrapping learning laboratory in parallel computation. This approach is paying off handsomely. To date, well over 500 individual investigators from 40 government and academic institutions have experimented in using the facility to tackle problems that take a prohibitively long time to solve when using conventional serial computers. Some of the problems undertaken are advanced weather prediction models, a large-scale Monte Carlo simulation, and 3-D underwater acoustic propagation. As a rough comparison of gains achievable, to date experience indicates that many algorithms, once adapted to parallelism, run 10 to 25 times faster than on a commercial high-speed supercomputer.

Figure 8 shows a 3-D acoustic field produced at NRL by the Connection Machine Facility. The underlying algorithm that includes performing integration involving complex arithmetic runs extremely fast on the Connection Machine because of the computer's high-speed parallel input/output capabilities, and because the algorithm is naturally highly parallel.

Figure 9 shows the results of colliding galaxies as an example of an algorithm that, once parallelized, can be solved very quickly. Although not mathematically complex, the task of keeping track of the mutual influences of over 500 stars is extremely slow on serial computers. On the Connection Machine, however, the calculations are performed fast enough to allow the galaxies to spin in real time.

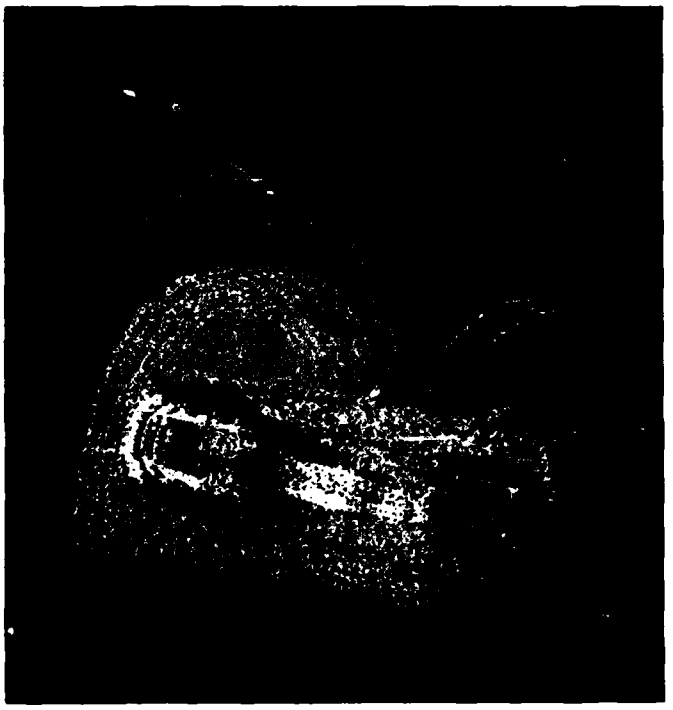

Fig. 8 — 3-D acoustic field. Program by Edward Jennings; graphics by Eric Hoffman.

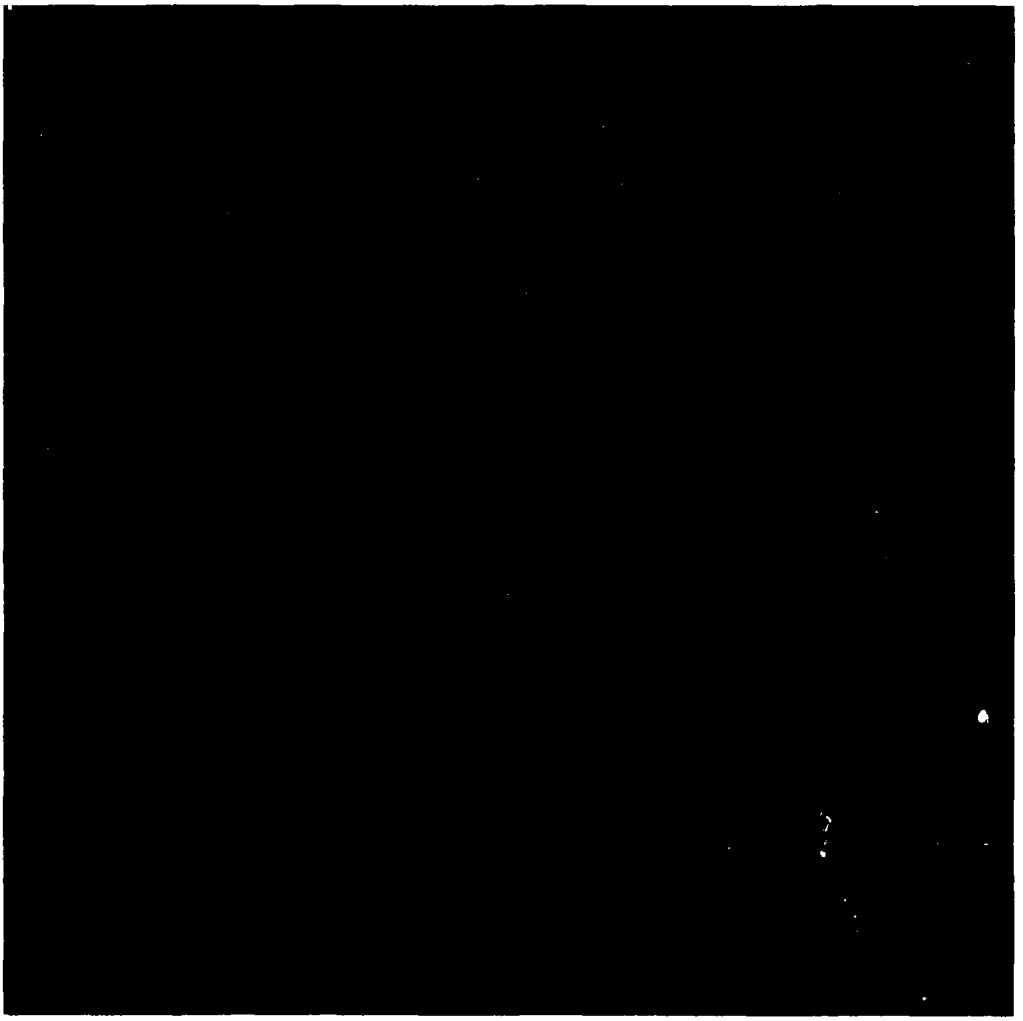

Fig. 9 — Colliding galaxies. Program by Paul Hertzen.

The success in parallel computation achieved by the Connection Machine Facility and the enthusiasm of the community for the learning laboratory approach give good reasons for optimism regarding both the potential of massively parallel computing and the speed with which we may reasonably expect to see it become a standard technique in large-scale computation. People wishing to use the Connection Machine Facility may write to Dr. Hank Dardy, Code 5153, Naval Research Laboratory, Washington, DC 20375-5000 or send electronic mail to the following address: dardy@ cmvax.nrl.navy.mil.

[Sponsored by NRL, ONR, DARPA] ■

Generic Monopulse Radar Simulation

C.-T. Lin
Radar Division

In the fields of electronics warfare technology and new radar development, it is essential to know how a radar sensor performs in natural and electronic countermeasure (ECM) environments and to identify whether the effectiveness of a proposed countermeasure (CM) is the result of a radar system peculiarity or a basic limitation of the radar design.

A generic monopulse model is being developed and actively used at the Naval Research Laboratory to demonstrate monopulse tracking

performance in various study aspects. The model performs target tracking runs, as a function of time, similar to actual radar tracking against modeled finite-size targets on a given trajectory. In experimental measurements, cause and effect are difficult to separate; oppositely, the monopulse radar simulation can turn on or off any environment available. Various monopulse radars can be modeled against different acquisition/tracking scenarios of interest. The monopulse locks on a target in range and angle to perform closed-loop tracking with range gates and monopulse-antenna sum and difference beams. Loss of track can be caused by CM, severe environmental conditions, target scintillation, or weak signal levels caused by small cross-section targets and/or long range. The generic monopulse model is sufficiently detailed to provide selection of a wide variety of antenna feeds with response to both normal and cross-polarization signals, complex targets with selectable size and configuration, most known deception CM, low-angle multipath, noise, chaff, and ocean surface clutter.

Monopulse Radar Model: A tracking radar typically measures target azimuth and elevation relative to its antenna beam axis and time of arrival of its echo relative to a range gate. Figure 10 shows how this information is used to close tracking loops. This monopulse-model example is a typical X-band, pencil-beam, tracking radar with approximately 1° beamwidth. It is a three-channel (sum, azimuth difference, and elevation difference) monopulse with a product-type angle-error detector [1]. It includes automatic gain control (AGC) that uses a control voltage generated from the detected sum signal and fed through a low-pass filter. The filter adjusts the AGC loop gain and bandwidth, and its output voltage controls the gain of the three receiver channels. A plot of relative AGC voltage is generated and used as a measure of signal level. An early-late gate range discriminator is used in the range tracking loop. The finite-size complex target consists of five scatterers that have different magnitudes and varying phase rates to represent target scintillation.

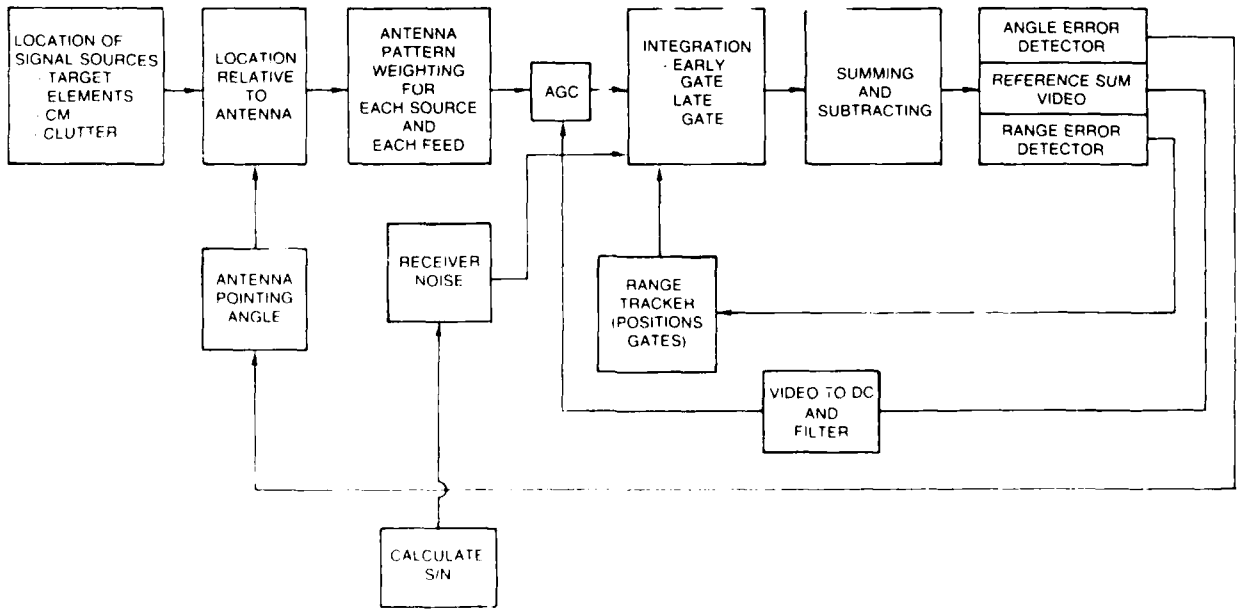

Fig. 10 — Monopulse radar modeling

Simulation Capabilities: Monopulse tracking performance in natural environments must consider the multipath and sea clutter effects, particularly in low-angle track. Sea clutter falling within the radar resolution cell has a specific angular location and finite extent and must be represented by a distribution of reflectors at the sea surface. Simulations demonstrate that strong clutter can move the average track toward the ocean surface. Multipath is modeled in detail and provides an exact mirror image of the target reflector configuration. It includes a detailed curved-Earth model of the sea-reflection coefficient with selectable sea state and inclusion of shadowing effects. Figure 11 illustrates a monopulse track in elevation for a complex target flying a typical trajectory. The severe almost periodic multipath error is observed. The more rapid error fluctuation occurs during target dives because of the more rapidly changing relative phase between target and image. The multipath error exhibits the random fluctuations of target elevation-angle, scintillation, and a shift in the average tracking point toward the sea surface.

The generic monopulse radar simulation has also demonstrated its capability in modeling basic noise-source and repeater CMs and some counter-countermeasure techniques. Examples include assessment of track performance against chaff, towed or forward-fired expendable decoys, and standoff jammers (SOJ). It illustrated the capability of the ECM to capture the radar track and the reacquisition of the target after expendable turn-off, or operator intervention. A simple leading-edge track was also demonstrated to show how it can prevent range-gate pull off by the expendable. The SOJs are modeled by scatterers collocated in azimuth and elevation having random-phases and Raleigh-distributed magnitudes that are independent of their ranges to the radar. A monopulse radar may track this continuous noise source in angle on a side lobe lock-on point that can be in a direction near the target either toward or away from the jammer.

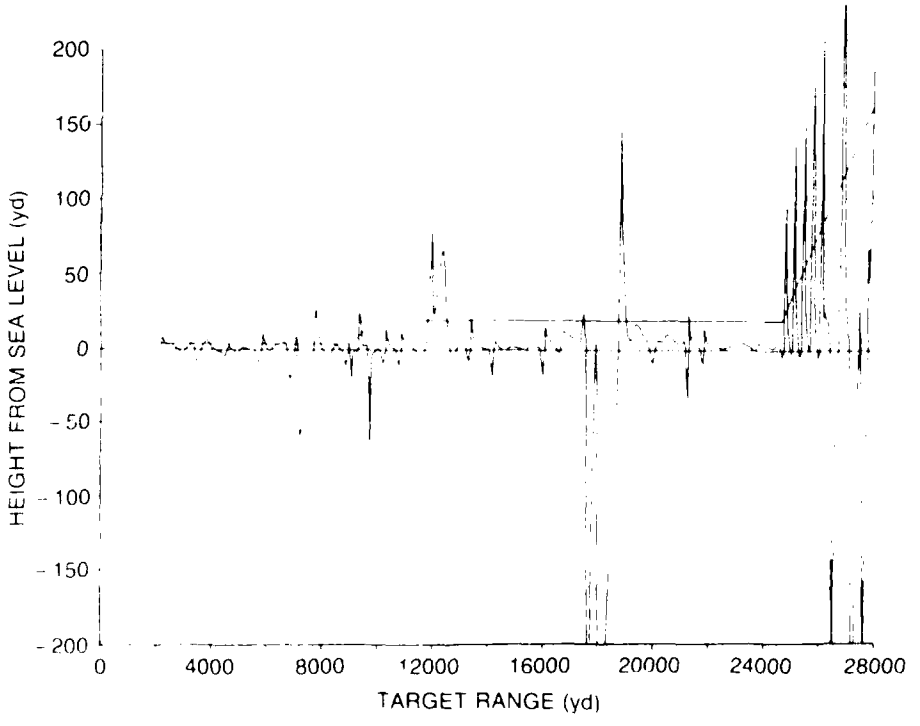

Fig. 11 — Simulation demonstrating low-angle track

In the ECM modeling, deception jamming sources can also be present along with the sources used as elements of the target. In the monopulse simulation, these jamming sources may be located relative to the target as desired and adaptively controlled in amplitude, phase, and delay-time to model, for example, fixed or modulated cross-eye, range-gate pull off, AGC stealer, cross-polarization, or blinking.

Conclusion: The generic monopulse model with its demonstrated capability offers a very convenient and economical means for assessing radar performance in a wide variety of operational scenarios. It is also a means for examining the performance of unavailable radar by using intelligence information about their characteristics.

Acknowledgment: Dean D. Howard, of Locus, Inc., made significant contributions to this research.

[Sponsored by NADC and NTIC]

Reference

1. C.T. Lin and D.D. Howard, "Track Performance Considerations for Monopulse Radars," NRL Report 9119, June 1988. ■

REAL Approach to Tracking and Correlation for Large-Scale Scenarios

J.B. Collins and J.K. Uhlmann
Information Technology Division

Introduction: Since the introduction of computing, research efforts have resulted in a variety of numerical tools that can track and correlate small numbers of objects to a high degree of precision. The application of this technology to scenarios that involve large numbers of objects has revealed that important algorithmic issues must be addressed. Specifically, it can be shown that the straightforward application of traditional tracking and correlation methods to scenarios consisting of N objects can lead to a computational effort proportional to N^2 or even N^3. For example, to track 10^4 objects, these approaches would require at least 10^8 to 10^{12} times the computation time required to track a single object. In response to this serious scaling problem, we have developed a general approach to tracking and correlation that maintains the same degree of tracking precision but incurs a computational expense that will always scale between $O(N \log N)$ and $O(N^2)$.

The REAL (Real-time Engagement Analyzer/Locator) project began with the goal of constructing a general tracking and correlation system with efficient worst-case scaling (less than $O(N^2)$) without sacrificing accuracy. The result is a modular system consisting of three principle components: (1) state estimation and filtering, (2) coarse assignment (i.e., gating), and (3) assignment. The result is fully extendable in terms of the dimensionality of the measured and estimated states for general multisignal processing applications. The approach requires only that compact volume be defined by the correlation or association measure for each state.

State Estimation and Filtering: Standard least mean square (LMS) filtering technology is employed to iteratively construct trajectory estimates from measurements received at semiregular intervals. (Although a scan period in which approximately one and only one report is received for each object (or signal) has been assumed for most tests, it is not a necessary condition to perform effective tracking and correlation.) Important functions of the filter include projecting state estimates to a given time and calculating the likelihood of association (or association weight) of a state estimate with a given measurement.

Coarse Assignment: Coarse assignment is primarily a preprocessing operation for eliminating infeasible (defined by a given probability threshold) association pairings of state estimates with measurements. This is accomplished by approximating trajectories over a given

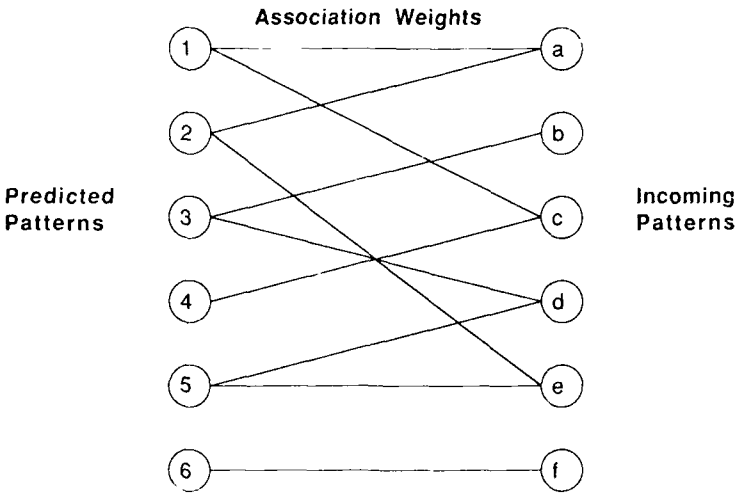

Fig. 12 — Coarse assignment generates a weighted bipartite graph of association weights (edges) between expected states (vertices 1–6) and measured states (vertices a–f)

time interval with a series of boxes. The process of finding feasible associations can then be transformed from a difficult problem in probability space to the relatively simple geometric problem of finding intersections of trajectory boxes and measurement boxes. Boxes are used to approximate more complicated volumes because they facilitate the use of optimal search algorithms that do not scale quadratically (the scaling required to compare each state estimate to each measurement) with the total number of boxes. In addition to a significant reduction in computational complexity, this operation also minimizes the number of potentially costly association weight calculations (Fig. 12).

Assignment: The gating procedure generates a weighted bipartite graph in which the state estimates and state measurements represent two disjoint sets of vertices and the candidate association weights that are above the gating threshold represent the weighted edges. The purpose of the assignment algorithm is to determine from this graph the subset of edges that represent correct associations and for which updated state estimates should be made. Many traditional approaches are based upon variations of the maximum weighted bipartite matching. They consist of finding a subset of edges, no two of which have a common vertex, whose associated weights have the maximum sum. Under certain conditions, these approaches are very accurate in their ability to identify correct associations. Unfortunately, besides large computational complexity ($O(N^3)$), the conditions required for good performance from these algorithms are often not satisfied (Fig. 13).

The assignment method employed by REAL derives a measure of logical independence for each state estimate from the structure of the graph. This independence measure provides an estimate of the amount of computational effort that would be required to unambiguously resolve the trajectory to which the state estimate corresponds. This provides a means for optimizing the use of available resources by amortizing the effort so that real-time performance constraints can be satisfied.

Performance Results: Tests to date show that 30-min strategic defense initiative (SDI) scenarios consisting of 65+ objects and 5 s scan periods can be processed in real time (including cold-start track initiation) on a SUN workstation when the probability of detection is high and the objects are relatively well separated.

When the objects are densely clustered, the process of initiating new tracks must be amortized over more scans to maintain real-time processing.

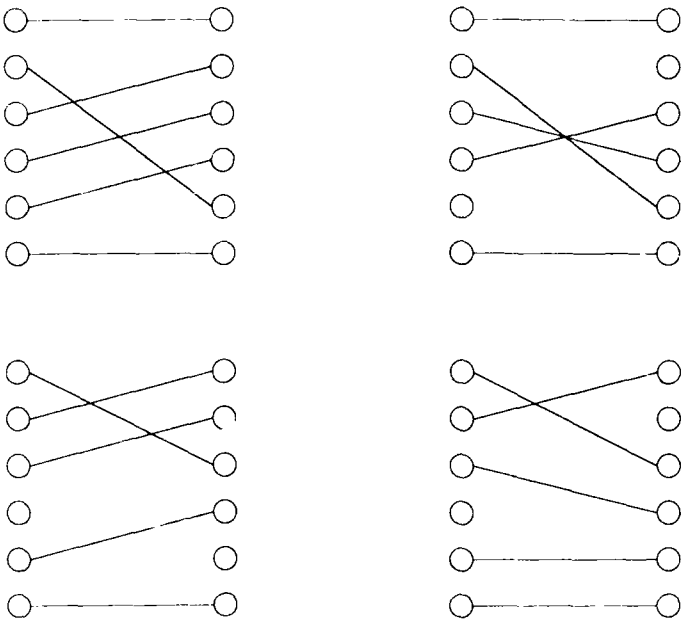

Fig. 13 — Final assignment of the measurements to logical representations of the objects requires consideration of the independent ways that an assignment may be made. These are four possible ways, based on Fig. 12, of marking global assignments so that each vertex of one set is assigned to only one vertex of the other set.

Thus, some estimates of trajectories at any given time during the scenario will be calculated from a shorter measurement history than others. This may result in some loss of estimate accuracy, but it permits the process of tracking and correlating to degrade gracefully in terms of computation time as the difficulty of the tracking environment increases. Tests also reveal that even with a sophisticated gating algorithm, the bulk of the total computing time is spent in the calculation of associations for state-estimate/measurement candidate pairs. This is true even when the size of the scenario is scaled to thousands of objects. Preliminary calculations suggest that components of the program that scale nonlinearly will not begin to dominate computationally even when the size of the scenario approaches 100,000 objects.

In sum, we have found that fundamental algorithmic problems that may easily arise in monitoring many objects can indeed be overcome and make it possible to effectively automate such tasks. Such tasks might include SDI surveillance, ocean surveillance, or monitoring maneuvering aerial objects. As the complexity of the objects increase, these tasks verge on robotic visual processing. Automating these tasks is of great interest to both military and civilian sectors.

[Sponsored by NRL and SDIO] ■

Shape Functions for Invariant Image Recognition

S. B. Gardner
Space Systems Technology Department

Many space technology applications require the automated recognition of visual targets within a broad field of view. In the human visual system, shape plays a major role in object recognition. We describe a method of invariant image recognition based on shape functions. The shape-function method is used to transform a closed contour into a scalar waveform. Since the magnitude of the Fourier transform of a shape function is scale and rotationally invariant, Fourier transforms of shape functions can be used to encode invariant feature

vectors. Near-term applications of the shape function method implemented with very-large-scale integration (VLSI) fast Fourier transform (FFT) chips, or digital signal processing (DSP) coprocessors, offer a potential for rapid image search and target recognition in satellite imagery [1,2].

Shape Functions: Shape information can be used in the construction of feature vectors for scale and rotationally invariant contour recognition. To compute the shape function, we start with a closed contour and select a centroid. The shape function is then defined as the distance from the centroid to the contour measured as a function of distance around the perimeter suitably normalized by the average size.

As an illustration of the shape-function process, Fig. 14 shows two aircraft shape contours with their corresponding shape functions. Figure 14 shows the aircraft shape functions measured from the aircraft nose (top). Individual features of each aircraft, such as the engines, can be clearly identified in the shape functions.

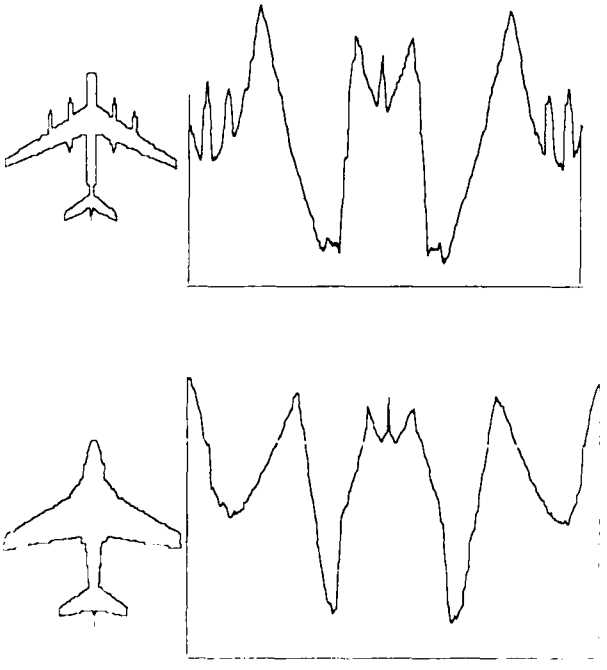

Fig. 14 — Aircraft contours and shape functions

We illustrate how LANDSAT data can be coded into a scalar function that characterizes the contour (outline) of an object after posterization and tracing between gray levels. The LANDSAT image is first posterized (quantized in gray level) and traced to obtain contours. Figure 15(a) shows a LANDSAT image that has been posterized to 1 bit (black/white). Figure 15(b) shows a trace of the image that contains a large number of individual contours. Figure 16 shows two LANDSAT data contours and their corresponding shape functions.

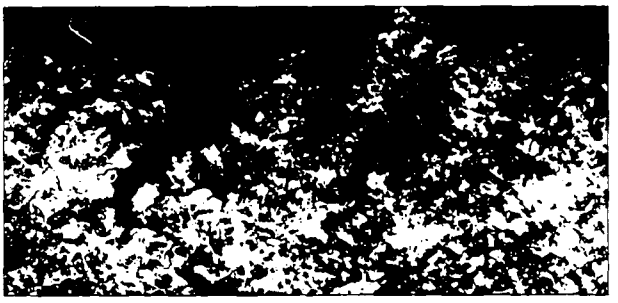

Fig. 15(a) — Single bit posterization of a LANDSAT image

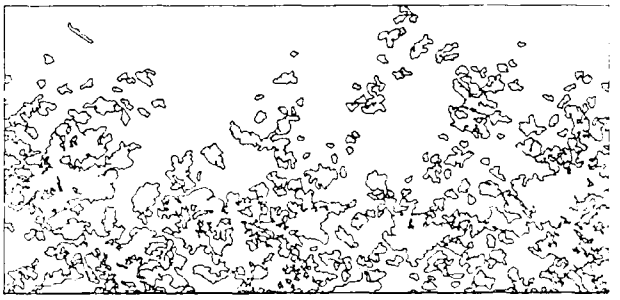

Fig. 15(b) — Trace of the LANDSAT image

Architectures and Algorithms: One of the advantages of the shape-function approach to image recognition is a potential reduction in computational complexity. Because of the unknown orientation of a target in a field of view, automated image recognition requires a rotational invariance in the image recognition algorithms. Straightforward approaches require template matchings that are too slow for many real-time applications. Since the magnitude of the Fourier transform of the shape function is rotation invariant, the Fourier transform magnitude

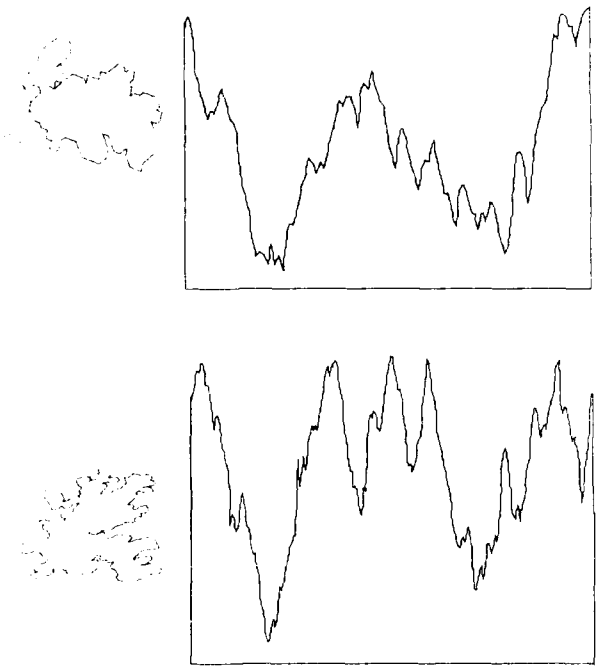

Fig. 16 — LANDSAT contours and shape functions

coefficients form a natural set of invariant features that can be used for coding a feature vector. The shape function method is well suited to real-time applications that require special purpose hardware, such as VLSI array processors implementing FFT algorithms. Shape function algorithms can also be simulated on a wide variety of current parallel computers (e.g., a Hypercube or a Connection Machine).

In the future, massively parallel computers based on neural network architectures will become available. To date, training of neural network computers based on popular learning algorithms such as backpropagation has been slow. Faster methods of unsupervised learning based on modified Hebbian algorithms are being developed [3]. In the future, when neural network computers become widely available, we expect that shape functions and their transforms may prove to be an effective method of image coding for invariant recognition.

[Sponsored by SPAWAR]

References

1. S. Gardner, "Neural Networks for Data Compression and Invariant Image Recognition," NASA International Workshop on Visual Information Processing, Williamsburg, VA, May 10-12, 1989.

2. S. Gardner, "An Approach to Multisensor Data Fusion Based Upon Complex Object Representations," Proc. 1988 Symposium on Command and Control Research, U.S. Navy Postgraduate School, Monterey, CA, June 1988.

3. T. Sanger, "Optimal Unsupervised Learning in a Single-Layer Linear Feedforward Neural Network," *Neural Networks* **2** 459 (1989). ■

Library-based Microcomputer Support Services

L. E. Stackpole
Technical Information Division

One place to go for all kinds of information. An impossible goal? Perhaps, but at the Naval Research Laboratory (NRL), 1989 brought that goal a little nearer to reality.

For over 60 years, the Ruth H. Hooker Technical Library has served as a focal point for meeting the information needs of the researchers and administrators at NRL. Underlying the Library's success as an information provider is its extensive research collection of books, journals, and reports selected for relevancy to the NRL mission and areas of interest. In 1987, in a major departure from its almost exclusive reliance on print media, the Library began to consider adding microcomputer software to the types of material with which it deals.

The impetus for expanding the library collection and services into the microcomputer software area was a proposal by an NRL researcher to the Laboratory's Computer Policy Panel that the Library purchase software for employees just as it purchases books and journals. Although such expanded procurement authority was not granted, once the Library's role in supporting Laboratory software needs was

addressed, several avenues for improving software availability and facilitating its implementation and use became evident. The first of these to be pursued was a software lending program, paralleling the circulation of bibliographic materials. A concurrent effort was the expansion of reference services to assist users in the identification and selection of microcomputer software for particular types of applications. After a period of planning and implementing, the Library opened a fully equipped and staffed Microcomputer Software Support Center that serves as a one-stop facility to address all facets of microcomputer software support.

Lending Software: In July 1988, the Library added commercial software packages to the materials it lends to Laboratory staff, starting with 10 of the most popular programs for IBM-compatible computers. This was a new approach for the Library in meeting Laboratory information needs arising from the increasing use of microcomputers for both office and research applications. Getting software into the hands of the users so they can test and evaluate it on their own machines is a major step beyond earlier Library efforts to provide staff with information about software through the purchase of relevant materials and searches of computerized databases covering the computer field.

Underlying the circulation of software are a number of carefully worked out controls and procedures to assure that the rights of the software publisher are properly observed and to provide the user with assurance that the software is complete and safe for use. Prospective users are asked to register as software borrowers by signing an agreement not to make or allow others to make copies. While the software may be copied to a hard disk for test and evaluation, any such copy must be erased before the package is returned to the Library. Upon returning the software, each user verifies in writing that no other copy exists. After each circulation, the software is checked for viruses using two types of antiviral programs, one that checks for specific viruses and the other that checks for changes in the disk by comparing it to the original. The computer used for checking has no hard disk so could not itself become infected.

At first, the software purchased for circulation were the more popular office-automation types of programs: word processing, spreadsheets, graphics, and database programs. It quickly became evident that NRL users were perhaps even more interested in having scientific software available for evaluation as well. Model simulation, mathematics solvers, neural computing, optical design, pattern recognition, and signal processing programs were soon added.

About 6 months into the program, all registered software borrowers were surveyed on their satisfaction with the lending program. Eighty users responded to this survey: 49 rated the program as excellent, 30 as satisfactory, and 1 as poor. Fifty-six believed the capability to "try before you buy" had saved them money. All recommended that the Library continue the program. A large number of respondents included comments on specific ways they had benefitted from the program. Many were variations on the theme that by testing and evaluating software they had avoided making inappropriate purchases and had saved both money and staff time they might have otherwise spent in implementing an unsatisfactory program.

By January 1990, the lending collection had grown to over 300 packages and included both IBM-compatible and Macintosh software. Lending services, which were originally limited to NRL employees, had been extended to the Office of Naval Research and to NRL on-site contractors as well. Over 400 users had registered as software borrowers. During calendar year 1989, there were 1,590 loans of software for test and evaluation purposes (Fig. 17).

Specialized Software Information Services: Lending software is an important first step in assisting users to identify the best available package for their particular needs. Although the

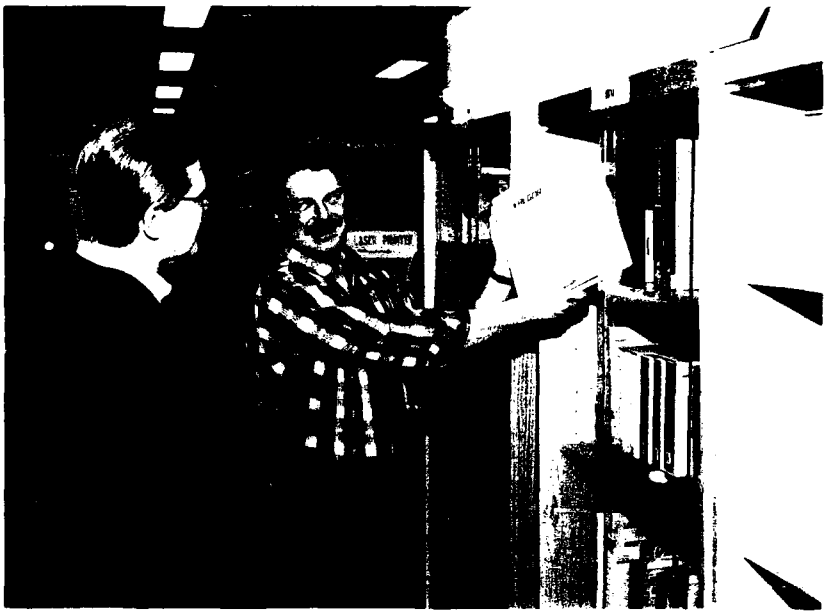

Fig. 17 — Dr. Terry Royt, of the Applied Optics Branch, is assisted by Laine Howell of the Microcomputer Software Support Center in selecting software for test and evaluation from the more than 300 packages available from the NRL Library for test and evaluation

Fig. 18 — Center manager, Dennis Blakey, searches an in-house database indexing and abstracting scientific software for Dr. Herbert Gursky, Superintendent of the Space Science Division

library reference staff were conversant in using existing catalogs and manuals and in searching online databases for software information, users appeared to need to interact with someone who had extensive microcomputer experience and who could serve as an advisor, or software "guru." In October 1988, the Library took advantage of an existing Research Computation Division contract to bring such a person on board to serve as the principal contact for users requiring software information and to participate in the planning for future support services.

To provide users with quickly accessible software information, a CD ROM product, which indexes over 130 computer publications and provides full text of the contents of some major magazines, was introduced. This product is available to end-users and is also used by Library and contract staff to respond to inquiries about particular software packages or types of products. In addition to descriptions of particular programs, evaluative articles that compare and rate packages with a similar purpose can be quickly located to assist in selection.

To meet the need for information about scientific software, which is not always readily available, the staff created an in-house database, called the scientific software database (Fig. 18). To lay the foundation for this database, various catalogs and directories were searched, and commercial vendors, government facilities, universities, and laboratories were contacted for current information on scientific software they had developed. The database indexes and in many

Fig. 19 — The Microcomputer Software Support Center features IBM-compatible and Macintosh user work stations. In the foreground are specialized newsletters and publications covering the microcomputer industry.

cases abstracts the information content of over 3000 vendor brochures. The brochures themselves are all on file and can be retrieved by a database search. Such searches have assisted users in identifying and selecting software in such diverse research areas as civil engineering, chaos, linear analysis, chemical structure modeling, optics, and neural systems.

An additional information source in the form of newsletters issued by computer user groups, software manufacturers, and industry associations was introduced to help users stay abreast of the software field. This information complements the more formal publications that have traditionally been part of the Library collection.

Microcomputer Software Support Center: Providing a one-stop location where users could get information about and assistance in using software was a part of the Library's overall plan from the start, but space limitations made this seem a distant goal. However, in late 1988, a change in program priorities and space allocations freed a computer room located within the Library. With a place to put a microcomputer center, the Library, with its contractor staffing, began to design a facility, order equipment and furnishings, and plan for expanded services.

The Center opened for business with a ribbon cutting by NRL's Commanding Officer, CAPT John Donegan, on 7 September 1989. Located in Room 348 of Building 43, the new Center offered IBM-compatible and Macintosh workstations for on-site use of software, a CD ROM user station for information searches and downloading of public domain software, a video station with software tutorials for individual or group use, a microcomputer for searching the scientific software database, and IBM and Macintosh virus-checking stations (Fig. 19). The staff

dedicated to Center activities and support of the lending program had now grown to three: a manger, a program administrator, and a technician, plus a summer student for data entry, and clerical support. A few months later, as workloads increased, an additional person was added to serve as the primary user contact for advice and training.

The Center was planned to assist NRL staff with the entire spectrum of needs associated with the use of microcomputers in a research environment. Added to the existing information services that had been developed to support the lending activity were now a user evaluation lab, expert assistance, and instructional capabilities. To address a need that had become evident as Center staff became identified throughout the Laboratory as software experts, field support services were introduced. Users can now ask for help in their offices to solve a variety of software-related problems, including configuration and setup, disk recovery, and virus checking. Additional services include vendor demonstrations and the showcasing of new equipment. Under consideration is a role for the Center, not fully defined, in facilitating software procurement through consolidated upgrades, bulk purchases, or site licenses. Center activities planned for the immediate future include a bulletin board system for software information exchange and a newsletter featuring reviews of scientific software along with news items of interest to microcomputer users.

On 30 and 31 October 1989, the Center hosted its first major vendor demonstration. Billed as ScannerFest '89, it featured data input devices and software from 26 vendors, 13 each day. Employees from the Office of Naval Research and Bolling Air Force Base were invited along with NRL staff. Over 550 people attended this event (Fig. 20). An expo highlighting presentation graphics software and devices is scheduled for spring 1990.

Fig. 20 — Some of the 500 participants tryout data input devices at ScannerFest '89

During the last three months of 1989 when the Microcomputer Center was open for business, 119 NRL employees registered to use its various services. Traffic was brisk as users took advantage of the Center's facilities to evaluate software, search the CD ROM and scientific software databases, and confer with the staff. As threats of viruses increased in October and November 1989, the Center's staff answered distress calls and was instrumental in keeping Laboratory microcomputers up and running and in providing peace of mind for concerned computer users.

In its few short months of operation, the Microcomputer Software Support Center has become an accepted and successful information facility that is well utilized by NRL staff. It has become NRL's "reference service" with a capital "R."

Want the latest research paper on superconductivity and advice on using Mathematica? What could be more natural? Go to the Library. ■

Ocean Acoustics and Surfaces

OCEAN ACOUSTICS AND SURFACES

The Navy's ability to operate effectively in the sea is dependent largely on continuing the development and use of advanced techniques and hardware for sensing acoustic signals generated by surface or submerged vessels. Reported in this chapter is work on environmental signal processing, reflection measurements on underwater acoustic panels, a shock test facility for sonar transducers, polymers for constrained layer damping, and ocean surfactant characterization.

Divisions contributing to this work are the Acoustics Division (5100), the Underwater Sound Reference Detachment (5900), and the Space Systems Technology Deparment (8300).

Other current research in acoustics includes:

- Compact underwater acoustic source
- Thermoacoustic wave propagation

Environmental Signal Processing

W. A. Kuperman and J. S. Perkins
Acoustics Division

Background: The performance of a passive array is normally simulated by numerically computing the complicated signal field; noise is either omitted, taken to be white, or represented by a set of plane waves whose distribution is not dependent on the specific local ocean environment. In fact, the structure of the noise is determined by the ocean environment in the same way as the signal field, and hence postulated array gains based on simplistic noise models for low signal-to-noise ratios will be erroneous. Our understanding of ocean acoustic phenomena is approaching the stage where exploring the possibilities of using the ocean itself (environmental signal processing or ESP) to construct signal processing schemes is now possible. We have studied the ESP application in a large ocean basin by using algorithms developed in our 6.1 program, "Unified Wave Theoretic Approach to Ocean Acoustic Propagation, Interference, and Signal Processing." These algorithms are collectively known as the Wide-area Rapid Acoustic Prediction (WRAP) model [1]. Two areas of these simulations require significant computation times: the computation of acoustic pressure fields on the receiver array from many source positions throughout a large region and the computation of the (surface-generated) noise cross-spectral density matrix for the receiver array. By using this model, we have shown that a vertical array in a complex 3-D ocean environment has a horizontal aperture if the asymmetries of the environment are used in the signal processing. This is a totally new combination of signal processing and wave propagation in inhomogeneous media. We summarize the first simulations of the "total" problem—signal, noise, and signal processing [2].

Simulation and the Ocean Environment: For the purpose of this simulation, we will search for the source location in range and horizontal position—an extension of earlier range-depth matched-field processing (MFP) [3] where both Bartlett (linear) and the maximum likelihood method (MLM) were explored in the context of MFP. MFP consists of comparing the data across an array with "replica" fields generated from trial positions. When the replica field from a trial position duplicates the data, the correlation between the two is a maximum, and localization is achieved.

Figure 1 shows our choice of a complex 3-D environment. The bathymetric contours were generated from archival data and the approximate position of the Gulf Stream, as it was in March 1983, is outlined in blue, as are two cold-core eddies and a small seamount. Note the variable bathymetry with the continental rise to northwest.

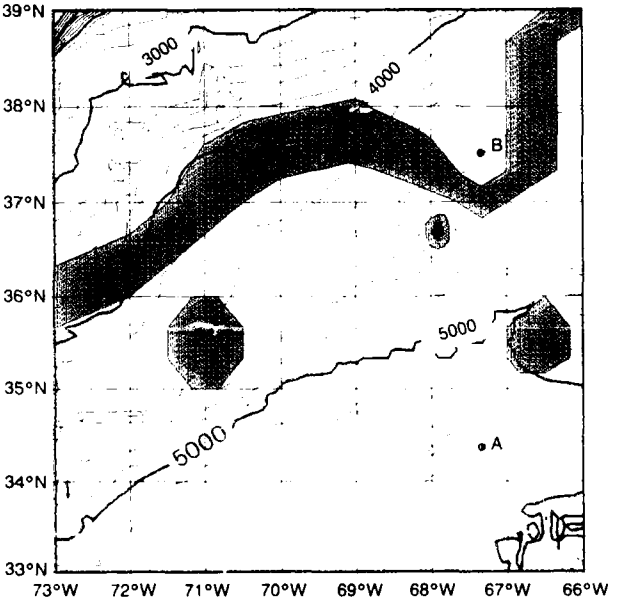

Fig. 1 — The Gulf Stream environment was used for the simulations. The Gulf Stream, two cold-core eddies, and a small seamount are shaded in blue over the bathymetric contours. The first source position is labelled "A" and the second is labelled "B".

Processing Results: We present here the simulation results for a 21-element vertical array with 75-m element spacing placed in the center of the region and covering a depth of 100 to 1600 m. The frequency of the simulation is 10 Hz. The

average signal-to-noise ratio at each hydrophone is approximately 0 dB. We use two source positions at a depth of 100 m. The first source is located southeast of the array toward a relatively homogeneous environment at position x = 527.5 km and y = 152.5 km. The second source is located northeast of the array at position x = 527.5 km and y = 502.5 km (in the "kink" of the Gulf Stream).

Figures 2 and 3 show the "ambiguity functions" as spatial plots of the correlation between the simulated data and the replicas, as just discussed. They were generated at a resolution of 5 km (the same resolution as our environment). The values were color coded so that the dynamic range of each figure covers the top 8 dB. Since we used eight colors, each color change represents a change of 1.0 dB.

Figure 2 shows the Bartlett and MLM results for the first source located to the southeast. For the Bartlett result, there is a maximum at the correct source position, but circular ambiguities indicate the nonuniqueness of the environment in which this source is located. Of course, in a totally range-independent environment, a source at any azimuth, but at the same range and depth as the true source, would propagate to the array exactly like the true source, and the ambiguities would be

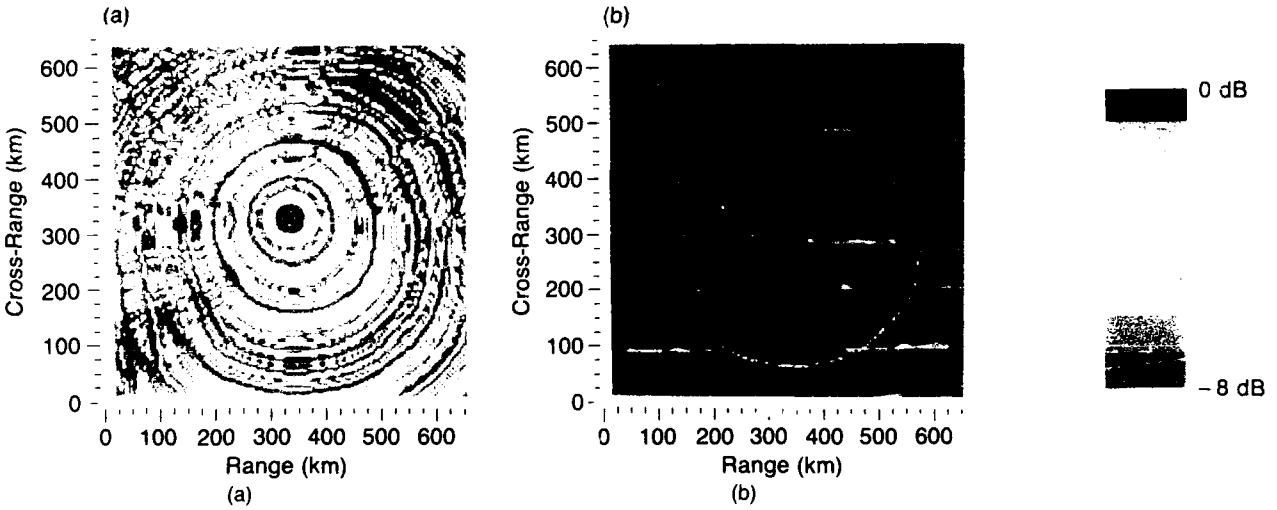

Fig. 2 — Ambiguity functions for the first source location x = 527.5 km, y = 152.5 km; (a) Bartlett and (b) MLM. Each function is color coded so that the dynamic range of the figure covers the top 8 dB.

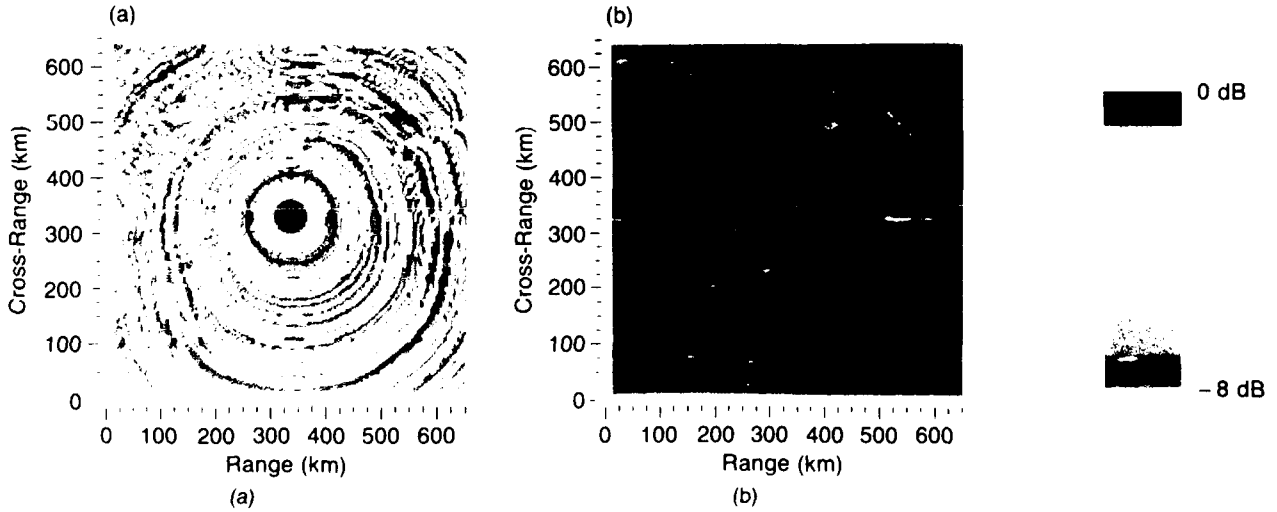

Fig. 3 — Ambiguity functions for the second source location x = 527.5 km, y = 502.5 km; (a) Bartlett and (b) MLM. Each function is color coded so that the dynamic range of the figure covers the top 8 dB.

full rings. Ambiguities in range alone generally result from the repetitive structure of the acoustic field in a convergence-zone environment. The "ring-ambiguities" in Fig. 2 are true ambiguities; they illustrate that when there is only mild range-dependance, there may well be some locations in azimuth that are not unique to the array. The MLM processor, which is high resolution and has lower sidelobes, reduces the ambiguities somewhat. This first location shows an ambiguous localization result.

The second location is in a rather unique environmental location—a kink in the Gulf Stream. Figure 3 shows the Bartlett and MLM results for this case. Here the Bartlett shows an absolute maximum at the true source location with some weaker, though significant, ambiguities that are more analogous to sidelobes. The MLM processor suppresses these sidelobe results for the unambiguous localization of the source.

Summary: A complex 3-D environment, if known, can enhance matched-field processing by providing more diversity to the acoustic structure across an array. We have shown by simulation that a vertical array can localize in azimuth as well as in range and depth. In effect, the environment can provide horizontal aperture for a vertical array.

[Sponsored by NRL]

References

1. W.A. Kuperman, M.B. Porter, J.S. Perkins, and A.A. Piacsek, "Rapid Three-Dimensional Ocean Acoustic Modeling of Complex Environments," Proc., 12th IMACS World Congress on Scientific Computation, R.R. Vichnevetsky, P. Borne, and J. Vignes, eds., Gerfidn, Villeneuve d'Ascq, France, 1988, pp. 231-233.

2. J.S. Perkins and W.A. Kuperman, "Environmental Signal Processing: Three-Dimensional Matched-Field Processing With a Vertical Array," *J. Acoust. Soc. Am.* **87**, (1990).

3. A.B. Baggeroer, W.A. Kuperman, and H. Schmidt, "Matched Field Processing: Source Localization In Correlated Noise As an Optimum Parameter Estimation Problem," *J. Acoust. Soc. Am.* **83**, 571-587 (1988). ■

Offnormal Incidence Reflection Measurements on Thick Underwater Acoustic Panels

J. C. Piquette
Underwater Sound Reference Detachment

Panel measurements are a standard technique whereby the effectiveness of a candidate coating material at reducing unwanted acoustic echoes is determined. Since the reflection coefficient varies as a function of incidence angle, it is important to determine sample performance under a variety of angles of incidence of the interrogating wave. The method described here can determine the reflection characteristics of sample panels of a small cross section as a function of incidence angle and, hence, may save the Navy tens of thousands of dollars compared to tests that heretofore have required a sample of much greater lateral extent.

Outline of the Technique: The present technique (Fig. 4) is a generalization of a technique described in the *1984 NRL Review*, pp. 117-119. This method is now known as the ONION method, based on an analogy to the layer-peeling process used by the technique to determine initial model parameters. The technique is based on least-squares fitting of a multiple-layer panel model to transient waveform data experimentally acquired in digital form.

The method described in the *1984 NRL Review* is restricted to a normal-incidence interrogating wave. The generalization of the algorithm to offnormal incidence involves three phases. In phase 1, the experimentally measured incident-pulsed waveform at *normal* incidence and the resulting experimentally measured reflected-pulsed waveform are used in a *normal* incidence

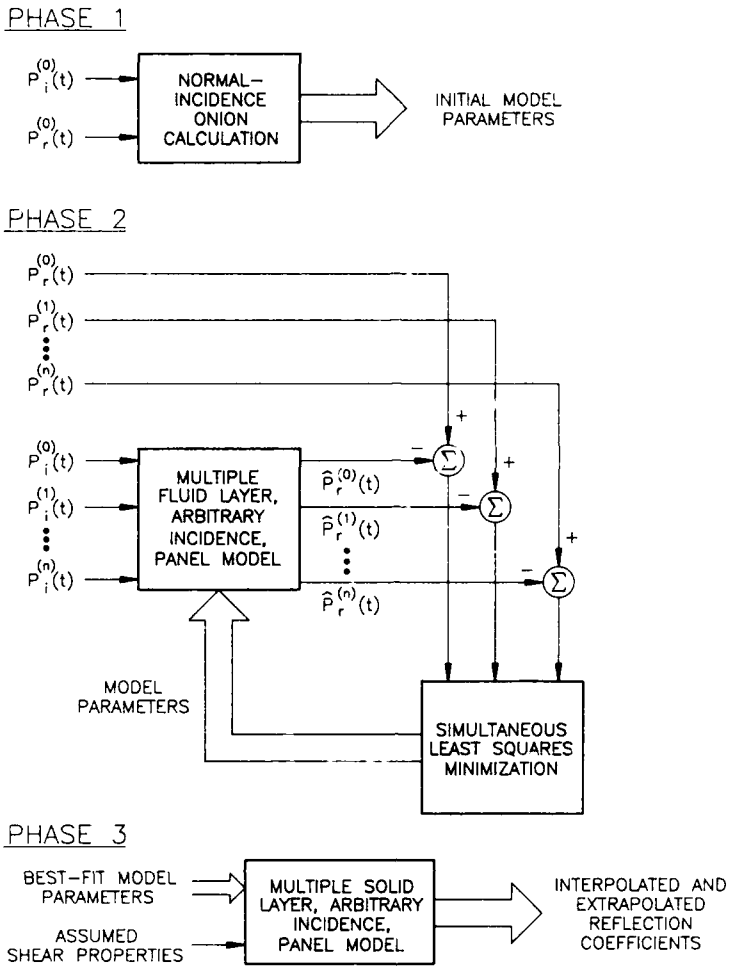

Fig. 4 — The ONION method. The symbol $p_i^{(k)}(t)$ denotes the measured incident-pulsed waveform at the k^{th} angle of interest, and $p_r^{(k)}(t)$ denotes the measured reflected-pulsed waveform at the k^{th} angle of interest. $\hat{p}_r^{(k)}(t)$ represents a computed reflected waveform, and n represents the maximum measurement angle.

ONION-method calculation to obtain starting model parameters. In phase 2, the model parameters are iteratively improved by using a nonlinear least-squares fitting procedure that simultaneously fits an offnormal incidence theoretical panel model to data acquired at all experimentally obtainable incidence angles. The layers of the panel are treated as fluids during this phase. In phase 3, the best-fit model parameters deduced by phase 2 are used with assumed shear properties for the layers in a calculation based on a *solid*-layer panel model to obtain interpolated and extrapolated reflection coefficients as a function of incidence angle θ.

Performance of the Method: Figures 5 and 6 show the effectiveness of the method. In Fig 5, results are presented for a 10 kHz test performed on a sample panel composed of three simple homogeneous layers. This sample consists of one layer of polymethylmethacrylate, one layer of water, and one layer of steel. The solid circles represent measured points. The dashed curve represents the output of the method; i.e., interpolated and extrapolated reflection coefficients. The solid curve, presented for comparison, is based on a theoretical calculation using the known acoustical properties of the layers.

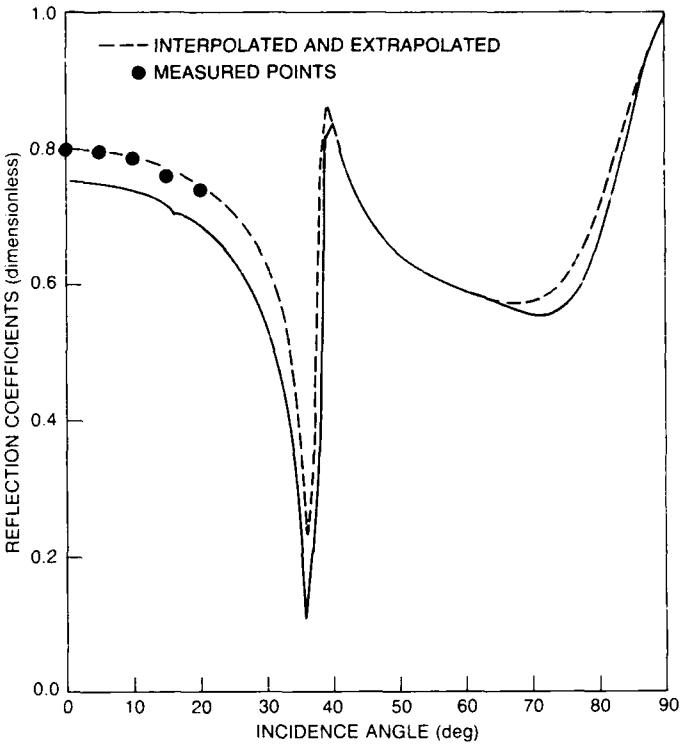

Fig. 5 — Experimental data points (solid circles) and interpolated and extrapolated reflection coefficients (dashed-line curve) compared to theory (solid-line curve) for a simple three-layer sample tested at 10 kHz. The sample layers are polymethylmethacrylate, water, and steel.

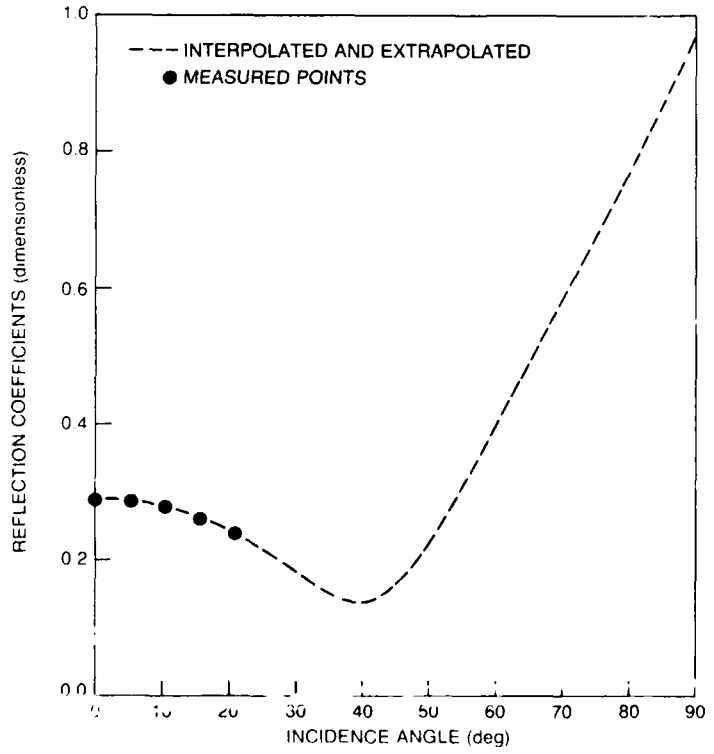

Fig. 6 — Experimental data points (solid circles) and interpolated and extrapolated reflection coefficients (dashed-line curve) for a thick sample panel containing three macrovoided viscoelastic layers affixed to a steel backing plate. Test frequency is 10 kHz. Overall sample thickness is 12.9 cm, and lateral dimensions are 76 x 76 cm.

In Fig. 6, results are presented for a test conducted on a much more complex sample; i.e., one containing three macrovoided viscoelastic sublayers affixed to a steel backing plate. The true properties of the layers are unknown, so no theoretical curve is presented for comparison. As in Fig. 5, the solid circles are measured points and the dashed-line curve presents the interpolated and extrapolated reflection coefficients produced by the generalized ONION method.

Potential Impact: To determine sample performance under offnormal incidence, it has heretofore been necessary to fabricate relatively large test samples (of the order of 2-m side lengths) so that the disturbing influence of the edge-diffracted wave might be reduced. The present method has been demonstrated to be effective for samples having side lengths of 0.75 m, or approximately one-seventh the volume of the larger samples. The use of smaller samples to perform the tests can potentially save the Navy tens of thousands of dollars on each sample. Also, the smaller samples are more amenable to placement into existing test facilities for evaluation under environmental conditions of temperature and pressure than are the larger samples. Thus the present method provides the Navy with a test capability not previously available.

References

1. J.C. Piquette, "The ONION Method: A Reflection Coefficient Measurement Technique for Thick Underwater Acoustic Panels," *J. Acoust. Soc. Am.* **85**(3), 1029-1040 (1989).

2. J.C. Piquette, "Offnormal Incidence Reflection Coefficient Determination for Thick Underwater Acoustic Panels Using a Generalized ONION Method," *J. Acoust. Soc. Am.* (scheduled to appear March 1990).

■

The Shock-Test Facility: A Water-Filled Conical Shock Tube

J. F. Zalesak and L. B. Poché
Underwater Sound Reference Detachment

Naval sonar transducers and related components mounted on the hulls of surface ships and submarines are subjected to an inertial shock and an acoustic pressure shock wave when an ordnance charge explodes underwater near the vessel. The potential damage and loss of capability are of great concern to the Navy. Consequently, naval sonar transducers are required to withstand a standard shock test performed, until recently, at the West Coast Shock Facility (WCSF) at Hunter's Point, San Francisco, CA. There transducers under test are attached to the bottom of a floating shock platform (FSP), and 60-lb explosive charges are detonated at a prescribed series of distances from the FSP [1]. The transducers are calibrated before and after the test to detect any shock damage. Tests are conducted only a few times each year because of environmental restrictions, and the large scale of the tests make the tests quite expensive. The Hunter's Point test facility is no longer available because of damage caused by the earthquake of October 17, 1989. An alternative test site is now being sought. Other types of shock testing machines cannot supply both parts of the shock exposure to the equipment being tested. The Navy requires an alternative test that is both inexpensive and frequently performed.

A closed-chamber shock-test facility has been developed at NRL's Underwater Sound Reference Detachment (USRD) to satisfy this need. It is a water-filled, conical-bore tube about 3-m long with an inner diameter of 15 cm at the large, or muzzle, end. Figure 7 shows the form of the tube. Our intention has been to develop a shock tube of adequate diameter to allow some of the most commonly tested sonar transducers to be evaluated. This design allows exposure to both shock-wave pressure and inertial shock in a single test by mounting the transducer on a piston that moves in a cylindrical reaction chamber. The

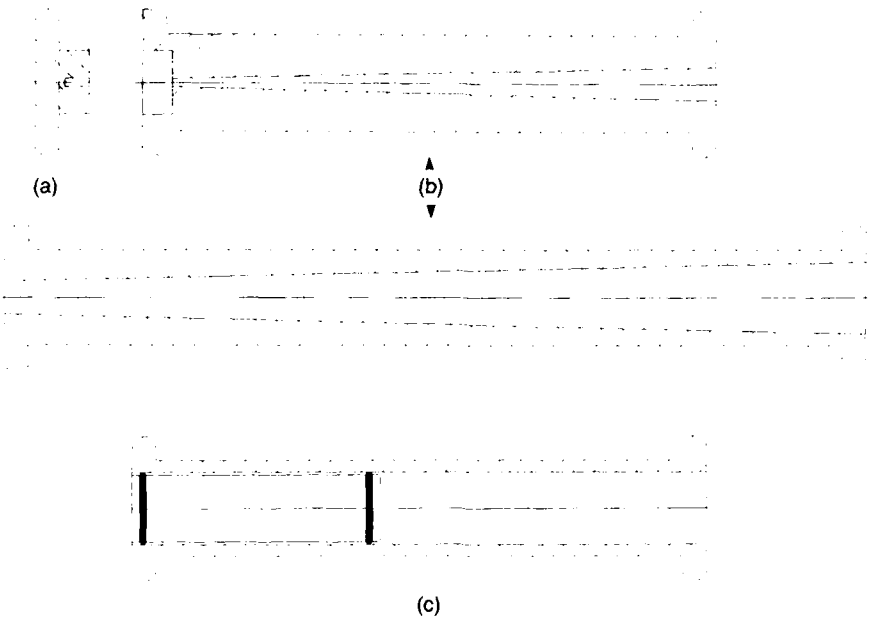

Fig. 7 — (a) breech block, (b) two-piece shock tube, and (c) reaction chamber with piston

shock-tube dimensions and explosive charge weight are chosen to closely simulate both the peak shock-wave pressure and the FSP's inertial motion during the most severe shot of the test schedule.

The environmental consequences of operating such a shock tube are much less likely to be considered objectionable than they are with the present test. Shock-tube tests can be performed with a frequency limited only by the mechanics of opening, loading, and filling the tube. Four test cycles per day seem to be a reasonable work load. In operation, the tube is mounted horizontally and a small explosive charge (1 to 6 gm TNT equivalent) is detonated in the breech, or small diameter end of the tube. This produces the pressure shock wave that quickly travels down the tube. The transducer under test is mounted on the face of a piston that is free to slide in a cylindrical chamber, forming the termination of the tube. After the shock wave strikes the transducer, the expanding gas bubble from the explosion accelerates the piston into the chamber, thus applying the inertial shock to the transducer. The gas bubble from the explosion acts as a spring, and the mass of the contained water, the piston, and transducer form a vibrating system that can be adjusted to mimic the inertial motion of the FSP in a single degree of freedom.

Figure 8 shows a typical sample of a shock-wave pressure measurement seen as the upper trace made in the closed tube and recorded with a 1/4-in. diameter tourmaline disk gage and digital waveform recorder. This pulse was generated by an electric blasting cap equivalent to 0.65 gm TNT that has an estimated peak pressure of 2380 psi. The high-frequency energy that visually dominates the pressure-wave signature does not contribute much to the total energy in the spectrum and seems to be characteristic of a shock wave generated in a conical tube with thick steel walls. The lower trace in the figure was recorded similarly at WCSF during a 30-ft standoff test (Shot 3 of MIL-S-901D). A secondary pressure pulse that may result from the reflection of the shock wave from the piston surface may be absorbed sufficiently by covering the piston surface with a water-soaked cypress wood cap of the proper grain orientation.

The inertial shock motion of the WCSF FSP in the vertical plane has been characterized as a half-sine pulse of approximately 600-ms duration

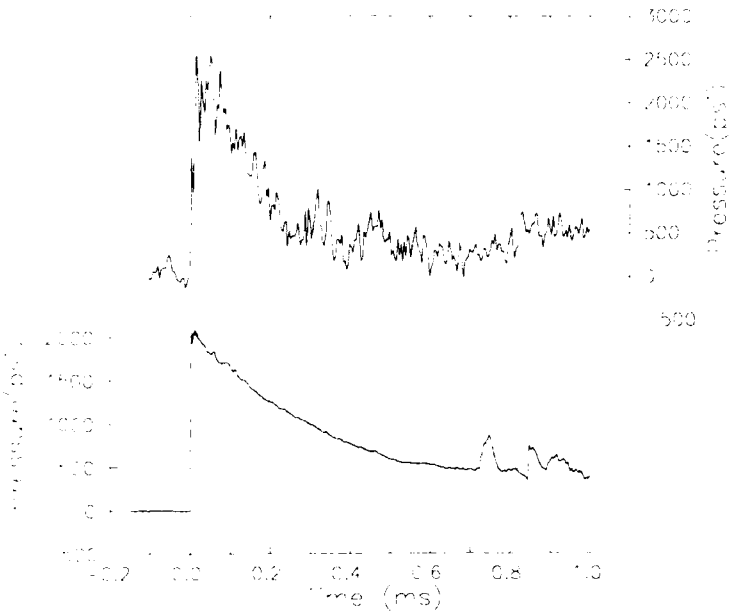

Fig. 8 — Typical shock-wave pressure signatures: upper trace from shock tube,lower trace from WCSF test

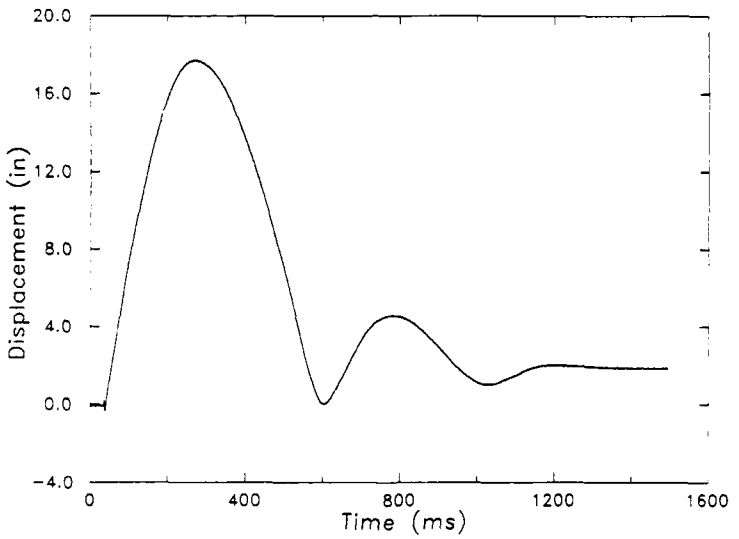

Fig. 9 — Reaction block motion in shock tube

and 16-in. peak displacement, with a peak velocity of about 11 fps. Figure 9 shows the inertial shock motion of our reaction chamber piston. Here the tube was driven by a charge consisting of an E-1A blasting cap and 0.7 gm of DuPont Detaprime GA. The piston was loaded with approximately 200 lb of lead. Our recorded waveform agrees quite well with the FSP's inertial motion.

[Sponsored by NAVSEA]

Reference

1. MIL-S-901D (NAVY), "Military Specification. Shock Tests, HI (High-Impact); Shipboard Machinery, Equipment, and Systems, Requirements for," 17 Mar 1989. ■

Development of Polymers for Constrained-Layer Damping

R. N. Capps
Underwater Sound Reference Detachment

Viscoelastic materials are widely applied for various noise and vibration problems. In particular, use of viscoelastic materials in constrained-layer damping treatments for decreasing structureborne noise in ships is becoming increasingly important in naval applications. In a constrained layer, a thin viscoelastic layer is constrained by a stiff cover plate. It experiences a relatively large shear strain and relatively small dilatation when the base plate to which it is attached is strained by some type of vibratory motion. Since most of the energy dissipation is caused by shear deformation and relatively little by dilatation, on an equal weight comparison, constrained layer damping provides a much more effective treatment than simple extensional damping from attached viscoelastic layers. Analyses presented in Ref. 1 show that the damping depends on the wavelength of bending waves in the damped structure, as well as the frequency- and temperature-dependent properties of the viscoelastic material. The thicknesses and extensional stiffnesses of the base and constraining layer also affect the damping.

Experimental Method: In the present case, we wanted to develop a viscoelastic material that would give as much damping as possible in a three-layer structure over a 100 Hz to 10 kHz range and a 0° to 20°C temperature range. Engineering considerations did not allow variations in the thicknesses of the various layers; therefore, it was necessary to maximize the damping through careful selection of the polymer and fillers.

The design of constrained-layer structures and the selection of materials for use in these structures require an accurate determination of the viscoelastic properties of the polymers used. Many commercially available instruments cannot operate at relatively low frequencies. To cover the desired frequency and temperature range, a transfer function technique was used that was based upon the measure of the transmissibility of a mass-loaded rod, with high internal damping, undergoing longitudinal sinusoidal excitation. Time-temperature superposition was used to extend the measured frequency-dependent Young's modulus and loss tangent curves at different temperatures into master frequency curves at a single reference temperature. The measured viscoelastic properties were then used with the Ross-Kerwin-Ungar (RKU) model [1] to calculate the expected damping.

The RKU model is a generalized solution for a three-layer beam configuration. The problem has been simplified by assuming that the extensional stiffness of the viscoelastic layer is small, and that shear deformations of the base plate and constraining layer are negligible. It is also assumed that the constraining material is purely elastic and dissipates no energy. Linear behavior of the viscoelastic layer is also assumed, with uniform shear effects throughout the viscoelastic layer. The loss factor of the three-layer beam is calculated by taking the ratio of the imaginary part of the bending rigidity to the real part.

To test the predictions of the model, scale-model plates were prepared from selected formulations and tested in air. The base plate was composed of 2.54-cm-thick piece of brass. The viscoelastic layer was 0.079-cm thick, with a 0.158-cm-thick brass top plate. The length of the plates was 1 m, and the width was 0.33 m. The plates were suspended in a shock chord. An impact hammer was used to tap the structure, and the outputs of the accelerometers fed into a Fourier transform-based spectrum analyzer to examine the envelope of vibration.

Selection of Materials: For broad-band damping, the glass-transition region of the polymer should be as diffuse as possible. Certain types of materials, such as acrylonitrile rubbers (NBR), may exhibit very high damping over a

relatively narrow temperature and frequency range. Other materials may exhibit loss factors that are as high but that show less temperature and frequency dependence. Figures 10 and 11 show the Young's modulus and loss tangent of an NBR and a chlorobutyl rubber (CIIR) as a function of temperature at 10 Hz. The two materials contain the same loadings of the same types of fillers and are crosslinked to approximately the same static stiffness. The CIIR is a better choice as a broad-band damping material, since it has a high loss tangent over a wider temperature range. It will also be a more effective damper over a broader frequency range.

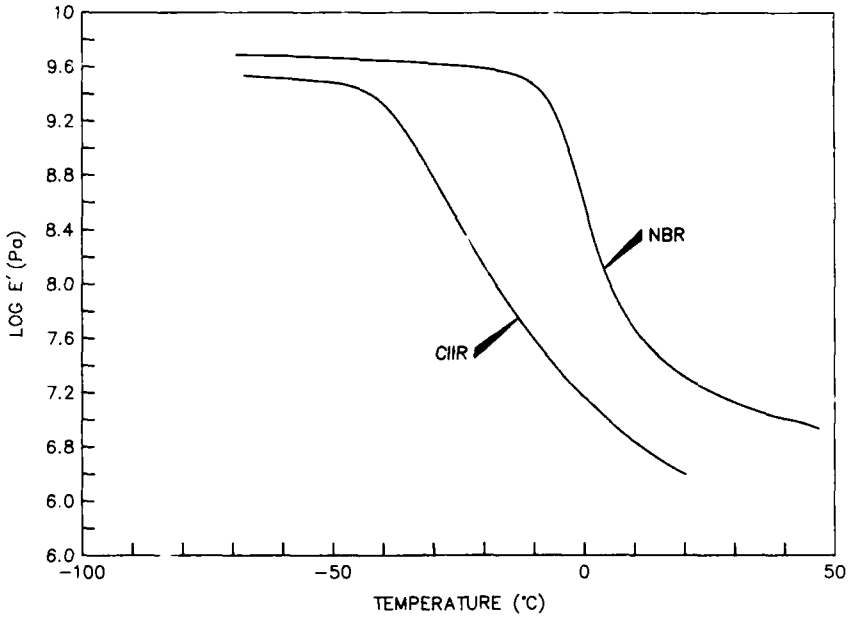

Fig. 10 — Young's storage modulus vs temperature in degrees Centigrade at 10 Hz for NBR and CIIR

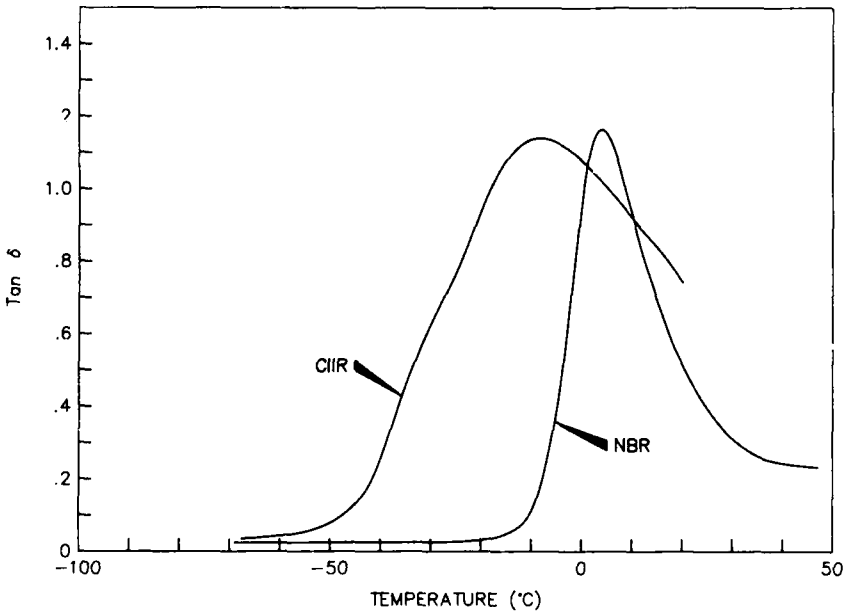

Fig. 11 — Loss tangent vs temperature in degrees Centigrade at 10 Hz for NBR and CIIR

The use of reinforcing fillers will broaden the transition region of many polymers, but the result will be an overall decrease in the magnitude of the loss tangent. Alternatively, use of platelet types of fillers such as mica and graphite may introduce additional loss mechanisms, increase the overall dampening, and simultaneously broaden the transition region. Carbon black at various loadings, as well as in combination with mica, and mica and flake graphite, was used. We found that lower loadings of carbon black alone did not give damping in the constrained layer structures that was as good as that obtained with combinations of mica and graphite.

In general, we found that the RKU model gave only qualitative agreement with the experimental damping results. Figure 12 shows the comparison between calculation and experiment of a CIIR rubber structure at 5°C. However, in all instances, the model was able to qualitatively predict the relative merits of the damping capability of different polymer layers. As the model predicted, relatively soft, lightly filled formulations gave the best damping performance.

The use of viscoelastic measurements, combined with the RKU model and plate-damping measurements, resulted in the successful development of a constrained-layer damping material. This CIIR used a combination of carbon black, mica, and graphite fillers.

Acknowledgments: Ms. Linda Beumel of TRI/TESSCO and Mr. Douglas Noll of David Taylor Research Center made significant contributions to this research.

[Sponsored by DTRC]

References

1. Rodger N. Capps and Linda L. Beumel, "Applications of Dynamic Mechanical Testing in the Development of Polymers for Constrained Layer Damping," ACS Symposium on Polymers in Damping, L. H. Sperling and R. D. Corsaro, eds., to be published by American Chemical Society Books in 1990.

2. Rodger N. Capps, "Effect of Cure Systems and Reinforcing Fillers on Dynamic Mechanical Properties of Chlorobutyl Elastomers for Potential Vibration Control Applications," *Rubber Chem. Technol.* **59**, 103–122 (1986). ■

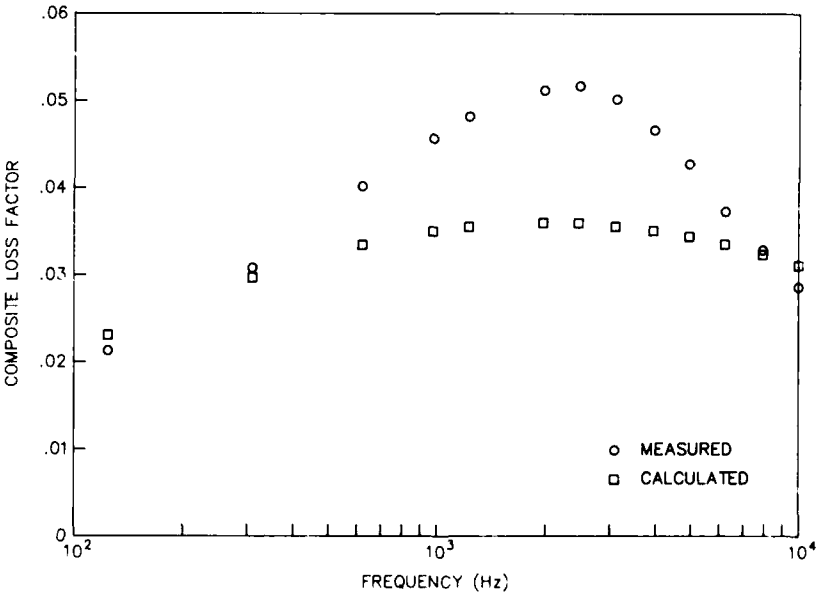

Fig. 12 — Comparison of experimental vs composite loss factor as predicted by the RKU model for three-layer constrained layer assembly as a function of frequency at 5°C for CIIR formulation

High-Resolution Surfactant Characterization in Ship Wakes

J. A. C. Kaiser
Space Systems Technology Department
and
R. D. Peltzer
Laboratory for Computational Physics and Fluid Dynamics

A modern adaptation of a traditional method to measure the surface tension of the ocean surface was developed at NRL and was deployed successfully to measure the distribution of surface-active chemicals (surfactants) in the wakes of surface ships. During an experiment in early 1989, this device—a small instrumented catamaran towed from a research platform—measured surface-tension profiles across ship wakes to 0.5 mN/m with a 1-m spacial resolution. Surface tension gradients of 20 mN/m were resolved with this modernized method—an order-of-magnitude improvement over the older measurement method.

These wake data are significant for two reasons. First, long (> 60 km) ship wakes have been observed from space [1,2]; surfactants are suspected of being the agent causing these long wakes to be imagable. Second, for the first time, these data have a much higher resolution revealing important fine structure in these long wakes.

Surfactants and Ship Wakes: Surfactants are biologically produced chemicals that have an affinity for the ocean surface and adsorb there in moderate to light winds. As they adsorb on the surface, they form films with reduced surface tension. These surfactant films are elastic and produce a viscous boundary layer just below the surface that dissipates short ocean waves ($\lesssim 10$ cm). This then reduces the surface roughness and produces visible slicks and dark areas in radar images if the surfactant concentration is high enough.

Near-surface convergent currents in the water can also increase surfactant concentrations sufficiently to deroughen the surface. The flow around the hull of a ship as it moves through the water produces such convergent zones in the wake [1]; this can make these wakes visible from space in radar or photographic images. In light winds ($\lesssim 4$ m/s or knots), these surfactant bands are highly persistent on the surface; it is these very long (>60 km) wakes that are observed from space.

Measurement Technique: Surface tension is measured with a set of calibrated spreading oils. Each oil is a mixture of paraffin oil and lauryl alcohol. The oil spreads on the water surface if the water surface tension is greater than the value ascribed to the oil (equilibrium spreading pressure (ESP)). It does not spread if the water surface tension is less than the oil's ESP. Therefore, by using a series of oils with known ESPs, we can bracket the water surface tension between two ESPs of contiguous oils in the set.

For our measurements, we used 23 oils. Their ESPs were separated by about 0.16 dyne/cm when the oil's ESPs were in the range of the clean water surface tension (70 to 74 mN/m), and the ESP separation of the oils increased to 8 mN/m for surface tensions around 50 mN/m.

The traditional method of using these oils is to dip a buoyant applicator (toothpick) into an oil, throw it on the water surface, observe whether or not the oil spreads at that location, and then move quickly to a new location to repeat the procedure. Different oils were tried until the water surface tension was bracketed by two contiguous oils at each location. If the water surface tension changes rapidly over a short distance, one has to move quickly and change the oils fast enough to keep up with the changes and still be able to bracket. Since this is a rapid procedure, small-scale features in surface tension change are usually missed.

Surface TEnsion Measuring System (STEMS): To overcome the resolution problem associated with toothpick application of the oils, we developed a towable device, called STEMS. Figure 13 shows the prototype device used in the ship-wake experiment. The towable catamaran is

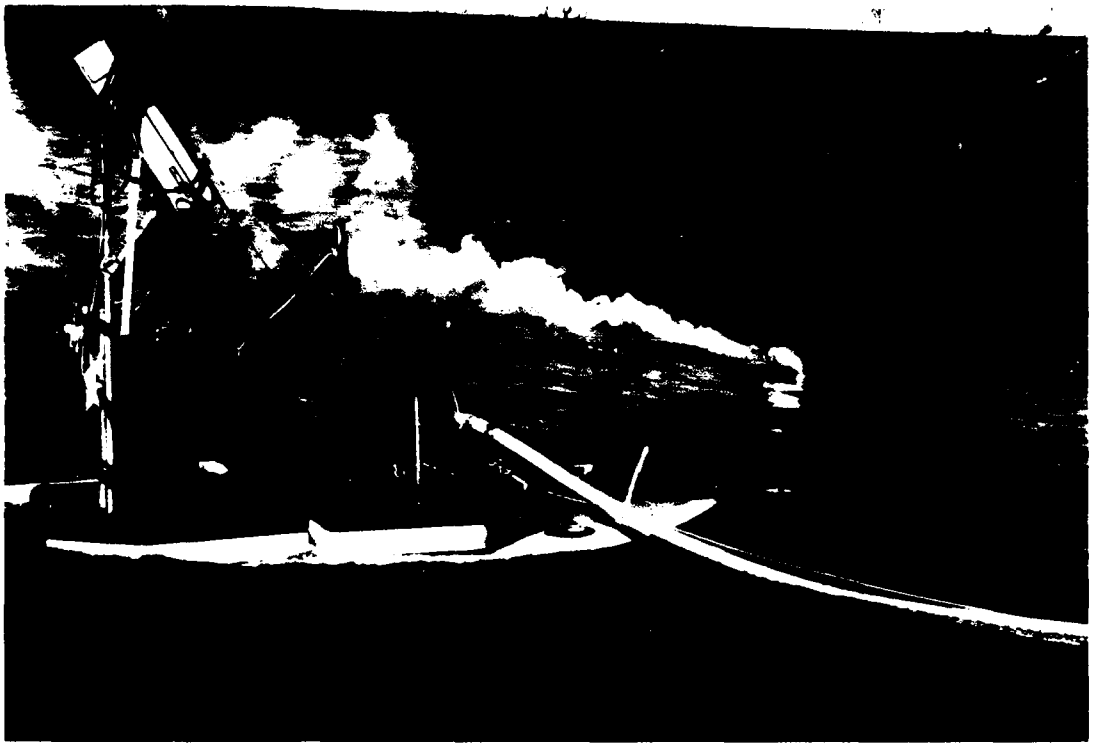

Fig. 13 — Surface TEnsion Measuring System (STEMS) being towed across the outer edge of a ship wake. (Note the slicked band just inside the smoke flare at the wake edge.) The oils drop between the hulls where the umbilical attaches. The video camera is mounted above the hull and to the rear.

3-m long and 2-m wide. In the forward portion of the region between the hulls, 23 spreading oils are released onto the water surface one drop at a time from individual hypodermic needles. The dropping rate for each oil varied between 0.2 and 0.5 Hz. The behavior of the oils on the water surface was recorded by a video camera on the sled shown in upper left-hand side of Fig. 13. The video tapes were analyzed at a later time to determine which oils did or did not spread, thus obtaining the surface tension profile. STEMS was towed at speeds ranging from 0.5 to 1.0 m/s in a serpentine pattern across ship wakes thus producing many surface tension profiles. Typically four crossings of each a wake were made in 1 h corresponding to distances in the wake of 3 to 22 km.

Sample Data: A comparison of the data from the traditional toothpick and modern methods reveals that STEMS produced higher resolution surface tension profiles. Figure 14 is a sample of STEMS-measured surface tension profiles made from behind a ship running at 25 knots. From top to bottom, the profiles correspond to distances behind the ship of 3.7, 12.0 and 21.3 km. The bands of surface-active materials are defined by the regions of reduced surface tension in the profiles. The edges of the wake are bounded by the outside bands.

Comparison with Synthetic Aperture Radar (SAR): An interesting comparison can be made with the corresponding SAR data that was obtained during a simultaneous overflight of the same ship wake. The SAR data are compared with the surface tension profile data at the location 3.7 km aft of the ship. Figure 15 shows radar cross sections for L-, C-, and X-bands at the polarizations indicated (HH is horizontal transmit and receive; VV is vertical transmit and receive) and the corresponding surface tension data. At L- and C-bands, the cross section is reduced about 6 dB in the surfactant bands (the ordinate tick marks

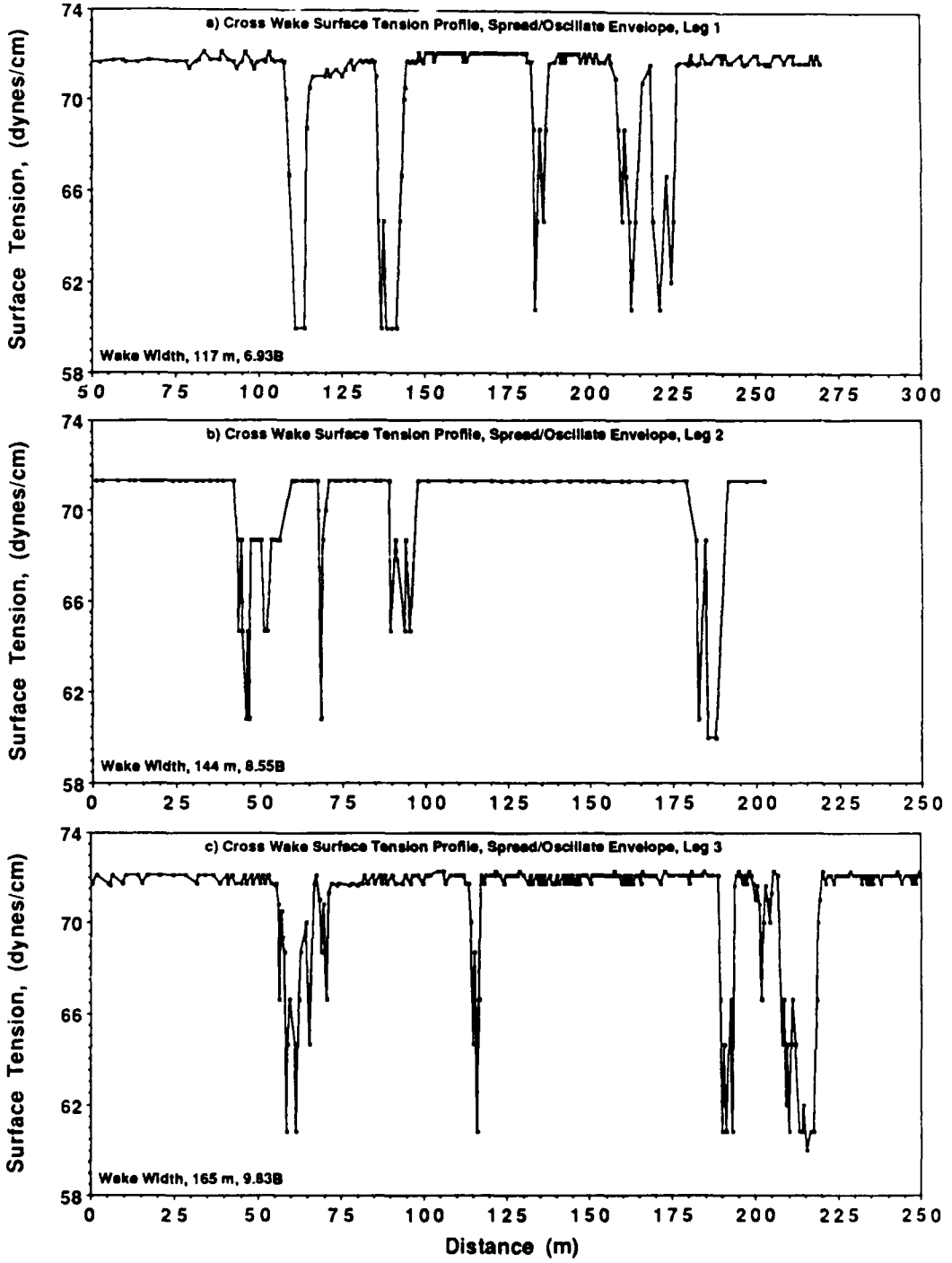

Fig. 14 — Three surface tension profiles across a ship wake measured with STEMS. Lower surface tension indicates the presence of a surfactant film. Note the ability at STEMS to measure rapid changes in surface tension and detect narrow (about 1 m) bands of surfactant material.

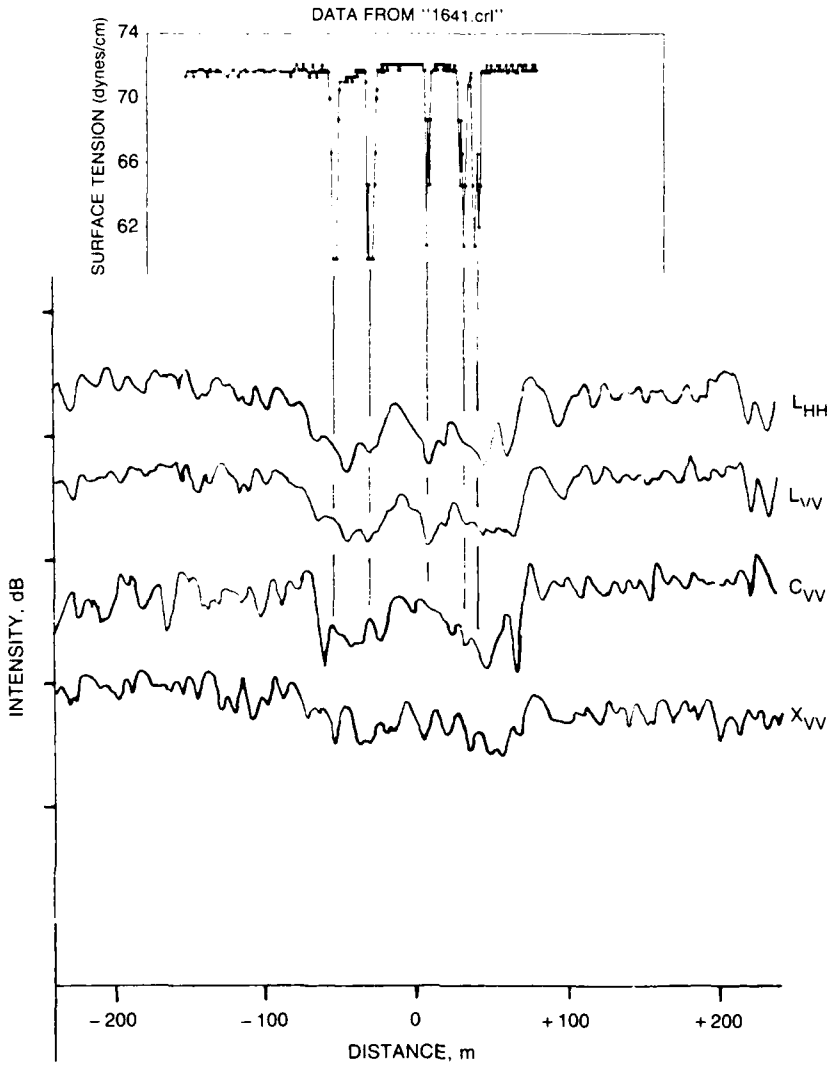

Fig. 15 — A comparison of one surface tension profile with the corresponding synthetic aperture radar cross-section (RCS) profile. Each tick mark on the vertical axis corresponds to 10 dB. Note that each band of surfactant corresponds reasonably well to a dip in the RCS.

are 10 dB apart), but at X-band, the radar was working at a noise floor, so there was no evident cross-section reduction in the wake.

This initial comparison is *ad hoc*, but these SAR images of ship wakes suggest that surfactants do play an important role in forming the dark centerline scar behind surface ships and that their influence remains at the surface many kilometers behind the surface ship in light winds.

The Future: STEMS-2, a new device that can either be towed from a host vessel or operated independently with two scientists aboard, is now being built. We will be able to increase the oil dropping rate to 2 Hz for each oil thus increasing our spatial resolution significantly. We will also have all oils drop simultaneously, which will greatly simplify the data reduction and evaluation procedure. STEMS-2 will be highly maneuverable and will be capable of supporting other instruments at sea, such as acoustic profilers, small thermistor chains, small radars, optical profilers, wave spectral measurement systems, and meteorological sensors.

We plan to refine the spreading oil technique (working with William Barger, Code 6170) to

obtain higher resolution in the measurement of surface tension.

[Sponsored by ONR]

References

1. J.A.C. Kaiser, W.D. Garrett, S.F. Ramberg, and R.D. Peltzer, "Ship Wake Experiment for Remote Sensing," *1986 NRL Review*, pp. 64-67.

2. P. Scully-Power, "Navy Oceanographer Shuttle Observations, STS 41-G Mission Report," NUSC Technical Document 7611, March 1986. ■

Optical Systems

OPTICAL SYSTEMS

Research in optical sciences is directed, in part, toward holography, optical warfare, optical data processing, space optics, laser–matter interactions, waveguide technology, and IR surveillance. Fiber-optics research and improved versatility and powers of lasers are also addressed. Reported in this chapter is work on infrared filters and mirrors, fiber-optic gyroscopes, optical phase conjugation, laser radar measurements, and photorefractive multibeam mixing.

This work is performed by the Condensed Matter and Radiation Sciences Division (4600), the Optical Sciences Division (6500), and the Space Systems Development Department (8100).

Other current research in optical systems includes:

- Infrared focal plane arrays
- Nonlinear frequency conversion of laser diode emission
- Single mode fiber radiation response
- Xe/Ar laser
- Quasi-optical gyrotron

High Performance Infrared Filters and Mirrors

E.P. Donovan
Condensed Matter and Radiation Sciences Division

Optical sensors including eyes, are susceptible to damage and/or dazzling at laser intensity levels far below those that damage structures. The Navy must protect sensors against known laser threats. A thin film in the light path, transparent except to the threat(s), is a solution. NRL has developed a new vacuum deposition method to produce optical interference coatings of novel designs to fill this need [1].

Ion-beam-assisted deposition (IBAD) deposits energetic atoms and molecules (e.g., nitrogen) from an ion beam onto the surface of the growing film, while low-energy atoms (e.g., silicon) are deposited by evaporation. Composition and refractive index of the film are computer controlled during the deposition by the relative arrival rates of the energetic and evaporated atoms. Many film properties (e.g., adhesion) are found to be superior to those of films of the same nominal composition produced other ways.

Optical Sensor Protection: When light is incident upon an optical filter, a fraction R is reflected, a fraction A is absorbed and the remainder T is transmitted (that is, $T = -R - A$). Absorption filters convert incident light to heat, and light from all incident angles is absorbed. However, it can be difficult to find materials that absorb only at predetermined wavelengths, and under high power, heat may cause such films to peel off or crack with loss of protection.

Interference mirror coatings use periodic variations of the refractive index with depth to reflect strongly at certain wavelength(s). The conventional quarter-wave dielectric stack, for example, has alternating layers of high- and low-index materials, each layer thickness being equal to one-fourth the peak R wavelength divided by the index. The peak optical density (OD = $-\log(T)$) increases linearly with the number of high/low index pairs for films with A = 0. These films allow a choice of peak R wavelength and have high T off peak but are sensitive to the angle of incidence of the light, protect only one wavelength, and may crack between layers if heated.

Design of Novel Optical Filters: The Naval Research Laboratory (NRL) can calculate the wavelength dependence of T or R (spectral response) of filter designs on substrates whose back surface is polished or rough. The index depth profile is input layer by layer or as a continuous function. Absorption and the index dependence on wavelength (dispersion) can be included.

An exciting class of novel filter designs is based on the "rugate" design (as in "corrugated") whose index varies with depth like a sine wave around the average index n_{av}. OD is again linearly dependent on the number of sine wave layers and depends on the amplitude of oscillation. The period of oscillation equals the peak reflection wavelength divided by $2n_{av}$. The design has no sharp interfaces to cause cracking, and several wavelengths can be reflected if the variation from n_{av} is a sum of variations of individual sine waves.

Ion-Beam-Assisted Deposition (IBAD): NRL has several vacuum systems similar to Fig. 1 to study the physical processes that occur in IBAD and to fabricate devices. The base pressure of this cryogenically pumped chamber is low compared to the operating pressure of the ion source. The substrate can be positioned directly over the 8-kW electron beam heating evaporator (1) normal to the ion source (2) or in the same plane but halfway between the two sources. Three charge collectors (Faraday cups) (3) surround the sample for ion current measurement during the deposition. The 200 to 1500 V ion beam can be centered on the substrate. The evaporation rate is monitored by means of a quartz crystal monitor or by an electron emission impact spectrometer (4), which allows much thicker films to be deposited. The substrate can be mounted on a water-cooled plug or on a

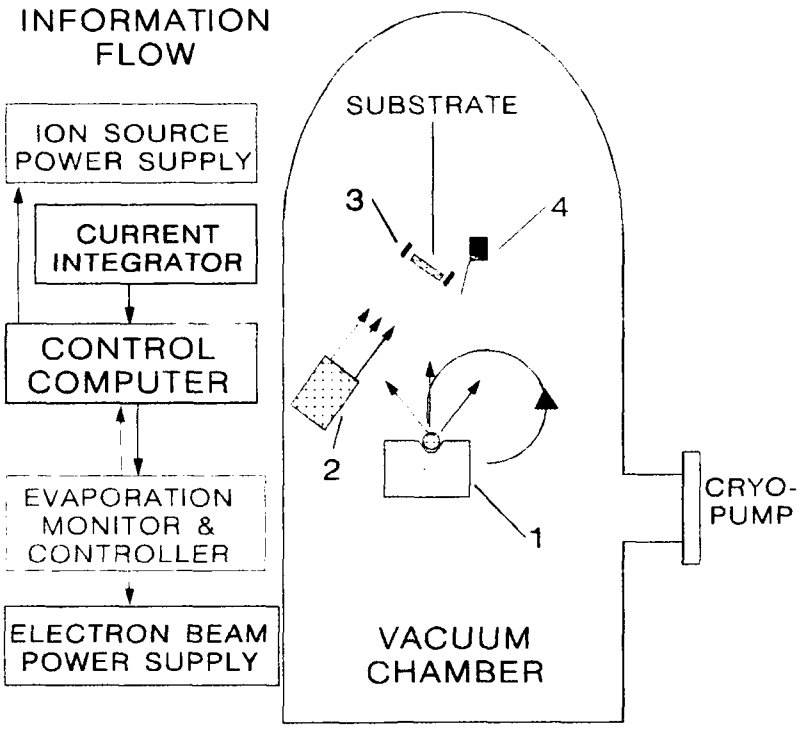

Fig. 1 — IBAD vacuum chamber with (1) electron beam evaporator, (2) ion source, (3) charge collectors, and (4) evaporation monitor

seven-sample rotating carousel. Materials that have been investigated include Si-N, Ti-N, B-N, Ti-deuterium, Si-O, Ti-C, and several evaporants with argon.

A personal computer (PC) controls the deposition. The design index profile is input either as a series of index-thickness pairs or as functions. Calibration curves for index and film thickness vs the ion-beam-to-evaporation ratio, such as those of Fig. 2, can be obtained with an ultraviolet-visible-infrared spectrometer and a surface profilometer or from Rutherford backscattering spectroscopy (RBS) measurements. NRL can further characterize the film after removal from the deposition chamber by auger electron spectroscopy, scanning electron microscopy, elastic recoil spectroscopy, RBS with channeling, proton-induced X-ray emission, hardness testing, optical microscopy, X-ray diffraction, and sliding friction and wear tester.

During the deposition, the PC receives output from the evaporation rate monitor and the current integrator attached to the Faraday cups. The PC calculates the current index and integrated film thickness (Fig. 2), then obtains the design index of the next incremental layer. It alters the ion beam current setting and/or the evaporation rate setting to obtain the proper ratio, pauses, then begins the cycle again. When complete, the deposition record is written to a file. The record can be used to calculate the spectral response from the deposition profile and compare it with that measured for the filter.

Optical Filters: Figure 3 shows the response of a silicon-nitride-on-silicon infrared rugate filter made to test the instrument rather than to protect against a particular laser wavelength. The optical density is very high in the peak region, and transmission is good outside the region. Similar rugate filters have been produced by using boron evaporation and a nitrogen ion beam.

The films produced at NRL by IBAD have been found to possess many superior properties.

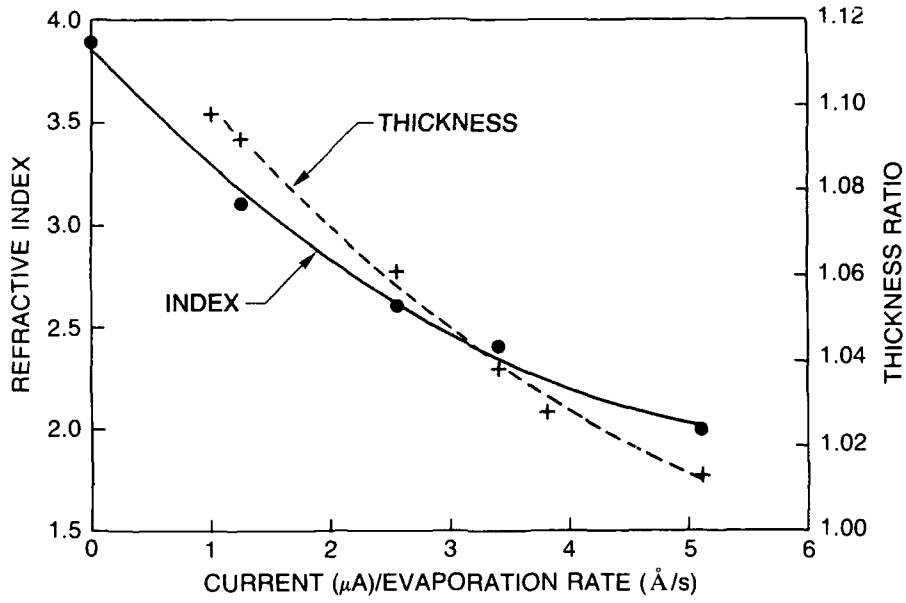

Fig. 2 — Typical calibration curves for the dependence on the ion-current-to-evaporation-rate ratio of refractive index and ratio of film-to-evaporant thickness.

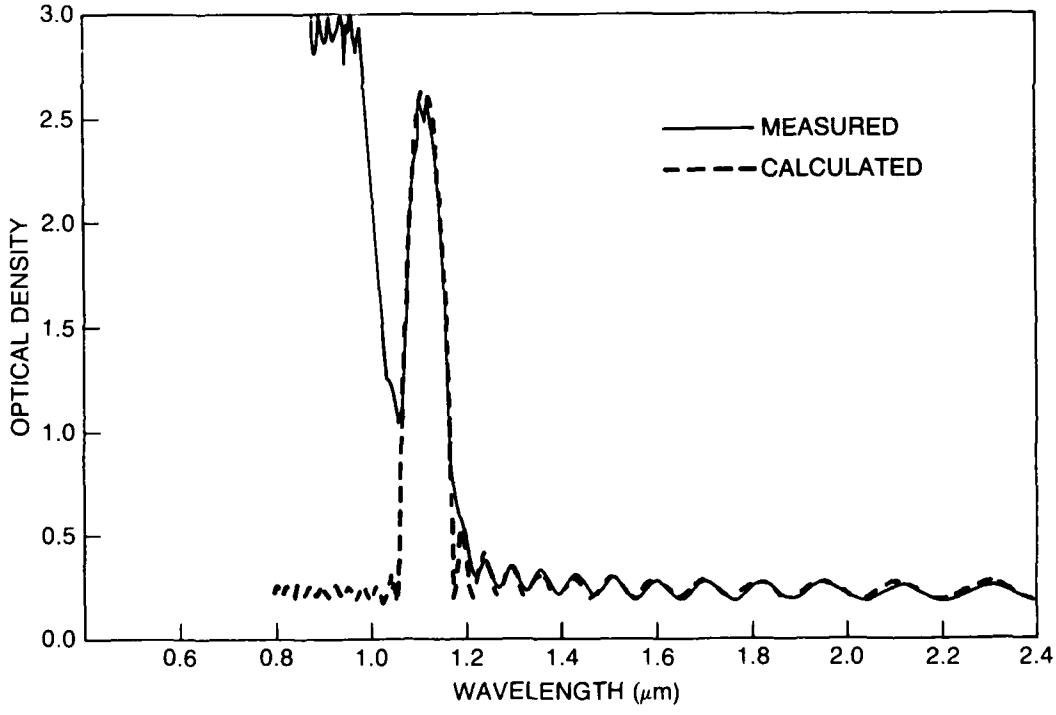

Fig. 3 — Optical density of a 23-cycle rugate band reflection filter. Transmission is less than 0.5% in the peak region.

For example, Si_3N_4 films have the density of the bulk material and less than 1% impurity levels of hydrogen, carbon, and oxygen. Chemical vapor deposition films, by comparison, may have 20% hydrogen. IBAD Si-N films have not peeled under the stress of ultrasonic cleaning and thermal anneals at 900°C.

Conclusion: The Si-N and especially the BN films are composed of low-atomic-number materials that are resistant to X-ray damage such as that from a nuclear blast. These ceramic materials are resistant to effects of high-power lasers and atomic oxygen in low-Earth orbits. Multifunction coatings of these materials would protect against both natural and hostile threats.

NRL can reliably produce high-quality films to test theories on the processes occurring in ion-beam assisted deposition. Many interference devices have been fabricated, including quarter-wave dielectric stack mirrors, rugate filters, broadband reflection coatings, anti-reflection coatings, and X-ray mirrors. These devices may all have importance for the Navy.

[Sponsored by ONT]

Reference

1. E.P. Donovan, D. Van Vechten, A.D.F. Kahn, C.A. Carosella, and G.K. Hubler, *Appl. Opt.* **28**, 2940-2944 (1989). ■

Superfluorescent Fiber Source for Fiber-Optic Gyroscopes

W. K. Burns and I. N. Duling III
Optical Sciences Division

Fiber-optic gyroscopes are becoming more important for rotation sensing applications because they offer a solid-state alternative to conventional spinning mass gyroscopes, with potential for lower cost and longer life. One of the key components in the fiber-optic gyroscope is the optical source, which should be spectrally broadband, compact, and have good lifetime characteristics. To date, semiconductor diodes operated as spontaneous emission emitters (superluminescent diodes) have been used as fiber-gyro sources. These devices have been able to couple up to 3 mW into a single mode fiber, but both lifetime and wavelength stability have caused problems. We have investigated the use of neodymium (Nd)-doped active fiber as a spontaneous or "superfluorescent" emitter to solve these problems.

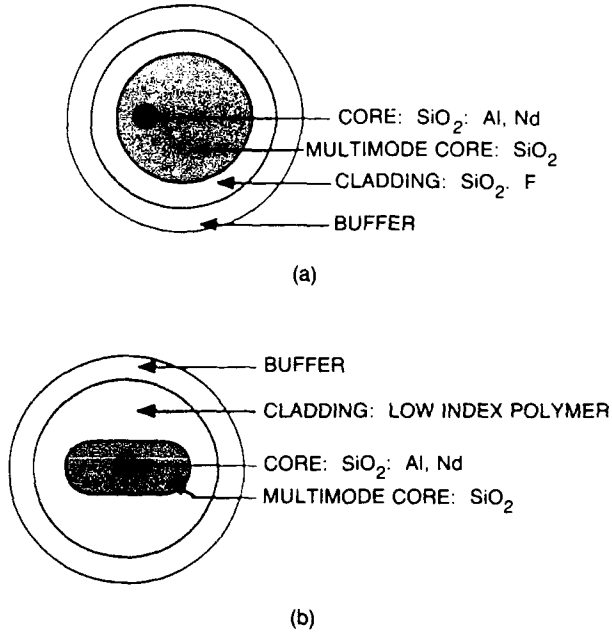

Fig. 4 — Geometry of dual-core fibers used to generate superfluorescent emission; (a) Fiber 1 with a plastic cladding layer and (b) Fiber 2 with a quartz cladding layer

Fiber Geometry and Pumping: The cross sections of the fibers we have used are shown in Fig. 4. These fibers were manufactured at the Polaroid Corporation [1]. In each case, a single-mode, Nd-doped core is surrounded by a multimode pump core, which in turn is surrounded by cladding and protective layers. Fiber 2 uses a plastic cladding layer, as opposed to a quartz cladding layer used in Fiber 1. This quartz cladding in Fiber 1 provides a larger refractive index change relative to the multimode core and allows more efficient coupling of the pump light.

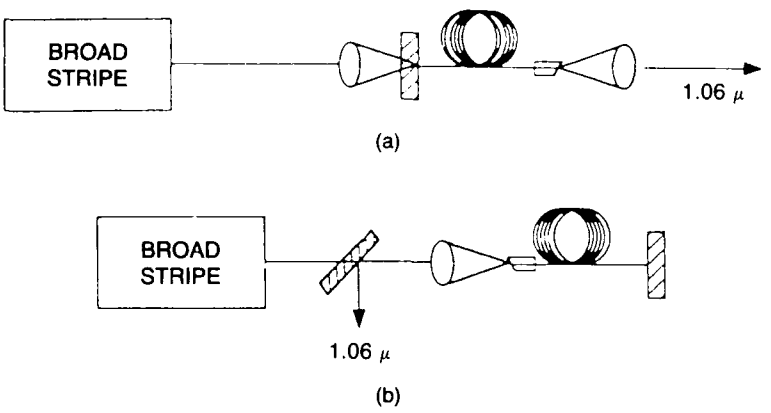

Fig. 5 — Configurations for pumping and extracting optical output from the active fiber. In (a) the output is taken parallel to the pump; in (b) the output is taken counterpropagating to the pump.

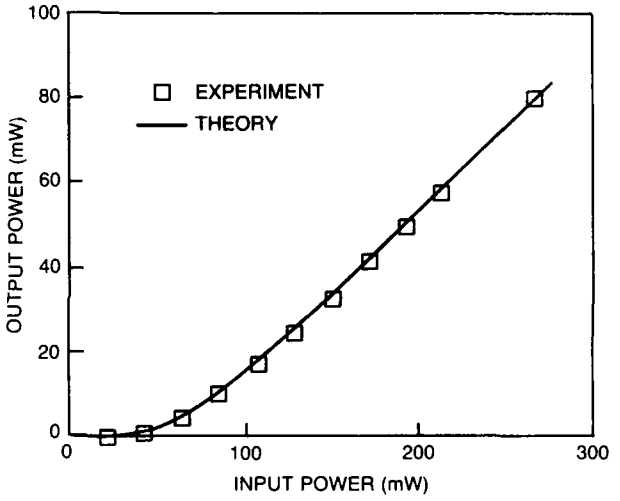

Fig. 6 — Output power vs pump power for Fiber 1 in the configuration of Fig. 5(b)

Since these fibers have a multimode pump core, they can be pumped by high-power, laser-diode arrays or broad-stripe lasers, which have multimode outputs. This allows higher power pumping and correspondingly higher source output.

Source Output: The fibers are pumped through their ends by broad stripe lasers with wavelengths near 0.81 μm as shown in Fig. 5. To avoid laser emission, reflectors are not used at all, or are used at one end of the fiber only, with the other end of the fiber cleaved at an angle to avoid back reflections. If back reflections are successfully avoided, a high-power, broadband, superfluorescent emission is observed from the Nd-doped core at 1.06 μm. An output characteristic for Fiber 1 in the configuration of Fig. 5(b) is shown in Fig. 6. We found that, with the configuration of Fig. 5(a), at high pump levels, Rayleigh backscattering in the fiber provided enough reflection to cause lasing rather than superfluorescent emission. This effect can be eliminated by removing the back reflector in Fig. 5(a). Fiber 2 was used in this manner to provide 40 mW of superfluoresent output in the forward direction.

Advantages of Fiber Sources: These fiber sources appear to have several significant advantages over semiconductor sources. Perhaps the most important advantage is related to the

thermal stability of the average emission wavelength; measurements at Stanford [2] indicate this is about an order of magnitude better than the semiconductor device. This emission wavelength stability translates directly into scale factor stability of the fiber gyroscope. Another significant advantage is the large optical power levels available. Since the signal-to-noise level improves with available optical power, sensitivity is improved. Also, a single source would have enough optical power to supply three gyros in a three-orthogonal-axis configuration, yielding three-axis-rotation information at lower cost. Finally, there is no lifetime issue for the fiber itself; the pump sources are expected to be long-life devices compared to the semiconductor spontaneous emission devices, so gyro lifetime should also be improved.

[Sponsored by ONT]

References

1 E. Snitzer, H. Po, F. Hakimi, R. Tumminelli, and B.C. McCollum, "Double Clad, Offset Core Nd Fiber Laser," Optical Fiber Sensor Conf., 1988 Technical Digest Series, Vol. 1, PD5, 1988.

2 K. Lice, M. Digonnet, K. Fesler, B.Y. Kim, and H.J. Shaw, "Broadband Diode Pumped Fiber Laser," *Electronics Lett.* **24**, 838-840 (1988). ■

High Performance Optical Phase Conjugation

P. S. Lebow
Optical Sciences Division

Optical phase conjugation (OPC) or wave front reversal is a nonlinear optical phenomenon that was first discovered in the early 1970s. Given a beam of light with a certain wave front, phase-conjugate replica is defined as having its wavefronts travel as though time were "running backward" when compared to the original beam. For instance, a beam diverging from a focal point will, in its phase-conjugate form, converge back to that point; a parallel beam traveling in some arbitrary direction will, after phase conjugation, be directed exactly opposite to the incoming light. Formally, if a wavefront is described by

$$\mathbf{E}(\mathbf{x}, t) = \mathbf{E}_0 e^{i(\omega t - \mathbf{k} \times \mathbf{x})} + c.c. \qquad (1)$$

then its phase-conjugate is written as

$$\mathbf{E}_{conj}(\mathbf{x}, t) = \mathbf{E}_0^* e^{i(\omega t + \mathbf{k} \times \mathbf{x})} + c.c. \qquad (2)$$

Comparing Eq. (1) to Eq. (2) shows that the conjugate wave has its spatial component complex conjugated relative to the initial wave. Thus, for increasing time, the spatial vector $\mathbf{x}$ must be decreasing to keep the overall amplitude constant; i.e., the conjugate wave is moving backward relative to the input.

It is particularly interesting to consider the behavior of this time-reversed wavefront as it experiences diffraction and refraction while propagating through a randomly distorting medium. It will, in fact, exactly retrace the path of the input wave as though a movie made of the incoming light wave were being played backward. The nonlinear device that generates this effect is called a phase conjugator or phase-conjugate mirror (PCM) because of this reversing property.

Practical Phase Conjugators: The most common form of PCM is based on the physical process called stimulated Brillouin scattering (SBS). In SBS, an intense light beam generates pressure fluctuations in a nonlinear medium, which in turn causes the incoming light to deviate or scatter from the path that it would normally take in a linear medium. In fact, the path that the scattered light does take turns out to be in the phase conjugate direction. Because these pressure fluctuations are by definition sound waves, they appear as moving index diffraction gratings that travel at the speed of sound for the medium.

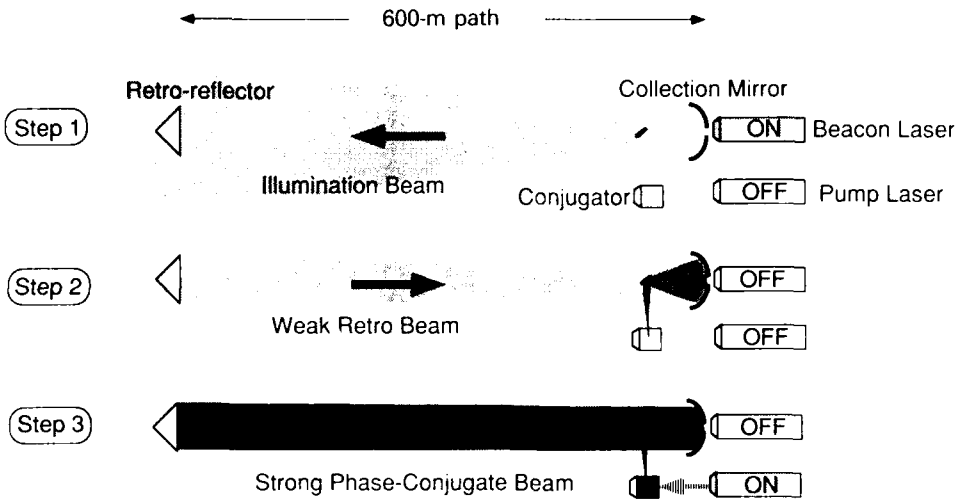

Fig. 7 — Atmosphere correction experiment

Because of this motion, the scattered light is Doppler shifted or *Brillouin shifted* with respect to the input.

An SBS conjugation falls within the general category of self-referencing conjugators because only one input and one output wave are involved. Techniques that use ancillary light beams in the phase conjugation process are called externally referenced conjugators. The most common of this variety are those that use four wave mixing (FWM). Typically the input signal beam is arranged to interfere with an oppositely directed pump beam. The nodes and antinodes in these interfering electric fields give rise to fluctuations in the polarization, or in effect, the index of refraction for the nonlinear medium. Again, as with SBS, a diffraction grating or hologram has been created. The difference in this FWM case is that a separate third wave, another pump wave opposite to the first pump wave, is simultaneously directed at this grating. The resulting scattered fourth wave is, as it turns out, phase conjugate to the input signal wave.

FWM PCMs can provide great practical advantages over self PCMs because the energy of the output beam is derived from the pump beams and not the input beam alone. Thus one can experience gain in the process of phase conjugation by converting pump energy to the phase-conjugate output beam. FWM techniques that are based on the same nonlinear effect used in SBS (electrostriction) have demonstrated extremely high gains. We have been able to demonstrate phase conjugation for light input levels as low as 10 picojoules with gains of more than 10 million. This technique, called Brillouin-enhanced four wave mixing (BEFWM) is being extensively studied in our laboratory [1].

Laser Pointing and Tracking: In addition to studies on the fundamental properties of BEFWM, we are actively pursuing applications involving laser beam transmissions over extended atmospheric paths [2]. In applications involving the direction of a laser beam at a remote object, a major source of loss is due to atmospheric turbulence. A laser beam experiences varying degrees of "beam spread" and "wander" depending on atmospheric conditions. These effects are beyond the reach of conventional optical correction techniques and are usually considered significant yet unavoidable loss factors. In certain situations, phase conjugation can be used to virtually eliminate these losses.

In a three-stage process, a divergent laser search beacon is sent out over an atmospheric test range (Fig. 7). A retroreflector is placed somewhere within this board area of illumination

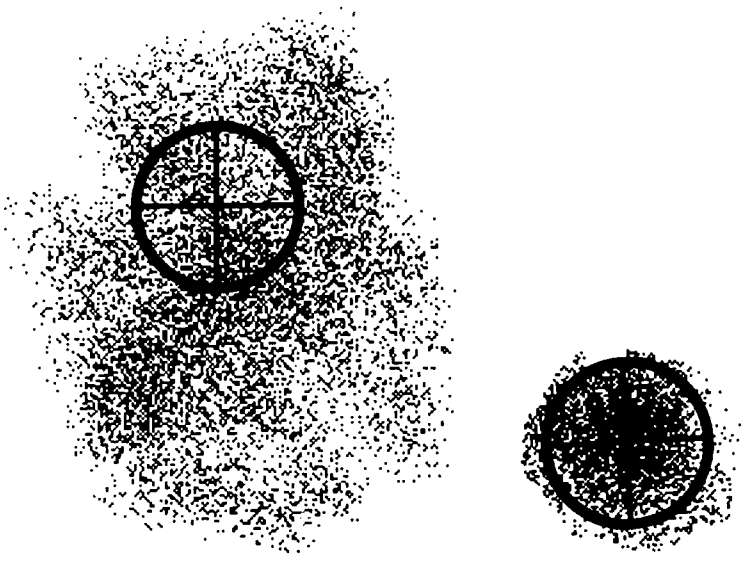

(a) Conventional mirror (b) Phase conjugator

Fig. 8 — Resulting target illumination patterns

and it sends back a very weak signal to a collection mirror. This weak light is focused into the phase conjugator, and simultaneously a strong pump laser also illuminates the conjugator. This turns the conjugator on, and an amplified phase-conjugate replica of the weak signal beam is sent back to the distant retroreflector. If a plane mirror were used in place of the conjugator, the laser beam profile back at the retroreflector would look similar to Fig. 8(a). With the conjugator, Fig. 8(b) shows the cancellation of the effects resulting from atmospheric turbulence. This, together with conjugator gains of more than a million, can greatly reduce the size and power requirements of lasers used in certain Navy pointing and tracking applications.

Phase conjugation, once considered an optical curiosity, has matured into a practical nonlinear optical technique. The ability to conjugate low light levels opens up new areas for applied research.

Acknowledgment: Dr. J.R. Ackerman of Sachs/Freeman Associates has made significant contributions to this research.

[Sponsored by NAVAIR]

References

1. J.R. Ackerman and P.S. Lebow, "Improved Performance from Noncollinear Pumping in a High-Reflectivity Brillouin-Enhanced Four-Wave Mixing Phase Conjugator," *IEEE JQE* 25, 479 (1989).

2. P.S. Lebow and J.R. Ackerman, "Phase Conjugation through Brillouin-enhanced Four Wave Mixing Over an Extended Atmospheric Path," *Opt. Lett* **14**, 236 (1989). ■

Coherent Laser Radar Measurements of High Velocity Targets

A. L. Huston and M. G. Roe
Optical Sciences Division

Laser radar is basically an extension of conventional radar to the shorter wavelength end of the electromagnetic spectrum. Virtually all known laser wavelengths between 250 nm and 10 μm are used for a variety of laser radar applications. Short wavelength operation provides better directionality, smaller sized optics, and

improved Doppler velocity and imaging resolution. Applications that use these advantages include remote wind velocity profiling for weather forecasting, atmospheric pollutant monitoring, wind shear detection for aviation safety, and target imaging for identification. We are developing a solid-state, coherent laser radar system that will combine both high-resolution velocity measurement and imaging capabilities of targets moving at velocities of several kilometers per second. These high velocities are typical of those that are expected for space-borne targets.

Doppler Velocimetry: Light scattered from a moving surface experiences a shift in frequency that is inversely proportional to the wavelength and directly proportional to the velocity of the target. The target velocity is obtained from a measurement of the frequency shift. Optical heterodyne detection provides a very sensitive, precise method for measuring frequencies. With this technique, scattered light from the target is mixed with a reference laser to produce a beat signal at a frequency that is equal to the difference between the reference and Doppler-shifted laser frequencies. For very high velocities, the beat signal frequency may exceed the frequency response capability of the detection system. In this case, the local oscillator must be frequency offset to compensate for the limited bandwidth of the detection system. The recent development of tunable, single frequency Nd:YAG lasers provides an ideal source for offset-frequency, heterodyne-detected Doppler velocimetry. The Nd:YAG laser wavelength is 1.06 μm and the Doppler shift factor is 1.89 GHz/km/s.

Laser Radar System: Figure 9 is a schematic of the coherent laser radar system. The output of a 40-mW, diode-pumped Nd:YAG laser is double-pass amplified in a flashlamp-pumped Nd:YAG rod operating 10 pulses per second. The amplified pulse is directed through a series of polarizing elements and is then transmitted to a target inside a vacuum chamber. Scattered light

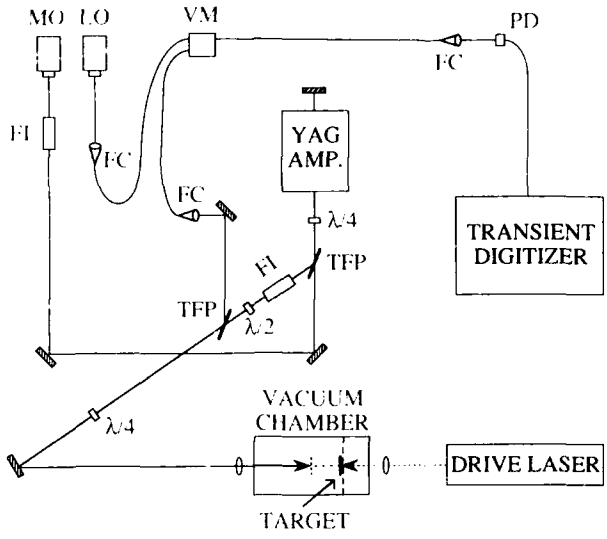

Fig. 9 — The two-oscillator laser radar system and the laser accelerated target apparatus (MO-master oscillator; LO-local oscillator; VM-variable ratio mixer; PD-photodiode; FI-Faraday isolator; FC-fiber coupler; TFP-thin film polarizer)

from the target returns along the same path and is reflected by a thin film polarizer and focused into a polarization-preserving, single-mode fiber. A 5-mW, frequency-offset Nd:YAG laser used as the reference or local oscillator, is focused into a similar fiber. The scattered return signal and the local oscillator are mixed in a variable ratio fiber coupler, and the resultant beat signal is detected with a 1 GHz frequency response avalanche photodiode. Signals are recorded and Fourier transformed to determine the frequency components in the return signals.

Targets are accelerated to very high velocities by using a laser ablative acceleration technique. Aluminum foils approximately 1 mm in diameter and 12 to 50 μm thick are attached to a silica window inside a small vacuum chamber. A 2-J, Q-switched ruby laser is focused through the window onto the foil target to generate a plasma that rapidly expands, driving the foil disk into the vacuum chamber.

Experimental Results: Figure 10 shows examples of waveforms obtained for 25-μm thick aluminum foils and their associated Fourier transforms. Waveform A is an example of a measurement with a good signal-to-noise ratio.

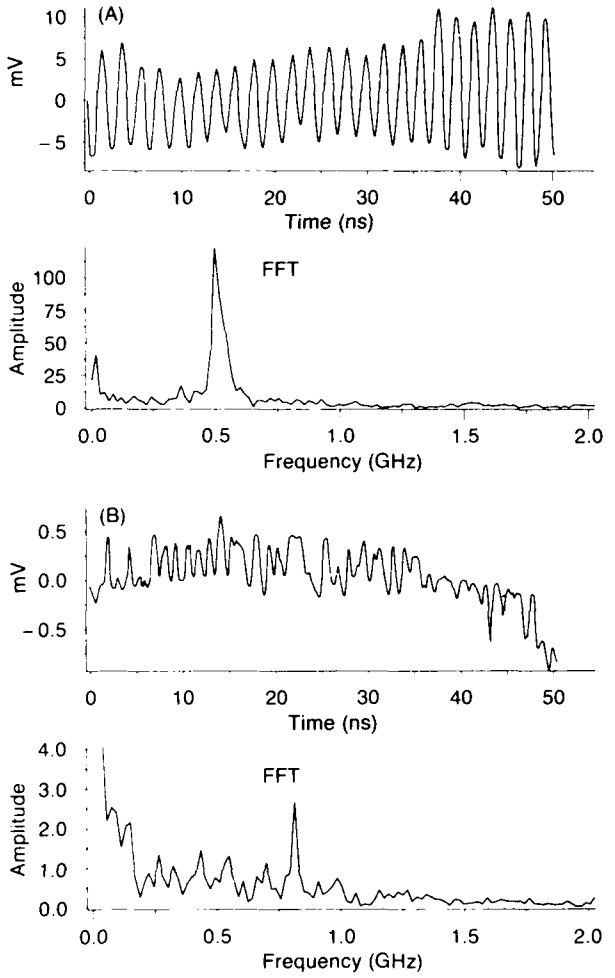

Fig. 10 — Typical waveforms from 25-μm-thick aluminum targets with associated Fourier transforms. A-offset frequency 2.5 GHz; v = 1.59 km/s; B-offset frequency 1.5 GHz, V = 1.23 km/s.

The Fourier transform shows a very distinct frequency at ~500 MHz. The local oscillator had an offset frequency of 2.5 GHz from which a velocity of 1.59 km/s is calculated. Without the local oscillator offset capability, the beat frequency would have been 3 GHz, which is well beyond the 1 GHz response of our detection system. Waveform B is an example of a low signal-to-noise measurement, yet the Fourier transform still shows a distinct peak at ~800 MHz. For this measurement, the local oscillator frequency offset was 1.5 GHz, and the velocity was calculated to be 1.23 km/s.

Figure 11 shows the results of a series of velocity measurements on aluminum flyers of

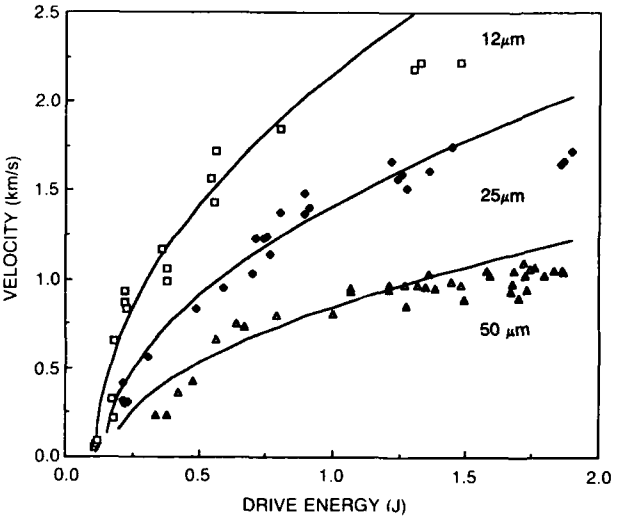

Fig. 11 — Velocities of aluminum disk targets as a function of ruby laser energy

three different thickness as a function of ruby laser energy.

Summary: We have developed a coherent laser radar system that can measure velocities of targets in the multikilometer-per-second range. The method for accelerating targets to very high velocities in a laboratory environment provides a convenient means for simulating conditions that would be encountered in space. We are working on a multiaperture, coherent receiver array that will allow us to simultaneously obtain image and velocity information.

[Sponsored by SDIO] ■

Forward Photorefractive Multibeam Mixing

G. Charmaine Gilbreath
Space Systems Development Department

In a spacecraft's optical communications link, maintaining a high signal-to-noise ratio is very important for sustaining a low bit error rate. Phasefront errors, even small ones, have a significantly deleterious effect on both of these parameters. Therefore, a method of correcting in real time the phasefront of the optical beam used in a satellite optical data link is very desirable.

Photorefractive coupling may provide the means to accomplish this goal. The photorefractive effect is one where a medium is modulated by incident light. The photorefractive medium can be erased and rewritten. Holograms can be written in photorefractive media that are self-developing, erasable, and rewritable. The photorefractive device has an additional important property. Energy from a strong beam can be made to couple into a weaker beam [1]. Hence, a kind of amplification can occur.

Previous work has been concerned with plane wave interactions. In this research, nonplanewave interactions, which reflect the more realistic case, are studied [2]. To do this, a given beam is seen as a family of plane waves where the external Poynting vectors span a given divergence. A theory is developed by using this multibeam approach to predict photorefractive gain as a function of the spread in the angular spectrum or the extent to which one or both the beams are phase aberrated. The theory is experimentally verified by using $BaTiO_3$ at 514.5 nm. Three-beam coupling is studied.

The theory for a diffusion-driven photorefractive material yields three coupled, nonlinear differential equations describing the interaction of beam intensities as they transverse the medium, i.e.,

$$\frac{dI_s(z)}{dz} = \frac{\Gamma}{I_0}\{I_s(z)I_{p1}(z) + I_s(z)I_{p2}(z)\}, \qquad (1)$$

$$\frac{dI_{p1}(z)}{dz} = \frac{\Gamma}{I_0}\{I_{p1}(z)I_{p2}(z) - I_s(z)I_{p1}(z)\}, \qquad (2)$$

and

$$\frac{dI_{p2}(z)}{dz} = -\frac{\Gamma}{I_0}\{I_s(z)I_{p2}(z)I_{p1}(z) + I_{p1}(z)I_{p2}(z)\}, \qquad (3)$$

where I_s is the intensity in the signal beam and I_{p1} and I_{p2} are the two pump components separated by an angle $\Delta\alpha$. I_0 is the total intensity prior to coupling, and Γ is the exponential gain coefficient determined by material parameters and geometry.

These equations do not have closed-form solutions and are numerically evolved by using a Runge-Kutta algorithm to gain insight to the effects of divergence on overall gain (gain is defined as the ratio of the energy coupled into the signal when the pump is present to the energy in the signal when the pump is not present). Figure 12 shows the results of one set of parameters in which the two pumps are separated by a large angle ($\sim 4°$ inside the medium). This figure shows that asymmetric depletion out of a pump beam characterized by large variations in phase is predicted, even for long interaction lengths. For short interaction lengths, although one pump component depletes, the other pump component experiences gain. This is to the detriment of the signal beam for which the gain is small. At longer lengths, both pumps eventually do deplete but asymmetry—hence, less efficient coupling—results even for long lengths.

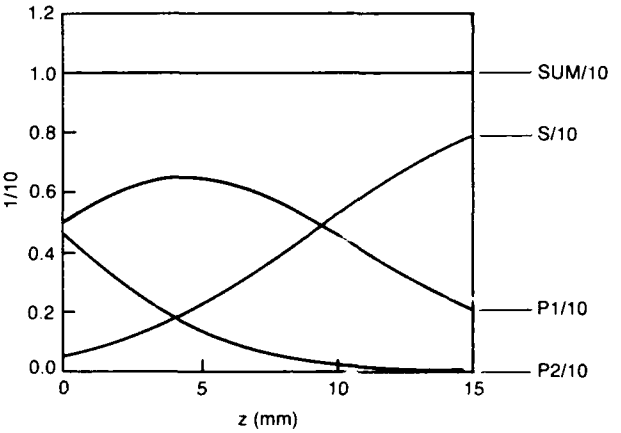

Fig. 12 — Normalized intensity vs interaction length for $BaTiO_3$: $\alpha_s = \alpha_{p1} = 1.85°$ (inside medium); $\alpha_{p2} = 5.93°$; $\Delta\alpha = 4.05°$; $m_{spi} = 10$, $m_{p1p2} = 1$. For short interaction lengths, P_1 exhibits gain. Over longer lengths, both pump components deplete but asymmetrically. Hence, a much longer crystal is required to reach saturated gains in the signal beam when large phase variations are present on the pump beam.

Figure 13 shows that these analytic results are borne out experimentally. Forward beam coupling was examined for varying geometries by using $BaTiO_3$, which is a photorefractive crystal with very high gain and a three-beam interferometric configuration. The interaction length for the

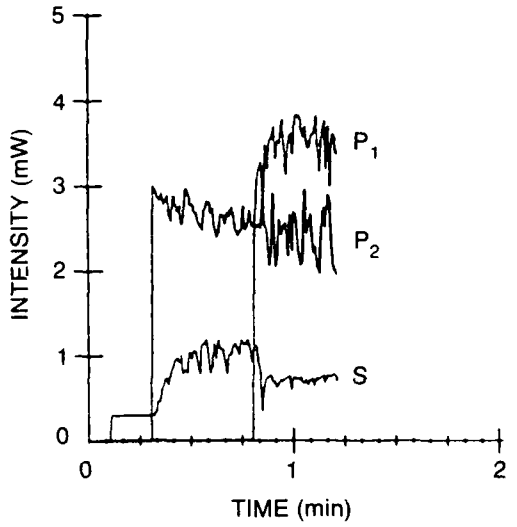

Fig. 13 — Intensity vs time for configuration described in Fig. 12. Signal component loses energy in the presence of three beams for the experimental interaction length (3 mm).

crystal was on the order of 3 mm. The shuttering sequence was varied. For $\Delta\alpha = 4.05°$ and Γs as noted in the figure caption, beams coupled as predicted in Fig. 12. $\mathbf{P}_2$ depleted but $\mathbf{P}_1$ experienced gain. The signal S actually lost energy in the presence of $\mathbf{P}_1$.

Further experimentation for various geometries showed that the shuttering sequence was irrelevant at steady state. The two-beam components that formed the largest exponential gain dominate the interaction. Consequently, large phase variations on the pump beam affect the nature of the energy coupling. If a large phase variation is present on the pump, asymmetric depletion can result. Hence, gains in the signal will be less, especially for materials with comparatively small ΓL_{eff} products.

Similar experiments studied the effects of phase variations on the signal beam when the pump beam was characterized as a plane wave. Asymmetric coupling was again observed, leading to the conclusion that large variations on the signal can mean nonuniform amplification of the signal beam's phasefront.

These results have important implications if the photorefractive device is to be used as a kind of optical amplifier, as in optical spacecraft communications. Geometry, beam ratio, and material parameters become critical in designing a system that anticipates large phasefront changes over the lifetime of the system.

[Sponsored by ONR]

References

1. D.L. Staebler and J.J. Amodei, "Coupled-Wave Analysis of Holographic Storage in $LiNbO_3$," *J. Appl. Phys.* **43**, 1042 (1972).

2. G.C. Gilbreath and F.M. Davidson, "Non-plane Wave Two-Wave Mixing Interaction in Diffusion-Driven Photorefractive Media," *S.P.I.E. Proc.* **1136**, 290 (1989). ■

Space Research and Technology

SPACE RESEARCH AND TECHNOLOGY

NRL has been involved for many years with various aspects of space research in the fields of astrophysics and astronomy, atmospheric science, and solar-terrestrial interactions, as well as with spacecraft engineering and systems development. Reported in this chapter is theoretical and observational work relating to high-speed solar wind streams, millisecond X-ray pulsars, Earth's magnetosphere, large space structures, and satellite theory.

This work was performed in the Space Science Division (4100), the Plasma Physics Division (4700), and the Spacecraft Engineering Department (8200).

Other current research in space includes:

- Ionospheric variability
- Accreting white dwarf stars
- Cosmic ray source abundance
- LIPS III spacecraft
- Low altitude/airspeed unmanned research aircraft (LAURA)

The Source of High-Speed Solar Wind Streams

K. P. Dere, J.-D. F. Bartoe,
and G. E. Brueckner
Space Science Division

Coronal Physics: The dynamics of the outer solar atmosphere are controlled by the solar magnetic field, which is generated below the solar surface. Because of the buoyancy of magnetic fields embedded in a dense plasma, the fields pop up through the surface in the form of active regions, sunspots, and small structures simply called emerging-flux regions that appear across the solar surface. Coronal holes are large regions on the sun where the magnetic field is primarily of one polarity. Instead of forming closed field line structures such as coronal loops, the field lines are open and extend outward from the sun into interplanetary space. The hot coronal gas at the base of the coronal hole expands, and the plasma is further accelerated along the open field lines to form high-speed solar wind streams. When these streams sweep past Earth as the sun rotates, they are accompanied by enhanced geomagnetic activity, such as is seen in auroral displays. Existing theories can explain some of the properties of coronal holes and high-speed solar wind streams in a general way, but the actual sources of the outward mass flux and the nonthermal acceleration mechanism are still not understood.

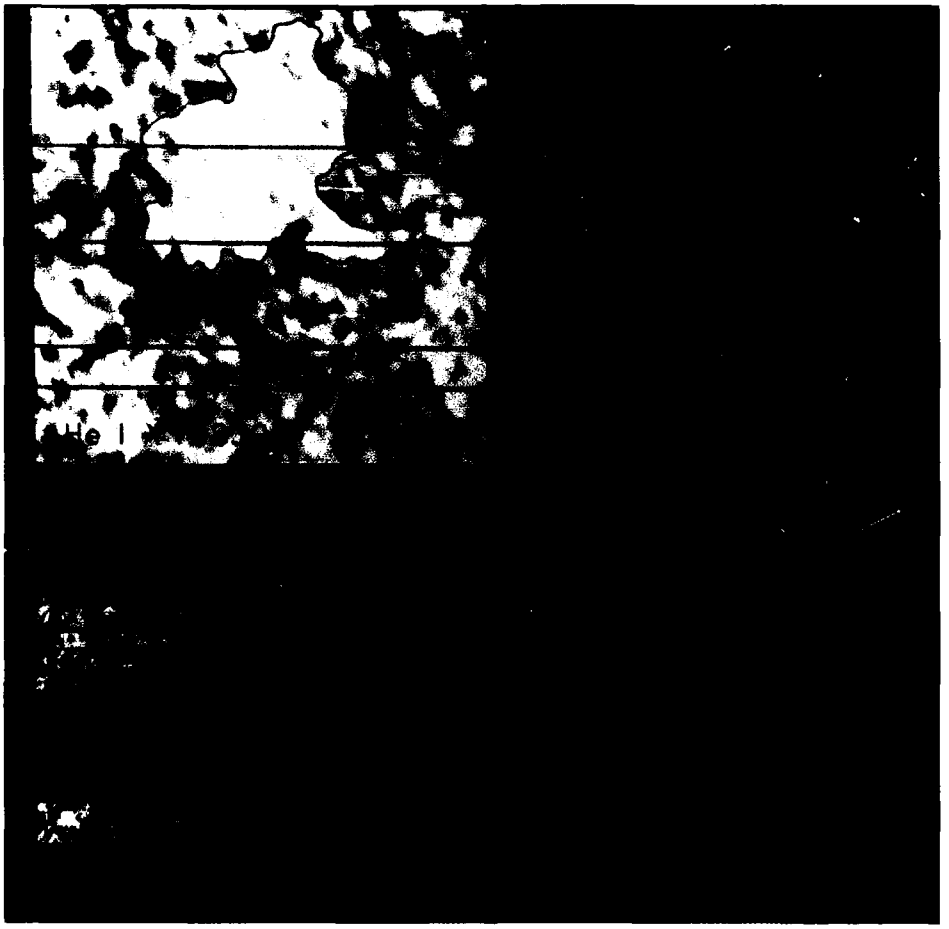

Fig. 1 — Upper left: He I λ10830 spectroheliogram of the sun with boundaries of the coronal hole outlined. Upper right: Intensity image of C IV λ1550 transition region emission. Lower left: Doppler image of C IV λ1550 transition region (blue – outflows; red – downflows; white – no net flow; black – insufficient intensity). Lower right: image of the nonthermal broadening in Ci IV λ1550 transition region.

Rocket Observations of the Coronal Source: The capabilities of the NRL High Resolution Telescope and Spectrograph (HRTS) are well suited to detect and characterize the sources of the solar wind mass flux at the coronal base. The HRTS consists of a 30-cm telescope and a stigmatic ultraviolet spectrograph that operates between 1200 and 1700 Å. On November 20, 1988, the HRTS was launched on a NASA Black Brant rocket to obtain ultraviolet spectra of a solar coronal hole. The observations are made by recording spectra along a slit that is half a solar radius long. This slit is repeatedly stepped across the solar disk so that spectra are obtained in long, narrow strips of the solar surface. The intensity, velocity, and linewidth of the ultraviolet spectral line profiles of the C IV ion, formed in the solar transition zone at 10^5 K, are measured; Fig. 1 shows the corresponding images (*The Astrophysical Journal* **345**, L95 (1989). The outline of the coronal hole is determined from the He I λ10830 spectroheliogram made at the Kitt Peak National Observatory (upper left corner of Fig. 1). The HRTS images show that the intensity of C IV in the coronal hole is somewhat less than in the quiet sun. The velocity data are displayed such that outflows from the solar surface are blue and downflows are red. The most important result of the rocket flight was the discovery that the outflows in the coronal hole cover only ~25% of the total area of the coronal hole and that most of the flows are downflows. Previous flights have shown that in the quiet sun, outflows cover only 7% of the total area. Some theories have predicted that, in addition to the thermal pressure of the hot plasma, a significant amount of wave motions could occur that could help accelerate the high-speed solar wind streams. These wave motions should show up as an enhanced line width in the coronal hole line profiles. The data show that the average line width inside the coronal hole is essentially equal to that outside the coronal hole so that these motions cannot explain the difference between the high- and low-speed solar wind streams.

These observations clearly show that more outflows are at the base of a coronal hole than in the quiet sun but that these outflows are in small, isolated structures. Longer term observations of these sites of the outward mass flux are now needed to understand the mechanism that injects this material into the solar wind streams.

[Sponsored by NASA] ■

The Search for Millisecond X-ray Pulsars

P. L. Hertz, J. P. Norris, and K. S. Wood
Space Science Division

Theorists have recently predicted that the brightest sources of cosmic X rays in our galaxy, the low-mass X-ray binaries (LMXBs), may emit periodic X-ray pulses with periods as short as 1 ms. These close binary star systems consist of a low-mass, normal companion star closely orbiting a neutron star, which is the collapsed remnant of a more massive star. The separation between the two stars is small enough that material from the atmosphere of the companion star is gravitationally captured by the neutron star. Up to 10^{31} W in X rays are produced in the accretion process through the conversion of the gravitational potential energy of the infalling matter to radiation. Although millisecond X-ray pulsations have not yet been seen, NRL scientists are using sophisticated data analysis techniques to search for the pulses as well as to better constrain the models used to predict their existence.

Predictions of Millisecond X-ray Pulsars: Two phenomena have recently been discovered that can be explained by theories incorporating millisecond spin periods for neutron stars in LMXBs. The first is the 1983 discovery of millisecond-period radio pulsars. The millisecond radio pulsars are quite old ($\sim 10^8$ yr) and are believed to have been spun up to their current spin rates. This can be best accomplished by means of the accretion process during which orbital angular momentum is transferred to the neutron star. If

correct, this scenario implies that some LMXBs should have millisecond-period spinning neutron stars. The second new observational result is the 1985 discovery of quasi-periodic oscillations (QPOs) in LMXBs [1]. In the popular beat-frequency modulated-accretion (BFMA) model, QPOs are the beat frequency between the Keplerian orbital period at the Alfven radius and the neutron star spin period. Shots of clumped accreting matter are chopped out of the accretion stream at the beam frequency and quickly (< 1 ms) fall to the neutron star surface, preserving the beat pattern. From the observed QPO frequencies (5 to 36 Hz) and the magnetic field ($\sim 10^9$ G), the spin period is ~ 5 to 10 ms.

Any rotating, accreting, magnetized neutron star will pulse. The amplitude for LMXB pulsars will be small because the magnetic fields are small and the signal is reduced by magnetospheric effects and gravitational lensing. The signal will be further degraded by Doppler smearing from the orbital motion of the neutron star.

Search for Millisecond X-ray Pulsars: The most sensitive search requires data with a high count rate, high time resolution, and long integration times. The long integration times allow significant Doppler smearing, and the orbits of the sources are not known with enough precision to correct the photon arrival times. Searching through the complete 3-D phase space of possible orbits (period, semimajor axis, phase) is prohibitively expensive for large data sets (> 106 samples), requiring millions of test orbits and millions of fast Fourier transforms (FFTs). We have developed an optimal 1-D search algorithm that is mathematically equivalent to fitting a parabolic approximation to the test orbit. For our data sets with submillisecond resolution and up to 4×10^6 samples, our method still requires 3000 FFTs.

We implemented the search routine on the NRL Connection Machine CM-2, a massively parallel computer containing 16,384 processors. Data were obtained from three of the most sensitive large-area X-ray satellites ever flown: the European EXOSAT satellite, the Japanese Ginga satellite, and NRL's experiment on HEAO-1. The LMXBs studied include Scorpius X-1, Cygnus X-2, GX5-1, GX9+1, and 4U1820-30. Sco X-1 is the brightest X-ray source in the sky, Cygnus X-2 and GX5-1 are classical QPO sources, GX9+1 is the brightest non-QPO LMXB, and 4U1820-30 is an exotic 11-min binary located at the core of a globular star cluster.

Our analysis yielded upper limits to the power emitted in short period pulsations of $\sim 1\%$ of the total flux [2]. The result is consistent with theory and represents the most sensitive search possible with existing data.

Testing QPO Theories: Since confirmation of the BFMA model through detection of millisecond pulsars is not currently possible, we have tested other aspects of the theory through direct study of QPOs. In the BFMA model, a correlation is expected between the QPO amplitude and the amplitude of the shot of clumped matter that carries the QPO beat pattern. Sensitive statistical techniques developed at NRL show that this correlation is not present in the data. Thus the underlying assumption of the BFMA model, that the Keplerian period is introduced into the accreting material by dividing it into shots, cannot be true. More sophisticated models are required to explain these new empirical properties, and new models might not require millisecond rotation periods for the neutron star.

Future Prospects: Our ability to detect millisecond pulsations in the frequency domain and individual QPO oscillations in the time domain are both limited by the X-ray signal collected during a single cycle. Future generations of orbiting X-ray detectors will require areas exceeding the 1 m^2 of current and recent missions. One possibility is the 100 m^2 X-ray Large Array that we have proposed to fly as an attached payload to Space Station Freedom. Until detectors with the requisite collecting area and time resolution are in orbit, progress will continue to be made by

developing advanced data analysis techniques that push existing data to its statistical limits.

[Sponsored by NASA and ONR]

References

1. J.P. Norris and P.L. Hertz, "QPOs: A New Astronomical Mystery," 1988 NRL Review, p. 206.

2. P. Hertz, J.P. Norris, K.S. Wood, B.A. Vaughan, and P.F. Michelson, "Search for Millisecond X-ray Pulsations from the Galactic Bulge X-ray Source GX9+1," *Astrophys. J.* **352**, in press (1990). ■

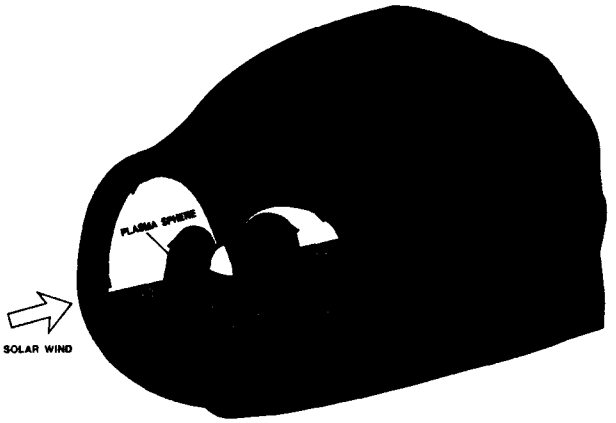

Fig. 2 — Cut-out view of the magnetosphere. The magnetotail stretches hundreds of Earth radii away from the sun. The sphere is Earth with the night side shaded. The lines with arrowheads represent magnetic field lines. The "magnetospheric" coordinate system is shown.

Chaos in the Magnetospheric Particle Dynamics

J. Chen
Plasma Physics Division

The dynamics of magnetospheric plasma plays an essential role in a wide range of space phenomena affecting the terrestrial environment. These phenomena include dramatic auroral displays and magnetic disturbances that can disrupt military as well as civilian facilities—communication networks (C^3I), navigation and radar systems, and power plants. These effects are manifestations of magnetospheric "substorms" arising from the interaction of the solar wind and Earth's magnetosphere. The substorm phenomenon is and has been a subject of keen interest to scientists throughout the world for a number of decades because of its scientific and practical importance. However, the underlying physical mechanism is still not well understood.

Figure 2 is a schematic diagram of the magnetosphere in relation to Earth (the sphere at the center) and the solar wind. The magnetosphere is a complex system filled with tenuous, highly ionized plasmas. A region of particular importance for substorms is the magnetotail, which is on the night (shaded) side of Earth.

Extensive research on particle motion in the magnetotail started in earnest in the 1960s. Recently, NRL scientists discovered [1] that particle motion in the magnetotail is stochastic and that the phase space available to the particles is partitioned into disjoint regions occupied by three distinct types of orbits—stochastic, transient, and integrable. An important property is that widely separated time scales are associated with the motion of these distinct types of orbits. This novel realization suggested that the phase space partition would cause a natural tendency for the plasma to develop various non-Maxwellian distributions. This process was referred to as "differential memory." Such distributions are known to have significant and profound influences on the magnetospheric plasma dynamics and, hence, on the terrestrial environment.

Figure 3 shows the structure of a representative constant-energy phase space surface. The horizontal axis is V_x and the vertical axis is V_y. The color scale gives roughly the time during which particles are "trapped" near the equatorial region of the magnetotail. The large dark blue region is the integrable region in which the particles are trapped indefinitely (computed to 2000 time units, each unit being ~1 s). The well-defined red-brown-yellow regions are the

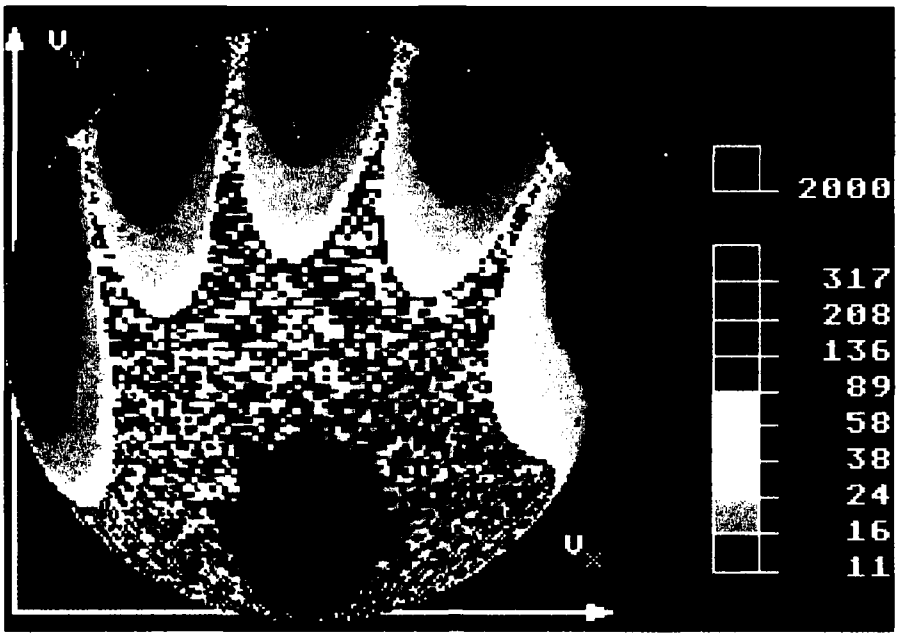

Fig. 3 — Partition of the phase space and separation of time scales between disjoint regions. The color of each "point" gives the amount of time in which a particle starting from that point spends near the equatorial plane before escaping from the system. One time unit is on the order of 1 s.

transient regions in which the particles spend relatively short periods of time. The remaining region is the stochastic region where the typical trapping time is intermediate to those of the transient and integrable regions.

We have recently verified the concept of differential memory. To elucidate the physical process, we first use a model in which the particle orbits can be calculated analytically [2]. This model possesses similar structures to those of Fig. 3. Figure 4 shows a time-sequence of the distribution function f in the equatorial plane plotted against $\log_{10}(h)$, where h is the particle kinetic energy. Initially ($\tau = 0$), f is taken to be an isotropic Maxwellian distribution f_{in}. The distribution function of the source region far away from the equatorial plane is f_{out}. If $f_{in} = f_{out}$, then the distribution f remains unchanged. As an example, we consider a scenario in which the source distribution function changes to $f_{out} < f_{in}$. As time τ progresses, the particles in the transient regions escape first, followed by those in the stochastic regions. Information concerning the

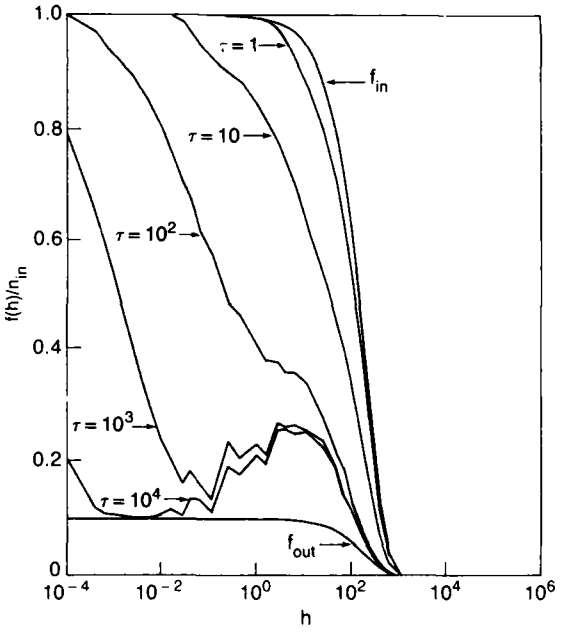

Fig. 4 — Time evolution of a distribution function $f(h)$

initial equatorial region plasma (f_{in}) is gradually lost. The particles from the source region then populate these regions, bringing with them information regarding the source plasma (f_{out}). The integrable orbits do not escape, and the particles

from the source region have no access to the integrable regions. The new distribution function f retains the memory of the initial particle distribution for different lengths of time in different regions of the phase space, hence the designation "differential memory." At $\tau = 10^4$, f is nearly equal to f_{out} except in the integrable regions, where the memory of the initial distribution ($f_{in} > f_{out}$) is retained indefinitely. This produces the peaks in the $\tau = 10^4$ curve. For some energy values (e.g., $h \sim 10^{-3}$ to 10^{-1}), only a small fraction of the phase space is occupied by integrable orbits so that $f \simeq f_{out}$ at $\tau = 10^4$. The distribution function is also predicted to develop specific, potentially observable anisotropies in the profiles of average velocity and temperature.

Note that the anisotropy results solely from the partition of the phase space, which is a property of this chaotic system. Contrary to usual expectations, chaotic particle dynamics give rise to more ordered (non-Maxwellian) rather than random (Maxwellian) distributions of particles in the magnetotail. We have shown that this leads to distinct and characteristic observable signatures not realized previously. These distributions represent rearrangement of the internal energy of the magnetospheric plasmas and can have important influences on the dynamics of the magnetosphere. Consequently, differential memory is a mechanism that allows the solar wind to profoundly and directly control the magnetospheric dynamics and its influences on the terrestrial environment. This is in contrast to a traditional scenario in which the solar wind energy is "loaded" into the magnetosphere in the form of a stressed magnetic field and is subsequently released (unloaded) in substorms.

When applied to the central plasma sheet, one characteristic signature predicted by our theory is that the valleys and peaks in the plasma distribution functions are nearly equally spaced if plotted against the fourth root of the particle kinetic energy. This scaling, a novel prediction, is a direct consequence of differential memory. We have found such features in distribution functions actually observed by satellites. This agreement is tentative at this time, and we are carrying out active research to establish it more definitively. If confirmed, it will be the first identification of observational signatures of differential memory in space and will provide a new means to understand the solar wind–magnetosphere interaction. This will help increase the predictive capabilities to forecast events in space that can cause disruptions to terrestrial activities.

We have also obtained the first documentation of fractal boundaries in the magnetotail particle dynamics. Illustration is provided in the Color Presentation section of this *Review*.

Acknowledgment: G. B. Burkhart, H. G Mitchell, and J. L. Rexford of Scienc Applications International Corporation have made significant contributions to this research.

[Sponsored by ONR and NASA]

References

1. J. Chen and P.J. Palmadesso, *J. Geophys. Res.* **91**, 1499 (1986).

2. J. Chen and H.G. Mitchell, and P. Palmadesso, accepted *J. Geophys. Res.* 1989.

■

Design of the LACE Flight Dynamics Experiment

S. Fisher
Spacecraft Engineering Department

An understanding of the dynamic behavior of large orbiting space structures is of supreme importance to the development of the modern spacecraft needed to address Navy requirements. With the complex geometric shapes, high-bandwidth controllers, and stringent antenna-pointing requirements of spacecraft now being planned, structural excitations generated by the attitude-control system or environmental forces are a critical concern in spacecraft design. Controls-structures interaction (CSI) research is

dedicated to the development of techniques for treating these effects. CSI methods are now needed for such applications as lightweight antennas and support structures, long booms for isolating sensors or power sources, large solar panels, radiators for cooling cryogenic sensors, and aerobrakes for atmospheric reentry. Furthermore, CSI techniques can be useful in "litesat" development by allowing a reduction of structural weight to improve payload size.

The Low Power Atmospheric Compensation Experiment (LACE) described here is a piggyback opportunity to provide an early assessment of the on-orbit dynamics of a large spacecraft. The dynamics experiment is a low-cost secondary experiment that exploits the characteristics of the LACE spacecraft.

Brief Description of the LACE Experiment: The LACE is designed to assess the effectiveness of compensating the atmospheric refraction of ground-based lasers aimed at an orbiting satellite. LACE includes ground apparatus and a spacecraft scheduled for deployment in early February 1990 on a DELTA 2 launch. The orbit will be circular, with a 556-km altitude and a 43° inclination. The spacecraft carries a retroreflecting array of glass corner cubes mounted at the end of a long boom attached to the leading side of the spacecraft bus. The spacecraft also has a zenith-directed boom for gravity gradient stabilization, a momentum wheel, and a trailing balance boom. In the experiment, the retro array is first targeted by an illuminating laser beam located near the ground site of the primary or scoring laser source aimed at the spacecraft base. Reflection from the retro array provides information about atmospheric refraction conditions to shape the optical surface of the source mirror of the scoring laser such that its wavefront will be spherical after the beam traverses the atmosphere. The scoring laser is then fired. After the laser beam strikes the LACE spacecraft, sensors on the base of the spacecraft bus measure the beam spread and energy deposition.

The LACE spacecraft is truly a large space structure. It has been described as a "flying chimney." The structure includes an aluminum bus 1.37-m square and 2.44-m tall, of mass 1409 kg. The three deployable/rectractable, fiberglass booms attached to the bus have diameters of 0.254 m and lengths of up to 45.72 m. The zenith-facing gravity-gradient boom has a tip mass of 90.6 kg, with each of the other two booms having a tip mass of 15.9 kg. Attitude stabilization is accomplished by gravity-gradient torques and by a momentum wheel. A magnetic damper is installed at the tip of the gravity-gradient boom to damp the libration oscillations. The lowest vibration frequency of this structure with the three booms deployed is ~ .02 Hz, i.e., a period of 50 s.

Design of the Flight Dynamics Experiment: The LACE dynamics experiment (Fig. 5) is a study of the on-orbit vibration characteristics of the spacecraft. The experiment hardware consists of germanium corner reflectors on the base of the bus and at the ends of the retro boom and balance boom. The FIREPOND laser radar at the MIT Lincoln Laboratory will illuminate the cubes to measure the relative range rate of the boom tips with respect to the bus. Absolute bus rotation rates will be measured by means of the on board Ultraviolet Plume Instrument (UVOI). Measurements will be made of vibration frequencies, damping ratios, and oscillation amplitudes, as well as the vibration intensity generated by boom deployments and retractions.

Issues Addressed by the Flight Dynamics Experiment: Structural modeling, environmental interactions, and boom deployment dynamics are areas where the LACE flight dynamics experiment can provide useful data. At the present time, estimates of the vibration frequencies are based on static ground tests of the boom structure. The flexural rigidity value obtained thereby ranges from $1.26 * 10^4$ N - m^2 to $1.6 * 10^4$ N - m^2, giving an uncertainty in the vibration frequencies of ~20%. Further uncertainties in the vibration

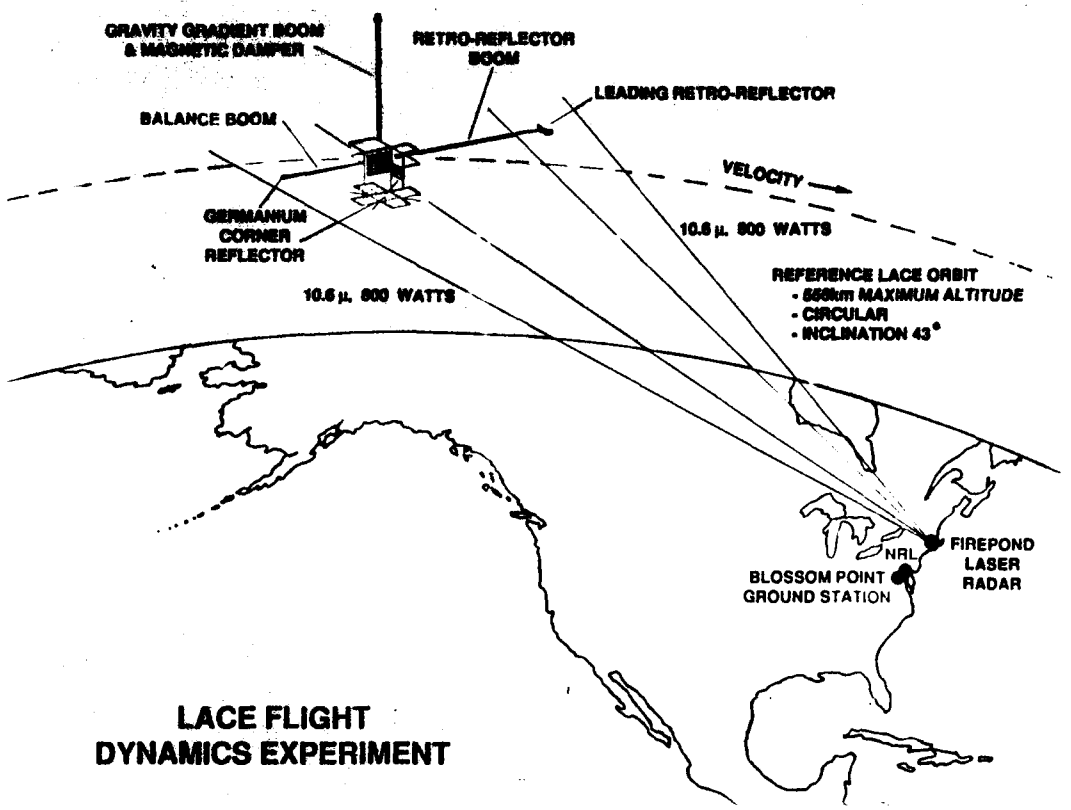

Fig. 5 — LACE Flight Dynamics Experiment showing targeting from FIREPOND laser radar at MIT Lincoln Laboratory

frequencies, as well as in the gravity-gradient libration frequencies, are generated by twisting from differential day/night heating. The amount of vibration damping is not well known; some ground testing of damping has been made. In the SAFE experiment of 1984 [1], a flexible, deployable "wing" of polymer film was attached to a boom similar to the LACE booms. Damping rates were observed to be nonlinear [2] with most of the damping induced by the attached wing. In the case of LACE with no boom attachments, the experiment will measure the damping intrinsic to the boom structure. A comparison of ground-based damping with the on-orbit damping will provide a mechanism to evaluate the microbehavior of unloaded joints.

Other outputs from the flight dynamics experiment are an estimation of the influence of magnetic torques, gravity-gradient torques, and atmospheric drag on a large, flexible structure. The experiment will furnish a comparison of boom deployment/retraction vibration amplitudes with those observed with the SAFE experiment.

Numerical Simulations of Spacecraft Structure and Dynamics: Since ground testing of the fully deployed LACE spacecraft is not possible, numerical simulations have been made by using data from the static ground tests of the boom structure. A NASTRAN finite-element analysis has been performed on the LACE system in its nominal operational configuration with the gravity-gradient boom and retro boom fully deployed at 45.72 m and the balance boom at 22.86 m. Figure 6 shows the two lowest modes with the frequencies and mode shapes viewed from different perspectives. The NASTRAN simulation provides a base for calculating the estimated

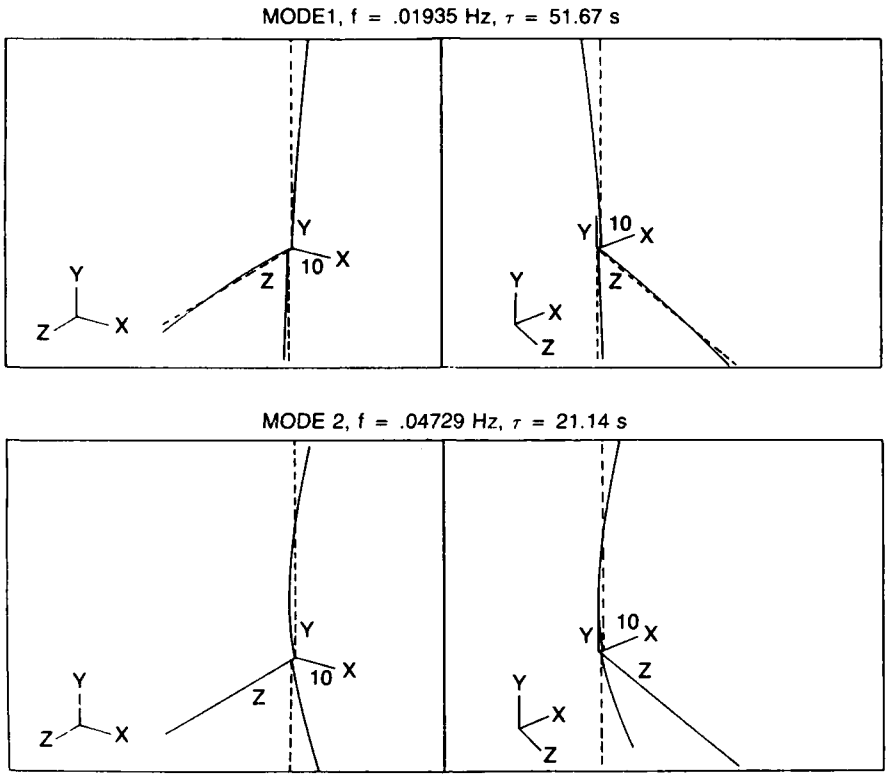

Fig. 6 — NASTRAN finite-element simulation of LACE spacecraft. Modes 1 and 2 are shown from two perspectives.

returns from the FIREPOND targeting, given nominal vibration amplitudes. Simulations have shown that tip amplitudes as low as .30 m will give the signal-to-noise ratio return of 10, thereby establishing confidence in the feasibility of the experiment. Parametric excitations, generated by raising and lowering the gravity-gradient boom at the fundamental frequency of the spacecraft, are now being designed to produce boom excitations of measurable amplitude.

Significance of the Flight Dynamics Experiment: The LACE dynamics experiment will provide an early on-orbit opportunity to validate ground testing, modeling, and computer simulation of the dynamics of large space structures. It will also serve as a test bed for development of laser methods for remote sensing of spacecraft dynamics. Such techniques could become standard methods for assessing the health of large, orbiting structures. It will help verify algorithms for system identification of orbiting spacecraft. It will also allow for an assessment of the utility of conventional attitude sensors such as horizon sensors, magnetometers, and sun sensors as tools for measuring the amount of spacecraft vibrations.

The LACE experiment, including spacecraft and ground stations, has been designed and built at the Naval Center for Space Technology of the Naval Research Laboratory. Boom deployment/retraction simulations have been made by Dr. Glenn Creamer of Bendix Corporation, and simulations of return from FIRPOND laser radar have been made by Professor John Junkins and Mr. Andy Browder of Texas A&M University.

[Sponsored by SDIO]

References

1. Lockheed Missiles and Space Company, "Solar Array Flight Experiment: Final Report," LMSC-F087173, submitted to

National Aeronautics and Space Administration, Marshall Space Flight Center, Alabama, April 1986.

2. L.E. Young and H.C. Pack, Jr., "Solar Array Flight Experiment/Dynamic Augmentation Experiment," NASA Technical Paper 2690, National Aeronautics and Space Administration, Marshall Space Flight Center, Alabama, February 1987. ■

Visualizing Phase Flows in Dynamical Systems

S. L. Coffey, E. M. Deprit, and L. M. Healy
Spacecraft Engineering Department

For an integrable dynamical system with one degree of freedom, "painting" the integral over the phase space proves to be very effective for uncovering the global flow. By coupling color graphics with the processing power of the Connection Machine, the dynamicist interactively searches the phase space for interesting phenomena. When applied to the zonal problem in artificial satellite theory, this painting technique vividly reveals the system's global behavior, both confirming and enhancing the mathematical analysis.

Artificial Satellites: The zonal problem is crucial to aerospace engineers designing satellite orbits. The utility of a satellite relies critically on maintaining the desired eccentricity and inclination. The useful lifetime of a satellite depends, in large part, on the amount of fuel spent on maneuvers to correct orbital deviations forced by irregularities in Earth's gravitational field.

By general agreement, physicists express the departures from sphericity in the gravity field as a series of spherical harmonics. For now, we ignore the nongravitational forces (drag and radiation pressure) and even those parts of Earth's gravity field dependent on the longitude and consider only those harmonics dependent on latitude—the zonal harmonics.

At the mission-design level, only the long-trend orbital variations matter. Having averaged out the short-period disturbances through formidable symbolic calculations, we seek to represent the totality of long-trend trajectories. These long period trajectories correspond to level curves of the averaged orbital energy over a sphere. Tracing these level curves, however, either by symbolic or numeric integration of the differential equations, is infeasible. Instead, by color contouring the phase flow, we "paint" maps where the design engineer can trace the evolution of all possible trajectories for a wide selection of orbital eccentricities and inclinations.

Contour Painting: At each point in the phase space, we compute the orbital energy. We convert this value to a color that then maps to a pixel on the display—in effect "painting the integral onto the phase space." On the screen, the contour painting produces strips of different colors, the boundaries between adjoining strips substituting for contour levels of the energy function.

Producing a medium resolution image of 512 by 512 pixels requires evaluation of the energy function at over a quarter million points, a task that overwhelms most serial machines. Since the energy computation proceeds independently at each point of the phase sphere, this painting technique fits naturally on a massively parallel processor such as the Connection Machine.

A straightforward painting of the Hamiltonian would suffer from the same problem as contour drawing—insensitivity to changes in scale. We are particularly interested in marking peaks, hollows, and passes, being especially attentive to details around these singularities. These features must be emphasized, even if it means losing all information about relative heights.

A uniform height scale, however, would require an enormous number of colors to enhance these very small features. This problem resembles the cartographer's dilemma in trying to preserve

detail while separating a huge mountain from a shallow lake at its foot. Whether shallow or high, the interesting points and their neighboring flows generally occupy about the same area in phase space. To draw a very fine scale around critical points, we weigh the assignment of colors by the distribution of values, so that all color strips contain approximately the same number of points. Once again, the painting technique exploits the processing power of the Connection Machine to sort the massive array of energy values into frequency bins.

Main Problem: To demonstrate the benefit of contour painting, consider the main problem in artificial satellite theory, where the gravitational perturbations are restricted to the second harmonic. Figure 7 shows the north pole of the phase sphere. The intricate configuration of three stable and two unstable equilibria corresponds to the classical cases of "frozen" orbits, i.e., Keplerian ellipses with fixed perigee.

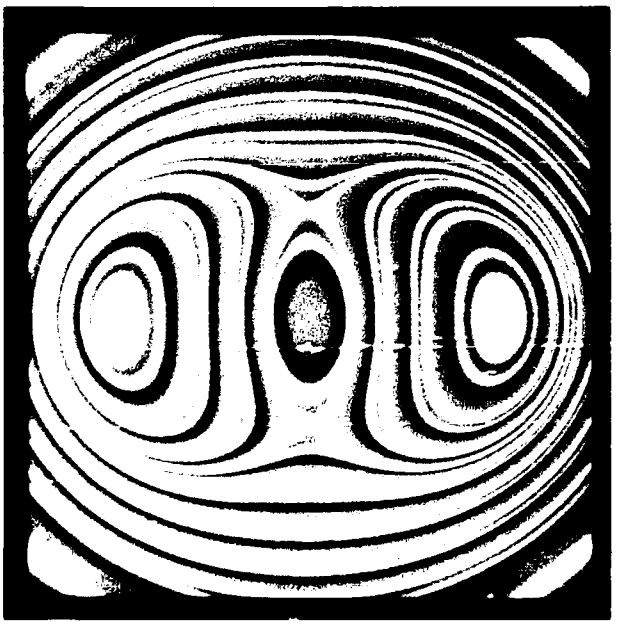

Fig. 7 — Phase flow in the main problem of artificial satellite theory; a view of the northern hemisphere after the second pitchfork bifurcation

To see how these equilibria develop, the dynamicist may view a sequence of phase flows as the polar component of the angular momentum increases. Figure 8 shows that the first bifurcation yields two stable and one unstable point from the stable equilibrium at the north pole. In the second pitchfork bifurcation, the unstable point becomes stable while spawning two unstable equilibria. Computing each of these frames at a resolution of 256 by 256 takes about 1 s on the Connection Machine.

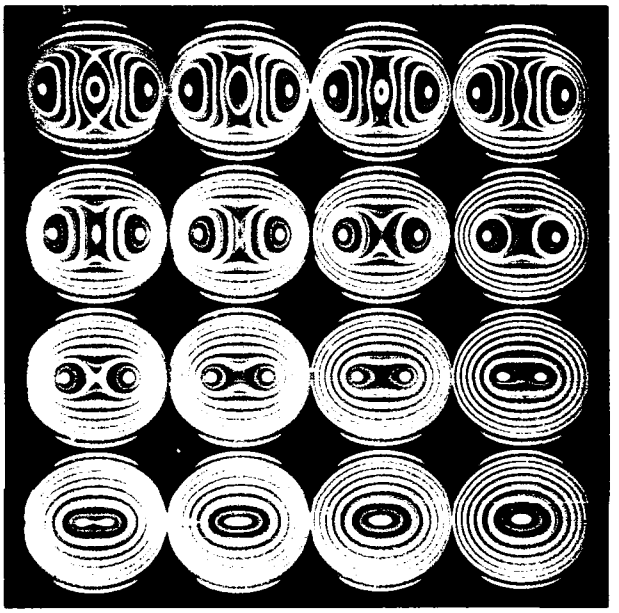

Fig. 8 — Phase flow around the north pole as the polar component of angular momentum increases

Higher Order Zonals: The second zonal harmonic, however dominant, does not completely account for the long-trend perturbations endured by an artificial satellite. To qualify as an engineering tool, our mathematical analysis must incorporate higher order zonal harmonics. To measure the painting technique against increasing analytical complexity, we retain zonal harmonics in the gravity field from second to ninth degree.

The equations in the averaged system appear so formidable that we must rely on visualizing the phase space to guide the mathematical analysis. Figure 9 shows how the odd zonals break the symmetry of the main problem by shifting the frozen orbit from its central position as a circular

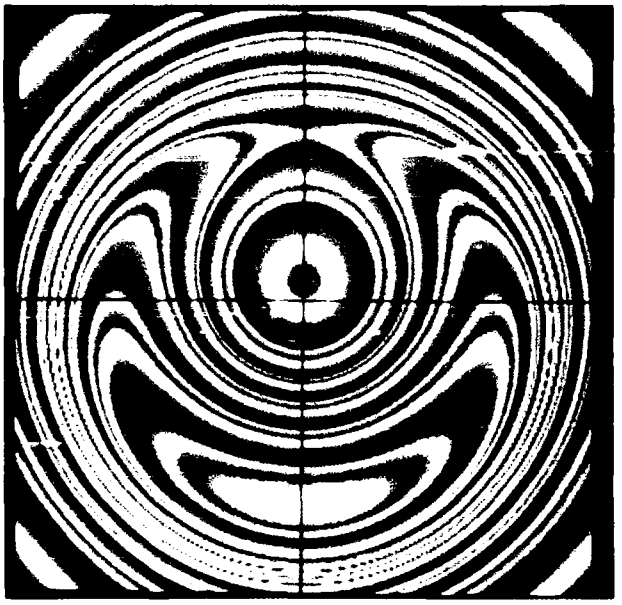

Fig. 9 — North pole of the phase space with zonal harmonics J_2 through J_9

orbit. This plot also reveals a new event buried deep in the differential equations: a saddle-node bifurcation that spawns a pair of equilibria, one stable and the other unstable. Including higher order zonals renders the energy function so complex that each phase map now takes nearly 30 times as long to compute compared with the main problem.

Conclusions: The contour-painting technique contributes crucially to our understanding of the artificial satellite problem, both confirming and augmenting the mathematical analysis. In addition, this flexible technique may be profitably applied to any integrable system with one degree of freedom (such as the Stark-Zeeman problem in semiclassical quantum mechanics). Just as in the satellite problem, the dynamicist may harness the processing power of the Connection Machine to rapidly search the phase space, identifying critical points and tracing their origins.

Acknowledgment: Dr. A. Deprit of the National Institute of Standards and Technology made significant contributions to this research.

[Sponsored by ONR]

Bibliography

S.L. Coffey, A. Deprit, E. Deprit, and L. Healy, "Painting the Phase Space Portrait of an Integrable Dynamical System," to appear in Science.

S.L. Coffey, A. Deprit, E. Deprit, L. Healy, and B.R. Miller, "A Toolbox for Nonlinear Dynamics," to appear in the *Proceedings of the Conference on Computer Assisted Proofs in Analysis*, Institute for Mathematics and its Applications, Springer-Verlag. ■

Excellence in Research for Tomorrow's Navy

AWARDS AND RECOGNITION

"We should ask ourselves, 'Are we, as an in-house laboratory, performing our job as Mr. Edison thought we should?' I believe the answer is that we are doing considerably better than he ever imagined we would. We have been responsive to Navy problems, we have maintained sustained technical competence over the many fields of Navy interest, and we have managed to maintain our intellectual independence."

"In the final analysis, these awards recognize exceptional commitment to continued productivity, intellectual integrity, and forefront work in science and technology."

Dr. Alan Berman, former Director of Research
10th Annual Research Publication Awards Presentation

SPECIAL AWARDS AND RECOGNITION

NRL is proud of its many distinguished scientists and engineers. A few of these have received exceptional honors for their achievements.

Dr. William R. Ellis
Associate Director of
Research for General
Science and Technology

PRESIDENTIAL RANK AWARD OF MERITORIOUS EXECUTIVE IN THE SENIOR EXECUTIVE SERVICE

Dr. Ellis was cited for his career achievements in managing and executing research and development programs of national importance. His initiative in undertaking studies of various administrative and management functions has contributed significantly to improving Laboratory operations.

Dr. Homer W. Carhart
Navy Technology Center for
Safety and Survivability

PRESIDENTIAL RANK AWARD OF MERITORIOUS EXECUTIVE IN THE SENIOR EXECUTIVE SERVICE

Dr. Carhart was cited for his distinguished contributions to the Navy's fire research and other programs. He has provided science, the Navy, and the nation with a flow of innovative discoveries, concepts, and devices that offer improved fuels performance and safety, ship/submarine/aircraft survivability against fires, and personnel protection, as well as new insights into the fundamental chemistry of combustion.

Robert E. Eisenhauer
Space Systems Development Department

DEPARTMENT OF THE NAVY SUPERIOR CIVILIAN SERVICE AWARD

"For his distinguished contributions to the Navy Space Program. Mr. Eisenhauer's conception and development of secure command systems and the development of radiation-hardened microprocessor based satellite control systems provide significant improvements and security for a critical Navy Space Program. He not only was the first to utilize these technologies in an operational spacecraft, but successfully transitioned them from government laboratory to industry production....Through his personal accomplishments and leadership, Navy space capabilities and the United States Space Program have been significantly enhanced."

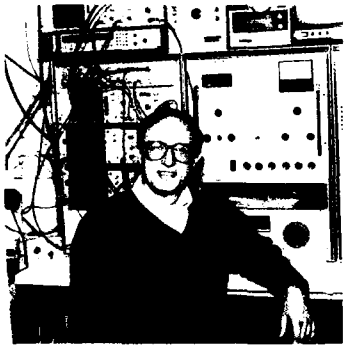

Dr. Wallace Manheimer
Plasma Physics Division

E.O. HULBURT ANNUAL SCIENCE AND ENGINEERING AWARD FOR 1988

"...for his outstanding contributions to and seminal work in the field of plasma physics as measured by his extremely high scientific productivity, the respect of his peers, and the applications of plasma physics to the solutions of real Navy problems."

Dr. Yue-Ying Lau
Plasma Physics Division

THE NRL-SIGMA XI APPLIED SCIENCE AWARD FOR 1989

"...for pioneering studies in the dynamics of electron beams and for ingenuous and elegant solutions of several problems in radiation and accelerator physics."

Dr. Philip R. Schwartz
Space Science Division

THE NRL-SIGMA XI PURE SCIENCE AWARD FOR 1989

"...for fundamental contributions to the fields of astrophysics and atmospheric spectroscopy, and remote sensing of the middle atmosphere, including the critically important problem of ozone depletion."

Carolyn J. Marks
Space Science Division

1988 COMMANDING OFFICERS'S AWARD FOR ACHIEVEMENTS IN THE FIELD OF EQUAL EMPLOYMENT OPPORTUNITY (Supervisory Category)

"In recognition of the many contributions she has made to promote equal employment opportunity at the Naval Research Laboratory, as well as innumerable community programs....As a highly regarded counselor, she was especially effective in resolving discrimination complaints....Mrs. Marks has especially gained recognition for her notable contributions to the Federal Women's Program. She served as chairperson of the Federal Women's Program subcommittee,...chaired task groups, conducted training,...planned programs and workshops...(and) as a member of the Federally Employed Women,...she has actively promoted equality and employment opportunities for women in the federal service."

Gladys L. Stuart
Public Works Division

1988 COMMANDING OFFICERS'S AWARD FOR ACHIEVEMENTS IN THE FIELD OF EQUAL EMPLOYMENT OPPORTUNITY (Non-Supervisory Category)

"In recognition of the many contributions she has made to promote equal employment opportunities (EEO) at the Naval Research Laboratory and in community programs....Mrs. Stuart has been instrumental in resolving conflicts between employees and supervisors....She relays the views and policies of the Commanding Officer on EEO-related topics at division meetings....Mrs. Stuart has also served on the Federal Women's Program Subcommittee...and on promotion selection panels....Mrs. Stuart enthusiastically worked with "Project Success" in the Prince Georges County Public School Program....Through Mrs. Stuart's dedicated commitment to the promotion of equal employment opportunity, better opportunities for minorities and women have been realized...."

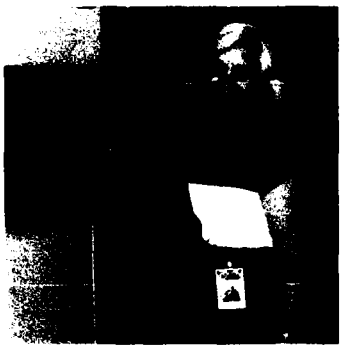

Dr. Isabella Karle
Laboratory for Structure
of Matter

RECIPIENT OF THE CITY COLLEGE OF NEW YORK'S CHEMISTRY ALUMNI ASSOCIATION'S BICENTENNIAL AWARD FOR SCIENTIFIC ACHIEVEMENT

Dr. Norman C. Koon
Materials Science and
Technology Division

***WASHINGTON TECHNOLOGY*'S TOP TEN TECHNOLOGY TALENT OF 1989**

Recognized as one of the best and brightest scientists in the local technology community. Selected from more than 50 organizations, including local federal laboratories, companies, national and regional associations, and universities.

Richard Foch
Tactical Electronic
Warfare Division

NAVY MERITORIOUS CIVILIAN SERVICE AWARD

"...for his meritorious contributions to the mission of the Department of the Navy in the Persian Gulf and the extraordinary role he played as a senior team member in the electronic warfare technical assistance team...he personally led a team of scientists and engineers in the rapid design, testing, fabrication, and implementation of three vital electronic warfare projects in the Persian Gulf. His exceptional technical prowess and support of electronic warfare are indicative of his total devotion to duty and commitment to excellence...."

Dr. William Howell
Tactical Electronic
Warfare Division

NAVY MERITORIOUS CIVILIAN SERVICE AWARD

"...for his meritorious technical and scientific contributions in the rapid development of two critical electronic warfare systems in response to urgent requests from the Fleet and an important Persian Gulf ally. His untiring efforts...resulted in the accelerated application of new critical technologies into operational systems that provide significant defense capabilities and have far-reaching impact into the design of future systems."

Waymon Humphries
Tactical Electronic
Warfare Division

NAVY MERITORIOUS CIVILIAN SERVICE AWARD

"...for his meritorious service and extraordinary contributions to the mission of the Department of the Navy in the Persian Gulf in the accelerated development and successful employment of critical new electronic warfare equipment and tactics. He provided comprehensive countermeasures tactics briefings to Middle East force escort commanders. He superbly led the initial in-theater electronic warfare technical assistance team in response to an urgent request from an important ally in the Persian Gulf. He was also a key member of the team in the subsequent development, deployment, and tactical employment of a critical electronic warfare resource for the U.S. Central Command...."

Dr. Francis Klemm
Tactical Electronic
Warfare Division

NAVY MERITORIOUS CIVILIAN SERVICE AWARD

"...for his meritorious contributions to the mission of the Department of the Navy in the Persian Gulf and to Fleet electronic warfare readiness. He orchestrated the development and testing of new countermeasures systems and tactics in response to the Persian Gulf missile threats. Equally significant were his vital contributions to the electronic warfare assistance team that responded to urgent requests from an important ally in the Persian Gulf and U.S. Central Command. He led three in-theater teams in the assembly, fabrication, testing, and deployment of critical electronic warfare hardware...."

Dr. Peter Matic
Materials Science and
Technology Division

THE "JIMMIE" HAMILTON AWARD FOR 1988

For the best original paper published in the *Naval Engineers Journal* during the year 1988. The paper, coauthored by Dr. Mitchell I. Jolles, is entitled "The Influence of Weld Metal Properties, Weld Geometry and Applied Load on Weld System Performance."

NAVY AWARD OF MERIT FOR GROUP ACHIEVEMENT

A team of nine scientists and engineers from the Optical Sciences and Acoustics Divisions was awarded the Navy Award of Merit for Group Achievement for their work in developing the first all–optical towed array (AOTA). Pictured in row 1 (l to r): Mr. Keith Williams, Mr. Gary Cogdell, Dr. Aileen Yurek, Dr. Anthony Dandridge, and Dr. Michael Marrone. Row 2: Dr. Alan Tveten, Dr. Frank Bucholtz, Dr. Alan Kersey, Dr. Nicholos Lagakos, and NRL's commanding officer CAPT John Donegan, Jr.

INDIVIDUAL HONORS

Laboratory employees received numerous scientific medals, military service awards, academic honors, and other forms of recognition, including election and appointment to offices in technical societies. The following is an alphabetical list of persons who received such recognition in 1989.

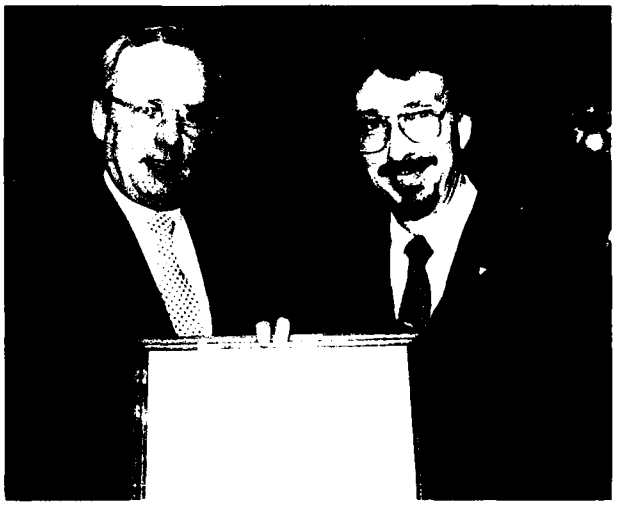

The Secretary of the Navy, the Honorable H. Lawrence Garrett III, presents a Presidential Rank Award of Meritorious Executive in the Senior Executive Service to Dr. Homer W. Carhart (in the left photo) and Dr. William R. Ellis (in the right photo)

Achille, L.B., Associate editor of Human Factors Society Visual Performance Technical Group.

Aggarwal, I.D., Member, American Ceramic Society; Member, Optical Society of America; Committee Member, International Halide Conference; and Member, Materials Research Society.

Baer, R.N., Fellow, Acoustical Society of America.

Barone, F.R., Co-chairman, Infrared Information Symposium on Infrared Countermeasures; and Co-chairman Coordinating Group on Aircraft Survivability.

Bassel, R.H., Fellow, American Physical Society; and Fellow, AAAS.

Batra, N.K., Elected Senior Member of IEEE; Associate Technical Editor, *Materials Evaluation*; reviewed book entitled *Polymer NDE*, ed., K.H.C. Ashbee, Technonic Publishing Co., Inc. (1986); Member, IEEE Ultrasonics, Ferroelectricity and Frequency Control Society's Technical Committee; and Member, Organizing Committee of 1989 IEEE UFFCS Symposium, Montreal, Canada.

Beal, R.T., Member, AIAA Space Transportation Technical Committee.

Beard, R.L., Appointed as principal U.S. representative to NATO Special Working Group (SWG) on Precise Time and Frequency Systems. This SWG reports directly to the NATO Tri-Service Group on Communications-Electronics Equipment and is charged with establishing a NATO standard for time and frequency interfaces for military communications systems; and appointed as a principal Navy Precise Time and Time Interval (PTTI) Coordinator with the Space and Naval Warfare Systems Command as a DOD PTTI Program Manager with the Naval Observatory.

Berman, D.H., Became a member of the Underwater Acoustics Technical Committee of the Acoustical Society of America.

Blue, J.E., Fellow, Acoustical Society of America; and Chairman, Membership Committee, Acoustical Society of America.

Bordley, T., Honored by ONT for work on the development of a sonar array that would improve the Navy's antisubmarine warfare and undersea surveillance capability.

Borenstein, M.D., Professional Engineer Registration, State of Maryland.

CAPT John Donegan, Commanding Officer (right), presents Ms. Wendy L. Lippencott with a 1989 Alan Berman Research Publication Award

Brady, R.F., Jr., Member, Admissions Committee and Membership Affairs Committee, American Chemical Society; and Member, Editorial Boards of the *Journal of Coatings Technology* and the *Journal of Protective Coatings and Linings*.

Brown, M., Became a member of AIAA Space Systems Technical Committee.

Brueckner G.E., Selected to Space Physics Subcommittee of the Space Science Applications Advisory Committee (SSAAC), NASA.

Bultman, J.D., Member, Committee on Creosote and Creosote Solutions of the American Wood-Preservers' Association; Member, Committee for the Evaluation of Wood Preservatives of the American Wood-Preservers' Association; Member of the Editorial Board for the *Journal of Industrial Crops and Products*; and Associate Editor of *BIOTROPICA*, published by the Association for Tropical Biology.

Burns, W.K., Member, Program Committee, Integrated and Guided Wave Optics Conference.

Campbell, F.J., Fellow, Institute of Electrical and Electronics Engineers; Fellow, American Institute of Chemists; Chairman, Awards Committee, Dielectrics and Electrical Insulation Society, IEEE; Member, Fellows Committee, Dielectrics and Electrical Insulation Society, IEEE; Member, Nuclear and Plasma Sciences Society, IEEE; Member, Power Engineering Society, IEEE; Member, Radiation Effects Committee, Dielectrics and Electrical Insulation Society IEEE; Member, Transactions Review Committee, Dielectrics and Electrical Insulation Society, IEEE; Member, Subcommittee on Electrical Tests, D-09 Electrical Insulating Materials, ASTM; Member, Subcommittee on Hookup Wire, D-09 Electrical Insulating Materials, ASTM; Member, Subcommittee on Thermal Capabilities, D-09 Electrical Insulating Materials, ASTM; Member, Subcommittee on International Standards, D-09 Electrical Insulating Materials, ASTM; Member, Division of Polymeric Materials, American Chemical Society; Member, Joint Board on

Science and Engineering Education of Washington Area; and Member, Naval Aerospace Vehicle Wiring Action Group.

Capps, R.N., Invited talk, "Applications of Thermal Analysis in the Development of Speciality Elastomers for Underwater Acoustic Applications," at the 18th North American Thermal Analysis Society Conference.

Carruthers, G.R., Editor, *National Technical Association Journal*.

Carter, R.C., CDR. USN, Received a second Navy Commendation Medal for performance as Navy Surgeon General VADM James Zimble's assistant for medical research and development from 1986-1989.

Cherkis, N.Z., Invited expert to Fourth, Fifth and Sixth Meetings of the General Bathymetric Chart of the Oceans (GEBCO) Subcommittee for Digital Bathymetry (1987, 1988, 1989); invited speaker to address Joint Intergovernmental Oceanographic Committee/International Hydrographic Organization (IOC/IHO) Guiding Committee for GEBCO, 1989; and Committee Member, U.S. Board on Geographic Names (Advisory Committee on Undersea Features), 1986-1989.

Cohen, R., Chairman, Division Colloquium Committee; and Visiting Scientist, Geophysical Laboratory.

Colton, R.J., Third year as member of advisory board of *Surface and Interface Analysis*; third year as member of advisory editorial board of *Applied Surface Analysis*; and elected member-at-large of ASTM E-42 Committee on Surface Analysis.

Commisso, R.J., Selected as Executive Secretary, DNA-fostered Advanced Pulsed Power Technical Review Workshop; Member, Executive Committee of the IEEE Nuclear and Plasma Sciences Society, Plasma-Science and Applications Committee (PSAC); Chairman for the PSAC Award Committee.

Cooper, J.C., Selected as University of Nebraska "Master," November 1988; appointed to University of Nebraska Chemistry Department, Industrial Advisory Board; and appointed Virginia Coordinator for American Junior High School Mathematics Exam.

Cooperstein, G., Fellow, American Physical Society; and Technical Program Committee Member, IEEE Pulsed Power Conference.

Cruddace, R.G., Member, ROSAT Cluster Working Group, Institut Fur Extraterrestrische Physik, Max Planck Institut, Garching, Federal Republic of Germany.

Dandridge, A., Appointed to the International Steering Committee of the Sixth International Conference on Optical-Fiber Sensors; appointed to Technical Program Committee of the Sixth International Conference on Optical-Fiber Sensors; and appointed to Associate Editorship of Applied Optics.

Dardy, H.D., Chairman, Technical Panel on Strategic Computing, Joint Directors of Laboratories.

Dasenbrock, R.R., Appointed to membership on Astrodynamics Technical Committee of the American Institute of Aeronautics and Astronautics (AIAA).

Davis, J., Fellow, American Physical Society; Associate Editor, *Physics of Fluids*; Associate Editor, *Journal of Quantitative Spectroscopy and Radiative Transfer*; and guest editor, *Journal of Quantitative Spectroscopy and Radiative Transfer*.

Davis, L.C., Elected to Sigma Xi, Spring 1989.

DeGiorgi, V.G., Appointed member of Fracture Control Technology Operating Assignment, The Technology Cooperation Program; appointed member of HSLA Steel Operating Assignment, TTCP; and 6th year as member of ASTM Committee E-24 on Fracture Testing.

Dere, K.P. Selected for the Organizing Committee for the Solar Wind Seven Meeting.

Diachok, O.I., Honored by ONT for work on the development of a sonar array that would improve the Navy's antisubmarine warfare and undersea surveillance capability, and elected as Chairman of the Instrumentation Committee (IEEE Oceans).

Donovan, E.P., Member, Optical Society of America; Member, Materials Research Society; Member, Condensed Matter and Radiation Sciences Division Computation Committee, and Member, Sigma Xi.

Dozier, C.M., Member, ASTM E10:07 Nuclear Technology and Applications Committee, Ionizing Radiation Dosimetry and Radiation Effects on Materials and Devices; and Member, ASTM F1:11 Electronics/Quality and Hardness Assurance Subcommittee.

Dragonette, L.R., Fellow, Acoustical Society of America.

Dubbelday, P.S., Fellow, Acoustical Society of America.

Duncan, M.D., Appointed committee member for Quantum Electronics and Laser Science Conference Publication Liaison for 1989; and appointed committee member for International Quantum Electronics Conference Publicity Liaison for 1990.

Edelstein, A.S., Program Committee, International Conference on the Physics of Highly Correlated Electron Systems, Sept. 11–15, 1989, Santa Fe, NM.

Eisenhauer, R.E., Navy Superior Civilian Service Award.

Elam, W.T., Continuing membership on External Advisory Committee, Biostructure PRT (X9), National Synchrotron Light Source; charter member of the Committee on Standards and Criteria for XAFS; and member, User's Executive Committee, National Synchrotron Light Source (XAS), Special Interest Group Representative.

Ellis, W.R., Presidential Rank Award of Meritorious Executive in the Senior Executive Service.

Mr. Robert Eisenhauer receives congratulations from CAPT George Wagner, Office of the Chief of Naval Research, for receiving the Navy Superior Civilian Service Award

Esman, R.D., Member, Program Committee, Conference on Lasers and Electro-optics (CLEO).

Fedder, J.A., American editor for the International Solar Terrestrial Environment Program Simulation Promotion Office (STEP SIMPO).

Feldman, B.J., Appointed member of Lasers and Electrooptic Society (LEOS) Committee on UV and Gas Lasers; and appointed co-editor of IEEE *Journal of Quantum Electronics*, special issue on electronic transition lasers.

Fischer, J., Continuing memberships in the International Astronomical Society and the American Astronomical Society.

Fitzgerald, J.W., Member, Committee on Atmospheric Aerosols and Nucleation of the International Commission on Cloud Physics; and invited keynote speaker at the International Conference on Aerosols and Background Pollution, Galway, Ireland.

Folen, V.J., Fellow, American Physical Society; appointed member, SDI Passive RF Survivability Steering Panel, and Fellow of the American Physical Society, continuing.

Ford, R.T., Elected treasurer and member of the Board of Directors of the Institute of Electrical and Electronics Engineer's Society on Electromagnetic Compatibility; and appointed as a technical expert (TE) on the National Institute of Standards and Technology

National Voluntary Laboratory Accreditation Program; and certified as an Electromagnetic Compatibility Engineer by the National Association of Radio and Telecommunications Engineers.

Fox, R.B., American Chemical Society: Councilor, Member, Society Committee on Publications, Meetings and Expositions Committee; Committee on Nomenclature, Polymer Division Nomenclature, Polymer Division Committee on International Activities; and Chemical Society of Washington: Member of Board of Managers, Section Liaison for National Meetings.

Friebele, E.J., Fellow, American Ceramic Society; Member, Tri-Service Fiber-Optics Coordinating Structure; Member, SDI Optics Coordination Committee; and Member, NATO Panel IV, Research Study Group 12 Nuclear Effects Task Group.

Fritz, G.G., Appointed to NASA X-ray Astronomy Program Working Group, June 1989; appointed to NASA Peer Review Panel on "U.S. Contributions to the ESA Cornerstone X-ray Multimirror Mission (XMM)," March 1989.

Gardner, J.H., Member, National Aerospace Plane CFD Technical Support Team; and Member, National Aerospace Plane Technical Maturation Team.

Garroway, A.N., Organized and chaired 30th Experimental NMR Conference (Pacific Grove, CA); and served on evaluation panels for the FAA and U.S. Customs.

Gauss, R.C., Became member of Sigma Xi and of the Management Committee on Bioacoustic Signal Classification (CNS Division of ONR).

Giallorenzi, T.G., 1989 IEEE/OSA John Tyndall Award, Chairman IEEE Lasers and Electro-optical (CLEO) Conference; Member, Board of Editors, Optical Society of America; Member, Technical Committee, IEEE Conference on Semiconductor Laser Device and Applications, IEEE Conference on Integrated Opto-electronics; Chairman, Tri-service Fiber Optics Conference; Chairperson, Tri-service Fiber Optics Committee; Member, National IRIS Executive Committee; Industrial Advisory Boards of University of New Mexico and University of Virginia; Member, National Research Council Panel on Photonics Science and Technology Assessment.

Gold, S.H., Became a member of Executive Committee of the Standing Technical Committee on Plasma Science and Applications of the IEEE Nuclear and Plasma Sciences Society.

Grabowski, K.S., Co-chairman and co-editor for proceedings of symposium on "Environmental Degradation of Ion and Laser Beam Treated Surfaces," Fall 1988 TMS Meeting, Chicago, IL.

Grefenstette, J.J., Elected to Sigma Xi in Spring 1989.

Griffin, O.M., Associate editor, *Journal of Fluids and Structures*, Academic Press, London (U.K.).

Griscom, D.L., Vice Chairman, Glass Division, American Ceramic Society; Fellow, American Ceramic Society; Member, NASA Micro-gravity Glasses and Ceramics Discipline Working Group.

Groshans, R.G., Member, Committee on Standards (Operations), The American Institute of Aeronautics and Astronautics (AIAA), Space-Based Observation Systems (SBOS); and re-elected (fourth year) Class Secretary, United States Military Academy Class of 1953.

Gubser, D.U., Selected chairman of the Naval Consortion for Superconductivity (NCS); invited speaker at Military Developments in Superconductivity (Nov. 1988); invited speaker at Superconductivity; Global Developments (Jan. 1989); session chairperson at American Physical Society Meeting, March 1989, and Global Developments in Superconductivity Meeting, Jan. 1989; Member, Planning and Review

Committee for OSTP Commission of National 5-Year Plan for Superconductivity; DOE Review Panel for Power Conductor Applications of Superconductivity; OTA Reviewer for Congressional Report on Superconductivity; and NSF reviewer for Science and Technology Center (STC) selection for Superconductivity Center.

Haber, I., Co-chairman of 14th Conference on Numerical Simulations of Plasmas.

Haftel, M.I., Chairman, CMRSD Colloquium Committee, 1987-1988.

Hayward, T.J., Honored by ONT for work on the development of a sonar array that would improve the Navy's antisubmarine warfare and undersea surveillance capability.

Heckathorn, H.M., Member, SDIO User Products Subpanel (subpanel of the Phenomenology Steering and Analysis Group (PSAG); and Chairman, SDIO Strategic Scene Generator Working Group.

Hertz, P.L., Member, NASA Peer Review Committee, ROSAT Guest Investigator Program; and Member, NASA HEAO X-ray Users Committee.

Hoover, J.E., Professional Engineer Registration, State of Arizona.

Hubler, G.K., Member, International Committee, Conference on Surface Modification of Metals by Ion Beams; Member, Joint Services Committee on Laser Eye Protection Program; and Member, Program Committee for Ion Beam Modification of Materials Conference, Summer 1990.

Idzerda, Y.U., A winner in the Poster Presentation Competition at the 35th American Vacuum Society National Symposium.

Imam, M.A., Member, Flow and Fracture Committee, American Society of Metals International; Member, Mechanical Metallurgy Committee, The Mineral Metals and Materials Society; and Member, Physical Metallurgy Committee, TMS.

Ingenito, F.L., Fellow, Acoustical Society of America.

Jacob, R.J.K., Appointed at-large member of ACM SIGCHI Conference Planning Committee, July 1989; and appointed senior referee for *IEEE Software* (journal).

Joyce, G., Elected as Fellow of the American Physical Society; Member, Program Committee of Annual DARPA Review; and Member, Program Committee of APS Spring Meeting 1990.

Kabler, M.N., Fellow, American Physical Society; and Member, National Synchrotron Light Source PRT Council.

Kailasanath, K., Member, AIAA Propellants and Combustion Subcommittee; Member, Program Subcommittee for the 23rd International Symposium on Combustion; and elected Senior Member, American Institute of Aeronautics and Astronautics (AIAA).

Karle, Isabella, Recognized as one of *Washington Technology*'s Top Ten Technology Talents of 1989; received the Outstanding Achievement Award from the Association for Women in Science, Detroit Area Chapter; and selected by the University of Michigan's Women's Studies Association to be inducted into the Michigan Women's Hall of Fame.

Kaufman, B., Chairman, Astrodynamics Technical Committee of American Institute of Aeronautics and Astronautics (AIAA) 1989-1990; selected as chairman of 1991 Astrodynamics Conference co-sponsored by American Astronautical Society (AAS) and AIAA.

Keskinen, M.J., Member, Executive Committee, Commission H, Waves in Plasmas, U.S. National Committee, International Union of Radio Science (URSI).

Kim, C., President, Korean-American Scholarship Foundation; Reviewer, *Journal of Composite Materials*; and Reviewer, National Science Foundation, Small Business Innovative Research.

King, S., Session Chairman, Second European Workshop on Low Temperature Detectors.

Klein, B.M., Chairman, Peer Review Committee, Pittsburgh Superconductor Center and National Center for Supercomputer Applications; and Member, Renewal Review Panels for NSF Supercomputers Centers.

Klemm, F.J., Navy Meritorious Civilian Service Award.

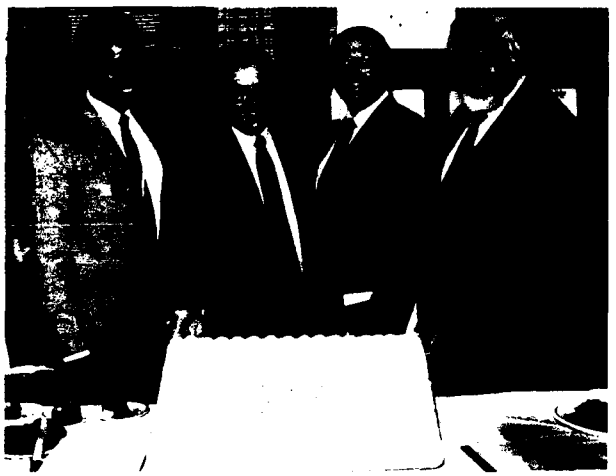

The Navy Meritorious Civilian Service Award was presented to these members of the Tactical Electronic Warfare Division. Pictured from left to right are Dr. William Howell, Dr. Francis Klemm, Mr. Richard Foch, and Mr. Waymon Humphries.

Kowalski, M.P., Member, NASA Peer Review Committee, ROSAT Guest Investigator Program.

Krebs, J.J., Fellow, American Physical Society.

Kuperman, W.A., Associate editor, *Journal of the Acoustical Society of America*; and consulting editor, *Encyclopedia of Applied Physics*, American Institute of Physics.

Kurfess, J.D., NRL representative for the Nuclear Power Mission Advisory Board.

Lambert, J.M., Member, Organizing Committee and co-chairman of Plenary Sessions of the 1988 Conference of the Applications of Accelerators in Research and Industry; Reviewer for *Physical Review Letters*, National Science Foundation, American Association for the Advancement of Science, and American Institute of Physics; appointed to Executive Council, College of Arts and Sciences, Georgetown University; continuing as chairman, Department of Physics, Georgetown University; and director, Georgetown University Bicentennial Lecture Series, "Frontiers in Science."

Landwehr, C.E., Member, Program Committee, IEEE Computer Society Symposium on Security and Privacy, 1989; appointed Program Committee Member for 1990 Symposium; completed two-year term as chairman, IEEE Computer Society Technical Committee on Security and Privacy; continued as Member, National Institute of Science and Technology Computer and Telecommunications Security Council; edited book, *Database Security, II: Status and Prospects*, North Holland, 1989; completed third year as U.S. National Leader and Chairman, Technical Panel 1 (Trustworthy Computing Technologies), Subgroup X (Computing Technology), of the Technical Cooperation Program; appointed second year as IEEE Computer Society Distinguished Visitor; delivered several lectures under this program, including keynote address to Conference on Computing Systems and Information Technology, Sydney, Australia; Invited Working Group Chair, group on example applications, Formal Methods '89 Workshop (organized by U.S.-NSA, Canada-CSE, UK-CESG); continued as Chairman of Working Group 11.3, Database Security, of Technical Committee 11 (Computer Security), International Federation for Information Processing (IFIP); appointed Chair of Federal Liaison Group for National Academy of Sciences, Computer Science and Technology Board study on computer security issues; and Invited Working Group Chair, Workshop on Integrity Protection in Computer Information Systems II, January, 1989.

Lau, Y.Y., Fellow, American Physical Society and recipient of the 1989 Sigma Xi Applied Science Award (NRL).

Dr. Yue-Ying Lau accepts the 1989 NRL-Sigma XI award for Applied Science from CAPT J. Donegan, Commanding Officer. Mrs. Lau looks on.

Lewis, J.S., Professional Engineer Registration, State of Virginia.

Ligler F.S., Elected to Board of Managers, the Chemical Society of Washington; and ONT Award (for Liposome Encapsulated Hemoglobin Program) for Exploratory Development (with B.P. Gaeber; J.M. Schnur, E. Chang, and A.S. Rudolph).

Mak, P.S., Second year membership in Infrared Scene Projector Ad Hoc Group, Simulation Committee, Technical Panel for Electronic Warfare, Joint Directors of Laboratories.

Marrowitz, A.E., Invited talk, "The Measurement Scientist's Role at NRL-USRD," at the Metrology Engineering Conference.

Marks, Carolyn J., recipient of the Chief of Naval Research Award for Achievements in the Field of Equal Employment Opportunity (Supervisory Category).

Marsh, E., Elected to Sigma Xi in Spring, 1989.

Matic P., Received "Jimmie" Hamilton award for best paper of 1988 appearing in *Naval Engineers Journal*, May 1989.

McCafferty, E., Member, Corrosion Monograph Committee, The Electrochemical Society; and Member, Honorary Membership Committee, The Electrochemical Society.

McLean, J., Invited panelist in 1989 IEEE Security Foundations Workshop; panel chairman for 1989 IEEE Security Foundations Workshop; Member, Program Committees of 1989 Symposium on Security and Privacy, 1989 IEEE Security Foundations Workshop, and 1989 ACM Software Testing and Evaluation Workshop; invited speaker at University of Maryland Institute of Advanced Computer Science's Formal Methods Workshop; and Member, National Computer Security Center's Verification Working Group.

McMahon, J.M., Appointed by Department of Energy to Microfusion Facility Review Committee; and appointed by Defense Nuclear Agency to DRAGSTER Review Panel.

Meadows, C.A., Invited to participate in Second RADC Database Security Workshop; Member, Program Committee for IEEE Symposium on Security and Privacy; also chaired sessions at IEEE Symposium on Security and Privacy; guest lecturer on cryptography at University of Maryland; and referee for NCSC Computer Security Conference, AIAA Computer Security Conference, and IFIP AG 11-3 Workshop on Database Security.

Mehl, M.J., Member, American Geophysical Union since 1985; Member, American Physical Society since 1977; and Member, Sigma Xi since 1978.

Meier, R.R., Advisory Committee for the Laboratory for Atmospheric and Space Physics, University of Colorado (3-year term, beginning May 1989); and Member, American Institute of Astronautics and Aeronautics' Environmental Interactions Panel to review the Air Force Technology Center Program, Spring 1989.

Metzbower, E.A., Chairman, Laser and Electron Beam Committee of the Joining Division Council of ASM International; Member, Board of Directors of Laser Institute of America (LIA); Chairman of International Conference on Lasers and Electro-Optics (ICALEO '89).

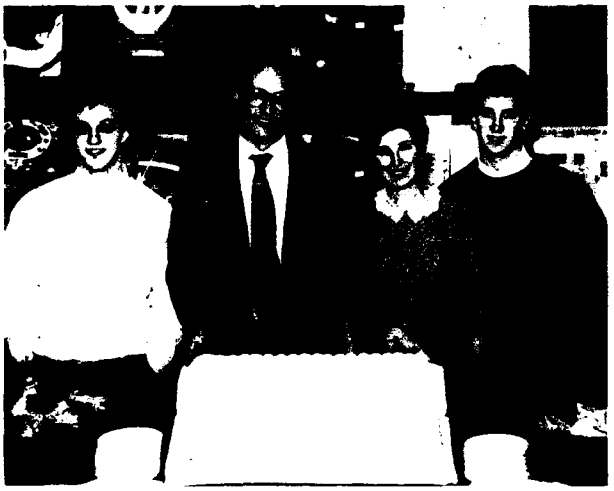

Dr. Wallace Manheimer was awarded NRL's highest scientific and engineering honor, the E.O. Hulburt Science and Engineering Award. His family shares in celebrating the award.

Michel, D.J., Elected Fellow, ASM International; Member, Technical Program Committee, Third and Fourth International Symposia on Environmental Degradation in Nuclear Power Systems-Water Reactors; Member, Nuclear Materials Committee, ASM International and TMS; and Professorial Lecturer, Engineering Materials, the George Washington University.

Moon, D.W., Member, American Society for Metals and American Welding Society; Committee Member, American Welding Society, C7 Committee on High Energy Beam Welding and Cutting, and C7C Subcommittee on Laser Beam Welding and Cutting.

Mowery, R.L., Lubricant Subcommittee Chairman DoD-IBWG (DoD Instrument Bearing Working Group).

Mueller, G.P., Session Chairperson, Organizing Committee for Seventh DoD Conference on DEW Vulnerability, Survivability and Effects.

Murday, J.S., American Institute of Physics - Member, Governing Board; Chairman, Nominating Committee; Chairman, Development Committee; Chairman Organizing Committee; Fifth International Conference on Scanning Tunneling Microscopy/Spectroscopy; First International Conference; Nanometer Scale Science and Technology; and coeditor, Proceedings of the Topical Conference on Probing the Nanometer Scale Properties of Surfaces and Interfaces.

Nagel, D.J., Chairman, Technology Panel, High Power Microwave Program Balanced Technology Initiative; Member, Proposal Review Committee, X-ray Lithography Program, Very High Speed Integrated Circuits (VHSIC) Program, Defense Advanced Research Projects Agency (DARPA); Member, Program Review Committee, National Laser Users Facility, Laboratory for Laser Energetics, University of Rochester; Member, NRL Management Training Committee; Member, Program Advisory Committee, National Synchrotron Light Source, Brookhaven National Laboratory, Department of Energy; Member, Program Committee, Ninth International Conference on Vacuum Ultraviolet Radiation Physics; Chairman, NRL Committee on Technology Transfer; co-chairman, NRL Technical Strategic Unit on Directed Energy Warfare.

Namenson, A., Member, DNA Hardness Assurance Committee.

Natishan, P.M., Chairman, Symposium on Marine Corrosion, 1989 NACE NE Regional Meeting, Baltimore, MD, Sept. 1989; Vice Chairman, Baltimore-Washington Section of NACE; 2nd Vice Chairman, National Capital Section of the Electrochemical Society; and representative to the Individual Membership Committee, The Electrochemical Society.

Oran, E.S., Editorial Board, Progress in Energy and Combustion Science; Committee on the Status of Women in Physics, American Physical Society; Chairman, Committee on Status and Bylaws, American Geophysical Union; Publication Committee and Chairman, Subcommittee on Technical Information Services, American Aeronautics and Astronautics; Board of Directors of the International Colloquium on the Dynamics of Energetic and Reactive Systems; Executive Committee, Topical Group in Computational

Physics, the American Physical Society; Plenary Lecture, Seminar on Flame Structure, Alma Ata, USSR; coeditor, Numerical Approaches to Combustion Modeling, to be published by AIAA, Washington, DC.

Ossakow, S.L., Organizer and co-convenor of special sessions on Theory and Computer Experiments of Plasma Processes at XXIII URSI General Assembly, Prague, Czechoslovakia, August-September, 1990; Advisor, ONR Ionospheric Research.

Ottinger, P.F., Session organizer for IEEE International Conference on Plasma Science.

Palmadesso, P.J., Second year as member of the National Research Council Committee on Solar-Terrestrial Relations.

Pande, C.S., Invited lecturer, NATO Advanced Study Institute Workshop on High T_c Superconductivity Germany (1989); invited author (with H.A. Hoff) on a chapter of a book on high T_c superconductivity entitled "*Twins in High T_c Superconductors*;" elected vice chairman, Physical Metallurgy Committee of The Metallurgical Society of America.

Papaconstantopoulos, D.A., Member, Organizing Committee of the 20th International Conference on the Physics of Semiconductors; co-chairman, Conference Committee, Fifth International Conference on the Physics of Electro-Optic Microstructures and Micro-devices; and appointed to the Editorial Board of *Journal of Superconductivity* (published by Plenum Publishing Company).

Parks, V.J., Elected fellow, American Society of Mechanical Engineers.

Parvulescu, A., Fellow, Acoustical Society of America.

Peterson, E.L., Selected as program area reviewer for New DNA Neutral Particle Beam Program; selected as editor for the *Journal of Radiation Effects Research and Engineering*, Special Issue on Single Event Hardening; selected as associate guest editor for Proceedings of HEART Conference to be published in *Journal of Radiation Effects Research and Engineering*.

Pickett, W.E., Appointed to the Editorial Board of *Journal of Superconductivity* (published by Plenum Publishing Company); and treasurer, Greater Washington Solid State Physics Colloquium Committee.

Ramaker, D.E., Recipient of the Hillebrand Prize from the Chemical Society of Washington (for five years of work on theory and application of surface spectroscopies).

Rife, J.C., Member, Condensed Matter and Radiation Sciences Divisions COMSPEC Committee.

Ripin, B.H., Fellow, American Physical Society; Senior Member, IEEE; Chairman, APS Division of Plasma Physics Publication Committee; appointed to the APS Publication Committee; appointed to the *Physical Review Letters* Review Panel; and on editorial boards of *Physical Review A* and *Lasers and Particle Beams*.

Ritter, J.C., Invited to address the International Commission on Radiation Units and Measurements at its 1988 meeting in Helsinki, Finland; selected by the Defense Nuclear Agency (DNA) to serve on the editorial board to prepare a special issue of the *Journal of Defense Research* (JDR) on System Generated Electromagnetic Pulse (SGEMP) (second year); invited to serve as SDIO radiation SIG representative to Long Duration Exposure Facility (LDEF) joint SDIO/NASA LDEF Retrieval Analysis Team; Session Chairman, DNA/DARPA Single Event Upset Symposium in Los Angeles, California; Member, Air Force Space Technology Center, Space and Missiles Environment Interaction Strategy Panel; and Tutorial Short Course Instructor at the 1989 IEEE Nuclear and Space Radiation Effects Conference for Radiation Effects in Marco, Florida, July 1989.

Robinson R.L., Appointed to the Joint Directors of Laboratories Technology Panel for Electronic Warfare (JDL-TPEW).

Roland, C.M., Associate editor Rubber Chemistry and Technology, American Chemical Society (ACS); and Member, Advisory Board for "Advances in Chemistry and Technology (ACS); and Member, Advisory Board for "Advances in Chemistry" and Symposium Series," (ACS).

Rolison, D.R., Appointed to the Advisory Board for Analytical Chemistry for *The American Chemical Society Journal*.

Rosen, M., Lethality assessment coordinator, DNA SDI Projects Office; Chairman, Lethality and Target Hardening Target Description Working Group; and Member, SDIO Follow-on Architecture Study Group.

Rudgers, A.J., Fellow, Acoustical Society of America; Member, American Association of Physics Teachers; Associate Member, U.S. Naval Institute; and Member, Technical Committee on Physical Acoustics, Acoustical Society of America.

Saenz, A.W., Honored with one-day symposium on "Fundamental Problems of Classical and Quantum Dynamics," Catholic University, 21 October 1988, in honor of 65th birthday.

Sartwell, B.D., General Chairman of 16th International Conference on Metallurgical Coatings, April 17-21, 1989, San Diego, California; editor of the journal *Surface and Coatings Technology* published by Elsevier Sequoia, Lausanne, Switzerland; editor of the Proceedings of the 16th International Conference on Metallurgical Coatings, published by Elsevier Sequoia, 1989; Member, Executive Committee of the Vacuum Metallurgy Division of the American Vacuum Society; and appointed an editor of the Proceedings of the International Conference on Thin Films, to be held April 2-6, 1990.

Schmidt-Nielsen, A., Continuing as Newsletter Editor for Division 21 of the American Psychological Association; appointed to Acoustical Society of America Committee on Standards (ASACOS).

Schnur, J.M., Chairman, 1990 Gordon Conference on Organic Thin Films; and Member, Organizing Committee for "Scanning 90."

Schultz, A.C., Appointed chairman of finance committee and treasurer of the Association for Computing Machinery's (ACM) Computer Science Conference 1990.

Severns, J.G., Presented an invited paper, "LIPS III—A Solar Cell Test Bed in Space," coauthored by R.M. Hobbs, N.P. Elliott, R.H. Towsley, R.W. Conway, and G.F. Virshup, at a plenary session of the 20th IEEE Photovoltaics Specialist Conference in Las Vegas, NV, in September 1988. The Proceedings were published in February 1989.

CAPT J. Donegan, Commanding Officer, congratulates Dr. Philip R. Schwartz and Mrs. Schwartz. Dr. Schwartz received the Sigma-Xi Pure Science Award for 1989.

Share, G.H., Member, NASA's High-Energy Astrophysics Management Operations Working Group (HEAMOWG).

Sheinson, R.S., Secretary, Eastern States Section of the Combustion Institute.

Shivanandan, K., Advisory Council, Defense Science Board; Science Advisory Committee, Laser and Plasma Physics, Costed, Paris; IR working group on sensors, STC,

Albuquerque, New Mexico; and Advisory Committee on Astronomy and Astrophysics, Indian Academy of Science.

Silberberg, R., Nominated to sit on the Masters of Science Thesis Committee, University of Atlanta, GA.

Skelton, E.F., Spokesperson for High Pressure Insertion Device Team at National Synchrotron Light Source, Brookhaven National Laboratory; and representative for Energy Dispersive Group (1989–1990) on Users Executive Committee, National Synchrotron Light Source, Brookhaven National Laboratory.

Smidt, F.A., Fellow, ASM International; Member, Navy Council on Materials and Structures; Member, U.S. Government-TTG-A, Sub-Group C (Technology Export Control Advisory Group on Coatings); Member, American Society for Materials (National Committee), Technical Awareness Advisory Committee; and Co-chairman, Organizing Committee for International Conference on Surface Modification of Metals by Ion Beams to be held in Washington, D.C., June 1991.

Smith, W.R., Member, Navy ASW Signal Processing Committee.

Spezio, A.E., Continuing Chairman, TTCP-QTP-14; appointed to Source Selection Committee, AN/ALR-67ASR; appointed to Source Selection Committee AN/WLQ-( ); Continuing Member, BTI Optical Processing Committee; Continuing Chairman, DoD-Sponsored OSP-TAG; and appointed Session Chairman, SPIE Spring Meeting.

Sprangle, P.A., Fellow, American Physical Society, continuing membership; Member, Executive Committee of 11th International FEL Conference; Member, National Organizing Committee for 13th Conference on Numerical Simulation of Plasmas, held Sept. 1989 in Santa Fe, NM; and Member, Program Committee of Division of Physics of Beams-APS.

Statler, R.L., Member, IEEE 21st Photovoltaic Specialists Conference Committee; and Member, Solar Photovoltaic Panel of the Interagency Advanced Power Group.

Stolovy, A., Chairman, Energetic Materials Panel, Particle Beam Weapons, SDI; and Member, Lethality Assessment Panel, Particle Beam Weapons, SDI.

Summers, G.P., Served as Session Chairman for IEEE Nuclear and Space Radiation Effects Conference, Mano Island, Florida; and served as Chairman, Physics Department at the University of Maryland in Baltimore County.

Tang, C.M., Member, Program Committee for IEEE Particle Accelerator Conference, 1989; and Member, Program Committee for 11th International FEL Conference.

Tatem, P.A., Arrangements Chairman, Eastern States Section of the Combustion Institute.

Temes, C.L., Appointed to committee by National Science Foundation for evaluating proposals for Small Business Innovation Research (SBIR) grants.

Timme, R.W., U.S. Navy Technical Representative to the Cooperative Committee for the International List of the Militarily Critical Technology List Meetings (COCOM for IL-1510 of MCTL).

Ting, R.Y., Translator and translation editor, Chinese Physics, American Institute of Physics; Member, National Research Council Research Advisor at Naval Research Laboratory; Navy Advisor, Pennsylvania State University, Materials Research Laboratory, Navy Piezoelectric Materials Program; associate editor for the *Journal of Wave-Material Interaction*; and Member, IEEE Sensors and Actuators Committee, Electronics Division, Naval Research Laboratory.

Tolstoy, A., Became a member of the Technical Specialty Group (ASA Committee); and invited to joint delegation of mathematicians to China (Association of Women in Math).

Ms. Gladys Stuart receives the NRL Commanding Officer's Award for Achievements in the Field of Equal Employment Opportunity in the Non-Supervisory Category from CAPT J. Donegan

Trunk, G.V., Second year as chairman of KTP-2 (this is a technical exchange on radar data processing under the auspices of subgroup K (radar) within The Technical Cooperation Program (TTCP)).

Trzaskoma, P.P., Elected Chairman of the Council of Local Sections of the Electrochemical Society; and Appointed Member, Board of Directors of the Electrochemical Society.

Turner, N.H., Elected Membership Secretary of the Division of Colloid and Surface Chemistry of the American Chemical Society; and third year as an alternate councilor for the Chemical Society of Washington, the Washington Section of the American Chemical Society.

Valenzuela, G.R., Co-chairman of panel of experts in National Science Foundation (NSF) Workshop "On Future Direction in Electromagnetics Research," 27 July 1989, Boston, MA; representative on the Scientific Committee on Oceanic Research (SCOR) for International Union of Radio Science (URSI); and International Council of Scientific Unions (ICSU).

Van Buren, A.L., Fellow, Acoustical Society of America; Member, Mathematics Advisory Group for the University of Central Florida; and Member, Acoustical Society of America Working Group to Develop ANSI Standard for Measurement of Phase Response of Transducers.

Vandermeer, R.A., Appointed Chairman, Recovery and Annealing Committee of ASM International; and appointed Vice Chairman, Surfaces and Interfaces Committee of ASM International.

Venezky, D.L., Alternate councilor, Washington Section, American Chemical Society; and Member, International Activities Committee, American Chemical Society.

Vogt, P.R., Committee Member, U.S. Science Advisory Committee, 1988, 1989.

Weller, J.F., Program Committee Member, Optical Fiber Communications Conference.

White, C.T., Appointed to the ONR Technical Advisory Group for Chemistry.

Wieselthier, J.E., Treasurer of the 1991 IEEE International Symposium on Information Theory; Senior Member of the IEEE.

Wieting, T.J., Program Committee and Session Chairman, Seventh DoD Conference on DEW Vulnerability, Survivability, and Effects; Member, Technical Program Committee, HPM and Broadband RF Propagation Solidace — Phenomenology Solidace — Methodology Workshop; editor, Proceedings of the 4th National Conference on High-Power Microwave Technology; Chairman, DoD Microwave Effects Panel; Member, DoD Systems Effects Assessment Team (SEAT); Member, DoD Team on Project Tiger Grip; Member, Review Group on AF Project Seek Needle; and Member, DoD Foreign Asset Assessment Team (FAAT).

Wilhelm, P.G., Elected a Fellow, American Institute of Aeronautics and Astronautics (AIAA).

Williams, A., Member, DARPA Kinetic Energy Blue Ribbon Panel for Review of Antiarmor Joint Program; and Recording Secretary, Aero-Ballistic Range Association.

Williams, F.W., Governing Board, Eastern States Section of Combustion Institute.

Wolf, S.A., Program Committee, 1990 Applied Superconductivities Conference; Second International Conference on Thin Film Superconductors; Organizing Committee, First International Conference on RF Properties of High T_c Superconductors; Chairman, Electrical, Optical and Magnetic Phenomenon Committee of TMS; editor, Proceeding of the First International Conference on the Science and Technology of Thin Film Superconductors.

Wolf, S.N., Fellow, Acoustical Society of America; Member, Acoustical Society of America Committee on Standards, representing Underwater Acoustics Technical Committee; ex officio member, Acoustical Society of America Underwater Acoustics Technical Committee.

Wood, K.S., Member, Space Science and Astrophysics Technical Committee of American Institute of Aeronautics and Astronautics.

Yang, T., Honored by ONT for work on the development of a sonar array that will improve the Navy's antisubmarine warfare and undersea surveillance capability.

Zedd, M.F., Completed second year as Secretary to the AIAA Guidance, Navigation, and Control Technical Committee.

ALAN BERMAN RESEARCH PUBLICATION AWARDS

The Annual Research Publications Awards Program was established in 1968 to recognize the authors of the best NRL publications each year. These awards not only honor individuals for superior scientific accomplishments in the field of naval research, but also seek to promote continued excellence in research and in this documentation. In 1982, the name of this award was changed to the Alan Berman Research Publications Award in honor of its founder.

There were 1080 separate publications published in 1989 that were considered for recognition. Of those considered, 31 were selected. These selected publications represent 78 authors, each of whom received a publication awards certificate, a bronze paperweight, and a booklet listing the publications that received special recognition. In addition, NRL authors share in their respective division's monetary award.

The winning papers and their respective authors are listed below by their research units. Non-Laboratory coauthors are indicated by an asterisk.

Office of Director of Research

Determination of Atomic Positions Using Electron Nanodiffraction Patterns from Overlapping Regions: Si[110]
John H. Konnert, Peter D'Antonio, John M. Cowley,* Allen Higgs,* and Herng-Ja Ou *

Space Science Division

On the Stability of Degenerate Dwarf Radiative Shocks: New One- and Two-Temperature Calculations
Michael T. Wolff,* John H. Gardner, and Kent S. Wood

Transition Zone Flows Observed in a Coronal Hole on the Solar Disk
Kenneth P. Dere, John-David F. Bartoe, Guenter E. Brueckner, and Frank Recely*

Laboratory for Computational Physics and Fluid Dynamics

Kinetics of the Methoxy Radical Decomposition Reaction: Theory and Experiment
Michael J. Page. M.C. Lin, Tarun Choudhury,* and Yisheng He*

Numerical Evaluation of the Complete Wave-Resistance Green's Function Using Bessho's Approach
Henry T. Wang and Joel C.W. Rogers*

Condensed Matter and Radiation Sciences Division

Electronic Structure of the High-Temperature Oxide Superconductors
Warren E. Pickett

Effect of Particle-Induced Displacements on the Critical Temperature of $YBa_2Cu_3O_{7-\delta}$
Geoffrey P. Summers, Douglas B. Chrisey, Edward A. Burk,*
Michael Nastasi,* and Joseph R. Tesmer *

Plasma Physics Division

Reduction of Raman Scattering in a Plasma to Convective Levels Using Induced Spatial Incoherence
Stephen P. Obenschain, Carl J. Pawley, Andrew N. Mostovych, John A. Stamper,
Andrew J. Schmitt, Stephen E. Bodner, and John H. Gardner, Jr.

Airglow Enhancements Associated with Plasma Cavities Formed During Ionospheric Heating Experiments
Paul A. Bernhardt, Craig A. Tepley,* and Lewis M. Duncan*

Acoustics Division

The Evolution of the Double-Diffusive Instability: Salt Fingers
Colin Y. Shen

Radar Division

S-Band Shipboard Surveillance Radar
Paul K. Hughes II

Radar Waveforms Derived from Orthogonal Matrices
Frank F. Kretschmer, Jr. and Karl Gerlach

Information Technology Division

Voice Preprocessor for Digital Voice Applications
George S. Kang, Lawrence J. Fransen, and Thomas M. Moran

A Wideband Radio-Frequency Architecture for U.S. Navy HF Communication
Charles E. Hobbis, Richard K. Royce, David H. Townsend, and John R. Davis

Tactical Electronic Warfare Division

Threat Functional Identification
Leo W. Lemley

Chaff-Ship Discrimination from Correlated Envelope Observations: Optimal and Near-Optimal Block Discriminations
Evaggelos Geraniotis* and Joseph P. Lawrence

Underwater Sound Reference Detachment

Elastomeric Materials for Acoustical Applications
Rodger N. Capps

Chemistry Division

High-Pressure Fast-Atom Bombardment Mass Spectrometry: Collisional Stabilization and Reactions of Alkali Halide Cluster Ions
John H. Callahan, Richard J. Colton, and Mark M. Ross

Ion-Beam Alloying and Thermochemistry of Ceramics at High Temperatures
Irwin L. Singer and Joseph H. Wandass

Materials Science and Technology Division

Chaos and Chaotic Transients in an Yttrium Iron Garnet Sphere
Thomas L. Carroll, Louis M. Pecora, and Frederic J. Rachford

Modeling Recrystallization Kinetics in a Deformed Iron Single Crystal
Roy A. Vandermeer and Bhakta B. Rath

Optical Sciences Division

Optical Phase Control of an Optically Injection-Locked FET Microwave Oscillator
Ronald D. Esman, Lew Goldberg, and Joseph F. Weller

Explosive Molecular Ionic Crystals
Walter L. Faust

Electronics Science and Technology Division

Surface Structure and Composition of β- and 6H-SiC
Raphael Kaplan

Interface Trap Formation by the Two-Stage H^+ Process
Nelson S. Saks and Dennis B. Brown

Space Systems Development Department

Finite Element Analysis of Thermal Transients in Multi-Stripe Laser Diode Arrays
Wendy L. Lippincott and Anne E. Clement

Performance of LIPS III Attitude Control System
Robert W. Conway* and Robert L. Burdett

Spacecraft Engineering Department

Massively Parallel Symbolic Computation
Andre Deprit* and Etienne Deprit

Application of Actuators to Control Beam Flexure in a Large Space Structure
Shalom Fisher

Space Systems Technology Department

SBR Clutter and Interference
Grealie A. Andrews and Karl Gerlach

Radar Surface Signatures Based on the Two-Dimensional Tidal Circulation of Phelps Bank, Nantucket Shoals, MA
Scott R. Chubb, Gaspar R. Valenzuela, and David A. Greenberg*

Programs for Professional Development

PROFESSIONAL DEVELOPMENT

NRL has established many programs for the professional and personal development of its employees so that they may better serve the needs of the Navy. These programs develop and retain talented people and keep them abreast of advanced technology management skills. Graduate assistantships, fellowships, sabbatical study programs, cooperative education programs, individual college courses, and short courses for personal improvement contribute to professional development.

Programs are also available for non-NRL employees. These enhance the Laboratory research program by providing a means for non-NRL professionals to work at the Laboratory and thus improve the exchange of ideas, meet critical short-term technical requirements, and provide a source of new, dynamic scientists and engineers. The programs range from two-year graduate fellowships, faculty and professional interchanges, and undergraduate work to an introduction of gifted and talented high school students to the world of technology.

PROGRAMS FOR NRL EMPLOYEES

During 1989, under the auspices of the Employee Development Branch, NRL employees participated in about 5000 individual training events. Many of these were presented as either videotaped or on-site instructed courses on diverse technical subjects, management techniques, and enhancement of such personal skills as efficient use of time, speed reading, memory improvement, and interpersonal communications. Courses are also available by means of computer-based training (CBT) and live television courses for monitoring nationwide.

One common study procedure is for employees to work full time at the Laboratory while taking job-related scientific courses at universities and schools in the Washington area. The training ranges from a single course to full graduate and postgraduate programs. Tuition for training is paid by NRL. The formal programs offered by NRL are described here.

GRADUATE PROGRAMS

• The **Advanced Graduate Research Program** (formerly the Sabbatical Study Program) enables selected professional employees to devote full time to research or pursue work in their own or a related field for one academic year at an institution of their choice without the loss of regular salary, leave, or fringe benefits. NRL pays all educational costs, travel, and moving expenses for the employee and dependents. Criteria for eligibility include professional stature consistent with the applicant's opportunities and experience, a satisfactory program of study, and acceptance by the institution selected by the applicant. The program is open to paraprofessional (and above) employees who have completed 6 years of Federal Service, 4 of which are required at NRL. Since the program began in 1964, 168 employees have participated.

Dr. Conrad M. Williams, of the Materials Science and Technology Division, participated in the Advanced Graduate Research Program, spending 9 months at Johns Hopkins University and 3 months at the Tokyo Institute of Technology

• The **Edison Memorial Graduate Training Program** enables employees to pursue advanced studies in their fields at local universities. Participants in this program work 24 hours each workweek and pursue their studies during the other 16 hours. The criteria for eligibility include a minimum of 1 year of service at NRL, a bachelor's or master's degree in an appropriate field, and professional standing in keeping with the candidate's opportunities and experience.

• To be eligible for the **Select Graduate Student Program**, employees must have a college degree in an appropriate field and must have maintained at least a B average in undergraduate study. Students accepted in this program devote a full academic year to graduate study. While

attending school, they receive one half of their salary, and NRL pays for tuition, books, and laboratory expenses. During the summer, they work at the Laboratory and receive normal pay and fringe benefits. Forty-three staff members have enrolled in the program since it began in 1967.

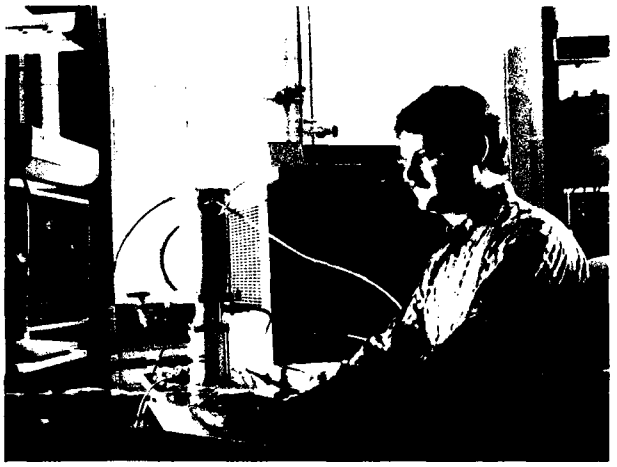

Gregory B. Tait, of the Electronics Science and Technology Division, participated in the Select Graduate Program at Johns Hopkins University

• Research conducted at NRL may be used as **thesis material for an advanced degree.** This original research is supervised by a qualified employee of NRL who is approved by the graduate school. The candidate should have completed the required course work and should have satisfied the language, residence, and other requirements of the graduate school from which the degree is sought. NRL provides space, research facilities, and supervision but leaves decisions on academic policy to the cooperating schools.

• The **Alfred P. Sloan Fellows Program** is designed for competent young executives whose job performance indicates senior management potential. The Sloan Fellows spend 1 year with the Massachusetts Institute of Technology faculty and with policymakers in industry and government. They study the theory and practice of effective and responsible management in a rapidly changing society.

• The **Education Program for Federal Officials** is directed to the needs of a small group of Federal employees who have demonstrated high competence and unusual promise. The Woodrow Wilson School of Princeton University has developed this program to enable selected mid-career officials to enlarge their knowledge in particular disciplines, to relate their fields of specialization to the broader concerns of government, and to sharpen their capacity for objective analysis of governmental problems.

• Federal Executive fellowships are available each year to employees who want to study in the **Brookings Institute Advanced Study Program.** In the program, the fellow is exposed to and participates in planning, developing, and conducting educational conferences on public policy issues for leaders in public and private life.

• The **Fellowship in Congressional Operations for Executives** provides an opportunity for some of the most promising young, technically oriented Federal executives to participate in a variety of assignments designed to develop their knowledge and understanding of Congressional operations.

• The **Maxwell Midcareer Development Program** of the Maxwell Graduate School of Citizenship and Public Affairs, Syracuse, New York, is designed to increase the managerial knowledge, ability, and skills of experienced Government officials who have been identified by their agencies as having potential for advancement to positions demanding progressively greater managerial and executive responsibilities.

• The **Practicing Engineer Advanced Study Program** of the M.I.T. Center for Advanced Engineering, Cambridge, Massachusetts, enables experienced engineers and applied scientists to work in-depth in technological areas pertinent to their professions.

• The **Science and Technology Fellowship Program**, a subsidiary of the Commerce Science

Program, includes a variety of special events, lectures, seminars, visits, conferences, field trips, and interactions with key persons from both the public and private sectors. Participants spend one week on Capitol Hill in an intensive, congressional orientation, and one week at the Brookings Institute Science Policy Conference. They also take two week-long field trips for on-site inspection of scientific institutions and industrial complexes.

• The **Stanford-Sloan Program of the Graduate School of Business**, Stanford, California, offers exceptional young executives an opportunity to make an intensive study of new concepts in business, to develop a top management perspective, and to broaden their intellectual horizons.

• The **Navy Postgraduate School** (NPS) in Monterey, California, provides advanced graduate study to selected Federal civilian employees who meet NPS academic requirements for the program in which they are interested, and whose employing agency is willing to act as sponsor.

CONTINUING EDUCATION

• Local colleges and universities offer **undergraduate and graduate courses** at NRL for employees interested in improving their skills and keeping abreast of current developments in their fields. These courses are also available at many other DoD installations in the Washington, DC area.

• The Employee Development Branch at NRL offers to all employees **short courses** in a number of fields of interest including technical subjects, computer operation, supervisory and management techniques, and clerical/secretarial skills. Laboratory employees may attend these courses at nongovernment facilities as well. Interagency courses in management, personnel, finance, supervisory development, and clerical skills are also available.

For further information on any of the above programs, contact the Employee Development Branch (Code 3840) (202) 767-2956.

TECHNOLOGY TRANSFER

• The **Office of Research and Technology Applications Program** ensures the full use of the results of the Nation's federal investment in research and development by transferring federally owned or originated technology to state and local governments and the private sector.

• The **Navy Science Assistance Program** establishes an information loop between the Fleet and the R&D shore establishments to expedite technology transfer to the user. The program addresses operational problems, focuses resources to solve specific technical problems, and develops a nucleus of senior scientific personnel familiar with the impact of current research and system performance on military operations.

The Navy's Scientists-to-Sea Program offers Navy researchers and R&D managers the opportunity to learn firsthand about factors that affect shipboard system design and operations. The program includes personnel from NRL. The trips generally lasts from three to ten days. The Scientists-to-Sea Program is scheduled to continue indefinitely with new embarkations offered on a quarterly basis.

Inquiries concerning NRL's technology transfer programs should be made to Dr. George Abraham (Code 1003.1), at (202) 767-3744.

PROFESSIONAL DEVELOPMENT

NRL has several programs, professional society chapters, and informal clubs that enhance the professional growth of employees. Some of these are listed below.

• The **Counseling Referral Service** (C/RS) helps employees to define short- and long-range career goals, to improve their job-seeking skills, and to deal with issues affecting job productivity. The C/RS provides individual counseling, career

development, and training workshops on such topics as stress management, relaxation techniques, substance abuse, and weight control. Additionally, the C/RS is available to help employees with any kind of personal problems that may be interfering with job performance. (Contact Dr. Valerie Hampson, Code 9012, (202) 767-6857.)

• A chartered chapter of **Women in Science and Engineering** (WISE) was established at NRL in 1983. Informal monthly luncheons and seminars are scheduled to inform scientists and engineers of women's research at NRL and to provide an informal environment for members to practice their presentations. WISE also sponsors a colloquium series to feature outstanding women scientists. (Contact Dr. Wendy Fuller at (202) 767-2793, Dr. Debra Rolison at (202) 767- 3617, or Dr. Cha-Mei Tang Hui at (202) 767-4148.)

• **Sigma Xi**, the Scientific Research Society, encourages original investigation in pure and applied science. As an honor society for research scientists, individuals who have demonstrated the ability to perform original research are elected to membership in local chapters. The NRL chapter, comprised of approximately 400 members, encourages original research by presenting awards annually in pure and applied science to outstanding NRL staff members. The chapter also sponsors lectures at NRL on a wide range of scientific topics for the entire NRL community. The lectures are delivered by scientists from all over the nation and the world. The highlight of the lecture series is the Edison Memorial lecture, usually featuring a Nobel laureate. (Contact Dr. Susan K. Numrich at (202) 404-7231.)

• Employees interested in developing effective self expression, listening, thinking, and leadership potential are invited to join either of two NRL chapters of **Toastmasters International**. Members of these clubs, who possess diverse career backgrounds and talents, meet three times a month in an effort to learn to communicate not by rules but by practice in an atmosphere of understanding and helpful fellowship. NRL's commanding officer endorses Toastmasters (NRLINST 12410.11), and the Employee Development Branch pays for membership and educational materials for those employees whose supervisors see a need for their active training in public speaking or organizational communication skills. (Contact Mrs. Kathleen Parrish at (202) 767-2782.)

Sid Pennington serves as toastmaster of the day at a meeting of the Forum Toastmasters Club

EQUAL EMPLOYMENT OPPORTUNITY (EEO) PROGRAMS

Equal employment opportunity is a fundamental NRL policy for all persons, regardless of race, color, sex, religion, national origin, age, or physical/mental handicap. The EEO Office's major functions include affirmative action in employment; discrimination complaint process; EEO training of supervisors, managers, and EEO collateral duty personnel; advice and guidance to management on EEO policy; and the following special emphasis programs:

• The **Federal Women's Program (FWP)** supports and enhances employment and

NRL employee, Dr. Ana Nash, tutors students from neighboring Leckie Elementary School as part of the Partners in Education Program, supported by NRL's Community Outreach Program

advancement opportunities for women and addresses issues that affect women in the workplace. It provides counseling and referral services and sponsors a chapter of Women in Science and Engineering to recognize outstanding female scientists and engineers. Distinguished women scientists are guest lecturers at quarterly presentations.

• The **Hispanic Employment Program (HEP)** focuses on working with supervisors, managers, and subcommittees to recruit and place qualified Hispanics. The program is involved with Hispanic community organizations and local schools and provides activities specifically designed to offer employment opportunities to Hispanics. "El Ingeniero" (The Engineer), which encourages Hispanic youth to pursue a career in engineering, is one such program.

• The **Black Employment Program (BEP)** concentrates on recruiting, placing, developing and advancing Black employees throughout NRL. It also encourages Black employees to achieve their maximum potential.

• The **Individuals with Handicaps Program (IHP)** assists management to improve employment and advancement opportunities for qualified handicapped and disabled-veteran employees. It also advises on accommodations necessary for handicapped persons. It recruits handicapped summer students from colleges and universities for technical positions in engineering and science and paraprofessional positions in accounting and administration; it also seeks Cooperative Education Program (Co-op) candidates who are pursuing degrees in engineering, computer sciences, or the physical sciences.

Local TV news anchorman and Emmy award-winner, Mr. James Adams, spoke at NRL at the invitation of the Black Employment Program Subcommittee

• The **Asian-American/Pacific Islander Program (API)** identifies areas of concern regarding the recruitment, selection, advancement, retention, and utilization of Asian-American/Pacific Islander employees throughout NRL. The program interacts with API professional/community organizations to address employment concerns.

• The **American Indian/Alaskan Native Employment Program (AI/ANEP)** focuses on the employment concerns of AI/ANEP employees. The program provides counseling and referral services for NRL's AI/ANEP on recruitment,

hiring, placement, promotion, retention, and other areas of employee interest.

• The **Federal Employment Opportunity Recruitment Program (FEORP)** is designed to establish, maintain, and update targeted recruitment programs to reduce the conspicuous absence or manifest imbalance categories of NRL employment through innovative internal and external recruitment. In addition, it fosters relationships with minority and women's institutions and organizations.

Special programs are held during the year to promote an awareness of the contributions and capabilities of women and minorities. (Contact the EEO Office at (202) 767-2486 for all EEO programs.)

OTHER ACTIVITIES

• The **Community Outreach Program** traditionally has used its extensive resources to foster programs that provide benefits to students and other community citizens. Volunteer employees assist with and judge science fairs, give lectures, tutor, mentor, coach, and serve as classroom resource teachers. The Program also sponsors Black History Month art and essay contests for local schools, a student Toastmasters Youth Leadership Program, and an annual Christmas party for neighborhood children. (Contact the Public Affairs Office at 767-2541.)

• Other programs that enhance the development of NRL employees include computer clubs (Edison Atari, Edison Commodore, and NRL-IBM PC) and the Amateur Radio Club. The Recreation Club accommodates the varied interests of NRL's employees with its numerous facilities, such as a 25-yard, 6-lane indoor swimming pool; a gymnasium with basketball, volleyball, and badminton courts; a weight room and exercise area; ping pong; meeting rooms; softball and basketball leagues; jacuzzi whirlpool; sauna; classes in karate, aerobics exercise, swimming, and swimnastics; and specialized sports clubs (running, skiing, biking, golfing). The Showboaters, a nonprofit drama group that presents live theater for the enjoyment of NRL and the community, performs in two major productions each year, in addition to occasional performances at Laboratory functions and benefits for local charities. The most recent productions were "Guys and Dolls" and "Godspell." Though based at NRL, membership in Showboaters is not limited to NRL employees.

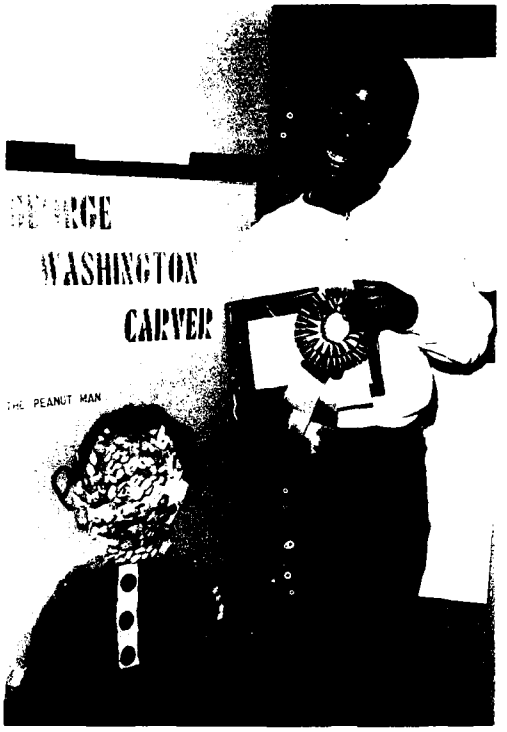

Craig Washington, of Turner Elementary School, displays a winning smile and a winning ribbon for his poster honoring George Washington Carver

PROGRAMS FOR NON-NRL EMPLOYEES

Several programs have been established for non-NRL professionals. These programs encourage and support the participation of visiting scientists and engineers in research of interest to the Laboratory. Some of the programs may serve as stepping-stones to federal careers in science and technology. Their objective is to enhance the quality of the Laboratory's research activities through working associations and interchanges with highly capable scientists and engineers and to provide opportunities for outside scientists and engineers to work in the Navy laboratory environment. Along with enhancing the Laboratory's research, these programs acquaint participants with Navy capabilities and concerns.

RECENT Ph.D., FACULTY MEMBER, AND COLLEGE GRADUATE PROGRAMS

• The **National Research Council (NRC)/ NRL Cooperative Research Associateship Program** selects associates who conduct research at NRL in their chosen fields in collaboration with NRL scientists and engineers. The tenure period is 2 years. The Office of Naval Research offers the associate posttenure research grants tenable at an academic institution.

• The American Society for Engineering Education (ASEE) administers the **Office of Naval Technology (ONT) Postdoctoral Fellowship Program** that aims to increase the involvement of highly trained scientists and engineers in disciplines necessary to meet the evolving needs of naval technology. Appointments are for 1 year (renewable for a second and sometimes a third year). These competitive appointments are made jointly by ONT and ASEE.

• The American Society for Engineering Education also administers the Navy/ASEE **Summer Faculty Research Program** for university faculty members to work for 10 weeks with professional peers in participating Navy laboratories on research of mutual interest.

• The **NRL/United States Naval Academy (USNA) Cooperative Program for Scientific Interchange** allows faculty members of the U.S. Naval Academy to participate in NRL research. This collaboration benefits the Academy by providing the opportunity for USNA faculty members to work on research of a more practical or applied nature. In turn, NRL's research program is strengthened by the available scientific and engineering expertise of the USNA faculty.

• The **Office of Naval Research Graduate Fellowship Program** helps U.S. citizens obtain advanced training in disciplines of science and engineering critical to the U.S. Navy. The 3-year program awards fellowships to recent outstanding graduates to support their study and research leading to doctoral degrees in specified disciplines such as electrical engineering, computer sciences, material sciences, applied physics, and ocean engineering. Award recipients are encouraged to continue their study and research in a Navy laboratory during the summer.

For further information about the above five programs, please contact Mrs. Jessica Hileman at (202) 767-3865.

• The **United States Naval Academy Ensign Program** assigns Naval Academy graduates to NRL to work in areas of their own choosing commensurate with their academic

qualifications. These graduates provide a fruitful summer of research assistance, while gaining valuable experience in the Navy's R&D program. (Contact CDR Tom Nadeau at (202) 767-2103.)

PROFESSIONAL APPOINTMENTS

- **Faculty Member Appointments** use the special skills and abilities of faculty members for short periods to fill positions of a scientific, engineering, professional, or analytical nature.

- **Consultants and experts** are employed because they are outstanding in their fields of specialization, or because they possess ability of a rare nature and could not normally be empioyed as regular civil servants.

- **Intergovernmental Personnel Act Appointments** temporarily assign personnel from the state or local government or educational institution to the Federal Government (or vice versa) to improve public services rendered by all levels of government.

UNDERGRADUATE COLLEGE STUDENT PROGRAMS

Several programs arc tailored to the undergraduate that provide employment and work experience in naval research. These are designed to attract applicants for student and full professional employment in the Laboratory's shortage category positions, such as engineers, physicists, mathematicians, and computer scientists. The student employment programs build an understanding of NRL job opportunities among students and educational personnel so that educators can provide students who will meet NRL's occupational needs. The employment programs for college students include the following:

- The **Cooperative Education Program** alternates periods of work and study for students pursuing bachelor degrees in engineering, computer science, or the physical sciences. Several universities participate in this program.

- The **Federal Junior Fellowship Program** hires students entering college to be assistants to scientific, professional, or technical employees.

- The **Summer Employment Program** employs students for the summer in paraprofessional and technician positions in engineering, physical sciences, and computer sciences.

- The **Student Volunteer Program** helps students gain valuable experience by allowing them to voluntarily perform educationally related work at NRL.

- The **1040-Hour Appointment** employs students on a half-time basis to assist in scientific work related to their academic program.

- The **Gifted and Talented Internship Program** provides a meaningful part-time employment experience for high school students who plan to pursue a bachelor's degree in engineering, computer science, or the physical sciences.

For additional information, contact Mrs. Cathy Downing at (202) 767-3030.

HIGH SCHOOL PROGRAMS

- The **DoD Science & Engineering Apprentice Program** employs high school juniors and seniors to serve for 8 weeks as junior research associates. Under the direction of a mentor, students gain a better understanding of research, its challenges, and its opportunities through participation in scientific programs. Criteria for eligibility are based on science and mathematics courses completed and grades achieved; scientific motivation, curiosity, and capacity for sustained hard work; a desire for a technical career; teacher recommendations; and achievement test scores. The Naval Research Laboratory Program is the lead program and the largest in the Department of Defense.

For additional information on these programs, please contact the Employee Development Branch, Code 3840, at (202) 767-2956.

The students who participated in the Science and Engineering Apprenticeship Program during the summer of 1989

Alexander Lurie, a Westinghouse Science Talent Search finalist from Illinois, talks with Dr. Elaine Oran of the Laboratory for Computational Physics and Fluid Dynamics

Diane Farrar, of NRL's Employee Development Branch, provides information about the Science and Engineering Apprenticeship Program (SEAP) to Jonathan Skroch, a student at Thomas Jefferson High School for Science and Technology in Fairfax, Virginia

General Information

GENERAL INFORMATION

"What incentives have resulted in the myriad of accomplishments over the past 66 years? Certainly, for the researchers, it is the freedom to think. I am convinced there are really no "breakthroughs," just a constant chipping away at understanding why something appears or behaves the way it does. I envy the scientist who understands, for that moment, something that no one else in the world understands. I envy the engineer who experiences the joy of using that *understanding* to make something *work* for the first time. I wish there were some way each of you could see the fruits of your labor as they find their ways into the ships and aircraft of the "service of choice," the Navy we sometimes take for granted, which will be there to defend that freedom to think and preserve the quality of life we so enjoy."

Captain W. G. Clautice, USN
Past Commanding Officer
at Change of Command Ceremony,
June 2, 1989

TECHNICAL OUTPUT

The Navy continues to be a pioneer in initiating new developments and a leader in applying these advancements to military requirements. The primary means of informing the scientific and engineering community of the advances made at NRL is through its technical output—reports, articles in scientific journals and books, papers presented to scientific societies, and topical conferences, patents, and inventions.

This section lists a portion of NRL's output for FY 1989. The omitted parts are oral presentations (about 1500), reports that carry a military security classification, and letter reports to sponsors.

Type of Contribution	Unclass.	Class.	Total
Papers in periodicals, books, and proceedings of meetings	803	0	803
NRL Reports	41	20	61
NRL Memorandum Reports	183	32	215
Books	1		1
Patents granted			21
Statutory Invention Registrations (SIRS)			8

The NRL Invention Evaluation Board was established in 1989 to assist in processing NRL invention disclosures. The Board is tasked to determine the best protection for government interests in inventions made by NRL employees and contractors. Shown standing are: Mr. R. Goodwin, Mr. G. Fritz, Dr. A. Robson, Dr. C. Temes, and Mr. T. Manuccia; Seated: Mr. T. McDonnel and Dr. J. Murday (not shown is Dr. J. Killiany).

A complete listing of the publications by NRL authors, including reports, articles in scientific journals and books, patents, etc. will appear in the *Bibliography of NRL Publications* as a separate publication.

Code	Office		Extension*
	EXECUTIVE DIRECTORATE		
1000	Commanding Officer	CAPT J.J. Donegan, USN	73403
1001	Director of Research	Dr. T. Coffey	73301
1002	Chief Staff Officer/Inspector General	CAPT R.W. Michaux, USN	73621
1003	Associate Director of Research for Strategic Planning	Dr. W.M. Tolles	73584
1004	Scientific Consultant to Director of Research	Dr. P. Mange	73724
1005	Head, Office of Management and Administration	Ms. M. Oliver	73086
1006	Head, Exploratory Development Program Office	Dr. S. Sacks	73666
1010	Associate Director of Research at Large	Mr. J.D. Brown	72879
1200	Head, Command Support Division	CAPT R.W. Michaux, USN	73621
1240	Safety Branch	Mr. J.N. Stone	72232
1270	Officer in Charge, Chesapeake Bay Detachment	CDR S.I. Kummer	301-257-4002
1280	Officer in Charge, Flight Support Detachment	LCDR G.R. Viggiano, USN	301-863-3751
1500	Head, Program Coordination Office	Dr. R.T. Swim	73314
3008	Legal Counsel	Mr. R.H. Swennes	72244
3803	Deputy EEO Officer	Mr. W. Williams	72486
4810	Public Affairs Officer	Mr. J.W. Gately, Jr.†	72541
	BUSINESS OPERATIONS DIRECTORATE		
3000	Associate Director of Research	Mr. R.E. Doak	72371
3200	Head, Contracting Division	Mr. J.H. Ablard	75227
3300	Comptroller	Mr. D.T. Green	73405
3400	Supply Officer	CDR W.E. Ralls, Jr., USN	73446
3500	Public Works Officer	CDR C.R. Allshouse, USN	73371
3800	Head, Civilian Personnel Division	Mrs. B.A. Duffield	73421
	GENERAL SCIENCE AND TECHNOLOGY DIRECTORATE		
4000	Associate Director of Research	Dr. W.R. Ellis	73324
4030	Center for Advanced Space Sensing	Dr. K. Johnston	72351
4100	Supt., Space Science Division	Dr. H. Gursky	76343
4400	Dir., Lab. for Computational Physics and Fluid Dynamics	Dr. J.P. Boris	73055
4600	Supt., Condensed Matter & Radiation Sciences Division	Dr. D.J. Nagel	72931
4700	Supt., Plasma Physics Division	Dr. S. Ossakow	72723
4800	Head, Technical Information Division	Mr. P.H. Imhof	73388
	WARFARE SYSTEMS AND SENSORS RESEARCH DIRECTORATE		
5000	Associate Director of Research	Mr. R.R. Rojas	73294
5100	Supt., Acoustics Division	Dr. D.L. Bradley	73482
5300	Supt., Radar Division	Dr. M.I. Skolnik	72936
5500	Supt., Information Technology Division	Dr. R.P. Shumaker††	72903
5700	Supt., Tactical Electronic Warfare Division	Dr. J.A. Montgomery	76278
5800	Head, Research Computation Division	Mr. R.F. Saenger	72751
5900	Supt., Underwater Sound Reference Detachment	Dr. J.E. Blue	407-857-5230
	MATERIALS SCIENCE AND COMPONENT TECHNOLOGY DIRECTORATE		
6000	Associate Director of Research	Dr. B.B. Rath	73566
6030	Head, Laboratory for Structure of Matter	Dr. J. Karle	72665
6090	Center for Biomolecular Science and Engineering	Dr. J. Schnur	73344
6100	Supt., Chemistry Division	Dr. J.S. Murday	73026
6300	Supt., Material Science & Technology Division	Dr. D.U. Gubser	72926
6500	Supt., Optical Sciences Division	Dr. T.G. Giallorenzi	73171
6800	Supt., Electronics Science and Technology Division	Dr. G.M. Borsuk	73525
6900	Engineering Services Officer	Mr. L.A. Sentiger	72300
	NAVAL CENTER FOR SPACE TECHNOLOGY		
8000	Director	Mr. P.G. Wilhelm	76547
8100	Supt., Space Systems Development Department	Mr. R.E. Eisenhauer	70410
8200	Supt., Spacecraft Engineering Department	Mr. R.T. Beal	76407
8300	Supt., Space Systems Technology Department	Mr. L.M. Hammarstrom	73920

*Direct-in-Dialing (202)76; Autovon 29-

†Additional duty

††Acting

ORGANIZATIONAL CHART
RESEARCH ADVISORY COMMITTEE

COMMANDING OFFICER
Code 1000
CAPT J.J. Donegan, Jr., USN

DIRECTOR OF RESEARCH
Code 1001
Dr. T. Coffey

ASSOCIATE DIRECTORS OF RESEARCH

OFFICE OF STRATEGIC PLANNING
Code 1003
Dr. W.M. Tolles

AT LARGE
Code 1010
J.D. Brown

BUSINESS OPERAT ONS DIRECTORATE
Code 3000
R.E. Doak

GENERAL SCIENCE AND TECHNOLOGY DIRECTORATE
Code 4000
Dr. W.R. Ellis

WARFARE SYSTEMS AND SENSORS RESEARCH DIRECTORATE
Code 5000
R.R. Rojas

MATERIALS SCIENCE AND COMPONENT TECHNOLOGY DIRECTORATE
Code 6000
Dr. B.B. Rath

NAVAL CENTER FOR SPACE TECHNOLOGY
Code 8000
P.G. Wilhelm

ORGANIZATIONAL CHART (Continued)
EXECUTIVE DIRECTORATE

EXECUTIVE COUNCIL (DIVISION DIRECTORS)

COMMANDING OFFICER
Code 1000
CAPT J.J. Donegan, Jr., USN

RESEARCH ADVISORY COMMITTEE

DIRECTOR OF RESEARCH
Code 1001
Dr. T. Coffey

CHIEF STAFF OFFICER
INSPECTOR GENERAL
INTERNAL REVIEW
Code 1002
CAPT R.W. Michaux, USN

SAFETY OFFICER
Code 1240
J. Stone

LEGAL COUNSEL
Code 3008
R.H. Swennes

ASSOCIATE DIRECTOR OF RESEARCH AT LARGE
Code 1010
J.D. Brown

DEPUTY EQUAL EMPLOYMENT OPPORTUNITY OFFICER
Code 3803
W. Williams

PUBLIC AFFAIRS OFFICER
Code 4810
J.W. Gately, Jr.

OFFICE OF STRATEGIC PLANNING
Code 1003
Dr. W.M. Tolles

SCIENTIFIC CONSULTANT TO THE DIRECTOR OF RESEARCH
Code 1004
Dr. P. Mange

OFFICE OF MANAGEMENT AND ADMINISTRATION
Code 1005
M. Oliver

EXPLORATORY DEVELOPMENT MANAGER
Code 1006
Dr. S. Sacks

DIVISION DIRECTORS

COMMAND SUPPORT DIVISION
Code 1200
CAPT R.W. Michaux, USN
- Security
- Military Operations
- Military Administration and
- Personnel
- Flight Support
- Flight Support Detachment
- Safety
- Chesapeake Bay Detachment

PROGRAM COORDINATION OFFICE
Code 1500
Dr. R.T. Swim

CHESAPEAKE BAY DETACHMENT
Code 1270
CDR S. Kummer, USN

FLIGHT SUPPORT DETACHMENT
Code 1280
LCDR G.R. Viggiano, USN

ORGANIZATIONAL CHART (Continued)

BUSINESS OPERATIONS DIRECTORATE
Code 3000
R.E. Doak

CONTRACTING DIVISION
Code 3200
J.H. Ablard

FINANCIAL MANAGEMENT DIVISION
Code 3300
D. Green

- Budget
- Accounting
- Disbursing
- Equipment Resource Management and Control
- Systems Operations

SUPPLY DIVISION
Code 3400
CDR W.E. Ralls, Jr., USN

- Purchasing/Requisition Control
- Receipt Control
- Material
- Automated Inventory Management
- Technical
- Material Issue

PUBLIC WORKS DIVISION
Code 3500
CDR C.R. Allshouse, USN

- Engineering
- Maintenance and Utilities
- Contract Administration
- Maintenance Control
- Administrative
- Planning
- Project Management
- Selective/Facilities Support Contracts

CIVILIAN PERSONNEL DIVISION
Code 3800
B. Duffield

- Staffing and Classification
- Employee Development
- Employee Relations
- Special Recruitment Programs

GENERAL SCIENCE AND TECHNOLOGY DIRECTORATE
Code 4000
Dr. W.R. Ellis

CENTER FOR ADVANCED SPACE SENSING
Code 4030
Dr. K. Johnston

SPACE SCIENCE DIVISION
Code 4100
Dr. H. Gursky

- Atmospheric Physics
- X-Ray Astronomy
- Radio & IR Astronomy
- Upper Atmospheric Physics
- Gamma & Cosmic Ray Astrophysics
- Solar Physics
- Solar Terrestrial Relationships
- Ionospheric Effects
- E O Hulburt Center for Space Research
- Engineering Management
- Ultraviolet Measurement
- Solar Spectroscopy

LABORATORY FOR COMPUTATIONAL PHYSICS AND FLUID DYNAMICS
Code 4400
Dr. J.P. Boris

- Reactive Flow and Dynamical Systems
- Fluid/Structure Interactions
- Fluid Dynamics Developments
- Computational Physics Developments
- Mathematical Physics

CONDENSED MATTER AND RADIATION SCIENCES DIVISION
Code 4600
Dr. D.J. Nagel

- Radiation Effects
- Directed Energy Effects
- Surface Modification
- Dynamics of Solids
- Complex Systems Theory

PLASMA PHYSICS DIVISION
Code 4700
Dr. S. Ossakow

- Plasma Radiation
- Laser Plasma
- High-Power Electromag Radiation
- Experimental Plasma Physics
- Plasma Technology
- Geophysical & Plasma Dynamics
- Plasma Theory
- Advanced Beam Technologies
- Charged Particle Physics
- Joint Programs for Plasma Physics

TECHNICAL INFORMATION DIVISION
Code 4800
P. Imhof

- Information Services
- Technical Library/Software Support
- Publications
- Graphic Design Services
- Systems/Photographic
- Historian

WARFARE SYSTEM AND SENSORS RESEARCH DIRECTORATE
Code 5000
R.R. Rojas

ACOUSTICS
Code 5100
Dr. D. Brac

- Acoustics M
  Characteri
- Applied Oce
- Physical Acc
- Ocean Dyna
- Marine Syst
- Signal Proce
- Acoustic Sy

RADAR DI
Code 5300
Dr. M.I. Sk

- Radar Analy
- Radar Techn
- Search Rada
- Target Chara
- Identificatior
- Airborne Rac
- Systems Cor
  Research

INFORMAT TECHNOLO DIVISION
Code 5500
Dr. R.P. Sh

- Navy Center
  Applied Re
  Artificial Int
- Communicati
- Transmissior
- Integrated W
- Human-Comp
- Secure Infor
  Technology

TACTICAL E WARFARE
Code 5700
Dr. J.A. Mc

- Offboard Co
- EW Suppor
- Airborne EW
- Ships EW Sy
- Advanced Te

RESEARCH COMPUTAT DIVISION
Code 5800
R.F. Saenge

- Software
- User Service
- Computer Op
  and Commu
- Information
  Manageme

UNDERWAT REFERENCE DETACHME
Code 5900
Dr. J.E. Blu

- Acoustic Ma
- Technical Se
- Electronics
- Transducer
- Measureme
- Computer

ATIONAL CHART (Continued)

WARFARE SYSTEMS AND SENSORS RESEARCH DIRECTORATE
Code 5000
R.R. Rojas

ACOUSTICS DIVISION
Code 5100
Dr. D. Bradley
- Acoustics Media Characterization
- Applied Ocean Acoustics
- Physical Acoustics
- Ocean Dynamics
- Manne Systems
- Signal Processing
- Acoustic Systems

RADAR DIVISION
Code 5300
Dr. M.I. Skolnik
- Radar Analysis
- Radar Techniques
- Search Radar
- Target Characteristics
- Identification Systems
- Airborne Radar
- Systems Control and Research

INFORMATION TECHNOLOGY DIVISION
Code 5500
Dr. R.P. Shumaker*
- Navy Center for Applied Research in Artificial Intelligence
- Communication Systems
- Transmission Technology
- Integrated Warfare Technology
- Human-Computer Interaction
- Secure Information Technology

TACTICAL ELECTRONIC WARFARE DIVISION
Code 5700
Dr. J.A. Montgomery
- Offboard Countermeasures
- EW Support Measures
- Airborne EW Systems
- Ships EW Systems
- Advanced Techniques

RESEARCH COMPUTATION DIVISION
Code 5800
R.F. Saenger
- Software
- User Services
- Computer Operations and Communications
- Information Resources Management

UNDERWATER SOUND REFERENCE DETACHMENT
Code 5900
Dr. J.E. Blue
- Acoustic Materials
- Technical Services
- Electronics
- Transducer
- Measurements
- Computer

MATERIALS SCIENCE AND COMPONENT TECHNOLOGY DIRECTORATE
Code 6000
Dr. B.B. Rath

LABORATORY FOR STRUCTURE OF MATTER
Code 6030
Dr. J. Karle

CENTER FOR BIOMOLECULAR SCIENCE AND ENGINEERING
Code 6090
Dr. J. Schnur

CHEMISTRY DIVISION
Code 6100
Dr. J.S. Murday
- Chemical Dynamics and Diagnostics
- Polymeric Materials
- Surface Chemistry
- Navy Technology Center for Safety and Survivability
- Biomolecular Engineering

MATERIALS SCIENCE AND TECHNOLOGY DIVISION
Code 6300
Dr. D. Gubser
- Physical Metallurgy
- Composites and Ceramics
- Mechanics of Materials
- Structural Integrity
- Material Physics

OPTICAL SCIENCES DIVISION
Code 6500
Dr. T.G. Giallorenzi
- Advanced Concepts
- Applied Optics
- Laser Physics
- Electro-optical Technology
- Optical Techniques
- Fiber Optics Technology

ELECTRONICS SCIENCE TECHNOLOGY DIVISION
Code 6800
Dr. G.M. Borsuk
- Solid State Devices
- Electronic Materials
- Surface Physics
- Microwave Technology
- Semiconductors
- Vacuum Electronics

ENGINEERING SERVICES DIVISION
Code 6900
L.A. Sentiger
- Mechanical Engineering and Manufacturing
- Electronic Engineering and Fabrication
- Industrial Engineering Services

NAVAL CENTER FOR SPACE TECHNOLOGY
Code 8000
P.G. Wilhelm

SPACE SYSTEMS DEVELOPMENT DEPARTMENT
Code 8100
R.E. Eisenhauer
- Spacecraft Engineering
- Advanced Systems Development
- Communication Systems Technology
- Terrestrial Systems
- SDI Office

SPACECRAFT ENGINEERING DEPARTMENT
Code 8200
R.T. Beal
- Design, Manufacturing and Processing
- Systems Analysis and Test
- Control Systems
- Concept Development

SPACE SYSTEMS TECHNOLOGY DEPARTMENT
Code 8300
L.M. Hammarstrom
- Space Sensing
- Space Applications
- Systems Engineering and Analysis
- Advanced Concepts and Processing

*ACTING

— — — ADDITIONAL DUTY

CONTRIBUTIONS BY DIVISIONS AND LABORATORIES

Space Science Division (4100)

Strategic Scene Generation Model
by Harry M. Heckathorn, Herbert Gursky, and Russell G. Groshans

The Source of High-Speed Solar Wind Streams
by Kenneth P. Dere, JohnDavid F. Bartoe, and Guenter E. Brueckner

The Search for Millisecond X-ray Pulsars
by Paul L. Hertz, Jay P. Norris, and Kent S. Wood

Three-Dimensional Spectral Simulations of the Solar Corona
by Russell B. Dahlburg (Laboratory for Computational Physics and Fluid Dynamics) and Spiro K. Antiochos

Laboratory for Computational Physics and Fluid Dynamics (4400)

Parallel Algorithms for Real-Time Tracking
by Jay P. Boris and Ronald L. Kolbe (Berkeley Research Associates)

Three-Dimensional Spectral Simulations of the Solar Corona
by Russell B. Dahlburg and Spiro K. Antiochos (Space Science Division)

High-Resolution Surfactant Characterization in Ship Wakes
by Jack A.C. Kaiser (Space Systems Technology Department) and Rodney D. Peltzer

Condensed Matter and Radiation Sciences Division (4600)

Solid-State Supercomputing
by Larry L. Boyer, Barry M. Klein, Dimitrios A. Papanstantatopoulos, and Warren E. Pickett

Anomalous Intense Electron Beam Deposition in Metals
by Alexander Stolovy, John M. Kidd, and Arthur I. Namenson

High Performance Infrared Filters and Mirrors
Edward P. Donovan

Plasma Physics Division (4700)

Charged Particle Beam Research for Directed Energy Applications: Experimental Program
by Robert A. Meger

Chaos in the Magnetospheric Particle Dynamics
by James Chen

Technical Information Division (4800; old 2600)

Library-based Microcomputer Support Services
by Laurie E. Stackpole

Acoustics Division (5100)

Investigating the Potential of Parallel Processing
by Helen F. Webb

Environmental Signal Processing
by William A. Kuperman and John S. Perkins

Radar Division (5300)

High-Resolution Waveforms in Radar Surveillance
by George J. Linde

At-Sea Support for SPS-49 Radar Improvements
by Robert M. Crisler, John L. Walters, and John P. Barry

Generic Monopulse Radar Simulation
by Ching-Tai Lin

Information Technology Division (5500)

Applying Formal Methods to the Analysis of Key Distribution Protocols
by Catherine A. Meadows

Certification Methodology for Trusted Application Systems
by Judith N. Froscher and John P. McDermott

Communication Network Research for SDI
by Edwin L. Althouse and Dennis N. McGregor

REAL Approach to Tracking and Correlation for Large-Scale Scenarios
by Joseph B. Collins and Jeffrey K. Uhlmann

Tactical Electronic Warfare Division (5700)

Airborne Infrared Signature Measurement Facility
by John W. Dries, Jamie S. Price, and Douglas S. Fraedrich
EWCM Prototype Readied for Deployment
by Gene E. Layman

Research Computation Division (5800; old 2800)

An Algorithm for Calculating Intramolecular Angle Dependent Forces on Vector Computers
by Jeffrey H. Dunn and Sam G. Lambrakos (Materials Science and Technology Division)

Underwater Sound Reference Detachment (5900)

Offnormal Incidence Reflection Measurements on Thick Underwater Acoustic Panels
by Jean C. Piquette
The Shock Test Facility: Water-Filled Conical Shock Tube
by Joseph F. Zalesak and Lynn B. Poché
Development of Polymers for Constrained Layer Damping
by Rodger N.Capps

Laboratory for Structure of Matter (6030)

Assembly of Membrane-Active Peptides
by Isabella L. Karle and Judith L. Flippen-Anderson

Center for Biomolecular Science and Engineering (6090)

Polymerized Vesicles Revisited
by Alok Singh

Chemistry Division (6100)

Ensuring Navy Fuel Availability and Performance
by Dennis R. Hardy
Combustion Chemistry Studied at High Temperature
by Nancy L. Garland, James W. Fleming, and Herbert H. Nelson
Epoxy Coatings for Shipboard Copper-Nickel Piping
by Robert F. Brady, Jr.

Materials Science and Technology Division (6300)

Ferrous Alloy Phase Transformations
by Roy A. Vandermeer
Glass Fibers with Metallic Cores
by Jack D. Ayers
Impact Angle Effects on Fracture
by V. Gensheimer DeGiorgi
Indicator of High-Temperature Oxide Superconductors
by Henry A. Hoff and Michael S. Osofsky
An Algorithm for Calculating Intramolecular Angle-Dependent Forces on Vector Computers
by Jeffrey H. Dunn (Research Computation Division) and Sam G. Lambrakos

Optical Sciences Division (6500)

Superfluorescent Fiber Source for Fiber-Optic Gyroscopes
by William K. Burns and Irl N. Duling III
High Performance Optical Phase Conjugation
by Paul S. Lebow
Coherent Laser Radar Measurements of High Velocity Targets
by Alan L. Huston and Mitchell G. Roe

***Electronics Science and Technology Division* (6800)**

New Frontiers in Electronics at NRL
by Gerald M. Borsuk
An Hydroxide Etch for β-SiC
by Paul E.R. Nordquist, Robert J. Gorman, and Philipp H. Klein
A Safe Storage and Delivery System for Hazardous Gases
by Roger S. Sillmon
Atomic Layer Electronics
by William E. Carlos, Daniel G. Gammon, Sharka M. Prokes, and Benjamin V. Shanabrook
Vacuum Microelectronics
by Henry F. Gray and Robert K. Parker
Light-Activated Resistance Switching: An Extremely Sensitive Solid-State Photodetector
by Eric S. Snow and Paul M. Campbell

Space Systems Development Department (8100)

A Novel Design of a 1.8 GHz Input Odd Ratio Frequency Divider
by David S. Korn

Forward Photorefractive Multibeam Mixing
by G. Charmaine Gilbreath

Spacecraft Engineering Department (8200)

Design of the LACE Flight Dynamics Experiment
by Shalom Fisher

Visualizing Phase Flows in Dynamical Systems
by Shannon L. Coffey, Etienne M. Deprit, and Liam M. Healy

Space Systems Technology Department (8300)

Global Weather Observations with the SSM/I
by James P. Hollinger and Glenn D. Sandlin

Shape Functions for Invariant Image Recognition
by Sheldon B. Gardner

High-Resolution Surfactant Characterization in Ship Wakes
by Jack A.C. Kaiser and Rodney D. Peltzer (Laboratory for Computational Physics and Fluid Dynamics)

EMPLOYMENT OPPORTUNITIES FOR ENTRY-LEVEL AND EXPERIENCED PERSONNEL

This *Review* illustrates some of the exciting science and engineering carried out at NRL as well as the potential for new personnel.

The Naval Research Laboratory offers a wide variety of challenging positions that involve the full range of work from basic and applied research to equipment development. The nature of the research and development conducted at NRL requires professionals with experience. Typically, there is a continuing need for electronics, mechanical aerospace, ceramic, and materials engineers; metallurgists with bachelor's and/or advanced degrees; and physical and computer scientists with Ph.D. degrees. Opportunities exist in the areas described below.

Ceramic and Materials Scientists/Engineers. These employees work on the mechanical properties, coating and materials processing, and materials research.

Electronics Engineers. These engineers work in the following areas: communications satellite design, analog and digital signal processing, information processing, strategic and tactical communication systems design, instrumentation, microcomputer design, satellite attitude-control systems, image processing, IR sensors, focal plane arrays, radar, inverse scattering phenomena, statistical communication theory, electro-optics, hardware/software interfacing, artificial intelligence, electromagnetic (EM) scattering, digital electronics, fiber optics, optical information processing, semiconductor device processing, microwave tubes, threat systems analysis, electroacoustic optics, RF measurement design, EM propagation, EM theory, HF radar propagation analysis, electronic warfare simulation, pulsed power technology, vacuum electronics, microwave technologies, networking techniques, speech processing, Navy C^3I, electronic countermeasure systems design, spacecraft attitude controls, and orbitology.

Mechanical and Aerospace Engineers. These employees may be assigned to satellite thermal design, structural design, propulsion, experimental fluid mechanics, experimental structural mechanics, solid mechanics, elastic/plastic fracture mechanics, materials characterization of composites, finite element methods, nondestructive elevation, characterization of fracture resistance of structural alloys, and combustion.

Computer Science Graduates. Employees in this field are involved with artificial intelligence, software engineering, software systems specifications, computer design/architecture, systems analysis, and command information systems.

Chemists. Chemists are recruited to work in the areas of inorganic and organometallic synthesis, solution kinetics and mechanisms, surface analysis, organic chemistry, combustion, colloid/surface chemistry, fire suppression, and nuclear decay.

Physicists. Physics graduates may concentrate on such fields as electromagnetics, image processing, inverse scattering phenomena, acoustics,

inversion theory, mathematical modeling of scattering processors, radar system development, electro-optics, focal plane arrays, signal processing, plasma physics, astrophysics, semiconductor technology, relativistic electronics, beam/wave interactions, low-temperature physics, superconductivity, physical/chemical vapor disposition of thin and thick coatings, wave propagation, ionospheric physics, computational hydrodynamics, computational atomic physics, and supersonic, gas-dynamic numerical modeling.

FOR FOREIGN NATIONALS

U.S. citizenship is required for employment at NRL.

APPLICATION AND INFORMATION

Interested applicants should submit a resume or an application for Federal Employment Form (SF-171), which can be obtained from local offices of the Office of Personnel Management and Personnel Offices of Federal agencies, to the address below.

Direct inquiries to;

Naval Research Laboratory
Civilian Personnel Division, Code 3830 RV 89
Washington, DC 20375-5000
202-767-3030

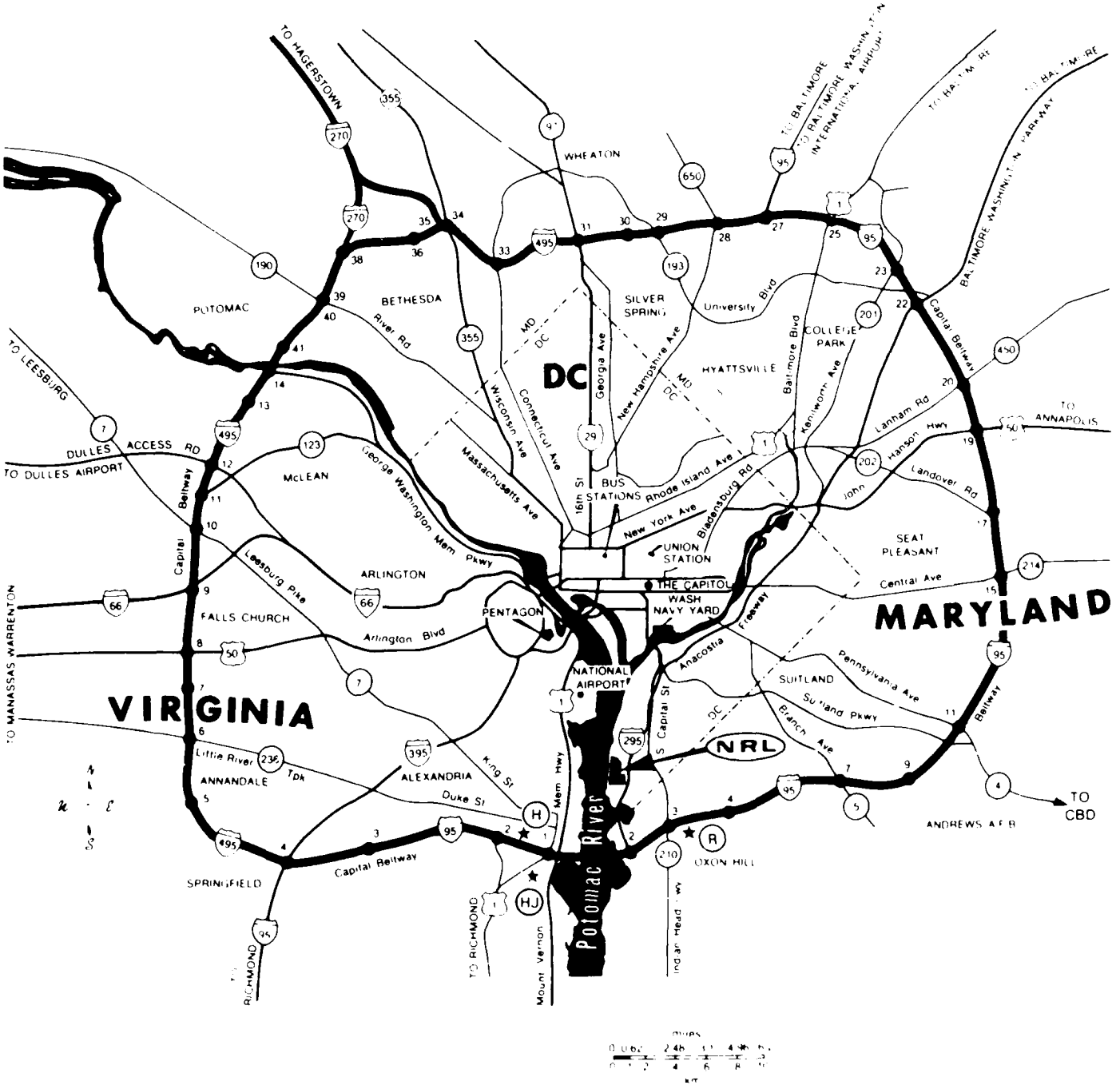

LOCATION OF NRL IN THE CAPITAL AREA

INDEX – 1989–1990 *NRL REVIEW*